8/8-94 9S(1)

ITRI-140
NOVEMBER 1993
CATEGORY: UC-408

INHALATION TOXICOLOGY RESEARCH INSTITUTE ANNUAL REPORT

1992 - 1993

by the Staff of the
Inhalation Toxicology Research Institute

INHALATION TOXICOLOGY RESEARCH INSTITUTE
LOVELACE BIOMEDICAL & ENVIRONMENTAL RESEARCH INSTITUTE
P.O. Box 5890 Albuquerque, NM 87185

PREPARED FOR THE OFFICE OF HEALTH
AND ENVIRONMENTAL RESEARCH
OF THE U.S. DEPARTMENT OF ENERGY
UNDER CONTRACT NUMBER DE-AC04-76EV01013

The research described in this report involved animals maintained in animal care facilities fully accredited by the Americal Association for Accreditation of Laboratory Animal Care. The research described in this report that involved humans was conducted in compliance with government regulations protecting human subjects.

Printed in the United States of America

Available to DOE and DOE contractors from the Office of Scientific and Technical Information, P. O. Box 62, Oak Ridge, TN 37831: prices available from (615) 576-8401, FTS 626-8401.

Available to the public from the National Technical Information Service, U.S. Department of Commerce, 5285 Port Royal Rd., Springfield, VA 22161.

ITRI-140
November 1993
Category: UC-408

Annual Report of the Inhalation Toxicology Research Institute Operated for the United States Department of Energy by the Lovelace Biomedical and Environmental Research Institute

October 1, 1992 through September 30, 1993

by the Staff of the
Inhalation Toxicology Research Institute
J. L. Mauderly, Director

K. J. Nikula, Senior Editor
S. A. Belinsky, Associate Editor
P. L. Bradley, Technical Editor

November 1993

Prepared for the Office of Health and Environmental Research of the U.S. Department of Energy Under Contract Number DE-AC04-76EV01013

I. AEROSOL TECHNOLGY AND CHARACTERIZATION OF AIRBORNE MATERIALS

TABLE OF CONTENTS

INTRODUCTION vi

PREVIOUS ANNUAL REPORTS viii

I. AEROSOL TECHNOLOGY AND CHARACTERIZATION OF AIRBORNE MATERIALS

Measurement of Thoron and Thoron/Radon Mixtures 1
Y. S. Cheng and H. C. Yeh

Use of a Two-Stage Virtual Impactor and an Electrical Classifier for Generation of Test Fiber Aerosols with a Narrow Size Distribution 5
B. T. Chen and H. C. Yeh

Performance of Respirator Filters for Aerosol Particles 8
Y. S. Cheng, H. C. Yeh, and E. E. Martinez

Characterization of Aerosols Produced During Total Hip Replacement Surgery in Beagle Dogs with ^{51}Cr-Labeled Blood 10
H. C. Yeh, B. A. Muggenburg, R. A. Guilmette, M. B. Snipes, R. S. Turner, and R. K. Jones

Design and Evaluation of an Annular Slit-Jet Virtual Impactor 13
B. T. Chen, M. D. Hoover, G. J. Newton, and H. C. Yeh

Particle Collection Efficiency of a High-Volume Annular Kinetic Impactor for Continuous Monitoring of Alpha-Emitting Radionuclides 15
B. T. Chen, S. J. Montaño, M. D. Hoover, G. J. Newton, and D. S. Gregory

Effects of Simultaneous Collection of Salt, Radon Progeny, and Plutonium on Alpha CAM Performance 18
M. D. Hoover and G. J. Newton

Characterization of Enriched Uranium Dioxide Particles from a Uranium-Handling Facility: Preliminary Evaluation of *In Vitro* Solubility 21
M. D. Hoover, R. A. Guilmette, G. J. Newton, R. J. Howard, and S. M. Trotter

Use of Lanthanide Oxides as Surrogates for Plutonium in Simulated Waste Retrieval 23
G. J. Newton, M. D. Hoover, A. W. Cronenberg, G. G. Loomis, and S. H. Landsberger

A Case Study on a NESHAP Evaluation for a Radioactive Materials Handling Area 26
G. J. Newton, M. D. Hoover, and H.-S. Hwang

II. DEPOSITION, TRANSLOCATION, METABOLISM, AND CLEARANCE OF INHALED TOXICANTS

Nasal Deposition of Ultrafine Aerosols in Humans 29
Y. S. Cheng, H. C. Yeh, S. Q. Simpson, and D. L. Swift

Transport of Inhaled Metals and Solvents Through the Olfactory Epithelium into the Olfactory Bulbs 32
J. L. Lewis, J. R. Harkema, A. R. Dahl, and Y. S. Cheng

Progress Toward an Experimentally Validated Model for Calculating Tissue Dosage of Inhaled Vapors 35
A. R. Dahl and P. Gerde

Particle-Associated Hydrocarbons and Lung Cancer: The Correlation Between Cellular Dosimetry and Tumor Distribution 38
P. Gerde, B. A. Muggenburg, R. F. Henderson, and A. R. Dahl

Retention Sites for Particles Deposited in Lung Conducting Airways of Beagle Dogs 40
M. B. Snipes, B. A. Muggenburg, K. J. Nikula, and R. A. Guilmette

The Fate of Inhaled Nickel Compounds in Cynomolgus Monkeys 43
J. M. Benson, Y. S. Cheng, B. A. Muggenburg, and F. F. Hahn

Methods for Labeling F344 Rat Alveolar Macrophages to Investigate Particle Transport and Clearance in Lung 45
J. M. Benson, D. L. Cassie, N. F. Johnson, and R. A. Guilmette

High Butadiene Monoepoxide Levels in Bone Marrow of B6C3F$_1$ Mice Inhaling Butadiene 47
K. R. Maples, W. E. Bechtold, A. R. Dahl, and R. F. Henderson

Urinary Excretion of Hydroquinone and Catechol by Workers Occupationally Exposed to Benzene 50
W. E. Bechtold and N. Rothman

III. CARCINOGENIC RESPONSES TO TOXICANTS

Exposure of F344 Rats to Aerosols of $^{239}PuO_2$ and Chronically Inhaled Cigarette Smoke 53
G. L. Finch, E. B. Barr, W. E. Bechtold, B. T. Chen, W. C. Griffith, M. D. Hoover, J. L. Mauderly, C. E. Mitchell, and K. J. Nikula

Effects of Combined Exposure of F344 Rats to Inhaled $^{239}PuO_2$ and a Chemical Carcinogen (NNK) 56
D. L. Lundgren, S. A. Belinsky, K. J. Nikula, W. C. Griffith, and M. D. Hoover

Combined Exposure of F344 Rats to Beryllium Metal and $^{239}PuO_2$ Aerosols 58
G. L. Finch, F. F. Hahn, W. W. Carlton, A. H. Rebar, M. D. Hoover, W. C. Griffith, J. A. Mewhinney, and R. G. Cuddihy

Effects of Combined Exposure of F344 Rats to $^{239}PuO_2$ and Whole-Body X-Radiation 61
D. L. Lundgren, F. F. Hahn, W. C. Griffith, W. W. Carlton, M. D. Hoover, and B. B. Boecker

Effects of Thoracic and Whole-Body Exposure of F344 Rats to X Rays 64
F. F. Hahn, D. L. Lundgren, W. C. Griffith, and B. B. Boecker

Effects of Intrapleural Innoculation of F344 Rats with Silicon Carbide Whiskers and Continuous Glass Filaments 66
N. F. Johnson and F. F. Hahn

Bone Tumor Incidence in Beagle Dogs that Inhaled Soluble Radionuclides 69
B. A. Muggenburg, F. F. Hahn, B. B. Boecker, K. J. Nikula, R. A. Guilmette, and W. C. Griffith

Growth Rate Patterns of Lung Tumors in Beagle Dogs Exposed to $^{239}PuO_2$ or $^{238}PuO_2$ 71
W. C. Griffith, J. H. Diel, B. A. Muggenburg, and S. J. Matthews

IV. MECHANISMS OF CARCINOGENIC RESPONSES TO TOXICANTS

Analysis of Sputum Samples and Lung Tumors from Uranium Miners for Altered Gene Expression 75
C. A. Carter, N. F. Johnson, S. A. Belinsky, and J. F. Lechner

A Scaffold-Attachment-Like Region on Human Chromosome 9 is Amplified in Some Lung Tumor Specimens 77
W. A. Palmisano, C. H. Kennedy, and J. F. Lechner

Isolation of a Putative p53-Controlled Gene by Polymerase Chain Reaction Amplification 79
C. H. Kennedy, W. A. Palmisano, and J. F. Lechner

p53, ErbB2, and K-ras Gene Dysfunctions are Rare in Spontaneous and Plutonium-239-Induced Canine Lung Neoplasia 81
L. A. Tierney, F. F. Hahn, and J. F. Lechner

p53 Alterations in ^{239}Pu-Induced Lung Tumors in F344 Rats 83
G. Kelly and F. F. Hahn

Wild-Type p53 Expression in Cultured Lung Epithelial Cells Exposed to Alpha Particles 85
N. F. Johnson, R. J. Jaramillo, and A. W. Hickman

K-ras and p53 Alterations in Lung Tumors Induced in the F344 Rat by X Irradiation 87
S. A. Belinsky, C. E. Mitchell, and F. F. Hahn

K-ras and p53 Alterations in Lung Tumors Induced in the F344 Rat by Diesel Exhaust or Carbon Black 89
D. S. Swafford, K. J. Nikula, and S. A. Belinsky

Epithelial Cell Kinetics in the Lungs of F344 Rats that Inhale Diesel Exhaust or Carbon Black 91
K. J. Nikula and I. Y. Chang

Rapid Detection and Quantitation of Mutant K-ras Codon 12 Restriction Fragments by Capillary Electrophoresis 94
C. E. Mitchell, S. A. Belinsky, and J. F. Lechner

An Improved Method for the Isolation of Type II and Clara Cells from A/J Mice 96
S. A. Belinsky, J. F. Lechner, and N. F. Johnson

V. NONCARCINOGENIC RESPONSES TO INHALED TOXICANTS

Induction of Nasal Carboxylesterase in F344 Rats Following Inhalation Exposure to Pyridine 99
K. J. Nikula, R. Novak, I. Y. Chang, A. R. Dahl, and J. L. Lewis

Tobacco Smoke-Induced Alterations of Rhodanese and Carboxylesterase in the Olfactory Mucosae of F344 Rats 102
K. J. Nikula, L. A. Sachetti, G. L. Finch, B. T. Chen, and J. L. Lewis

Effects of Inhaled Endotoxin on Intraepithelial Mucosubstances in F344 Rat Nasal and Tracheobronchial Airways 105
J. R. Harkema and T. Gordon

Effects of Chronic Ozone Exposure on Airway Mucosubstances in the F344 Rat 108
J. R. Harkema, K. E. Pinkerton, and C. G. Plopper

Comparison of Type II Cell and Neutrophil Alkaline Phosphatases 110
R. F. Henderson, G. Kelly, G. G. Scott, and J. J. Waide

VI. MECHANISMS OF NONCARCINOGENIC RESPONSES TO INHALED TOXICANTS

Construction of F344 Rat and Human cDNA Libraries and Isolation of Species-Specific Cytochrome P450 Family 4 cDNAs 113
J. A. Hotchkiss, S. H. Lowell, and A. R. Dahl

Effect of Neutrophil Depletion on Endotoxin-Induced Mucous Cell Metaplasia in Pulmonary Airways of F344 Rats 116
J. A. Hotchkiss and J. R. Harkema

The Role of Antigen in the Development of Pulmonary Immune Memory 119
D. E. Bice, M. E. Cunniffe, G. E. Snow, and B. A. Muggenburg

Progress Toward a Murine Model of Granulomatous Lung Disease from Inhaled Beryllium 122
G. L. Finch, K. J. Nikula, D. S. Swafford, M. D. Hoover, and D. E. Bice

VII. DEVELOPMENT OF THERAPEUTIC MODALITIES

Treatment of the Prostate Gland Using a Diode Laser 125
B. A. Muggenburg, F. F. Hahn, W. C. Griffith, V. Esch, and R. L. Conn

VIII. THE APPLICATION OF MATHEMATICAL MODELING TO HEALTH ISSUES

Mathematical Model of Particle Deposition from Inhaled Polydisperse Aerosols 127
H. C. Yeh, Y. Zhuang, and I. Y. Chang

Sensitivity Analysis of the ITRI ^{238}Pu Biokinetic Model 130
A. W. Hickman, W. C. Griffith, and R. A. Guilmette

Intake Assessment for Workers that Inhaled ^{238}Pu Aerosols 133
R. A. Guilmette, W. C. Griffith, and A. W. Hickman

New Tools for Evaluating Respiratory Tract Intake of Alpha-Emitting Particles 136
B. R. Scott, M. D. Hoover, and G. J. Newton

Risk of Lung Cancer Mortality after Inhaling Beta-Gamma- or Alpha-Emitting Radionuclides 139
B. R. Scott, M. E. Mueller, and B. B. Boecker

IX. APPENDICES

A. Status of Longevity and Sacrifice Experiments in Beagle Dogs 143

B. Organization of Personnel as of November 30, 1993 144

C. Organization of Research Programs. October 31, 1992 - November 30, 1993 153

D. Publication of Technical Reports. October 1, 1992 - September 30, 1993 156

E. ITRI Publications in the Open Literature Published, In Press, or Submitted Between October 1, 1992 - September 30, 1993 157

F. Presentations Before Regional or National Scientific Meetings and Educational and Scientific Seminars. October 1, 1992 - September 30, 1993 165

G. Seminars Presented by Visiting Scientists. October 1, 1992 - September 30, 1993 175

H. Adjunct Scientists as of November 30, 1993 177

I. Educational Activities at the Inhalation Toxicology Research Institute 178

J. Author Index 180

INTRODUCTION

The Institute

The Inhalation Toxicology Research Institute (ITRI) is a Federally Funded Research and Development Center operated for the U. S. Department of Energy (DOE) by the Lovelace Biomedical and Environmental Research Institute, a nonprofit subsidiary of the Lovelace Medical Foundation. ITRI is designated as a "Special Purpose Laboratory" within the DOE Office of Health and Environmental Research, Office of Energy Research. Approximately 80% of the Institute's research is funded by DOE; the remainder is funded by a variety of governmental, trade association, and industry sources.

The mission of ITRI is to conduct basic and applied research to improve our understanding of the nature and magnitude of the human health impacts of inhaling airborne materials in the home, workplace, and general environment. Institute research programs have a strong basic science orientation with emphasis on the nature and behavior of airborne materials, the fundamental biology of the respiratory tract, the fate of inhaled materials and the mechanisms by which they cause disease, and the means by which data produced in the laboratory can be used to estimate risks to human health. Disorders of the respiratory tract continue to be a major health concern, and inhaled toxicants are thought to contribute substantially to respiratory morbidity. As the largest laboratory dedicated to the study of basic inhalation toxicology, ITRI provides a national resource of specialized facilities, personnel, and educational activities serving the needs of government, academia, and industry.

The Institute's multidisciplinary staff works in specialized facilities and takes a collaborative research approach to resolving scientific issues. ITRI is located on Kirtland Air Force Base East, approximately 10 miles southeast of Albuquerque, New Mexico. The more than 290,000 square feet of laboratory and support facilities include unique facilities and equipment for basic biological research and exposures of animals to all types of airborne toxicants. The staff of approximately 200 includes doctoral-level scientists in physical, chemical, biological, medical, and mathematical disciplines. Working with the scientists are highly trained scientific technicians, laboratory animal technicians, and a full range of support staff. The entire range of biological systems is employed, including macromolecules, cells, tissues, laboratory animals, and humans. The research includes both field and laboratory studies. Strong emphasis is placed on the quality of research and resulting data; the Institute has a Quality Assurance Unit and is fully capable of research in adherence to Good Laboratory Practices guidelines.

The Institute's scientific and support staffs are organized into disciplinary and functional scientific groups and support units (see Appendix B). The research is organized into programs which are administered by the Assistant Directors (see Appendix C). The programs are composed of projects having common research themes, but which typically cut across research disciplines. For example, the Pathogenesis Program contains projects oriented largely toward the development of non-cancerous respiratory tract disease, but the projects involve molecular biology, biochemistry, pathology, physiology, and inhalation exposure technology.

The Report

The papers in this report are organized along topical lines, rather than by research program, so that research within specific disciplines is more readily identified. The papers include summaries of research funded by both DOE and non-DOE sources, to represent the full scope of Institute activities. The source of funding is acknowledged for each paper. The appendices summarize the organization of the Institute's staff and research programs, publications and presentations by ITRI Scientists, seminars by visiting scientists, collaborations with scientists in other institutions, and a description of ITRI's educational activities.

A separate series of reports entitled, Annual Report on Long-Term Dose-Response Studies of Inhaled or Injected Radionuclides, summarize the design and status of the long-term studies of the health effects of radionuclides in dogs, conducted at ITRI and the University of Utah. This separate report also contains the status of each dog, the detailed tables which were previously included as appendices in the ITRI Annual Report. The dog report can be obtained from NTIS, and by request from the Institute.

Joe L. Mauderly, D.V.M.
Director

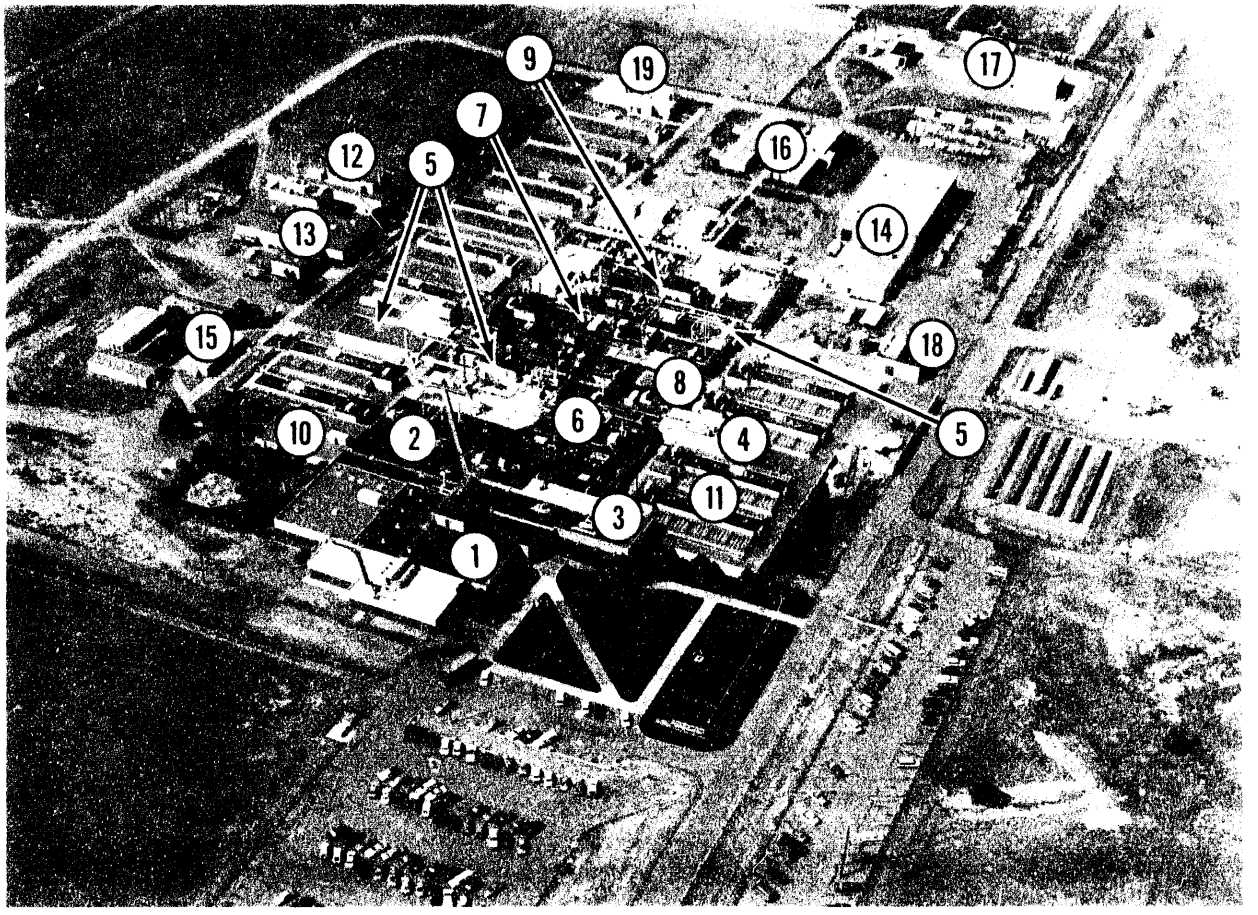

An aerial view of the Inhalation Toxicology Research Institute which was constructed in several increments, starting in June 1962. The Institute's facilities consist of (1) an administrative area, including housing for the directorate, personnel, business and purchasing offices, editorial offices, a cafeteria, conference rooms, and health protection operations; (2) a central laboratory and office area, including aerosol science, radiobiology, pathology, chemistry and toxicology laboratories; (3) cell toxicology laboratories; (4) pathophysiology laboratories; (5) a specially designed and equipped chronic inhalation exposure complex with some laboratories suitable for use with carcinogenic materials; (6) an exposure facility for acute inhalation exposures to chemical toxicants and beta- and gamma-radionuclides; (7) exposure facilities for acute inhalation exposures to alpha-emitting radionuclides; (8) a veterinary hospital and facilities for detailed clinical observations; (9) small-animal barrier-type housing facilities; (10) a modern library and quality assurance facilities; (11) 13 kennel buildings, nine capable of housing 100 dogs each and four for housing 120 dogs each; (12) an analytical chemistry building; (13) an engineering and shop support building; (14) a receiving, property management, and storage building; (15) a health protection building; (16) several temporary laboratories; (17) a hazardous waste storage and treatment facility; (18) standby power facility; and (19) animal quarantine facility.

PREVIOUS ANNUAL REPORTS

Selective Summary of Studies on the Fission Product Inhalation Program from July 1964 through June 1966;

LF-28, 1965 LF-33, 1966

Fission Product Inhalation Program Annual Report 1966-1972;

LF-38, 1967 LF-41, 1969 LF-44, 1971

LF-39, 1968 LF-43, 1970 LF-45, 1972

Inhalation Toxicology Research Institute Annual Report 1972-1990;

LF-46, 1973 LMF-84, 1980 LMF-120, 1987

LF-49, 1974 LMF-91, 1981 LMF-121, 1988

LF-52, 1975 LMF-102, 1982 LMF-126, 1989

LF-56, 1976 LMF-107, 1983 LMF-129, 1990

LF-58, 1977 LMF-113, 1984 LMF-134, 1991

LF-60, 1978 LMF-114, 1985 LMF-138, 1992

LF-69, 1979 LMF-115, 1986

Long-Term Dose-Response Studies of Inhaled or Injected Radionuclides 1988-1990;

LMF-128, 1989 LMF-130, 1990 LMF-135, 1991

MEASUREMENT OF THORON AND THORON/RADON MIXTURES

Y. S. Cheng and H. C. Yeh

Thoron and radon mixtures are found in many environments. Although there are techniques to measure radon, techniques for simultaneous measurement of both substances are needed. A team from ITRI participated in the First International Intercomparison and Intercalibration Meeting on Thoron and its Progeny, and Thoron/Radon Mixtures at Elliot Lake, Canada, November 2-6, 1992. The meeting was organized by Dr. J. Bigu, Canada Centre for Mineral and Energy Technology (CANMET). The ITRI team participated in all phases of the intercomparison studies. The methods, procedures, and results are summarized here.

Thoron or thoron/radon mixtures have been maintained in the Radon/Thoron Test Facility at CANMET. During the meeting the ITRI team used several instruments to measure thoron and its progeny, and thoron/radon mixtures. A calibrated Lucas cell was used to determine the concentrations of thoron gas and thoron/radon mixtures during the day when the thoron concentrations were higher. Electret ion chambers were used to determine the gas and gas mixtures at night when gas concentrations were lower. The thoron and thoron/radon progeny and their size distributions were determined using an ITRI graded diffusion battery (GDB) (Cheng, Y. S. *et al. J. Aerosol Sci. 23*: 361, 1992).

A cylindrical Lucite® cell (10.16 cm ID, 17.3 cm long) coated with ZnS on the inner wall was used to collect the thoron gas and the thoron/radon mixture. A filter was placed in front of the cell inlet to remove progeny particles. Samples were taken from a port located outside the thoron/radon test chamber. After sampling, the cell was placed inside a Radon Flask Counter (Model 218, Ludlum Measurements, Sweet Water, TX) with a Smart Radiation Monitor (Model SRM-200, Eberline Inc., Santa Fe, NM). The counting efficiency of the Lucas cell in the counter was 15.4% based on a calibration by the Environmental Measurement Laboratory (New York, NY). The continuous counting of α decay started 1 min after filling the cell with gas. For thoron gas, the counting stopped after 8 to 10 min, when the α counts approximated the background value. For an experiment done on November 5, the thoron/radon mixture was counted initially in Elliot Lake for 1580 min, and the counting continued up to 7154 min after the ITRI team returned to Albuquerque. The data (count rate as a function of time) were analyzed to obtain an estimate of thoron or thoron/radon air concentrations, using equations derived from a series of radioactive decays for both ^{220}Rn and ^{222}Rn. The data were analyzed using the non-linear fit procedure of SigmaPlot (Jandel Scientific, San Rafael, CA) on an IBM-compatible PC.

Four Standard E-PERM chambers and four Thoron E-PERM chambers (Rad Elec Inc., Frederick, MD) were used to measure thoron and radon concentrations overnight. Voltage readings on standard electret substrates were measured using an Electret Voltage Reader (Rad Elec Inc., Frederick, MD) before and after sampling. The samplers were placed inside the test chamber on the third rack. The sampling time ranged from 13.6 to 18.4 h. The Standard chamber has a 100% response for radon and a 15% response to thoron, whereas the Thoron chamber has a 100% response for thoron and radon. A simultaneous measurement made at the same location at the same time using both chambers led to an estimation of time-averaged radon and thoron concentration.

The ITRI GDB was used to determine the activity size distribution, the progeny concentration, and the unattached fraction. The design, calibration, and performance of this device have been described (Cheng *et al.*, 1992; Cheng, Y. S. *et al. Health Phys.*, in press). For this study, five stainless steel screens with 24, 50, 145, 200, and 635 mesh numbers (Tetko Inc., Briacliff, NY) were used. A 47-mm type A/E glass fiber filter (Gelman Co., Ann Arbor, MI) was used to collect all particles that penetrated the screens. The flow diameter of the GDB was 38.1 mm. The flow rate was controlled by a calibrated rotameter. A 6 L/min flow rate was used. After a 10-min sampling period for thoron gas and a 5-min sampling period for the gas mixtures, screens and filters were placed into individual gross alpha counters (Model TM-372A2, Tri-Mets Instruments) with calibrated efficiency between 0.447 to 0.463. Only the front side of the screen was counted. Two counting intervals (2-17 and 92-107 min) were used for thoron-only experiments, and five counting intervals (2-5, 6-20, 21-30, 245-305, 401-446 min) for the thoron/radon mixture.

Activity concentrations of thoron progeny (^{212}Pb and ^{212}Bi) were calculated from the two counts by solving simultaneous equations (Raabe, O. G. and M. E. Wrenn. *Health Phys. 17*: 593, 1969). For mixtures, the thoron

and radon progeny (^{218}Po, ^{214}Pb, and ^{214}Bi) concentrations were calculated from five counts using a non-linear least square method (Raabe and Wrenn, 1969). Data were analyzed using both Quattro Pro (Borland International, Scotts Valley, CA) and SigmaPlot (Jandel Scientific, San Rafael, CA) softwares. After progeny concentrations collected at each screen and filter were estimated, the activity size distribution was calculated from the collection data using the expectation-maximization method (Maher, E. F. and N. M. Laird. *J. Aerosol Sci. 16*: 557, 1985) as described previously (Cheng *et al.*, 1992). Because only the front side of the screen was counted, front-to-total correction on the screens and interstage screen loss were accounted for using equations derived by Soloman, S.G. and T. Ren (*Aerosol Sci. Technol. 17*: 69, 1992). The computer code was written in Fortran 77 Code and run on a PC. Forty size intervals between 0.5 to 50 μm were used in the data analysis.

Figure 1 shows the experimental data and curve fit for the case of the thoron/radon gas mixture. Thoron (C_{Th}) and radon (C_{Rn}) concentrations were calculated from the best fit to the data. The average thoron concentrations measured during the day were between 70,000 to 100,000 Bq/m^3.

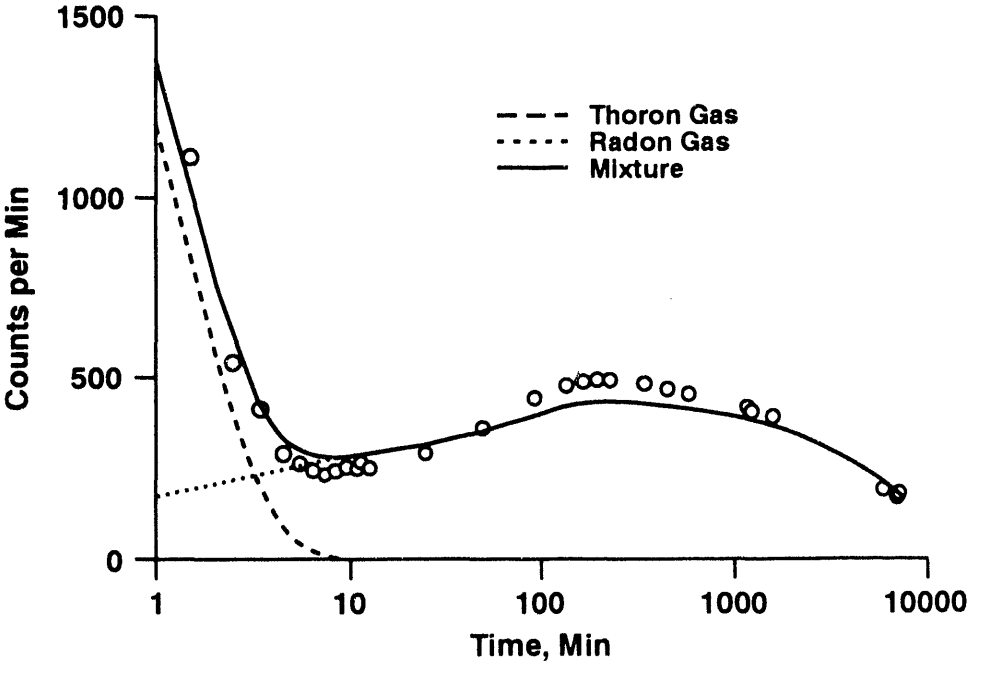

Figure 1. Measurement of thoron/radon mixture concentrations in a Lucas cell. The data points are counts/min, and the solid curve is the combined thoron/radon counts from the fitted equation. The dashed curve is the contribution from the thoron gas; the dotted curve is the contribution from the radon gas.

Four pairs of electret ion chambers were used to measure the thoron concentration and thoron/radon gas mixture during overnight sampling. The relative standard deviations of four measurements at the same location ranged from 15 to 35% for the thoron concentration and 2.2 to 30% for the radon concentration. In the first two samples, pure thoron gas was introduced; therefore, only low levels of background radon concentrations would be expected. However, measurements of between 200 to 250 Bq/m^3 of radon gas showed a high level of background concentration when this method was used to determine both radon and thoron concentrations. This result suggested that the current electret method is not suitable for determining thoron/radon gas mixture.

Of seven GDB samples, two samples of thoron/radon mixtures were taken. The experimental conditions and the resultant potential alpha energy concentration (PAEC) for each run are listed in Table 1. The working level of thoron progeny increased as the aerosol concentration in the chamber increased from 300 to 16,300 particles/cm^3, even though the thoron gas concentration remained relatively stable between November 3-4. For thoron progeny (^{212}Pb and PAEC), bimodal size distributions with modes at 0.75 and 47.2 nm were found,

Table 1

Thoron and Thoron/Radon Progeny Size Distributions by Graded Diffusion Battery

			Thoron Progeny			Radon Progeny		
Date	Run No.	CNC Conc. (#/cc)	Size Mode	AMD/σ_g	Unattached Fraction	Size Mode	AMD/σ_g	Unattached Fraction
11/3/93	CANMET 2	1100	0.75 nm /47.2 nm	22.8 nm /4.78	17.8 %			
11/3/93	CANMET 3	1060	0.75 nm /47.2 nm	24.1 nm /4.62	16.7 %			
11/4/93	CANMET 4	312	0.84 nm /47.2 nm	4.3 nm /7.00	60.5 %			
11/4/93	CANMET 5	355	0.75 nm /47.2 nm	13.9 nm /6.51	29.9 %			
11/4/93	CANMET 6	16300	47.2 nm	47.2 nm /1.0	0 %			
11/5/93	CANMET 7	200	0.75 nm /47.2 nm	16.0 nm /6.12	26.3 %	0.53 nm /47.2 nm	1.02 nm /4.64	86.5 %
11/6/93	CANMET 8	22000	0.53 nm /4.72 nm	44.8 nm /1.62	1.2 %	0.53 nm /47.2 nm	47.2 nm /1.07	0.02 %

except for cases with extremely high aerosol concentrations (> 16,300 particles/cm^3). At very high aerosol concentrations, almost all thoron progeny particles were attached to the aerosol; therefore, a single modal size distribution was found. The unattached fractions for thoron progeny, as calculated from the working level in the smaller size mode, decreased from 61 to 0 % when the aerosol concentration increased from 310 to 16,300 particles/cm^3. In the case of the gas mixture, the radon progeny also showed a bimodal distribution with size modes at 0.53 and 47.2 nm. The unattached fractions of both thoron and radon progeny almost disappeared at an aerosol concentration of 22,000 particles/cm^3.

Our measurements of the thoron and thoron/radon mixtures agreed well with data obtained from other laboratories (data not shown). These methods will be useful in measuring thoron/radon mixtures indoors.

(Research sponsored by the Office of Health and Environmental Research, U.S. Department of Energy under Contract No. DE-AC04-76EV01013.)

USE OF A TWO-STAGE VIRTUAL IMPACTOR AND AN ELECTRICAL CLASSIFIER FOR GENERATION OF TEST FIBER AEROSOLS WITH A NARROW SIZE DISTRIBUTION

B. T. Chen and H. C. Yeh

Fiber particles with well-defined diameters and lengths are important in studying the physical behavior, lung deposition and clearance, and toxicity of fibrous aerosols. This report describes the use of a two-stage virtual impactor and an electrical classifier to produce fibrous aerosols that have a narrow distribution of fiber diameter and length. A two-stage virtual impactor was used to classify fibers based on diameter. An electrical classifier, containing a unipolar-ion charger and a differential mobility analyzer, was used to segregate fibers based on length (Chen, B. T. *et al. Aerosol Sci. Technol. 19*: 109, 1993).

Four different manmade fibers, including carbon fibers (Test Article 31, Hercules, Inc., Wilmington, DE), glass fibers (X7484 and X7999, Owens Corning, Inc., Granville, OH), and MMVF10 glass fibers (Manville, Inc., Littleton, CO), were used in this study. The first three types of fibers were monodisperse in diameter and polydisperse in length; the MMVF10 glass fibers were polydisperse in diameter and length (Table 1).

Table 1

Size Distributions of Fiber Aerosols Before and After Classification by a Two-Stage Virtual Impactor and an Electrical Classifier

Types of Fibers	Size Distribution of the Bulk Materials		Impactor Cutoff Size (μm)	Classifier Total Flow (L/min)	Size Distribution of the Classified Materials	
	CMD/GSD (μm)	CML/GSD (μm)			CMD/GSD (μm)	CML/GSD (μm)
Carbon Fiber (Test Article 31)	3.74/1.06	35.8/2.08	3.0	20	–	16-200/ 1.17-1.28
				30	–	28-190/ 1.21-1.30
				40	–	30-170/ 1.18-1.25
Glass Fiber (X7484)	2.83/1.13	18.5/1.63	2.0	20	–	13-34/ 1.22-1.29
				30	–	15-35/ 1.26-1.29
Glass Fiber (X7779)	1.83/1.18	16.5/1.71	2.0	20	–	12-37/ 1.19-1.29
				30	–	19-43/ 1.22-1.26
Glass Fiber (MMVF10)	1.06/1.80	16.1/2.35	4.7, 3.3[a]	20	0.72-1.29/ 1.18-1.37	6.6-29/ 1.29-1.44

[a]A two-stage virtual impactor with two different cutoff sizes was used.

The experimental setup for this study is schematically shown in Figure 1. Each fiber material was aerosolized using a small-scale powder disperser (Model 3433, TSI, Inc.). The aerosol was passed through a ^{85}Kr bipolar ion source to reach a state of Boltzmann charge equilibrium. Because the aerodynamic diameter of a fiber-like particle depends primarily on the fiber diameter, a one- or two-stage virtual impactor was used to classify fibrous aerosols according to their diameters. For carbon and glass fibers with monodisperse diameters, a one-stage virtual impactor was used to reduce the numbers of fine nonfibrous particles, which exist in the bulk fibrous material and in the aerosol, and to concentrate the fiber-particle fraction. For polydisperse MMVF10 fibers, a two-stage virtual impactor was used to classify fibers with a narrow range of diameters. The count median diameter (CMD) and geometric standard deviation (GSD) of this distribution depend on the selection of the cutoff sizes and can be adjusted by varying the flow rate and nozzle diameter in the impactor. The fibers classified by the virtual impactor were introduced into an electrical classifier (Fig. 1) which was designed based on results from a previous study (Chen *et al.*, 1993).

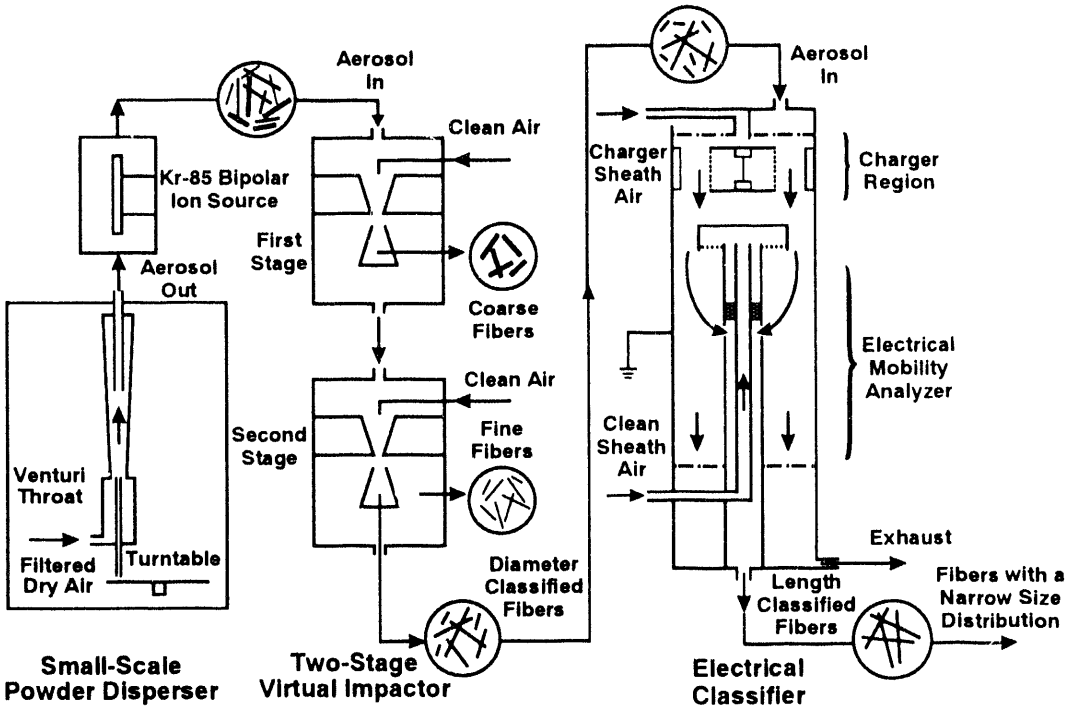

Figure 1. Schematic diagram of the experimental setup for fiber classification studies. The two-stage virtual impactor was used in classifying bulk fibers with polydisperse diameters and lengths. For classifying bulk fibers with monodisperse diameters, only one-stage virtual impactor was used.

This electrical classifier was fabricated by modifying the mobility analyzer section in the electrical aerosol analyzer (Model 3030, TSI, Inc.). This modified section consisted of two concentric stainless steel cylinders: a central rod and an outer cylinder. The aerosol stream was introduced into the analyzer near the outer cylinder, while a laminar flow of clean sheath air was delivered through the inner tube of the central rod and introduced around the rod. The outer cylinder was grounded, while a negative high voltage was applied to the central rod to form a cylindrical condenser with concentric cylindrical electrodes. Under a given set of operating conditions, charged fibers in the aerosol stream flow along the outer cylinder and are deflected through the clean air core. If these particles have the appropriate electrical mobility, they will be drawn into a slit (slit width = 1.6 mm) in the central rod, through the outer tube of the central rod, and extracted at the exit slit with a classification flow rate of 2 L/min. Due to the finite width of the aerosol stream entering and leaving the mobility analyzer, the mobility of the particles classified by the device is spread over a finite range of values, which, in turn, classifies fibers with a finite range of length (count median length, CML). The classified fibrous aerosol samples were collected on membrane filters (SSWP25, Millipore Corp., Bedford, MA) for size analysis. The particle size distributions were determined by tracing the digitized images of fibers using a semi-automatic image analysis system.

Table 1 shows the size distributions of these four types of fibrous aerosols. The classified aerosols show a narrow size distribution in fiber diameter and length. As an example, the GSDs of the classified MMVF10 glass fibers were 1.18-1.37 in diameter and 1.29-1.44 in length, compared to the corresponding values of 1.80 and 2.35 in the bulk fibrous aerosols. The results showed that this device, which combines a virtual impactor with an electrical classifier, can successfully classify fibers based on both dimensions and, consequently, produce fibers with a narrow size distribution. This device has the potential to classify other micrometer-sized, irregularly shaped particles and will be used to produce aerosols with narrow size distribution.

(Research sponsored by the Office of Health and Environmental Research, U. S. Department of Energy, under Contract No. DE-AC04-76EV01013.)

PERFORMANCE OF RESPIRATOR FILTERS FOR AEROSOL PARTICLES

*Y. S. Cheng, H. C. Yeh, and E. E. Martinez**

The goal of this research was to quantify the performance of respirator filters used to protect workers in environments where they may be at risk of exposure to asbestos and manmade fibers. Current OSHA guidelines require the use of respirators that are fitted with high-efficiency filters. These filters must be approved under NIOSH certification criteria based on penetration tests in which spherical aerosols are used. Fiber aerosols are known to have different aerodynamic behaviors than spherical particles and usually carry higher electrostatic charges. Because the carcinogenicities of asbestos and other fibers are known to be due, in part, to fiber dimensions, it is very important to know the efficiency of a respirator filter in relation to fiber dimension. It is also difficult to predict how fiber aerosols will penetrate respirator filters as compared to the NIOSH testing results using spherical particles.

As a part of the evaluation of the respirator, we quantified performance of respirator filters and determined the effects of charge on the filter performance using spherical Di-Octyl Sebacate (DOS) aerosols. Four types of respirator filters were used in the study: (1) a HEPA filter AOR57A (American Optical Corp., Southbridge, MA), (2) a high-efficiency filter cartridge (Type S, MSA, Pittsburgh, PA), (3) a filter for powered respirators (Type A, MSA, Pittsburgh, PA), and (4) a disposable, low-efficiency filter (3M8710, 3M, St. Paul, MN). Following the current NIOSH test procedures, the HEPA and high-efficiency filters, which are used in dual cartridges, were tested at 16 and 42.5 Lpm, and the disposable-type filters were tested at 32 and 85 Lpm, as was the filter for powered respirators.

The experimental setup is shown schematically in Figure 1. A TSI condensation aerosol generator (model 3076 and 3072) was used at a flow rate of 2 Lpm. The particles then flowed through a Kr-85 discharger, which lowered their charge to the Boltzmann equilibrium charge level. The flow rate was increased prior to the particles reaching the test chamber in order to meet the test requirements. A mixing fan was placed inside the cone located before the chamber to increase aerosol uniformity. A honeycomb flow straightener was placed between the fan and the chamber to reduce the turbulence created. The test chamber was a cylinder (12 in I.D. x 17 in long); flow in the test chamber was laminar, and aerosol concentration was uniform. Pre-filter and post-filter probes were located in the test chamber to sample the aerosols. A magnehelic pressure sensor measured the pressure differential across the test filter. A change in pressure indicated that aerosol particles had built up on the filter. The RAM-1 (MIE, Bedford, CT) was connected to the sample probes and measured the mass concentrations before and after the filter. A QCM particle impactor determined the aerosol size to be about 0.25 μm.

The hypothesis postulated was that an increased electrical charge on the filter cartridge would increase the efficiency of the filter. To test this hypothesis, filter cartridges were used both untreated from the box and after treatment in isopropyl alcohol, which discharges the filters. The surface charge on the filters before and after the treatment was measured with an electrostatic fieldmeter (Model 245, Monroe Electronics, Lyndonville, NY). Only the low-efficiency filter had an initial charge.

Figure 2 shows the results obtained for the disposable, low-efficiency filter (3M8710). As can be noted from the differences in percent deposition, charge played an important role in increasing the efficiency of the filter, while flow rate had little effect on the efficiency of the filter.

Results were also obtained for the high-efficiency filter cartridge, which had no initial charge. As expected, it was considerably more efficient than the disposable filter. The differences between the discharged and untreated filter cartridges were negligible. The differences due to flow rate were also negligible. The results obtained from the other test filters with no charge were similar. The only differences were in the level of efficiency due to the rating of the filters.

*Department of Energy/Associated Westei Universities Summer Student Research Participant

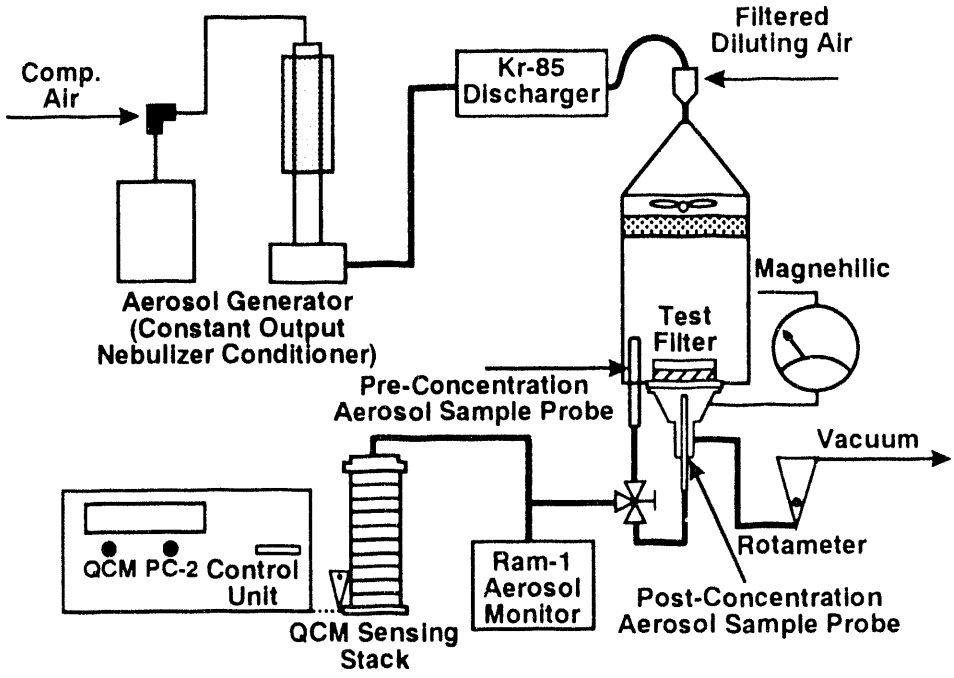

Figure 1. The experimental setup.

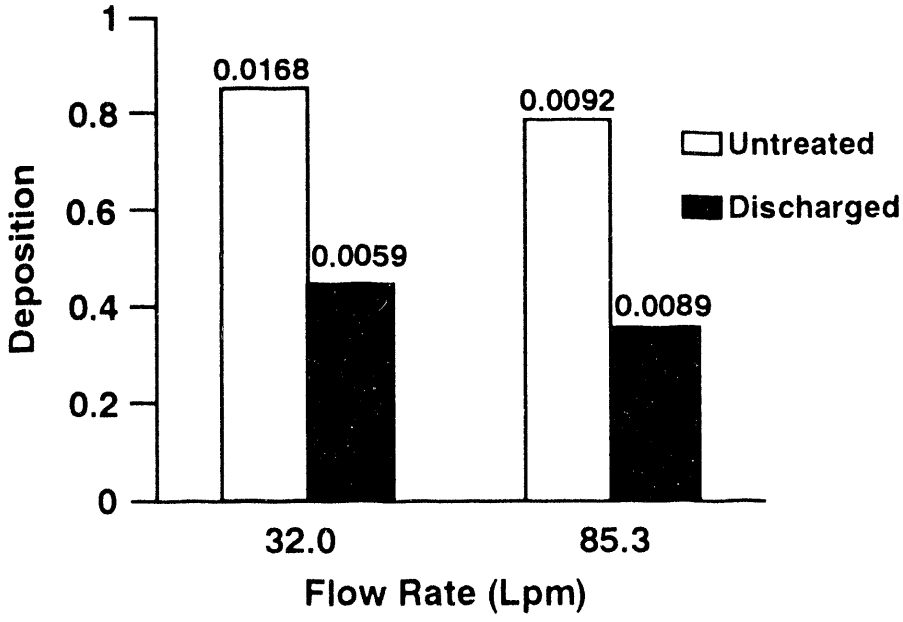

Figure 2. Aerosol deposition in a disposable filter (3M8710).

Overall, the electrostatic charges on the respirator filters did affect the filter efficiency; flow rates had negligible effect on the efficiencies of filters. Filters treated with anti-electrostatic spray and under high-temperature and high-humidity conditions (data not shown) had a reduced charge. A penetration test using asbestos fiber is in progress.

(Research sponsored by the PHS/CDC under Grant R01-OH02922-01A1 from the National Institute of Occupational Safety and Health in facilities provided by the U.S. Department of Energy under Contract No. DE-AC04-76EV01013.)

CHARACTERIZATION OF AEROSOLS PRODUCED DURING TOTAL HIP REPLACEMENT SURGERY IN BEAGLE DOGS WITH ^{51}Cr-LABELED BLOOD

H. C. Yeh, B. A. Muggenburg, R. A. Guilmette,
M. B. Snipes, R. S. Turner, and R. K. Jones*

The potential for transmitting blood-associated pathogens from infected patients to health care workers via inhalation of blood-containing aerosols, particularly during orthopedic surgery, has added to concerns about the hazards of working with these patients (Day, L. *Can. Med. Assoc. J. 139*: 1935, 1988; Goldman, B. *Can. Med. Assoc. J. 138*: 736, 1988). Previous studies have demonstrated that respirable, blood-associated aerosols are produced during orthopedic surgery (Heinsohn, P. and Jewett, D. L. *Am. Ind. Hyg. Assoc. J. 54*: 446, 1993; 1991-92 Annual Report, p. 48). In those studies, the identification and estimation of blood-associated aerosols were based upon Hemastix or Chemstrip 9 analysis of samples. These indicating strips will respond to either hemoglobin or myoglobin, but will not differentiate between the two. Furthermore, the results from the Hemastix and Chemstrip 9 analyses are only qualitative, because the responses are classified into four discrete categories, based on changes in color. This study was designed to quantify the blood-containing aerosols that might be produced during orthopedic surgical procedures using five Beagle dogs whose blood was labeled with radioactive ^{51}Cr immediately before the surgery.

The primary surgical procedure chosen for the study was total hip replacement, similar to those described previously in humans (1991-92 Annual Report, p. 48). The dog was chosen as the experimental model because its size permitted the use of the same surgical procedure and equipment as used in humans. The surgical tools used included an electrocautery, bone drill, saw, reamer, hammer, and water pulse irrigation/suction. The blood was labeled by incubating 19 GBq (500 mCi) of ^{51}Cr(VI) with fresh or refrigerated whole blood from a donor dog and by washing and centrifuging the blood to remove the reduced Cr(III). The labeling was about 90% efficient. Following radiolabeling and purification, the blood was transported to the surgical suite and intravenously infused into an anesthetized dog.

The relatively large amount of radioactivity used in this study and the considerations of potential contamination and decontamination of equipment limited the types and numbers of aerosol sampling instruments used. They were as follows: (1) a Marple personal cascade (MPC) impactor (to be worn by the chief surgeon), (2) two Lovelace Multi-Jet (LMJ) cascade impactors, and (3) filter samplers. These instruments were cleaned and decontaminated for each of the five experimental runs.

A lead shield covered the torso of the dog to reduce the potential radiation dose to personnel performing the experiment. The aerosol sampling probe was attached to the top of the lead shield that covered the torso of the dog. The distance of the probe from the surgical site was about 15-25 cm. One LMJ cascade impactor was also placed next to the probe on top of the lead shield. This approximated the configuration used in previous studies with humans at a local hospital. After radiolabeled blood was injected into the dogs, aerosol measurements were taken during the total hip replacement procedures in the surgical suite at ITRI. Aerosol samples were obtained using one MPC impactor, two LMJ cascade impactors (one placed near the surgical site, and the other that sampled through an aerosol chamber), and two consecutive filters taken from the aerosol chamber during each experiment.

At the conclusion of each surgical procedure, the MPC impactor, the LMJ cascade impactors, and the filters were disassembled, the impactor substrates and filters were removed, and the samples were weighed using a Cahn balance. After weighing, each sample was assayed for ^{51}Cr using an automated gamma counter (Beckman, Model 8000, Fullerton, CA). More than 30 samples (including background and standard samples) were counted per experiment. These counting data represented aerosolized red blood cell (RBC) samples. An intravenous blood sample was obtained from the dog prior to and post surgery, and was used as the counting standard and to establish counts per RBC for samples for that dog. This conversion factor could be used to estimate the

*Lovelace Medical Center, Albuquerque, New Mexico

number of RBCs collected on each impactor substrate from the counting data of the labeled ^{51}Cr activity. After counting, these filter and impactor substrate samples were washed with 20 μL of distilled water, and the hemoglobin content was quantified by using Chemstrip 9.

Similar to previous results from humans (1991-92 Annual Report, p. 48), the aerosol size distributions varied from experiment to experiment, apparently due to the dynamic nature of the surgical procedures. However, the shapes of the size distribution were similar among the five dogs. Figure 1 shows a typical result obtained from the MPC impactor worn by the chief surgeon. Also included are the results analyzed by Chemstrip 9 on each impactor stage for quantifying blood content. The estimated number of RBCs was obtained from the amount of ^{51}Cr in the sample, assuming that all of the ^{51}Cr was in the RBCs. Even though the Chemstrip 9 readings were qualitative and somewhat subjective, they correlated fairly well with the radioactivity (and thus to the estimated number of RBCs). In general, all of the size distributions obtained by weight and by radioactivity also correlated very well.

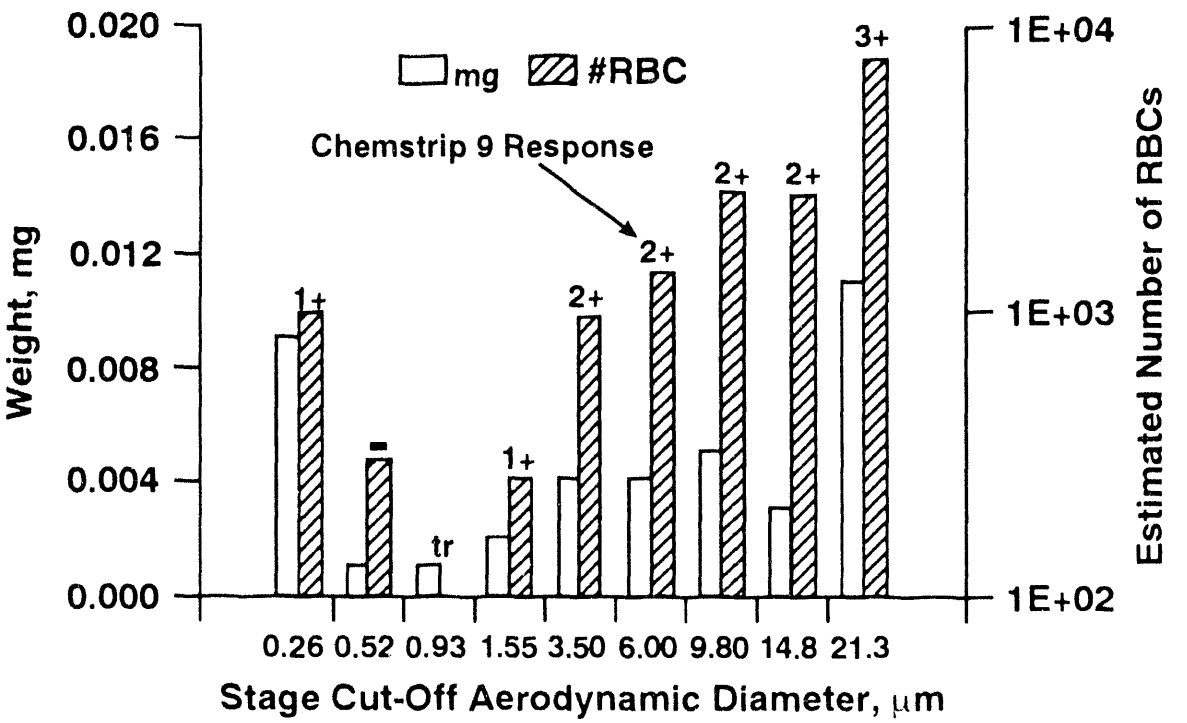

Figure 1. Histogram of the mass and estimated number of RBCs observed in each size interval of a MPC impactor. (^{51}Cr-labeled dog: Run #1) (The amount of hemoglobin detected on each stage by Chemstrip 9: negative = 0 erythrocytes/μL, trace ≈ 5 ery/μL, 1+ ≈ 10 ery/μL, 2+ ≈ 50 ery/μL, 3+ ≈ 250 ery/μL. Sample size = 20 μL.)

Table 1 summarizes data obtained from all five dogs. The aerosol mass concentration and estimated RBC (or activity) concentration were obtained from the MPC impactor, two LMJ cascade impactors, and the filter samples. A relatively large standard deviation indicates large variability between the surgeries. The total average sample weight collected by the MPC impactors was 0.038 ± 0.021 mg (mean ± S.D.; n = 5); the total estimated number of RBCs was $2.9 \times 10^4 \pm 1.5 \times 10^4$; and the sampled volume was 0.134 ± 0.020 m^3. Table 1 shows that data obtained through the probe (LMJ8106 and filters) were lower than those obtained by either the personal impactor or LMJ8380. This may suggest some losses in the sampling line for the LMJ8106 (and filters that sampled through the aerosol chamber via a sampling probe). It may also suggest spatial nonuniformity of the aerosol concentration around the surgical area and within the surgical room.

Table 1

Aerosol Mass and RBC Concentrations (from Radiation) Measured by Different Instruments
(Mean ± S.D.; Number of Samples or Experiments)

Instrument	Mass Concentration (mg/m^3)	RBC Concentration ($\#/m^3$)	RBC Concentration ($\mu g/m^3$)
Personal Impactor	0.368 ± 0.203 (5)	$2.18 \times 10^5 \pm 1.40 \times 10^5$ (5)	6.54 ± 4.20 (5)
LMJ8380	0.382 ± 0.059 (5)	$1.72 \times 10^5 \pm 0.97 \times 10^5$ (4)	5.16 ± 2.91 (4)
LMJ8106	0.122 ± 0.055 (5)	$7.53 \times 10^4 \pm 2.07 \times 10^4$ (5)	2.26 ± 0.62 (5)
Filters	0.134 ± 0.045 (5)	$6.34 \times 10^4 \pm 2.63 \times 10^4$ (5)	1.90 ± 0.79 (5)

The good correlation between the Chemstrip 9 response and the estimated number of RBCs (or radioactivity of ^{51}Cr) indicated that the Chemstrip 9 response was obtained primarily from blood-associated (hemoglobin) aerosols rather than from myoglobin, because only hemoglobin was labeled with ^{51}Cr. Examination of hemoglobin responses observed on Chemstrip 9 revealed that the MPC impactor data were similar to those derived from previous orthopedic surgeries at a local hospital (1991-92 Annual Report, p. 48). Thus, this study confirmed that blood-associated, respirable aerosols were produced during orthopedic surgical procedures.

(Research sponsored by the National Institute for Occupational Safety and Health under Interagency Agreement No. 92-05 with the U.S. Department of Energy under Contract No. De-AC04-76EV01013.)

DESIGN AND EVALUATION OF AN ANNULAR SLIT-JET VIRTUAL IMPACTOR

B. T. Chen, M. D. Hoover, G. J. Newton, and H. C. Yeh

Continuous air monitors (CAMs) have been developed to detect airborne plutonium or other actinide alpha emitters. Recently, DOE Order 5480.11 has specified that alpha CAMs for plutonium must meet an 8 derived air concentration-hour (DAC-h) sensitivity requirement. It is unclear whether alpha CAMs that have been installed with the existing technology in nuclear weapon fabrication facilities can meet these stringent air monitoring requirements. Furthermore, in many future DOE operations involving decontamination, decommissioning, and environmental restoration activities, this requirement will be impossible to meet with existing technology. Eight DAC-h represents about 35.5 dpm/m^3 that must be detected in a background of naturally occurring, alpha-emitting radon progeny ranging from 400 to 40,000 dpm/m^3.

A virtual impactor that would reduce interferences from radon progeny could be a solution to the problem. A virtual impactor (Marple, V. A. and C. M. Chien. *Environ. Sci. Technol. 14*: 976, 1980; Chen, B. T. and H. C. Yeh. *J. Aerosol Sci. 18*: 203, 1987) is similar to a conventional impactor that collects particles by inertial impaction onto a solid substrate placed under a high velocity jet of sampled air. A virtual impactor classifies particles larger than the desired cutoff aerodynamic diameter into a column of relatively stagnant air (minor flow) and diverts particles smaller than the desired diameter into the major flow. This study involved the design and evaluation an annular-jet virtual impactor (Fig. 1) that could be adapted as a sampling inlet to a standard alpha CAM. The impactor would allow high-volume sampling (300 L/min) of ambient air to reduce the response time of an alpha CAM. In addition, it would have a cutoff diameter of 0.5 μm to aerodynamically separate particles containing alpha-emitting radon progeny (mainly attached to submicrometer-sized particles) from micrometer-sized actinide particles (e.g., plutonium) and to reduce background interferences from naturally occurring radon progeny to an alpha CAM and, consequently, increase the sensitivity of the CAM.

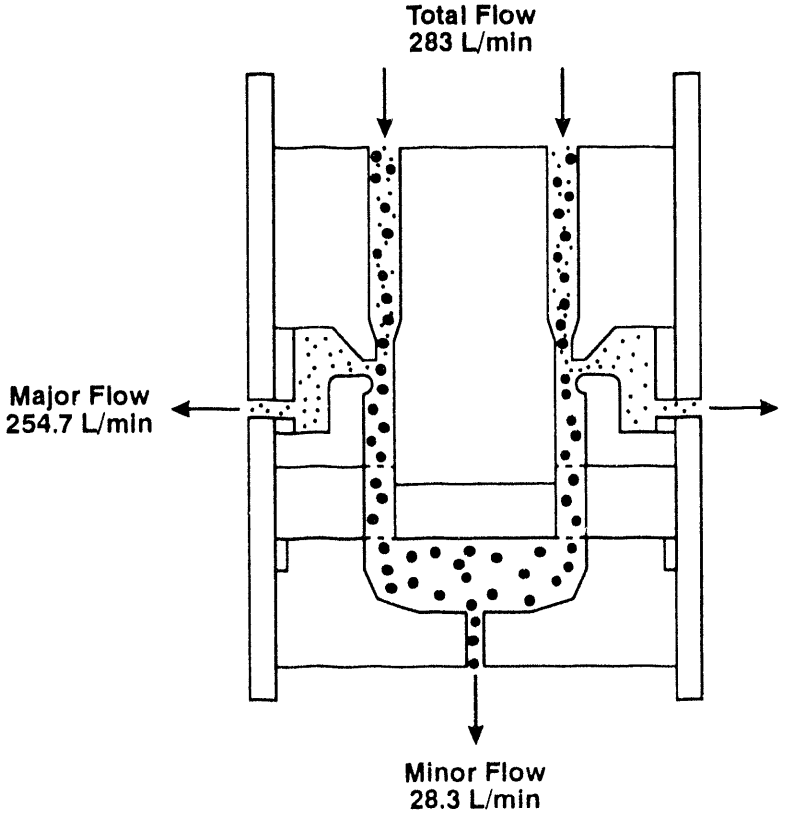

Figure 1. Schematic diagram of the prototype annular-jet virtual impactor. Larger particles are concentrated in the minor flow. Smaller particles, including radon progeny, are removed in the major flow.

Monodisperse, fluorescence-tagged oleic acid (OA) liquid particles with a count median geometric diameter between 0.5 and 10 μm were generated using a vibrating-orifice generator (Model 3053, TSI, Inc., St. Paul, MN). Clean, dry air was used to suspend the droplets and completely evaporate the solvent in the droplets. The dried aerosols were exposed to a ^{85}Kr bipolar ion source to bring the particles to a state of charge equilibrium. An aerodynamic particle sizer was used periodically to monitor the size distribution of the OA aerosols before they entered the virtual impactor. The monodispersity of the aerosols was controlled by adjusting the feeding pressure, vibrating frequency, and flow rate in the aerosol generator. Aerosols were introduced into the prototype, high-volume, annular-jet virtual impactor (Fig. 1), and the particles were separated into two fractions based on the separation efficiency of the impactor. Glass fiber filters (Gelman A/E) in the minor flow and major flow of the aerosol were used to collect the coarse and fine particle fractions of the aerosol, respectively. After each run (30-50 min), the filter samples were washed separately and subjected to ultrasonic agitation in a solution (50 mL) containing 50% isopropyl alcohol and 50% pH 10 Tris buffer. The impactor was disassembled, and the parts were separately rinsed with 50 mL of the same solution. Two aliquots of each washing from the filters and the parts were quantitated for fluorescence content with a Hitachi spectrofluorometer (Model F-1200).

Table 1 shows the percentage of fluorescence content found on the impactor walls and the exhaust filters of the major and minor flows. The impactor walls represent the section between the flow separation point and the exhaust filters. Separation efficiency was determined by taking the ratio of fluorescence content in the minor flow to the total fluorescence content on the impactor walls and the exhaust filters. Results indicated that the particle separation efficiency increased with particle size, and the 50% cutoff size was approximately 1.2 μm. Wall losses appeared to be high in both major and minor flow sections. Although wall losses in the major flow section will mainly contain radon progeny and will not affect the performance of the CAM, wall losses in the minor flow section are significant (8-38%) and could reduce the concentration of alpha-emitting actinide aerosols to be detected by the alpha detector. In future studies, the modification of this prototype impactor to minimize wall losses in the minor flow section will be emphasized. Several operating and design parameters such as the jet flow Reynolds number, the ratio of jet size to collector size, the separation between jet and collector, and the flow rate will be investigated to optimize the particle separation efficiency and to minimize the wall losses.

Table 1

Percentage of Fluorescence Content in the Prototype Annual-Jet Virtual Impactor[a]

	Major Flow		Minor Flow		
Particle Size (μm)	Impactor Walls (%)	Exhaust Filter (%)	Impactor Walls (%)	Exhaust Filter (%)	Separation Efficiency (%)
0.5	46	25	8	21	29
1.0	33	27	13	27	40
1.9	7	11	32	50	82
3.0	1	6	38	55	93
4.1	0.8	2.2	23	74	97

[a]The values of separation efficiency were determined by dividing the fluorescence content in the minor flow by the total fluorescence content.

(Research sponsored by the Assistant Secretary for Defense Programs, U.S. Department of Energy, under Contract No. DE-AC04-76EV01013.)

PARTICLE COLLECTION EFFICIENCY OF A HIGH-VOLUME ANNULAR KINETIC IMPACTOR FOR CONTINUOUS MONITORING OF ALPHA-EMITTING RADIONUCLIDES

B. T. Chen, S. J. Montaño, M. D. Hoover, G. J. Newton, and D. S. Gregory***

Continuous air monitors (CAMs) are used to detect airborne radioactive plutonium or other actinide aerosols in nuclear facilities. Generally, a CAM requires a filter or an impactor stage to collect actinide particles for alpha detection, and uses either spectroscopic techniques or an inertial mechanism to minimize background detection of naturally occurring, alpha-emitting radon progeny. The purpose of this study was to evaluate the particle collection efficiency and internal losses of a high-volume, impactor-type CAM used at the Savannah River Site (SRS). This study is part of a comprehensive evaluation of the technical basis for use of this CAM in order to determine its ability to meet the requirements of the U.S. Department of Energy RADCON Manual (DOE/EH-0256T) and DOE Order 5480.11.

The impactor-type CAM is an innovative, high-volume, real-time alpha air monitoring system which was developed at SRS (Collins, D. C. *U.S. AEC Report DP-188*, Savannah River Plant, 1956; Tait, G. W. C. *Nucleonics 14*: 53, 1956) and has been used reliably for many years.

Available results indicate that it has a nominal flow rate of 40 cubic feet per minute (cfm) and a collection efficiency of approximately 90% for particles greater than 0.5 μm in geometric diameter (Alexander, J. M. *Health Phys. 12*: 553, 1966). Tait (1956) reported that, when the device is operated at 25 cfm, it has a 50% collection efficiency of 0.5 μm (in diameter) dust particles with a 2.3 g/cm^3 density. In addition, results from environmental samplings indicate that the collection efficiency is 95% for plutonium and 5% for radon progeny (Hoy, J. E. *DPSPU 56-11-30*, Savannah River Plant, 1956). However, results from these studies do not provide adequate data to determine the ability of the SRS CAM to meet the current DOE regulations and, therefore, a thorough evaluation of the impactor-type CAM is being performed.

To evaluate this instrument (Fig. 1), monodisperse, fluorescence-tagged, polystyrene latex (PSL) aerosol particles with a count median aerodynamic diameter of between 0.5 and 10 μm were produced and introduced through the CAM with a 90-mm diameter backup filter (Fluoropore, Millipore Corp., Bedford, MA) The sampling flow rate of the instrument was 30 cfm without the filter and 20 cfm with the filter using a Meriam flow element (Model 50MC2-2). This test flow rate of 20 cfm was selected in part to evaluate the ability of the CAM to function at a lower-than-normal flow rate which might occur during an actual operation in the workplace. After each experiment, the CAM (Fig. 1) was dismantled, and various internal parts, including the aluminum delivery tube, bottom surface, impactor cone, impaction plate (planchet), brass tube, and fluoropore backup filter were rinsed with ethyl acetate to dissolve the PSL particles. Samples were then analyzed using a fluorescence spectrophotometer.

Table 1 shows the percentage of fluorescent PSL deposits at four different sections. The inlet section includes the internal surfaces of the delivery tube, the bottom surface, and the impactor cone upstream of the planchet, where particles are normally collected for alpha radioactivity counting; the outlet section represents the internal surfaces between the planchet and the backup filter; and the backup filter collects any particles exiting the impactor.

Results indicated that the particle collection efficiency (%) on the planchet increases with particle size with a 50% cutoff diameter of 3.1 μm (Fig. 2). Similarly, the percentage of fluorescent PSL particles on the inlet section increases with particle size, indicating that larger particles had more difficulty in negotiating the deflection of flow stream lines and, as a result, were more susceptible to impaction and collection on the bottom surface of the CAM. However, internal losses in the CAM were < 5% for particles smaller than 6 μm in diameter.

---

*Department of Energy/Associated Western Universities Summer Student Research Participant
**Health Protection Department, Westinghouse Savannah River Company, Aiken, South Carolina

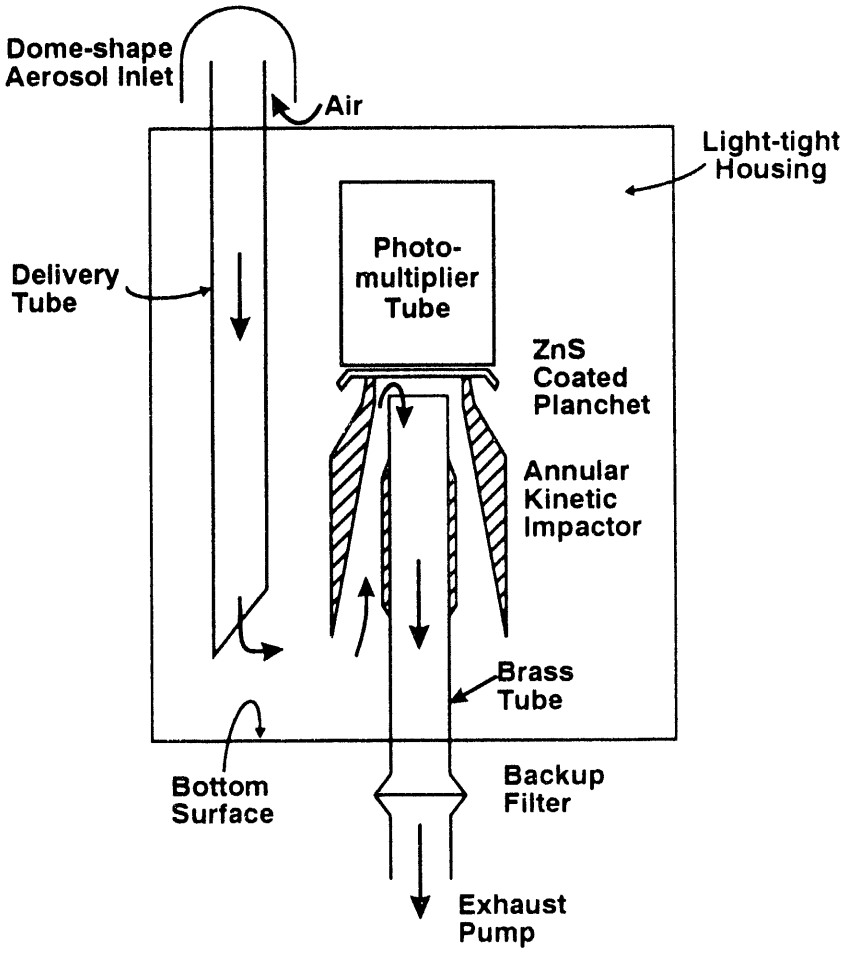

Figure 1. Schematic of the SRS CAM test apparatus.

Table 1

Percentage of Fluorescent Content on the Inlet Section, Planchet, Outlet Section, and Backup Filter of the Impactor-Type, SRS CAM

	Aerodynamic Diameter of PSL Particles (μm)					
	0.5	1	2	3	6[a]	10[a]
Inlet Section	0	1	2	1	5	8
Planchet	1	10	34	48	88	88
Outlet Section	0	1	4	1	0	1
Filter	99	88	60	50	7	3

[a]These aerosols were generated from dry powders; others were generated from liquid suspensions.

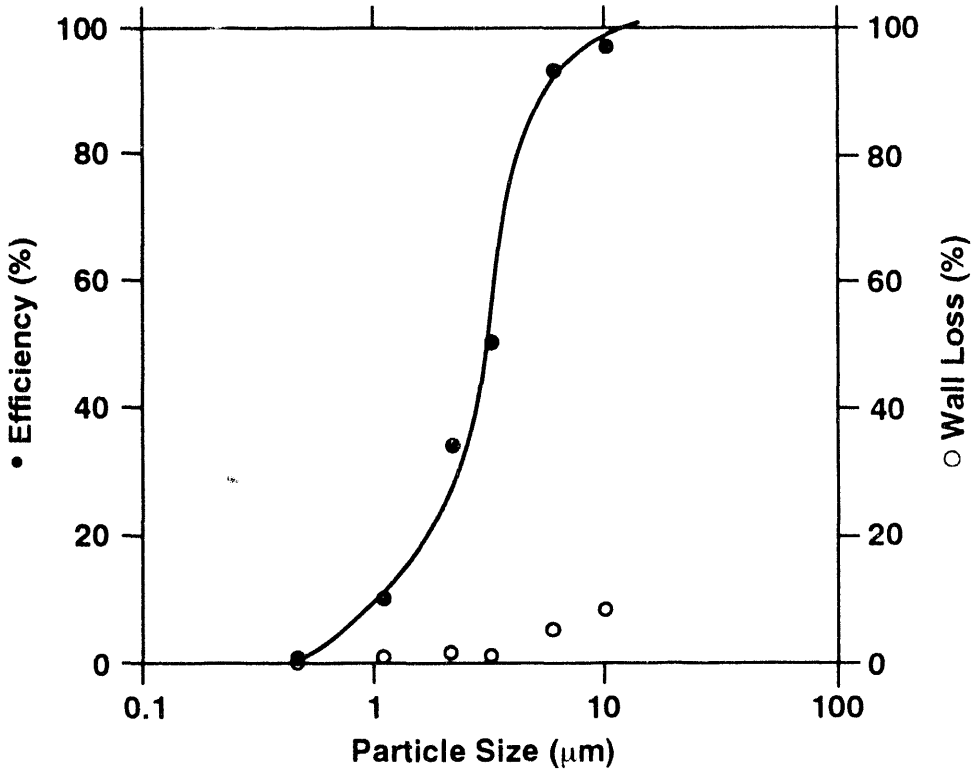

Figure 2. Particle separation efficiency curve and wall losses of the SRS impactor.

Because the data presented are based on a sampling flow rate of 20 cfm rather than 30 cfm when no backup filter was used (during field operation), the 50% cutoff diameter of the impactor during field operation must be calculated using the conversion of dimensionless Stokes number. With this approach, the 50% cutoff diameter is approximately 2.5 μm if the CAM is operated at 30 cfm, a value slightly greater than those reported by others. The cutoff diameter is calculated to be 2.1 μm if the CAM is operated at 40 cfm.

Overall, results obtained from this study indicate that the SRS CAM performs well with small wall losses using the solid, spherical particles. Future studies will include radon and actinide aerosols to provide additional information on the technical basis for use of the SRS impactor CAM.

(Independent Testing and Evaluation of SRS-Provided Impactor-Type Continuous Air Monitor and Lapel Air Samplers for the Westinghouse Savannah River Company under Purchase Order No. AA-71928 with the U.S. Department of Energy under Contract No. DE-AC04-76EV01013.)

EFFECTS OF SIMULTANEOUS COLLECTION OF SALT, RADON PROGENY, AND PLUTONIUM ON ALPHA CAM PERFORMANCE

M. D. Hoover and G. J. Newton

Tests have been conducted at the ITRI to evaluate the ability of the Eberline Alpha-6 continuous air monitor (CAM) to correctly measure plutonium aerosol concentrations in the presence of airborne salt and radon progeny concentrations that might be encountered at the U.S. Department of Energy Waste Isolation Pilot Plant (WIPP). This is a continuation of work reported in previous annual reports (1987-88, p. 29; 1988-89, p. 3; 1990-91, p. 4, 20; and 1991-92, p. 11) in which plutonium alone, radon progeny alone, plutonium and radon progeny, and plutonium and salt were tested.

Tests with plutonium alone showed that the CAM correctly reports collected plutonium with a predictable efficiency which depends on the detector and filter geometry, and an uncertainty which is consistent with Poisson statistics for radioactivity counting. Tests with radon progeny alone and with plutonium and radon progeny have shown that the background subtraction algorithm correctly subtracts alpha radioactivity of radon progeny from the plutonium-alpha-energy region of interest. The uncertainty in the correction is also based on Poisson statistics for radioactivity counting, and increases with the concentration of radon progeny (1991-92 Annual Report, p. 1). Tests with plutonium and salt have shown that accumulation of salt on the collection filter of the CAM reduces the energy of alpha radiation reaching the detector and may result in underestimation of the amount of plutonium on the filter. This interference is not a concern for detection of sudden, large releases of plutonium because an alarm will occur before burial becomes significant. Concern is for the slow release of plutonium over a long period of time in a dusty environment. In our 1991-92 Annual Report (p. 11) we demonstrated that expansion of the plutonium region of interest to channels 50 to 126 results in the proper report of plutonium concentration at dust concentrations up to 0.6 mg/m^3. This is a substantial improvement over the 60% error associated with the previous plutonium region of interest covering channels 92 to 126.

In the current tests, the CAM was challenged with plutonium, radon progeny, and salt to confirm proper performance under conditions relevant to WIPP. Aerosols were formed by nebulization of suspensions of plutonium and montmorillonite clay, with varying amounts of salt, to provide plutonium concentrations on the order of 1 disintegration per minute (dpm) to the CAM. The accumulation of 60 dpm on the CAM filter is equivalent to 8 DAC-h (derived air concentration hour); based on use of a 25-mm detector, with a 25-mm diameter collection filter, operating at 28.8 L/min sampling rate. Radon progeny aerosols were sampled from ambient air or from a specially designed radon progeny generation system (1991-92 Annual Report, p. 14). Approximately 50 tests were done. Tests involved three time sequences for sampling of radon progeny, plutonium, and salt: (1) collection of all three aerosols onto a fresh filter; (2) collection of radon progeny alone for 2 h, followed by collection of plutonium and salt; and (3) collection of radon progeny alone for 3 or more days (to simulate weekend conditions at WIPP), followed by collection of plutonium and salt.

Table 1 shows a typical set of test conditions used in the evaluation program. Figure 1A shows the minute-by-minute reports of the plutonium counts per minute (cpm) before and after collection of salt and plutonium. The radon progeny concentration in this test was approximately more than twice the concentration normally encountered at WIPP. Note that collection of about 14 DAC-h of plutonium was easily detected by the CAM. Figure 1B shows the alpha energy spectrum at the conclusion of the test. Although the plutonium counts are a negligible addition to the total spectrum, the CAM provided a proper report of Pu cpm. Note that the recommended expansion of the plutonium region of interest to channels 50 to 126 results in the proper report of plutonium concentration, despite interference from salt aerosol. Results show that the ambient concentrations of salt and radon progeny found at WIPP do not alter the basic ability of the CAM to provide a proper alarm at the 8-DAC-h level.

Table 1

Example of Experimental Conditions and Results for a Test of Simultaneous Collection of Plutonium, Salt, and Radon Progeny in the Eberline Alpha 6A

Parameter	Value
ITRI Test Number	29
CAM Identification	Eberline Alpha 6A, SNR 254
Detector Diameter	2.5 cm
Collection Filter Diameter	2.5 cm
Collection Filter Area	5.07 cm^2
Collection Filter Type	Versapor 3000
Average ^{218}Po Concentration	0.2 pCi/L
Estimated Radon Concentration	0.4 pCi/L
Duration of Radon Progeny Sampling before Start of Plutonium and Salt Generation	90 h
Duration of Plutonium and Salt Generation	60 min
Time to 8-DAC-h Alarm	38 min
Effective Salt Concentration	0.2 mg/m^3
Total Mass of Salt Collected	2.78 mg
Mass of Salt Collected per cm^2	0.5 mg/cm^2
Final Alpha 6A Pu DAC-h (for Pu ROI 92-126)	10 DAC-h
Final Alpha 6A Pu DAC-h (for Pu ROI 50-126)	15 DAC-h
Final Pu DAC-h from ZnS(Ag) Method	14 DAC-h

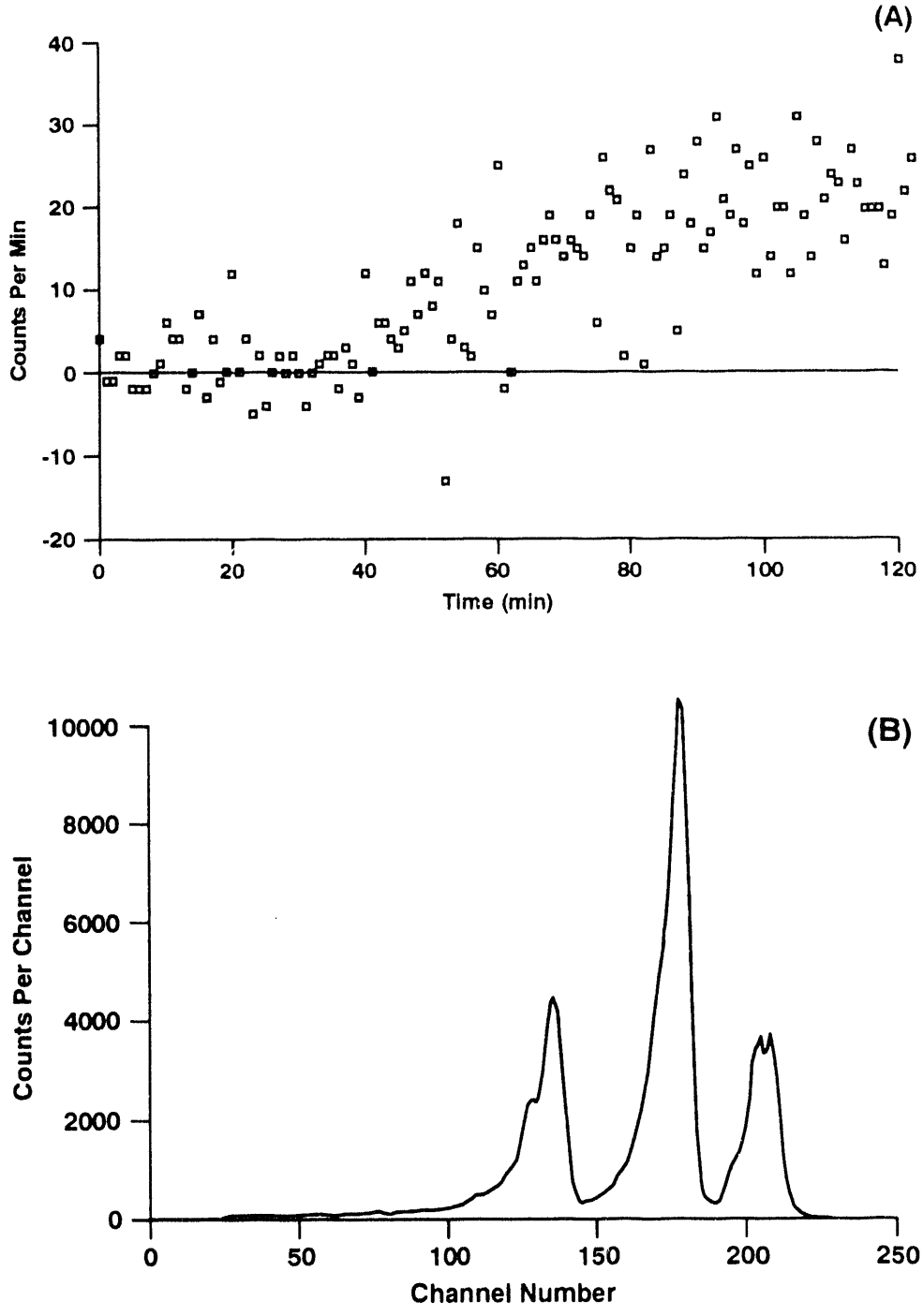

Figure 1. Results for simultaneous collection of plutonium, salt, and radon progeny in the Eberline Alpha 6A showing (A) minute by minute reports of plutonium cpm observed and (B) the alpha energy spectrum at the conclusion of the test. Radon progeny were sampled for 90 h prior to start of plutonium and salt generation. The slow, continuous release of plutonium and salt began at the 30-min time point in panel (A) and continued for 60 min. The plutonium accumulation is barely visible near channel 110 on the spectrum, but the CAM easily detected the collected plutonium. See Table 1 for additional details of the test conditions.

(Research sponsored by the Albuquerque Operations Office, U.S. Department of Energy, under Contract No. DE-AC04-76EV01013.)

CHARACTERIZATION OF ENRICHED URANIUM DIOXIDE PARTICLES FROM A URANIUM-HANDLING FACILITY: PRELIMINARY EVALUATION OF *IN VITRO* SOLUBILITY

M. D. Hoover, R. A. Guilmette, G. J. Newton, R. J. Howard, and S. M. Trotter**

Information about the amount and characteristics of radioactive particles that might be released in the workplace is needed to set appropriate aerosol control levels and to assess the effective dose to workers from inhalation exposures. A cooperative ITRI/Y-12 Plant study is underway to characterize the concentration, aerodynamic size, and biological solubility of uranium aerosols to which Y-12 workers might be exposed.

The ICRP-30 method (*Limits for Intakes of Radionuclides by Workers*, Report of Committee 2 of the International Commission on Radiological Protection, Pergamon Press, Oxford, 1979) for determining an annual limit on intake (ALI) and the derived air concentration (DAC) for radioactive aerosols involves three variables: the type of radionuclide, its particle size distribution, and its solubility. In our 1991-1992 Annual Report (p. 37), we reported on the characterization of the particle size distribution and composition of uranium oxide from cleanup of the uranium melting and casting process at the Y-12 Plant. Uranium-234 is the major radionuclide of concern for inhalation exposures to enriched uranium. It comprises less than 1% of the mass of the uranium, but contributes 96% of the radioactivity. The default assumption in ICRP-30 is a particle size of 1 μm aerodynamic diameter. We found the particle size distribution of the uranium oxide powder to be substantially larger than 1 μm aerodynamic diameter. This results in an increased ALI, with the magnitude of the increase depending on the solubility class of the material. The solubility classes assumed by ICRP-30 are class D (dissolution half time of 0.5 days), W (half time of 50 days), and Y (half time of 500 days). For the less soluble forms of ^{234}U (dissolution half times on the order of weeks or years), the pulmonary region of the lung is the target organ because particles deposited in the naso-pharyngeal and tracheobronchial region are quickly cleared to the gastrointestinal tract by mucociliary action or swallowing. Pulmonary deposition for the particle size distribution of the collected material was only 41% of the pulmonary deposition for 1-μm diameter particles, resulting in an ALI and DAC which are 2.4 times higher than the default values for both the class W and class Y forms of uranium. For the more soluble forms of ^{234}U (dissolution half time on the order of days), material deposited in all three regions of the respiratory tract can dissolve and be translocated to the bone surface, kidneys, and red bone marrow. Some radiation dose to the pulmonary region of the lung can also occur. For the soluble material, radiation doses for the larger particle size distribution are only 81% of the doses from 1-μm particles, and the ALI and DAC are therefore 1.24 times higher than the default values.

Barber, J. M. and R. Forest have proposed a class Q clearance model for uranium oxides at the Y-12 Plant (*Class Q: A Modification of the ICRP Lung Model for Uranium Oxides*, Y/DQ-39, Oak Ridge Y-12 Plant, Oak Ridge, TN, March 1992). Their model, based on exposures of workers at the Y-12 Plant, estimates that 90% of the material dissolves with a modified class W half time of 120 days, and that 10% of the material dissolves with a class Y half time of 500 days.

The current phase of our evaluation involves determination of the solubility class of the uranium oxide powders for comparison with the model of Barber and Forest and determination of an appropriate site-specific ALI and DAC for the Y-12 Plant. Samples of the size-separated materials were shipped from the Y-12 Plant to ITRI, and preliminary *in vitro* dissolution tests were conducted on uranium oxide particles from the 2.9 μm to 4.3 μm aerodynamic diameter size fraction. We used two solvents alone: serum ultrafiltrate or SUF (Kanapilly, G. M. *et al. Health Phys. 24*: 497, 1973), and HCl at pH 5.0, the pH that has been measured in phagolysosomes of alveolar macrophages. In a third system, we used SUF for 1 day, followed by HCl for the remainder of the study, to simulate the realistic biological situation in which particles are deposited on the lung epithelium, then engulfed by macrophages within about 1 day (1989-90 Annual Report, p. 68).

*Martin Marietta Energy Systems Y-12 Plant, Oak Ridge, Tennessee

Figure 1 shows the amount dissolved as a function of time for the three test conditions. The particles were more soluble in the SUF solvent than in the HCl. In tests using SUF followed by HCl, the initial dissolution matched that of SUF alone, and the later dissolution was similar to the rate observed for HCl alone. Solubility in both solvents appeared to be biphasic, with approximately 2% and 6% of the material dissolving with a half time of approximately 0.5 days in the HCl and SUF, respectively. The balance of the material appeared to dissolve with a half time greater than 500 days in HCl and with a half time of about 120 days in SUF.

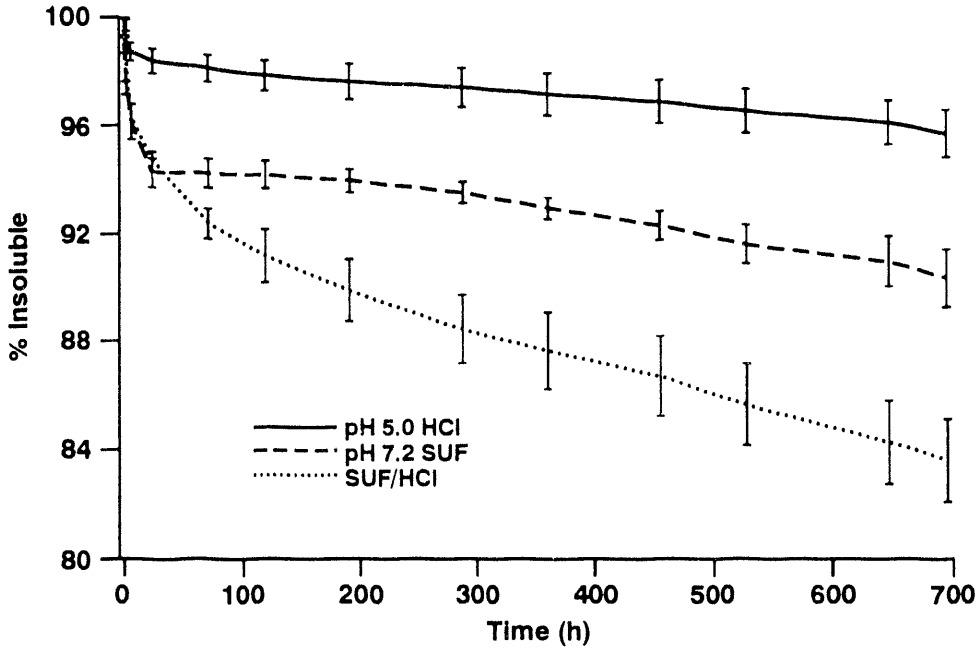

Figure 1. Amount of uranium oxide dissolved as a function of time for these three test conditions: serum ultrafiltrate (SUF) alone, HCl at a pH typical of lysosomes in macrophages, and SUF for 1 day, followed by HCl, to simulate the realistic situation in which particles are deposited on the lung epithelium, then engulfed by macrophages. Error bars are standard deviation.

The greater dissolution of uranium in pH 7 SUF, as compared to pH 5 HCl, was not expected because U_3O_8 is increasingly soluble in solutions of increasing acidity (decreasing pH). The studies of Ansoborlo, E. P. *et al.* (*Radiat. Prot. Dosim. 26*: 101, 1989) have shown that the *in vitro* dissolution rates for uranium oxides are significantly affected by the presence of redox and complexing agents such as phosphate, bicarbonate, peroxide, and pyrogallol. Such agents may be required both at pH 7 and pH 5, and may in fact control U oxide dissolution *in vivo*. Future studies will involve longer dissolution times to provide improved estimates of the half times, tests of additional size fractions, work with other solvents or combinations of solvents, and comparison of our results with the model of Barber and Forest. Completion of the work will provide a technical basis for selection of an appropriate ALI and DAC for uranium at the Y-12 Plant.

(Research sponsored by the Assistant Secretary for Defense Programs, U.S. Department of Energy under DOE Contract No. DE-AC04-76EV01013.)

USE OF LANTHANIDE OXIDES AS SURROGATES FOR PLUTONIUM IN SIMULATED WASTE RETRIEVAL

G. J. Newton, M. D. Hoover, A. W. Cronenberg, G. G. Loomis**, and S. H. Landsberger****

Between 1952 and 1970 large amounts of liquid and solid waste contaminated with transuranic radionuclides were emplaced at the Idaho National Engineering Laboratory (INEL) in shallow land-filled pits. In 1987, organic solvents (e.g., trichloroethylene and carbon tetrachloride) containing trace amounts of plutonium were claimed to be found in an aquifer, 112 ft below the buried waste at INEL. Because of these findings, the waste may be retrieved for processing and final disposal.

The INEL project demonstration plans call for retrieval of simulated buried waste from a cold test pit containing waste forms labeled with nonradioactive, stable lanthanide oxides that will serve as nonradioactive surrogates for $^{239}PuO_2$. In support of this effort, INEL contracted with ITRI to conduct a series of smaller-scale tests, in a well-controlled environment, using the lanthanide oxide surrogates in INEL soil, to determine the aerosol particle size distributions and the concentration of the various lanthanides within these distributions. This study determined aerosol characteristics of (1) dispersed soils and (2) dispersed soils containing trace amounts of lanthanide oxides. Results of these aerosol experiments have been compared to assess and rank the adequacy of lanthanide oxides as surrogates for $^{239}PuO_2$, and to guide interpretation of the full-scale INEL tests of buried waste retrieval operations.

At INEL, four different lanthanide oxides were placed in four different zones of the cold test pit. Concentrations of lanthanide labels were 50 g/ton for dysprosium oxide (Dy_2O_3), ytterbium oxide (Yb_2O_3), and terbium oxide (Tb_4O_7); and 455 g/ton for neodymium oxide (Nd_2O_3). The soil used for the ITRI tests was never contaminated and was supplied by the INEL in a 55 gal drum. Soil for the experiments was taken from the drum in separate containers of about 5 kg each. The soil was homogenized by placing it in a drum roller for about 1 h. Next, the soil was desiccated with gentle heat (50°C) for about 2 h. Lanthanide oxides including Dy_2O_3, Yb_2O_3, Tb_4O_7, and Nd_2O_3 were obtained from the same commercial source (Unocal, Division of Molycorp, Los Angeles, CA) as was used in preparation of the cold test pit. Lanthanides were mixed with the soil using a V-mixer. Samples of 300 g of INEL soil were labeled with 16.5 mg each of the Dy_2O_3, Yb_2O_3, and Tb_4O_7, and 150 mg of Nd_2O_3. The soil mass and mass of the label were weighed and placed in the V-mixer for 30 min. A Venturi dust blower and screw feeder system developed at ITRI was used to disperse the aerosol (1988-89 Annual Report, p. 365). The first set of aerosol runs was delivered directly to a five-stage cyclone sampler for aerodynamic size distribution determinations of gram-sized samples. The second set of runs delivered aerosol to a cylindrical sample chamber. Filter samples for mass concentration, cascade impactor samples for aerodynamic size distribution determinations, and a point-to-plane electrostatic precipitator for electronmicroscopic size analysis were taken, in parallel, from the chamber.

The entire output from the Venturi dust blower entered the five-stage cyclone sampler. Extrapolating the fitted line of the plot of effective cutoff diameter (ECD) versus probability provided an estimation of the MMAD of the soil. The aerodynamic size of the aerosolized INEL soil was, MMAD = 44.6 μm ± 11.3, σ_g = 6.3 ± 1.2. Lovelace multi-jet cascade impactors were used to collect airborne samples for aerodynamic size distribution measurements of the aerosolized soil. A pre-cutter prior to the cascade impactor consisted of the first stage of the five-stage cyclone train to remove larger particles (ECD > 6.0 μm). Disks of stainless steel shimstock (37 mm diameter) were coated with Apiezon L grease dissolved in toluene to reduce bounce. After the toluene evaporated from the 37 mm diameter shimstock disks, cascade impactor substrates and filters were stored in a desiccator and the tare weights determined with a Cahn microbalance before use. After aerosol collection, all sample substrates were again placed in a desiccator for 3 h before weighing. The aerosol sampling flow rate was 12 L/min to minimize particle bounce. Results for eight different cascade impactor runs sampling the raw INEL soil, after the 6.0 μm pre-cutter, were MMAD = 2.2 ± 0.3 μm, σ_g = 1.7 ± 0.2. For the lanthanide-labeled

*Private Consultant, Albuquerque, New Mexico

**Idaho National Engineering Laboratory, Idaho Falls, Idaho

***Department of Nuclear Engineering, University of Illinois, Champaign, Illinois

studies, cascade impactor samples from three separate runs were pooled and the amount of the lanthanide content determined by instrumental neutron activation analysis (INAA) at the Department of Nuclear Engineering at the University of Illinois.

Figure 1 illustrates the size distribution parameters obtained for the total mass of collected dust and for one lanthanide oxide, Yb_2O_3. Data for each of the four lanthanide oxides used in this evaluation are listed in Table 1. Based on the data in Table 1, all size distribution determinations appear to be similar.

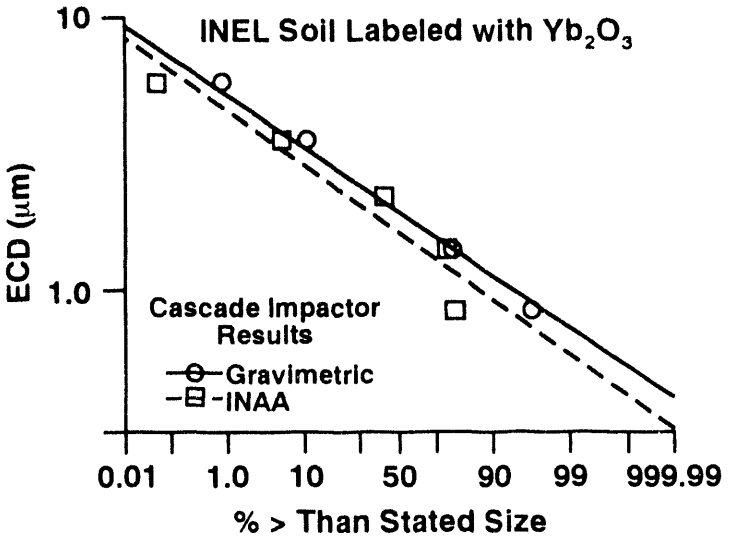

Figure 1. Mass median aerodynamic diameter (MMAD) of Y_2O_3-labeled INEL soil as determined using a Lovelace multi-jet cascade impactor. Data for the total mass are denoted by the circles (MMAD = 1.95 μm, σ_g = 1.53), whereas the squares indicate the MMAD as determined by INAA of cascade impactor samples (MMAD = 1.63 μm, σ_g = 1.56). Lines are fitted values using a nonlinear least squares fitting technique.

Table 1

Size Distribution Parameters for INEL Soil
Labeled with Various Lanthanide Oxides

Aerodynamic Size Distribution Parameters Determined from Cascade Impactor Samples Preceded by a 6.0 μm ECD Cyclone Pre-Cutter by Total Airborne Mass and INAA[a] Mass Median Aerodynamic Diameter (MMAD) (μm), Geometric Standard Deviation (GSD) (σ_g)				
	Gravimetric		INAA	
	MMAD (μm)	GSD (σ_g)	MMAD (μm)	GSD (σ_g)
Yb_2O_3	1.95	1.53	1.63	1.56
Tb_4O_7	1.93	1.53	2.20	1.45
Dy_2O_3	1.84	1.84	2.53	1.38
Nd_2O_3	2.01	1.61	1.86	1.54
Mean ± S.D.	1.93 ± 0.07	1.63 ± 0.15	2.06 ± 0.39	1.48 ± 0.08

[a]INAA is instrumental neutron activation analysis.

If the lanthanide-labeled soil in the cold test pit was as thoroughly mixed as were the samples for these tests, aerosol data derived from lanthanide quantification will be a useful surrogate for $^{239}PuO_2$. This will enable INEL to evaluate various dust suppression techniques and operational procedures without the added expense of working with $^{239}PuO_2$-contaminated soils during the demonstration phase of buried waste retrieval.

From a qualitative assessment, the Nd_2O_3 had the best match with the size distributions determined from the gravimetric analyses of cascade impactor samples, although all four lanthanide oxides can be used as surrogates for PuO_2 for the purposes of evaluating buried waste retrieval operations.

(Research sponsored by the Assistant Secretary for Environmental Restoration/Waste Management, U.S. Department of Energy, under Contract No. DE-AC04-76EV01013.)

A CASE STUDY ON A NESHAP EVALUATION FOR A RADIOACTIVE MATERIALS HANDLING AREA

*G. J. Newton, M. D. Hoover, and H.-S. Hwang**

The National Emission Standards for Hazardous Air Pollutants (NESHAP) 40 CFR Part 61, Subpart H refers to Department of Energy-owned facilities. The requirement is that no facility operated by DOE can release radionuclides that will expose a member of the general public to 10 mrem/yr which is defined as the national standard. Furthermore, a facility that could expose the reference individual to 1% of the standard, 0.1 mrem/yr or more, requires continuous monitoring of effluent stacks. Otherwise, only periodic confirmatory measurements are required to demonstrate compliance.

Several methods are available to estimate source terms for the purpose of dose assessment. If a facility handles or generates radionuclides, then it falls under the NESHAP standard and its attendant monitoring and reporting requirements. The 40 CFR 61, Appendix D methodology is given below:

(1) Determine the amount (in Curies) used at facilities for the period under consideration. Radioactive materials in sealed packages that remain unopened and have not leaked during the assessment period should not be included in the calculation.

(2) Multiply the amount used by the following factors, which depend on the physical state of the radionuclide. They are: (a) 1 for gases; (b) 10^{-3} for liquids or particulate solids; and (c) 10^{-6} for solids. If any nuclide is heated to a temperature of 100°C or more, boils at a temperature of 100°C or less, or is intentionally dispersed into the environment, it must be considered to be a gas.

(3) If a control device is installed between the place of use and the point of release, multiply emissions from (2) by an adjustment factor. These are presented in 40 CFR 61, Appendix D, Table 1. However, if the dose assessment is to determine the monitoring criteria of the source, no credits of any control efficiencies should be used in the calculation.

At Sandia National Laboratories, Albuquerque (SNL, NM) Technical Area V, the Hot Cell Facility (HCF), which includes the Hot Cell with Steel Containment Boxes (SCB), the Glove Box Laboratory (GBL), and ancillary equipment and instrumentation in the support area have been designed and developed to support SNL, NM experimental programs in which Special Nuclear Material (SNM) or other radioactive materials are used. The underground facility includes four radiation control zones with zone 1 handling the most radioactive materials. Zone 1 is within SCBs and is accessed with remote manipulators.

Release parameters for the HCF for NESHAP calculations are: stack height = 38.1 m, diameter at the top = 1.8 m, flow velocity = 8.7 m/sec, and exit temperature = 21°C. Volumetric flow rate = 22.14 m^3/sec.

Operations include the preparation of materials for test, experiment assembly, post-test disassembly, preparation of samples for post-test examination, and post-test microscopy and wet chemical analyses. In addition, the HCF and GBL are used for preparation and packaging of SNM for reprocessing of radioactive and contaminated waste for final disposition. Disassembly and sample preparation are conducted in zone 1 or within a shielded glovebox in zone 2, depending on the hazard level. Materials requiring polishing prior to microscopic examination are vacuum encapsulated in a selected resin. The choice of encapsulating materials is dictated by the characteristics of the sample. After the mount has cured, the sample (mount and sample) is ground and polished.

We have performed calculations using the NESHAP methods given above to determine an appropriate scenario for the SNL, NM HCF. Figure 1 shows the decision tree we developed for this effort. We based the reference scenario on the experiment handling the largest inventory of radionuclides conducted in the HCF.

*Sandia National Laboratories, Albuquerque, New Mexico

Historically, the HCF handled irradiated fuel with radioactivities of about 6000 Ci or less. During 1990, the HCF conducted experiments on a Mark 22 fuel element from the Savannah River Site's Tritium Production Facility. The SNL, NM used a typical value of 5.0 x 10^{-4} Ci in a 150-in long Al-U fuel element, with 1868 g of uranium per Al-U fuel element. The specific activity of the fuel was, therefore, 26.8 Ci/g.

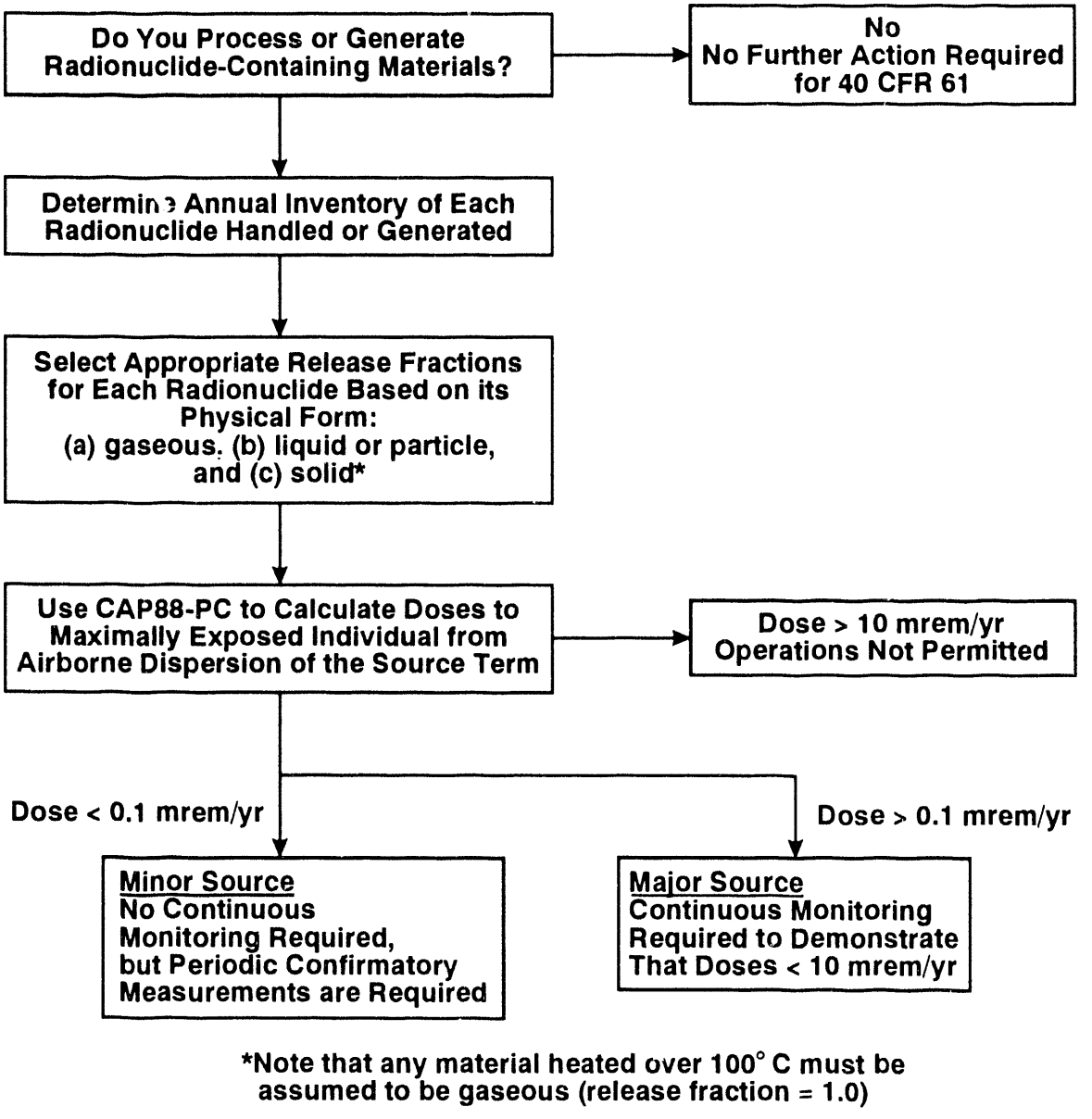

Figure 1. Decision tree to guide a facility in NESHAP compliance. For a calculated dose < 0.1 mrem/yr, no continuous monitoring required. For a calculated dose > 0.1 mrem/yr, continuous monitoring is required to verify that the dose is < 10 mrem/yr. For a calculated dose > 10 mrem/yr, operations not permitted.

The first scenario used an assumed release fraction (see methodology in step 3 above) from solids of 10^{-6}, or a calculated release of 5.0 x 10^{-2} Ci. A second scenario involves assumptions about the fines created during material science preparations. Dusts were collected and weighed during mounting, grinding, and polishing of samples for metallurgical studies. Records show that a total of 30 g of fines were actually created during the preparation (Don Bragg, 1993, personal communication). The total radioactivity of the fines was 30 g * 26.7 Ci/g = 803 Ci. The Clean Air Act Assessment Package of 1988 for a Personal Computer (CAP88-PC) specifies

an assumption that 10^{-3} of the available fines is released, along with all gaseous fission products in the disrupted fuel. Therefore, the total release estimate is (10^{-3})*(803 Ci) = 0.8 (total max. release) Ci plus a small number of Ci for ^{3}H and ^{85}Kr. The calculated release in Ci from the 30 g of fines, 0.86 Ci, is larger than the calculated release from the solids. This suggests that the creation of 30 g of fines from the historical preparation of sawing and polishing is the reference operation for NESHAP calculations rather than the total inventory of radionuclides in the fuel element. The assignment of the fuel element to the category of solids is valid because the fuel element is an alloy of aluminum and enriched uranium and as such does not have the structure of oxide fuels with grain boundaries and headspace between the oxide fuel and the cladding.

A total of 44 radionuclides that comprised the inventory of the Mark 22 fuel element was actually used for the material science studies. The Ci quantities for each radionuclide in the 30 g of fines are multiplied by a 10^{-3} release fraction except for the gaseous fission products, ^{3}H and ^{85}Kr, which are assumed to be released with a release fraction of 1.

The next step was to program the calculated maximum releases into the EPA-mandated program, CAP88-PC, to calculate the dose to the closest NESHAP receptor. The significant dose estimate from these exercises is the cumulative dose to the maximally exposed NESHAP individual. All of the radioactivities in this HCF scenario have a cumulative dose to this reference individual of 0.032 mrem/yr, less than 0.1 mrem/yr; therefore, the HCF qualifies as a minor source and does not require continuous monitoring.

In estimating doses to the NESHAP reference individual, we became aware of a series of errors that are incorporated into CAP88-PC. These errors result in an underestimate of the dose to the reference individual for certain two-member chains of beta-gamma-emitting radionuclides. The CAP88-PC can handle two complex, naturally occurring chains of radionuclides (^{238}U and ^{232}Th) and four simple chains (^{137}Cs-^{137}Ba, ^{140}Ba-^{140}La, ^{99}Mo-^{99}Tc, and ^{210}Pb-^{210}Bi). CAP88-PC does not calculate the dose correctly from at least five other biologically important, simple, two-member chains (^{90}Sr-^{90}Y, ^{95}Zr-^{95}Nb, ^{103}Ru-^{103}Rh, ^{106}Ru-^{106}Rh, and ^{144}Ce-^{144}Pr). The underestimate of dose caused by these errors in CAP88-PC is not significant when the code is used to broadly classify potential emission sources (for example, less than 20% in the SNL, NM HCF example given above). Care should be used in utilizing this program for other purposes.

(Research supported by Sandia National Laboratories for National Emissions Standard for Hazardous Air Pollutants under Purchase Order No. AB-5225 through U.S. Department of Energy Contract No. DE-AC04-76EV01013).

II. DEPOSITION, TRANSLOCATION, METABOLISM, AND CLEARANCE OF INHALED TOXICANTS

NASAL DEPOSITION OF ULTRAFINE AEROSOLS IN HUMANS

Y. S. Cheng, H. C. Yeh, S. Q. Simpson, and D. L. Swift***

Particles that deposit in the nasal airways are usually very large or very small (Cheng, Y. S. *et al. Radiat. Prot. Dosim. 38*: 41, 1991). Human volunteers have most often been used in studies of particles larger than 0.5 μm, whereas recent data on ultrafine particle deposition came from physical airway models (Cheng, Y. S. *et al. J. Aerosol Sci. 19*: 741, 1988; Yamada, Y. *et al. Inhal. Toxicol. Premier Issue 1*: 1, 1988). Studies in airway models provide large data sets with which to evaluate the deposition mechanism. However, data obtained in human subjects are needed to validate the results obtained with these models because of possible artifacts in the models. The only published study of *in vivo* deposition of ultrafine particles (George, A. and A J. Breslin. *Health Phys. 17*: 115, 1969) examined both total respiratory deposition of radon-progeny-bearing particles in mining and laboratory environments, and nasal deposition in laboratory experiments on three subjects. The nasal deposition for "unattached ^{218}Po " was found to range from 80% for a 3 L min^{-1} flow rate to 60% for flow rates in excess of 30 L min^{-1}. Unfortunately, the particle size of the radon progeny was not determined; therefore, it was not possible to relate the deposition to the particle size and flow rate without making certain assumptions for the particle size. Thus, human studies are needed for nasal deposition of ultrafine particles in the size range of 1 to 500 nm.

Four adult male, nonsmoking, healthy human volunteers (ages 40 to 57 yr) participated in this study. Each person underwent nasal deposition experiments at the constant flow rates of 4, 10, and 20 L/min. The exposure was conducted in the Human Exposure Laboratory at ITRI, and the exposure system has been described (1991-92 Annual Report, p. 28). The system included the aerosol generator, charge neutralizer, diluting air, nasal mask, mouth tube, and two condensation particle counters (CPC). Monodisperse aerosols of silver particles (5, 8, and 20 nm) and polystyrene latex particles (50 and 100 nm) were used.

For this study, a human subject sat comfortably in a chair in front of the exposure apparatus. He was fitted with a nasal mask (Silicon Contour Mask, Respironic, Inc., Murrysville, PA) and mouth tube (Small Rubber Mouth Tube, Warren E. Collins, Braintree, MA). He breathed filtered air normally through the nasal mask and mouth tube for several minutes to ensure that he was comfortable in wearing the mask and tube, and in holding his breath. He continued to breathe the filtered air normally for a few more minutes, then the aerosol flow was switched on by pushing a button. Two-way and three-way solenoid ball valves (Quality Control, Inc., Tilton, NH) were used to control the flow direction. The subject then held his breath for at least 30 sec but not over 1 min. During that time, an aerosol was drawn through the nasal airway and exhausted through the mouth tube. Aerosol concentrations in the supply and exhaust air were measured. The same maneuver was repeated eight times for each experimental condition.

Aerosol number concentrations (particles/cc) were determined by one TSI CPC (Model 3025, St. Paul, MN). The inlet and outlet concentrations were determined by sampling the aerosol through a three-way Delta solenoid valve (Fluorocarbon, Anaheim, CA). The signals from the CPC, the temperature probe, and the flow sensors were electronically connected to a data acquisition and control system (Analogue Connection, Strawberry Tree, Inc., Sunnyvale, CA) and an IBM 386-based PC. Labtech Note software (Wilmington, MA) was used to control and manage the system.

The deposition efficiency in the nasal airway was calculated as follows:

$$D_e = 1 - \frac{P_{measured}}{P_{system}}, \qquad (1)$$

*Department of Medicine, University of New Mexico, Albuquerque, New Mexico

**School of Hygiene and Public Health, Johns Hopkins University, Baltimore, Maryland

where $P_{measured}$ is the measured penetration estimated from the aerosol concentrations of inhaled and exhaled air ($P_{measured} = C_{ex}/C_{in}$); and P_{system} is the aerosol penetration in the sampling system including tubes, mask, and mouth tube. P_{system} was determined for each experimental condition with all components intact, but without the subject.

Figure 1, which shows the inspiratory deposition efficiency of the four subjects at 4 L min^{-1}, indicates considerable variability in the deposition among subjects. Figure 2 shows the mean inspiratory depositing efficiency at 4, 10, and 20 L min^{-1}. The curves in the figures are the predicted deposition at the corresponding flow rate based on the turbulent diffusion theory and data obtained from a deposition study using nasal airway casts (Cheng, Y. S. *et al. Aerosol Sci. Technol. 18*: 359, 1993). In general, the *in vivo* data agree with the turbulent diffusion theory. The differences in deposition between those obtained at 4 L min^{-1} and 20 L min^{-1} are more than those predicted by the theory. We are looking into the reasons for that, and are comparing the results obtained by using a MRI nasal cast. We are also examining the reasons for the inter-subject variations.

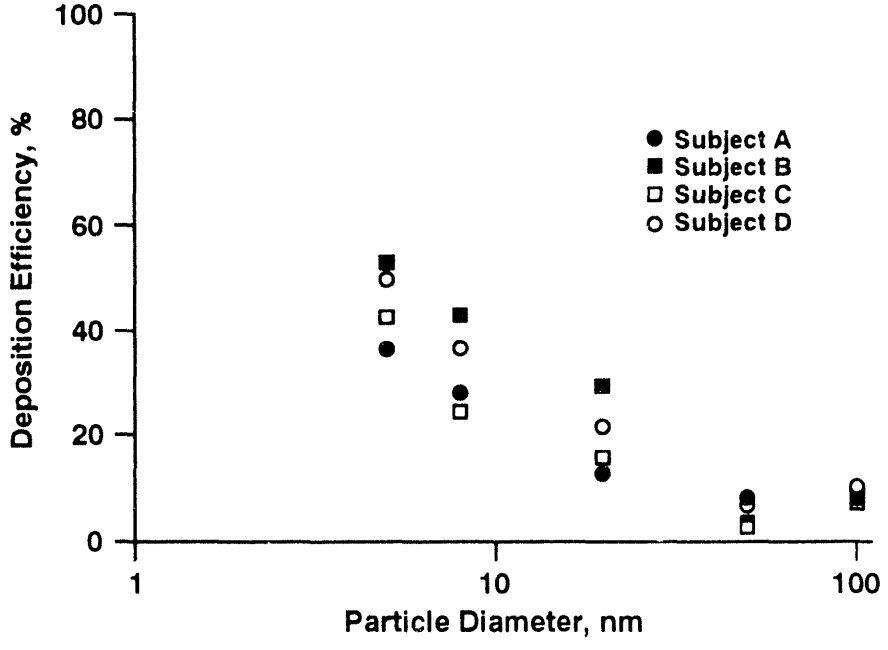

Figure 1. Inspiratory nasal deposition for four human volunteers at 4 L min^{-1}.

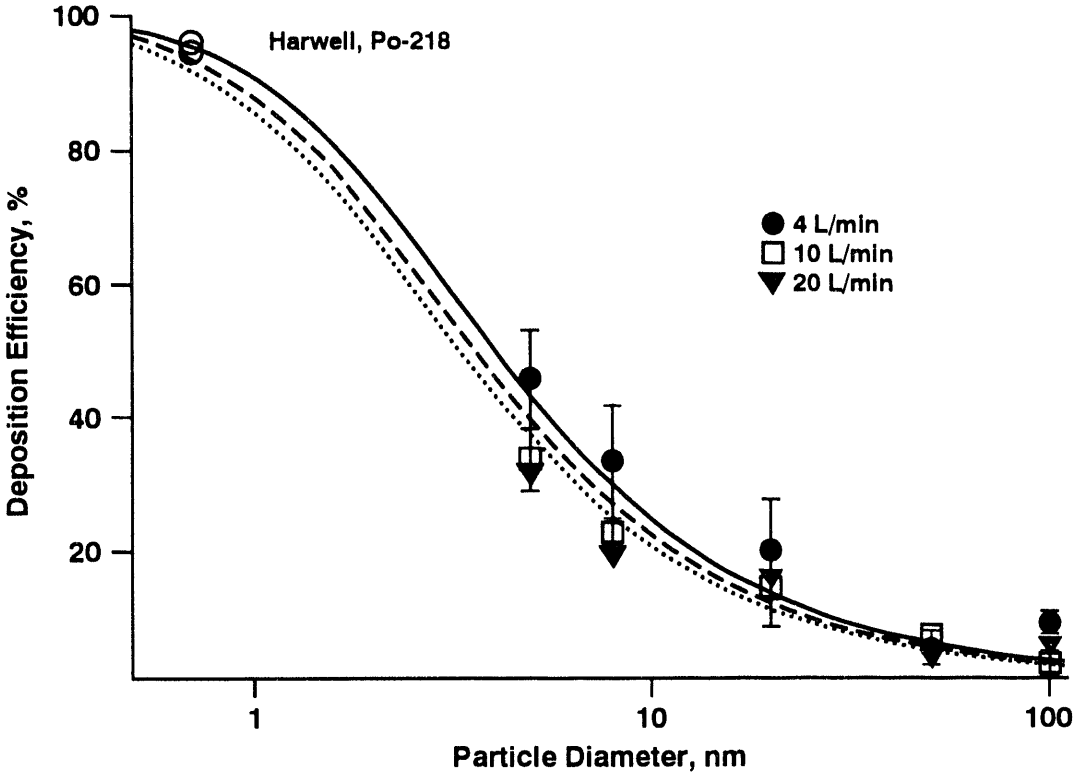

Figure 2. Mean nasal deposition for inspiratory flows in four human subjects are indicated by the symbols. The curves are predicted depositions (Cheng *et al.*, 1993). Error bars are standard deviations.

(Research sponsored by the Office of Health and Environmental Research, U.S. Department of Energy under Contract No. DE-AC04-76EV01013).

TRANSPORT OF INHALED METALS AND SOLVENTS THROUGH THE OLFACTORY EPITHELIUM INTO THE OLFACTORY BULBS

J. L. Lewis, J. R. Harkema, A. R. Dahl, and Y. S. Cheng

Transport of inhaled toxicants directly into the central nervous system (CNS) through the olfactory epithelium has been proposed to play a role in the development of neurodegenerative diseases. This transport is suggested primarily because of the anatomy of the olfactory epithelium where dendrites of olfactory receptor neurons contact the nasal lumen and axons of these same cells and project through the cribriform plate before synapsing within the olfactory bulb (Fig. 1). The need for systematic study of toxicant transport of inhaled materials from the olfactory epithelium to the brain is indicated by the following: (1) Theories implicating aluminum and other airborne, inhaled environmental toxicants as causal in Alzheimer's and related diseases have been debated, with no clear resolution, since 1973 (Roberts, E. *Neurobiol. Aging* 7: 561, 1986). (2) Several materials including metals and solvents (the toxic effects of which including learning and memory deficits) translocate to the olfactory bulb following nasal *instillation* and can show anterograde and retrograde transport within the brain (Lewis, J. L. and A. R. Dahl. In *The Vulnerable Brain and Environmental Risks, Vol. 3* [R. L. Isaacson and K. F. Jensen, eds.], Plenum, New York, 1993, in press). (3) The hippocampus, the brain region most often implicated in learning and memory, is only two synapses removed from the olfactory epithelium (Schwerdtfeger, W. K. *et al. Neurology 292*: 163, 1990). (4) To date, no experimental test of the central hypothesis of these theories of neurotoxicity has used inhalation as a route of exposure or attempted to assess what characteristics of either the epithelium or inhalants govern what materials enter the CNS (Lewis and Dahl, 1993).

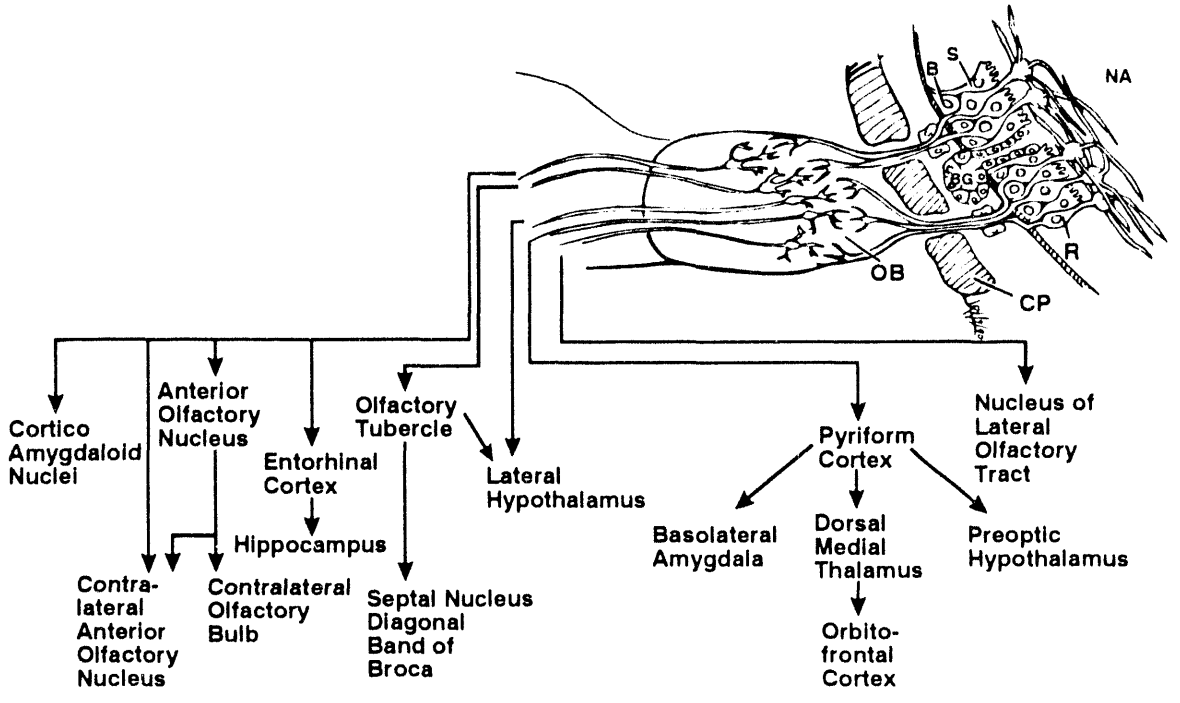

Figure 1. Anatomy of the olfactory mucosa, bulbs, and efferent projections. Diagram not to scale. All structures are bilaterally represented. (NA = nasal airway; S = sustentacular cells which support receptor neurons; R = bi-polar olfactory receptor neurons with cilia projecting into the nasal cavity and a single axon projecting through the lamina propria, forming nerve fascicles which penetrate the skull at the cribriform plate to synapse in the olfactory bulb; B = basal cells, progenitor cells for replacement of lost receptors; BG = Bowman's glands, primary secretory cells in this epithelium; CP = cribriform plate - perforated portion of skull through which olfactory nerves enter CNS; OB = olfactory bulb.)

In many of the studies mentioned above, either material in solution was instilled or material impregnated with the substance of interest was surgically packed in the nasal cavity. In addition, high concentrations of test substances were used. In humans, inhalation is the route of exposure most likely to result in olfactory transport, and environmental concentrations of materials are likely to be limited by industrial exposure standards well below the concentrations tested. Because airflow characteristics in the nasal cavity result in only 15% of inhaled air reaching the olfactory epithelium during normal breathing (Kimbell, J. S. *et al. Toxicol. Appl. Pharmacol. 121*: 253, 1993), actual concentrations of toxicants reaching this tissue are likely to be very low.

The CNS is protected from materials in the systemic circulation by a blood-brain barrier composed of tight junctions between endothelial cells lining the blood vessel, and high enzymatic capacity in those cells. The olfactory epithelium also has tight junctions between cells lining the nasal lumen and high xenobiotic-metabolizing capacity within these cells (Lewis and Dahl, 1993). Therefore, the blood-brain barrier may provide a useful model to begin examining what characteristics of the olfactory epithelium provide a barrier to inhaled toxicants (a nose-brain barrier) and under what conditions this barrier may be penetrated. It is likely that a nose-brain barrier will also include a role for the mucous secretions lining the tissue and the high immune/inflammatory capacity of the nasal epithelium (Lewis and Dahl, 1993). However, the model of the blood-brain barrier provides a conceptual framework to begin unraveling protective mechanisms in the olfactory system.

Using the F344/N Hsd rat as a model, a four-tiered approach is being followed in our laboratory to examine the nose-brain barrier and its role in the etiology of CNS disease:

(1) The role of toxicant solubility on transport to the CNS is being examined by using histopathological and quantitative tissue analytical techniques to compare the localization within the CNS of inhaled soluble and insoluble compounds of the metals aluminum and nickel, as well as the solvents xylene, amyl acetate, and ethanol that vary 60-fold in blood-air partition coefficients. All exposures will consist of inhalation of toxicants at the threshold limit values used for industrial exposures. Collaboration with Drs. Quintas Fernando and Dean Carter at the University of Arizona will allow cellular localization of the metals using micro-proton-induced X-ray-emission (micro-PIXE). Subcellular localization will be accomplished through collaboration with Dr. Terry Mitchell at Los Alamos National Laboratories using electron energy loss or X-ray energy dispersive spectroscopy. Solvents will be examined by quantitative autoradiography.

(2) The role of the physical structure of the olfactory mucosa on transport will be examined by causing lesions in the olfactory epithelium by pre-exposure to methyl bromide. This exposure will produce loss of sustentacular cells and mature receptor cells (Hurtt, M. E. *et al. Toxicol. Appl. Pharmacol. 94*: 311, 1988). The epithelium will regenerate, but whether the epithelium is more penetrable during the period of disruption can be examined using this technique. The question of transport in the presence of epithelial lesions is important because this is a common response of the epithelium to toxicant exposure.

(3) Inhibition of xenobiotic metabolism could allow substrates normally metabolized and cleared in the nasal mucosa to be transported to the olfactory bulb. In some cases, metabolism in the bulb could increase clearance of materials at that level, but if bulb clearance is compromised, transport to other CNS regions in the olfactory system may occur. The solvents used in this study vary not only in solubility, but in the nasal enzymes that metabolize them. Prior administration of enzyme inhibitors will allow assessment of the effect of xenobiotic metabolism on CNS distribution. This should allow assessment of the interactions between solubility and metabolism as well.

(4) Because both aluminum and nickel have been reported to accumulate in olfactory pathways following nasal instillation, but only aluminum is considered a neurotoxicant, the neurotoxicity of transported materials may be a function of distribution and rate of clearance as well as initial transport. Providing details of the differences in sites of accumulation and rate of clearance within the CNS for these two metals may increase our understanding of aluminum neurotoxicity.

To date, we have replicated and characterized the methyl-bromide-induced lesions of the olfactory epithelium in rats and have begun subsequent exposures to nickel sulfate. In conjunction with Dr. Fernando at the University of Arizona, methodology is being developed for quantitation of nickel in tissues using the micro-PIXE system. Radiolabeled solvents for localization of inhaled solvents following enzyme inhibition have been synthesized, and procedures for enzyme inhibition are being validated.

By incorporating environmentally relevant concentrations of toxicants and route of exposure (inhalation) into the experimental design, the above body of work should allow us to determine (1) if olfactory transport of toxicants is an important factor to be considered in determining human risk in industrial settings; (2) whether transport through the olfactory epithelium plays a role in the etiology of late-developing neurodegenerative diseases; and (3) the importance of olfactory mucosal lesions on this process. Demonstration of the occurrence of toxicant transport via the olfactory epithelium with *inhalation* of concentrations of materials which *mimic environmental exposures* is critical in resolving the debate on the etiology of memory-related disorders and in assessing the potential health risk of airborne toxicants.

(Research sponsored by PHS/NIH under Grant R01-DC01714 from the National Institute on Deafness and Other Communication Disorders in facilities provided by the U.S. Department of Energy under Contract No. DE-AC04-76EV01013.)

PROGRESS TOWARD AN EXPERIMENTALLY VALIDATED MODEL FOR CALCULATING TISSUE DOSAGE OF INHALED VAPORS

*A. R. Dahl and P. Gerde**

Tissue dosage of inhaled gas molecules is dependent on two linked phenomena: resistance to transfer of the molecules from the air to the airway surfaces, and events that occur in the liquid phase of the mucosa. Because of the rapid diffusion of gases, as well as the convective forces in inhaled air, air phase resistance in the narrow passages of the nasal cavity and smaller airways of the lung will be important only when there is a steep gradient in vapor concentration between the inhaled air and the surface of the mucosa. Such a gradient is set up for rapidly reactive gases, such as formaldehyde, that essentially "disappear" on first contact with the moist nasal mucosa. In the larger airways of the lung, where gas molecules may traverse relatively long distances from the air to the mucosa, airway resistance may be important even for relatively nonreactive and insoluble vapors. In the liquid phase of the mucosa, transport of gas molecules from the mucosal surface to the capillaries is effected by diffusion, by chemical reaction with components of the mucosa, or by both of these phenomena.

Different types of models are useful for predicting uptake of gases having different chemical reactivities or solubilities. For rapidly reactive gases, dosage to tissue is a function of flow patterns (Kimbell J. S. *et al. Toxicol. Appl. Pharmacol. 121*: 253, 1993): The higher the proportion of air flow over a particular portion of the mucosa, the larger the dose that tissue receives. So-called super computer models are used to calculate flow patterns and dose rates in the torturous chambers of the nasal cavity. At the other extreme of reactivity, gases that are unreactive and poorly soluble (having water/air partition coefficients of less than approximately 50) interact minimally with the respiratory tract, and uptake of such gases occurs mostly in the gas exchange region of the lung.

Vapors with properties between the two extremes of solubility and reactivity include important toxicants for which modeling efforts require sophisticated analysis of subtle and complex phenomena. For example, tissue dosage of ozone (which is not so rapidly reactive that it cannot reach sufficient backpressure in the nasal mucosa to reach the deep lung) and common air pollutants such as alcohols and ketones are difficult to model because the air/mucosa boundary condition (the concentration of the vapor at the boundary between the mucosa and the air) cannot be set to zero - as is the case for formaldehyde and other rapidly reactive gases - nor can it be assumed to be approximately given by the inhaled gas concentration and the partition coefficient - as is the case for common anesthetics and other unreactive, relatively insoluble gases. The most difficult modeling case is that where chemical reaction occurs at a moderate rate in the mucosa, ozone being an example. Methods to address such cases *a priori* involve all the complexities of chemical reaction kinetics of a gas in a complex mixture - in this case the mucosa - and satisfactory methods are still not at hand. On the other hand, for gases that are relatively soluble but unreactive in the mucosa - in which case uptake is effected solely by ventilation patterns, diffusion into the capillary blood, and the rate of perfusion - we have methods to calculate dosage to the tissues of the respiratory tract (Gerde, P. and A. R. Dahl. *Toxicol. Appl. Pharmacol. 109*: 276, 1991).

We are currently extending an experimentally validated mathematical model developed for uptake of vapors in the canine nose to include both uptake of vapors in discrete sections of the canine lower respiratory tract and uptake in the rat upper and lower respiratory tract. The method for carrying out the experimental validation in the rat has been reported (1991-92 Annual Report, p. 69), and the mathematical model developed for uptake in the canine nose has been adapted to accept appropriate physiological parameters to determine the dosage to tissue in the rat respiratory tract (Fig. 1). For the development of a model of uptake in the lower respiratory tract, we will use a mathematical model similar to that published previously (Gerde and Dahl, 1991) with modifications, taking into account air phase resistance to uptake in the larger lung airways. To validate the lung model, we have developed techniques by which we can place dual catheter tubes down as far as the eighth generation of the dog bronchial tree, using a bronchoscope as a guide for placement. We will use the dual catheters to determine uptake in discrete portions of the dog lower respiratory tract. The data will then be used to validate a mathematical model describing uptake in the entire respiratory tract for unreactive but soluble gases.

*Part-time employee of ITRI and of the National Institute of Occupational Health, Solna, Sweden

Rat

Respiratory Rate (breaths/min):	132.0
Tidal Volume (mL):	1.5
Number of Breaths Simulated:	12
Number of Timesteps Per Breath:	2400
Thickness Air/Blood Barrier (μm):	30.00
Nasal Mucosa Blood Flow ($m^3/m^2/sec$):	0.60000E-05

Solvent Vapor

Blood/Air Partition Coefficient:	185.000
Effective Diffusivity in Tissues (m^2/sec):	0.5000E-09
Vapor Concentration Exiting Lung:	0.3000
Sampling Flow Rate to GC (mL/min):	0.5

Output Data

Nasal Uptake (fraction of inhaled):	0.5186
Sampled Nasal Uptake:	0.5301
Nasal Desorption:	0.3407
Sampled Nasal Desorption:	0.3624
Blood Absorption:	0.1717
Mass Balance:	0.993777
Stability Criteria (less than 0.5):	0.0421
Dispersion Criteria (less than 1.0):	0.1562

Figure 1. Input parameters and output data.

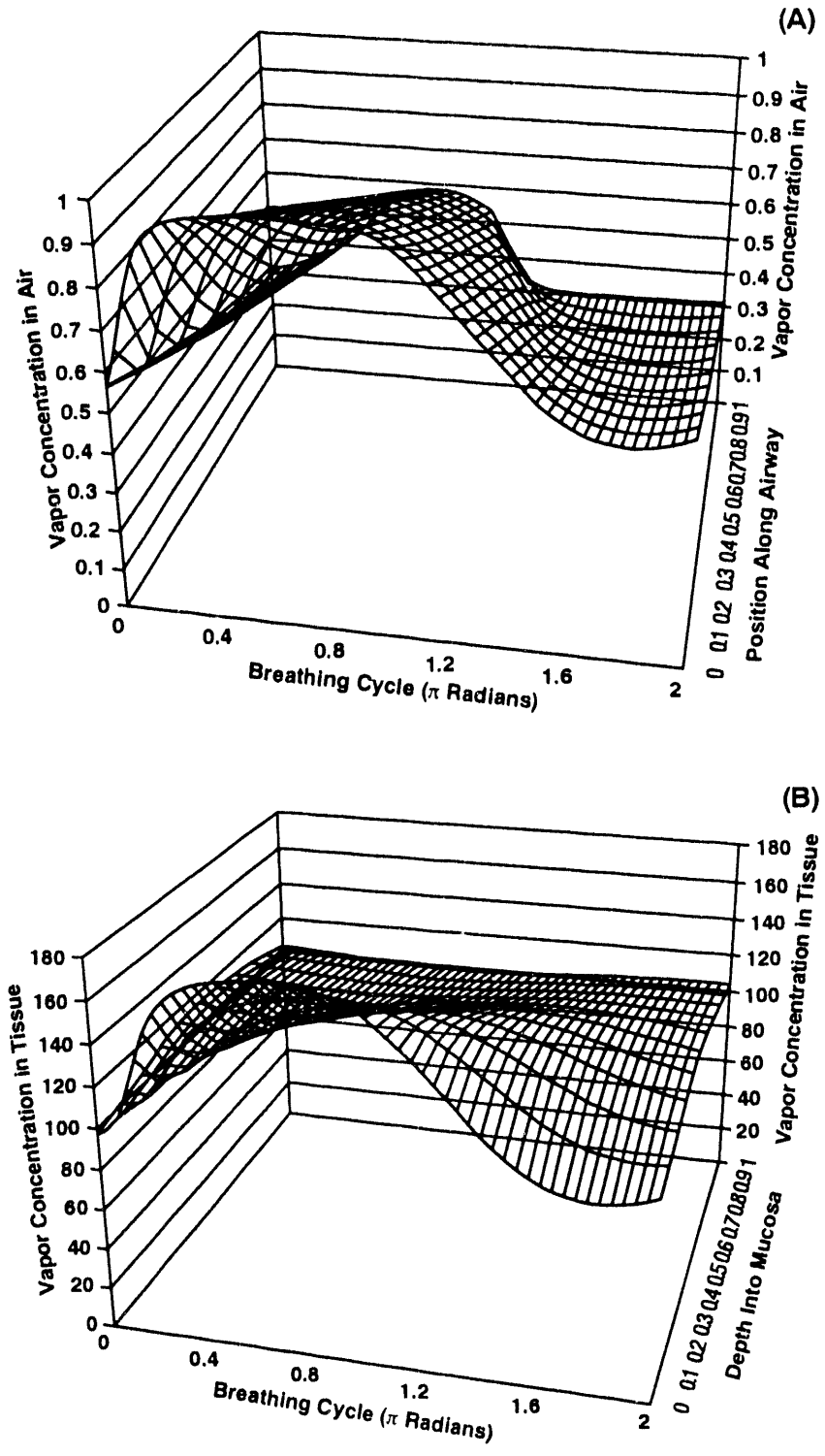

Figure 1 (continued). Computer simulation showing (A) concentration of vapor in air as a function of breathing cycle and the distance into the nasal airway from the tip of the nose, and (B) concentration of vapor in the mucosa at a cross-section perpendicular to the air space, taken at 10% of the distance from the tip of nose to the nasopharynx.

(Research sponsored by the PHS/NIH under Grant R01-ES04422 from the National Institute for Environmental Health Sciences in facilities provided by the U.S. Department of Energy under Contract No. DE-AC04-76EV01013.)

PARTICLE-ASSOCIATED HYDROCARBONS AND LUNG CANCER: THE CORRELATION BETWEEN CELLULAR DOSIMETRY AND TUMOR DISTRIBUTION

P. Gerde, B. A. Muggenburg, R. F. Henderson, and A. R. Dahl*

The well-known correlation between patterns of particle deposition in the human bronchial tree and the apparent sites of origin of primary bronchial tumors (Schlesinger R. B. and M. Lippmann. *Environ. Res. 15*: 424, 1978) is paradoxical because clearance of inhaled particles from the bronchi is comparatively rapid, leading to short exposure time. However, there may be a dosimetric link between deposition of highly lipophilic carcinogens such as polycyclic aromatic hydrocarbons (PAHs), reversibly adsorbed on inhaled particles, and the distinctive distribution of preneoplastic and neoplastic lesions in the lungs. This study was based on the assumption that the dosimetry of PAHs is determined primarily by the behavior of the dissolved hydrocarbons in the tissues after release from their carrier particles.

We measured clearance of PAHs from the respiratory tract of the Beagle dog via three different routes: alveolar clearance, mucociliary clearance, and penetration of the tracheobronchial epithelium. Alveolar clearance was measured by exposing the dogs to an aerosol bolus of PAHs in a single breath, then monitoring the appearance of the PAHs in the blood entering and leaving the lungs (Gerde, P. *et al. Toxicol. Appl. Pharmacol. 121*: 313, 1993a). Mucociliary clearance of dissolved PAHs was measured by instilling onto the mucous blanket in the trachea small volumes of PAHs dissolved in saline, followed by lavage of the mucous-retained materials (Gerde, P. *et al. Toxicol. Appl. Pharmacol. 121*: 319, 1993b). Retention of BaP in the bronchi was determined by instilling the hydrocarbons onto the airway walls followed by measuring the tissue concentration at different times after instillation (Gerde, P. *et al. Toxicol. Appl. Pharmacol. 121*: 328, 1993c).

Results show that clearance of the highly lipophilic carcinogen benzo(a)pyrene (BaP) to the blood takes only minutes in the alveoli, while in the thicker epithelium of the bronchi, clearance may take hours. The data were sufficient to demonstrate that once desorbed from the particles, highly lipophilic PAHs are diffusion-limited during clearance through the airway epithelium to the capillary blood (Gerde *et al.*, 1993c). A direct result of slowed clearance is a high concentration of the PAH in the bronchial epithelium and an increased opportunity for metabolism to reactive forms on first-pass penetration to the capillary blood. Figure 1 shows the calculated tissue concentration of BaP in three important tissue compartments following exposure to BaP at an even density of deposition over the entire surface of the lungs. A prolonged elevation of the concentration of BaP-equivalent activity in the thicker bronchial epithelium is the most important consequence of diffusion-limited clearance of BaP in the lungs. In contrast, less lipophilic substances are perfusion-limited during clearance, and are likely to clear within minutes from all regions of the lungs to the circulating blood. Perfusion-limited toxicants are more likely to induce toxicity in richly perfused tissues such as the alveoli.

For organic compounds, both lipophilicity and the tendency of gaseous organics to adsorb onto airborne particles increase with increasing molecular weight. As a consequence, the greater likelihood of highly lipophilic toxicants to induce first-pass toxicity during diffusion-limited clearance links the seemingly independent parameters of lipophilicity and particle-association: highly lipophilic organic toxicants will be carried into the lungs adsorbed on particles, and not as gases. Highly lipophilic toxicants desorbed from particles are more likely to induce first-pass toxicity near the location of their deposition than less lipophilic compounds. This coincidence of physicochemical properties may provide a plausible explanation for the correlation between particle deposition patterns and the distribution of tumors in the bronchial tree. This new information on the microdosimetry of PAHs in the lungs should improve risk assessments of exposure to inhaled particle-associated hydrocarbons.

*Part-time employee of ITRI and of the National Institute of Occupational Health, Solna, Sweden

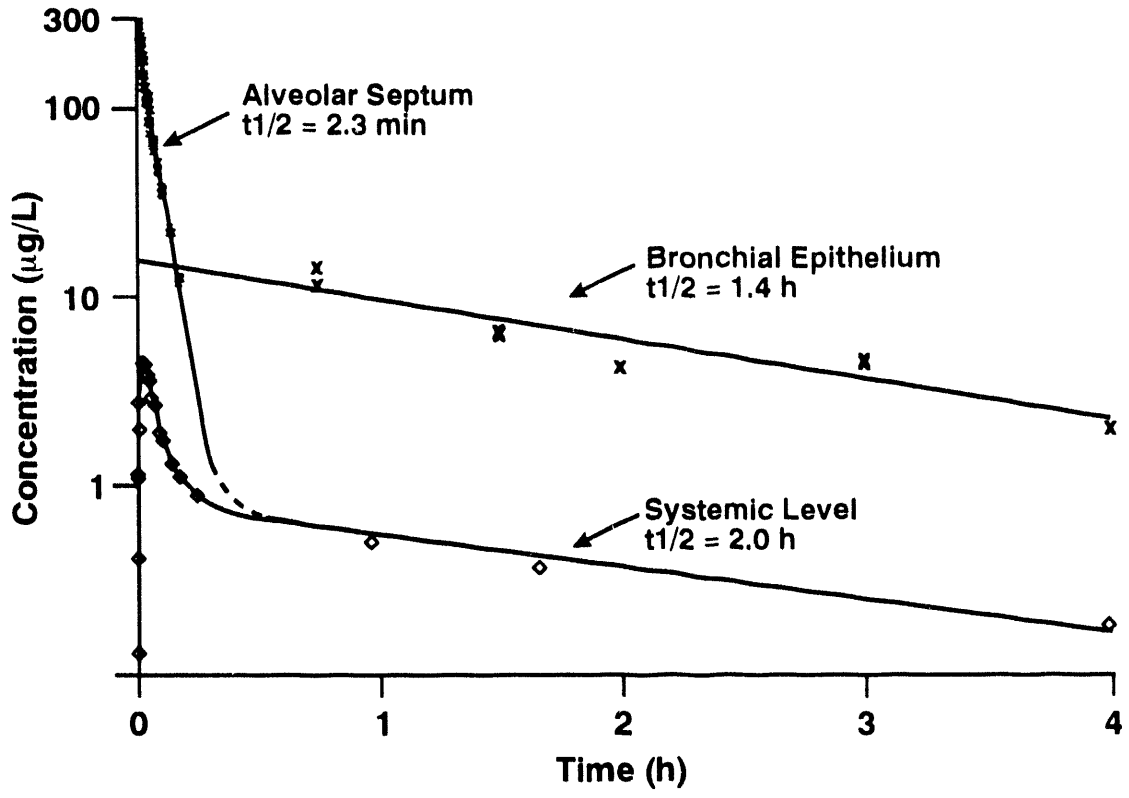

Figure 1. Calculated tissue concentrations of BaP-eq in the Beagle dog following an even deposition of 0.5 $\mu g/m^2$ of BaP over the entire surface of lungs and airways. The thicknesses of the alveolar air/blood barrier and the bronchial epithelium have been assumed to be 1.6 and 30 μm, respectively. Note the prolonged elevation of the concentration in the bronchial epithelium caused by the diffusion-limited absorption of the highly lipophilic carcinogen BaP. Based on data from Gerde *et al.* (1993a,b).

(Research sponsored by the PHS/NIH under Grant R01-ES05910 from the National Institute of Environmental Health Sciences in facilities provided by the U.S. Department of Energy under Contract No. DE-AC04-76EV01013.)

RETENTION SITES FOR PARTICLES DEPOSITED IN LUNG CONDUCTING AIRWAYS OF BEAGLE DOGS

M. B. Snipes, B. A. Muggenburg, K. J. Nikula, and R. A. Guilmette

The International Commission on Radiological Protection (ICRP) has incorporated long-term retention of radioactive particles in conducting airways into its newly approved respiratory tract dosimetry model (ICRP Report No. 66, 1993, in press). This model is purported to provide a better basis for assessing risk associated with human inhalation exposures to radioactive particles. However, applying the new model requires an understanding of particle retention patterns in conducting airways of the lung. Beagle dogs and a unique airway dosing procedure were used to quantify long-term retention patterns for particles deposited at specific sites in conducting airways. The dog was selected as a model because long-term retention and clearance patterns for particles deposited in the lungs of dogs and humans are similar (Snipes, M. B. *CRC Crit. Rev. Toxicol. 20*: 175, 1989). Male and female Beagle dogs, 2 to 4 yr old, were obtained from the Institute's closed colony. A fiberoptic bronchoscope was used to position the dosing device, a microspray nozzle (Hoover, M. D. *et al. J. Aerosol Med. 6*: 67, 1993), in specific airway sites in dog lungs. The sites selected for dosing had 15-mm, 8-mm, or 4-mm diameters. A suspension of test particles in 20 μL or 6 μL of saline solution was expelled through the microspray nozzle using 1 mL of air.

Three kinds of test particles were used: (1) monodisperse 3-4 μm diameter polystyrene latex (PSL) microspheres, radiolabeled with either ^{85}Sr, ^{59}Fe, or ^{46}Sc (3M Company, Minneapolis, MN), were suspended in 0.9% saline containing 0.05% Tween-80 surfactant (3M Company); (2) polydisperse fused aluminisilicate particles (FAP) radiolabeled with ^{46}Sc or ^{169}Yb, with an activity median aerodynamic diameter of 1.6 μm, and a geometric standard deviation of 1.8; and (3) monodisperse yellow-green fluorescent PSL microspheres (1.1 or 3.2 μm; Polysciences, Inc., Warrington, PA), used in combination with radiolabeled PSL microspheres or alone to allow visual localization of retained particles in histological slides.

Details about the procedures used to spray particles onto airways of dogs, as well as results relevant to clearance determined by *in vivo* whole-body counting, have been previously described (1989-90 Annual Report, p. 49; 1990-91 Annual Report, p. 59; 1991-92 Annual Report, p. 77). This report emphasizes the results obtained from examination of histological sections of airways and parenchyma obtained from dosing sites and attempts to determine the extent to which the spraying procedure influenced the results. In some cases, the dogs were alive at the time of dosing. However, to eliminate lung movement resulting from breathing or heart beat as factors that could influence particle locations immediately after dosing, lungs of dead dogs were also dosed. After dosing, lungs were removed from the thoracic cavity, inflated with air, and either fixed with 10% neutral buffered formalin by vascular perfusion or inflation-dried. The drying procedure became the method of choice because the potential for dislocation or movement of particles in the lung during the drying procedure is minimal. Lungs were dried while inflated at 30-cm H_2O pressure in a microwave oven using a procedure similar to one previously described (Valberg, P. A. *et al. J. Appl. Physiol. 53*: 824, 1982).

The volumes of lung tissue of interest at and near the dosing sites were mapped and carefully dissected free of the surrounding lung tissue. The total volume of lung tissue removed was about 2-3 cm^3 for each site. These specimens of lung tissue were cut into about 20 pieces and embedded in glycol methacrylate (Polysciences, Inc., Warrington, PA). Plastic embedding was necessary to maintain the integrity of the PSL microspheres. Embedded tissues were sectioned at 3 to 5 μm and mounted on glass slides for light and epifluorescent microscopy to determine the locations of retained microspheres. We anticipated finding the microspheres associated with airway epithelium near the dosing site. Unexpectedly, most of the instilled microspheres remaining in the lung longer than 6 days after dosing were in parenchyma distal to the dosing sites.

These direct observations of lung tissue examined 6 days or longer after dosing consistently demonstrated long-term retention of test particles in lung parenchyma, but not in conducting airways. This result may have been the consequence of retrograde movement of particles from airways into the lung parenchyma, as hypothesized in a series of studies with dogs during the late 1960s and early 1970s which evaluated powdered tantalum metal as a radiographic contrast medium (Morrow, P. E. *et al. Radiology 121*: 415, 1976). Large

amounts of tantalum were insufflated into the conducting airways of the dogs, and significant alveolar burdens of tantalum were present in essentially all of the dogs after about 1 day. Wolff, R. K. *et al.* (*J. Aerosol Med.* 2: 261, 1989) used a fiberoptic bronchoscope and dry powder dispersion technique to disperse 3 μm and 9 μm monodisperse radiolabeled or fluorescent PSL microspheres to a depth of about the sixth generation of lung airways in dogs. The microspheres were forced through the dosing apparatus using air, and the dogs were sacrificed immediately after dosing. Most of the fluorescent microspheres found after dissection of the lung were in the fifth to tenth generation airways, but some were as far into the lung as the terminal bronchioles and alveoli.

After concluding that the dosing procedure might have influenced our results, a study was conducted to determine the locations of particles immediately after dosing. Dogs were available from another study at the Institute, not involving the lung, and had been exsanguinated about 0.5 h prior to the time that particles were sprayed into their lung airways. A mixture of 3-4 μm ^{46}Sc-labeled PSL and 3.2 μm fluorescent microspheres was used in one study. The dosing volume was 20 μL (1.5 x 10^7 microspheres) for four dogs and 6 μL (5 x 10^6 microspheres) for one dog; three, 4-mm diameter airway sites were dosed in each dog. The lungs were removed about 30 min after dosing, inflated, and dried in a microwave oven. After the lungs were dried, locations of the microspheres were identified using a radiation detector. The volumes of lung tissue containing all detectable radioactivity, about 1-3 cm^3 for each dosing site, were dissected from the lungs and cut into pieces small enough to rehydrate and embed in plastic. Most of the microspheres seen in tissue sections were on bronchial surfaces proximal to the deposition sites. This indicates mucociliary clearance was still occurring, even though the dogs were dead at the time of dosing. However, when either the 20 μL (1.5 x 10^7 microspheres) or 6 μL (5 x 10^6 microspheres) dose was used for microspheres were invariably found in alveoli distal to the dosing site.

To evaluate the effect of particle number on subsequent distribution in lung, five dogs were exposed that were dead about 30 min before they were dosed. A dosing volume of 6 μL was used that contained about 3 x 10^5 1.1 μm fluorescent microspheres, and two, 4-mm diameter airway sites were dosed in the lungs of each dog. One day prior to dosing, the deposition sites to be used were marked by positioning the tip of the bronchoscope about 1 cm from the designated site, inserting a hypodermic needle, on the end of a polyethylene tube, about 0.5 mm into the airway mucosa, and injecting a small amount of India ink. This effectively marked a spot about 1 cm from the location at which the microspheres would be sprayed the following day. The microsphere dosing procedure and lung drying were the same as for the first part of this study, except that two dogs were suspended vertically with their heads pointed down during the dosing procedure. This modification of the dosing procedure was included to test the possible effects of gravity on retrograde movement of the microspheres after spraying them into the airway. After drying the lungs in a microwave oven, the dosing sites were found by locating the ink marks. The lung tissue occupying a volume of about 1.2 cm diameter by about 3 cm long and distal to the ink tattoo was carefully dissected from the lung and cut into pieces small enough to embed in plastic. The pieces of lung tissue were mapped relative to the ink tattoo and each other and labeled for later reference. The pieces of lung were hydrated, embedded in plastic, and representative 3 μm sections were mounted on glass slides for light and epifluorescent microscopy to determine the locations of retained microspheres. Two-hundred-and-one fluorescent microspheres were located in tissue sections prepared from pieces of lung near five of the airway locations. The microspheres were all observed on airway surfaces; none of the observed microspheres were within or under the airway epithelium or in alveoli. No fluorescent microspheres were found at or near the other five locations dosed with 3 x 10^5 microspheres/6 μL. Additionally, results were not influenced by the orientation of the lung relative to gravity when the 6 μL doses were used.

Even though the 20 μL dosing volume was relatively small, large numbers of 3-4 μm PSL microspheres were deposited per unit area of airway epithelium. The 1.5 x 10^7 microspheres were delivered to an estimated 50 mm^2 of airway surface at the 4-mm diameter sites (6 μg/mm^2) and to 500 mm^2 at the 15-mm diameter airway sites (0.6 μg/mm^2). The volume of dosing suspension for the FAP was also 20 μL, but the numbers and mass of particles deposited per unit area of airway epithelium were both substantially less than for the PSL microspheres. These results suggest that using small volumes of particle suspensions may be necessary to avoid alveolarization of a portion of the dose.

An important point to make is that in many cases the entire dose of particles, within the ability to measure them with the counting system used, cleared from the dosing site within 3 days (1989-90 Annual Report, p. 49;

1990-91 Annual Report, p. 59; 1991-92 Annual Report, p. 77). Therefore, these results suggest that the dosing procedure may result in alveolarization of a portion of the particles sprayed onto airways; if the particles do not become alveolarized, they are effectively removed from the airways via the mucociliary escalator.

In summary, the microspray dosing procedure is adequate for depositing particles in a liquid vehicle on predefined segments of conducting airways as small as 4 mm diameter. No evidence for long-term retention of particles in conducting airways was observed, but some particles were retained in alveoli. This was apparently due to retrograde movement of particles subsequent to deposition, particularly when a dosing volume of 20 μL was used. This phenomenon may have been due to effects of surface tension, gravity, or the physicochemical composition of the suspension vehicle.

(Research sponsored by the Office of Health and Environmental Research, U. S. Department of Energy, under Contract No. DE-AC04-76EV01013.)

THE FATE OF INHALED NICKEL COMPOUNDS IN CYNOMOLGUS MONKEYS

J. M. Benson, Y. S. Cheng, B. A. Muggenburg, and F. F. Hahn

We evaluated the fate of nickel oxide (green oxide; NiO), nickel sulfate hexahydrate ($NiSO_4 \cdot 6H_2O$), and nickel subsulfide (Ni_3S_2) administered by nose-only inhalation to cynomolgus monkeys in order to provide information that will aid in extrapolating toxicity and toxicokinetic data obtained in rodent inhalation studies to humans. Specific endpoints evaluated included retention of inhaled Ni in lung, extent of distribution of Ni to extrarespiratory tract tissue, pathways of Ni excretion, and histopathological changes in lung resulting from the acute Ni compound exposures.

A total of 34 monkeys were exposed individually to the nickel compounds. Before the exposure, the monkeys were anesthetized using ketamine and xylazine. For the exposures, each monkey was fit with a fiberglass face mask that allowed nose-breathing only. The mask covering the monkey's face was connected to the main aerosol exposure line through a secondary line fitted with a non-rebreathing valve. After the monkey was made apneic by hyperventilation for approximately 5 min, he was sealed in a ventilator box where his rate and depth of breathing were controlled using a Harvard respiratory pump.

Test compounds were synthesized with a ^{63}Ni label to facilitate detection and quantitation of Ni in the monkey tissue samples. Briefly, ^{63}NiO was prepared by reacting $^{63}NiCl_2$ with ammonium carbonate to form $^{63}NiCO_3$ which was subsequently calcined at 1200°C to form the ^{63}NiO. $^{63}NiSO_4 \cdot 6H_2O$ was formed by recrystallizing $NiSO_4 \cdot 6H_2O$ from an aqueous solution containing $^{63}NiCl_2$. $^{63}Ni_3S_2$ was prepared by reducing $^{63}NiSO_4$ with H_2 at 500°C. Each monkey was exposed for approximately 45 min to mean concentrations of 29.5 mg NiO/m^3, 12.5 mg $NiSO_4 \cdot 6H_2O/m^3$, or 16.4 mg Ni_3S_2/m^3. The mass median aerodynamic diameters of the NiO, $NiSO_4 \cdot 6H_2O$, and Ni_3S_2 aerosols were 2.2, 1.2, and 1.6 μm, respectively. Ten to 12 monkeys were exposed to each compound and groups of two monkeys were sacrificed at five or six time points after exposure.

NiO-exposed monkeys were sacrificed at 0, 1, 8, 30, 100, and 200 days post exposure. On day 0, Ni was present in the nasal turbinates, larynx, trachea, and lungs. Ni was cleared rapidly from the upper respiratory tract, but little clearance occurred from lung. No Ni was detected in extrarespiratory tract tissues except for the lung-associated lymph nodes. The retention half-time for inhaled NiO in monkeys was estimated at > 200 days. $NiSO_4 \cdot 6H_2O$-exposed monkeys were sacrificed at 0, 2, 8, 16, and 32 days post exposure. As expected, the $NiSO_4 \cdot 6H_2O$ cleared rapidly from lung and upper respiratory tract distributed to the liver, kidney, and carcass. The pattern of Ni clearance from lung was fit with a two-component, negative exponential equation. Approximately 96% of the initial Ni body burden cleared with a half-time ($t_{1/2}$) of 5 h. The remaining 4% of material cleared with a $t_{1/2}$ of approximately 10 days. Ni_3S_2-exposed monkeys were sacrificed at 0, 2, 4, 8, and 16 days post exposure. As with $NiSO_4 \cdot 6H_2O$, the deposited Ni_3S_2 cleared rapidly from the lung and upper respiratory tract and distributed to extrarespiratory tract tissues. The clearance pattern of Ni from lung was fit using a single-component, negative exponential equation. The half-time for clearance was approximately 4 days.

Ni was excreted in both urine and feces of the monkeys exposed to each form of Ni compound. No histopathological changes attributable to Ni exposure were present in the lung.

The prolonged retention of NiO in monkey lung and general lack of distribution of Ni to extrarespiratory tract tissues were not unexpected, based in its high calcination temperature (1200°C) and retention pattern in rats (1991-92 Annual Report, p. 83). By comparison, pulmonary retention half-times of 500 - 900 days have been reported for another highly insoluble particle, PuO in monkeys (Nolibe, D. *et al.* In *Inhaled Particles IV, Part 2* [Walton, W. H. and B. McGovern, eds.), Pergamon Press, Oxford, UK, p. 597, 1977; LeBauve, R. J. *et al. Radiat. Res. 82*: 310, 1980). The mean (sem) Ni lung burden for 12 NiO-exposed monkeys was 2.2 μg ± 0.32 Ni/g lung. This concentration of Ni, presumably in the form of undissolved NiO, was not sufficient to produce histopathological changes in lung even at 200 days post exposure. By comparison, only macrophage hyperplasia was observed histopathologically in lungs of rats exposed to NiO for 13 wk and possessing accumulated burdens of 80 μg Ni/g lung (Dunnick, J. K. *et al. Fundam. Appl. Toxicol. 12*: 584, 1989).

Patterns of Ni retention in lungs of $NiSO_4 \cdot 6H_2O$ and Ni_3S_2-exposed monkeys were consistent with those expected for soluble particles. Due to the solubility of the particles, lung retention and tissue distribution patterns observed in monkeys were similar to those we have observed for these compounds in rats (Benson, J. M. *et al. Inhal. Toxicol.* in press; 1990-91 Annual Report, p. 42). Estimated initial Ni lung burdens in the $NiSO_4 \cdot 6H_2O$ and Ni_3S_2-exposed monkeys were < 3 μg Ni/g lung. These initial Ni burdens did not produce a toxic response in lung observed histologically. By comparison, similar initial lung burdens of Ni administered as $NiSO_4 \cdot 6H_2O$ and Ni_3S_2 to rats by a single intratracheal instillation produced mild to moderate inflammatory responses in lung observed 7 days after dosing (Benson, J. M. *et al. Fundam. Appl. Toxicol.* 7: 340, 1986).

Results of this study, in combination with rodent inhalation studies on these nickel compounds indicate that high temperature nickel oxides inhaled by humans will be retained in the lung for hundreds of days, but small lung burdens may not produce an inflammatory response. Soluble nickel compounds inhaled by humans are expected to clear rapidly from the respiratory tract and distribute to other tissues, especially kidney, and are more likely to produce an inflammatory response in lung than the nickel oxides.

(Research sponsored by the Nickel Producers Environmental Research Association, under Funds in Agreement No. DE-FI04-87AL44742 with the U.S. Department of Energy under Contract No. DE-AC04-76EV01013.)

METHODS FOR LABELING F344 RAT ALVEOLAR MACROPHAGES TO INVESTIGATE PARTICLE TRANSPORT AND CLEARANCE IN LUNG

J. M. Benson, D. L. Cassie, N. F. Johnson, and R. A. Guilmette*

Inhaled particles deposited in the lung are generally phagocytized by alveolar macrophages (AM) and either transported out of the lung via the mucociliary escalator or transported into the interstitium and to the lung-associated lymph nodes. Species differences exist in the prevalence of these two pathways. In rodents, clearance via the mucociliary escalator is the predominant pathway, while in larger species, such as dog, transport of particles into the lung interstitium and lymph nodes predominates. Macrophage-mediated particle transport in lung has been investigated (Harmsen A. R. *et al. Science 230*: 1277, 1985; Corry, D. *et al. Am. J. Pathol. 115*: 321, 1984); however, in these studies, AM were labeled with fluorescent particles or radiolabeled materials that were rapidly lost from the cells. In order to more accurately define mechanisms of macrophage-mediated particle transport in the lung, an improved method is needed to label AM. Ideally, the label should be easy to detect, stable, and should not affect cell viability and function.

The usefulness of the nuclear stain Hoechst 33342 for labeling rat AM was investigated. The toxicity of the dye to AM was evaluated *in vitro*, then cells were labeled with nontoxic concentrations of dye to evaluate the usefulness of the labeled cells in following particle transport *in vivo*. AM were obtained from F344/NHsd rats by bronchoalveolar lavage (Benson, J. M. *J. Toxicol. Environ. Health 19*: 105, 1986). The cells were washed once in RPMI culture medium containing 10% fetal bovine serum and 0.1% gentamicin and centrifuged to sediment the cell suspension. The cell pellet was resuspended in saline containing 0.1% gentamicin. Aliquots of cells were dosed with 0, 2.5, 5.0, 10, or 15 μg Hoechst/mL and incubated for 30 min at 37°C. At the end of the incubation period, the cells were recovered by centrifugation and resuspended in RPMI. Cell viability and phagocytic and migratory abilities were determined on the day cells were dosed and after 1, 2, and 4 days in culture. Based on the results of these studies, the 2.5 μg/mL concentration was chosen for use in the *in vivo* studies.

For the *in vivo* studies, AM were obtained and dosed with 2.5 μg Hoechst/mL saline for 30 min as described above. Half of the Hoechst-stained population was incubated in petri dishes at 37°C in a 5% CO_2 atmosphere with red-fluorescing polystyrene latex microspheres (1.7 μm), while the other half was incubated with green-fluorescing spheres for 18 h. Cells were recovered, combined to form a single population of cells containing either red or green fluorescent beads and concentrated to a density of approximately 6 million cells/mL incubation medium. Approximately 3 million cells were administered to nine recipient rats by intratracheal instillation. Groups of three recipient rats were sacrificed 1, 3, and 6 days later. The lungs of two rats per group were lavaged, and cytospin preparations of the recovered cells were evaluated for the distribution of red and green particles among the donor (Hoechst-stained) and resident (nonstained) cells. The presence of fluorescent beads of one color in Hoechst-stained cells over time would indicate the stability of the stain and provide indication that the Hoechst-stained cells remained viable over the time period investigated. The presence of beads of one color in unstained AM would suggest that the dye was unstable over the time period evaluated. Finally, the presence of both color beads in Hoechst stained or unstained AM would indicate the donor Hoechst-stained cells were dying and particles they once contained were being phagocytized by viable AM. The lungs of the third rat per group were inflated with air and "fixed" by slow drying in a microwave oven. The fixed lungs were subsequently formalin fixed, embedded in methacrylate, and sectioned at 3 μm for examination by light microscopy. The distribution of free particles and particles contained in Hoechst-stained or unstained cells was examined in the tissue samples.

Hoechst-labeled AM containing red or green fluorescent particles were recovered from lung by lavage up to 6 days after instillation into recipient rats (Table 1). Only a few of the cells recovered by lavage contained both red and green beads, indicating that the donor cells remained viable over the 6-day period. The percentage of donor cells among the AM recovered from lung diminished from approximately 34% to about 4% over the

*Department of Energy/Associated Western Universities Teacher Research Associates Program (TRAC) Participant

6-day period. It is expected that many of them were removed by mucociliary clearance. However, labeled cells were also identified in lung tissue of recipient rats up to 6 days post exposure. The fact that Hoechst-stained AM are present in lungs up to 6 days after instillation coupled with low percentages of AM containing both colored beads suggest that Hoechst 33342 may be useful for evaluating mechanisms of particle transport in the rat.

Table 1

Characteristics of Cells Recovered From Recipient Rats
by Bronchoalveolar Lavage
(Percents; Mean ± Standard Deviation)

	Days After Donor Cell Instillation		
	1	3	6
Cells With Hoechst			
Hoechst Alone	8.6 ± 1.3	7.0 ± 3.5	0.7 ± 0.3
Hoechst + Red Beads	10.0 ± 2.3	1.3 ± 0.7	0.6 ± 0.3
Hoechst + Green Beads	13.2 ± 1.0	5.8 ± 3.7	1.2 ± 0.5
Hoechst + Both Colors	2.1 ± 0.5	4.0 ± 2.6	1.2 ± 0.7
Total	33.9 ± 2.9	18.1 ± 5.8	3.7 ± 0.69
Cells Without Hoechst			
No Label	62.5 ± 0.3	83.7 ± 4.6	91.8 ± 3.7
Red Beads	1.3 ± 0.1	1.1 ± 0.5	1.5 ± 0.7
Green Beads	2.1 ± 0.4	2.0 ± 1.0	3.0 ± 1.3
Both Colors	0.1 ± 0.1	0.2 ± 0.1	0.5 ± 0.3
Total	66.0 ± 0.52	87.0 ± 4.7	96.8 ± 4.0

(Research sponsored by the Office of Health and Environmental Research, U.S. Department of Energy, under Contract No. DE-AC04-76EV01013.)

HIGH BUTADIENE MONOEPOXIDE LEVELS IN BONE MARROW OF B6C3F$_1$ MICE INHALING BUTADIENE

K. R. Maples, W. E. Bechtold, A. R. Dahl, and R. F. Henderson*

1,3-Butadiene is a major industrial chemical used primarily in the manufacture of styrene-butadiene and polybutadiene rubbers. Recently, chronic toxicity tests in B6C3F$_1$ mice exposed to either 625 or 1250 ppm butadiene had to be ended after 60 wk of exposure due to high mortality from lymphocytic lymphomas (Huff, J. E. *et al. Science 277*: 548, 1985). These tests were subsequently repeated at exposure levels ranging from 6.25 to 625 ppm (Melnick, R. L. *et al. Environ. Health Perspect. 86*: 27, 1990), and an increased incidence of lung tumors was observed in B6C3F$_1$ mice at levels of butadiene exposure equivalent to or greater than 6.25 ppm or 62.5 ppm for females and males, respectively. Hemangiosarcomas of the heart were obtained at concentrations as low as 20 ppm in males and 62.5 ppm in females. Increased incidences of neoplasms in the Harderian gland, liver, mammary gland, and ovary were also observed. As seen in the first study, lymphocytic lymphomas were the primary cause of death for mice of both sexes exposed to 625 ppm butadiene and were increased in females exposed to 200 ppm. In addition to causing lymphocytic lymphoma in mice, chronic exposures to 650 ppm cause bone marrow toxicity. In contrast, inhalation exposure of Sprague-Dawley rats to either 1,000 or 8,000 ppm butadiene yielded no hematopoietic tumors (Owen, P. E. *et al. Am. Ind. Hyg. Assoc. J. 48*: 407, 1987). Instead, increased incidences of pancreatic exocrine adenoma, uterine sarcoma, Zymbal gland sarcoma, mammary tumors, thyroid follicular cell tumors, and testis Leydig-cell tumors were found. Because of the species differences in response to butadiene exposure, an expanding scientific controversy has arisen as to the appropriate rodent species to use for assessing human health risks from butadiene exposure.

Evidence from studies conducted *in vivo* and *in vitro* indicates that, while metabolism of butadiene is qualitatively similar among species, there are major species differences in the quantitative rates of metabolism of butadiene and its metabolites. The two major oxidative metabolites of butadiene are the mono- and diepoxide; both have been shown to be mutagenic and are the putative ultimate carcinogens. Mice are much more efficient at forming the monoepoxide, the most abundant metabolite, than are rats or primates; in contrast, mice are much less efficient at hydrolyzing the monoepoxide, a detoxication process, than are rats and primates. This suggests that the toxic monoepoxide might accumulate to a greater level in mouse tissues than in those of other species.

In the present study, we determined the levels of butadiene monoepoxide in probable target tissues, bone marrow, blood, heart, lung, and liver, of B6C3F$_1$ mice exposed to 1,3-butadiene. We analyzed the samples using a GC/MS isotope dilution assay with a cryogenic distillation technique.

Twelve, 11-wk-old male B6C3F$_1$ mice (Charles River Laboratories, Kingston, NY) were exposed nose-only to either filtered air (n = 4) or 1,3-butadiene gas at 100 ppm (n = 8) for 4 h. Butadiene concentration was monitored by infrared spectroscopy (Wilks Miran 1A-OVF) and quantitated using a GOW-MAC gas chromatograph (series 750) equipped with a flame ionization detector.

After exposure, the mice were sacrificed (thiamylal sodium, 5%, 0.5 mL intraperitoneal). Within 4 min of the cessation of respiration, we obtained blood from the heart and removed the femurs, lungs, liver, and heart. The bone marrow was obtained by removing the fur and muscle surrounding the femur, clipping the ends of the femur, attaching a syringe to the bone via plastic tubing, and forcing the bone marrow out using pH 7.2 water into a round-bottom flask that was cooled to liquid nitrogen temperature. Marrow from both femurs was pooled. The blood samples were collected in round-bottom flasks precooled to liquid nitrogen temperature. These flasks had been prespiked with 100 nmoles of [d_6]-butadiene monoepoxide. Three water blanks were also prepared and spiked with equivalent amounts of the internal standard on the day of exposure. Due to difficulties in spiking whole tissues with the standards, the lung, liver, and heart samples were handled in a different manner than the more fluid blood and bone marrow. The heart, lung, and liver samples were frozen immediately in liquid nitrogen and placed in precooled, labeled vials. These tissue samples were spiked with the internal standards on the day of distillation. All samples were stored in a liquid nitrogen freezer (-120°C) until analyzed.

---

*Currently at Centaur Pharmaceuticals, Sunnyvale, California

At least one control tissue (tissue from an air-exposed mouse) and one water blank were analyzed for every 10 samples. The weights of the blood and bone marrow samples were adjusted prior to distillation by the addition of water to yield 1 g weights for all samples. In the case of the lung, liver, and heart tissue, samples were pulverized at liquid nitrogen temperature to yield a fine powder. A 0.2 g aliquot of the powder was transferred to a precooled flask (-120°C), spiked with 25 nmoles of [d_6]-butadiene monoepoxide, and was cryogenically distilled into septa-port U-tubes immersed in liquid nitrogen. The same stock of standard was used for the water blanks as for the tissue samples.

Following distillation, the septa-port U-tubes were brought to room temperature, the vacuum was released, and a 1-μL aqueous sample was removed from the trap and injected onto a GC/MS (Hewlett-Packard, GC model 5890, 5970B series mass selective detector), equipped with a DB-Wax capillary column (40 m column length, 0.18 mm i.d., and 0.3 μm film thickness; J&W Scientific, Folsom, CA). The concentrations of butadiene monoepoxide in the distilled samples were calculated by comparing their GC/MS peak areas to those of the internal standards. The identity of each peak was confirmed by comparison of the intensities of the three ions scanned for each compound with those obtained using pure standards.

Following distillation of the bone marrow samples, we dissolved the lyophilized tissue remaining in the round-bottom flasks using sodium hydroxide, adjusted the solutions to pH 10, and assayed the samples for protein content using the Lowry protein assay, with bovine serum albumin as the standard. In order to convert the bone marrow data into units comparable to those used for the other tissue data (nmoles metabolite/g tissue), we determined the amount of protein per milligram wet tissue weight by examining bone marrow samples obtained from naive mice using pressurized air to extrude the tissue samples.

Based on the standard deviation of the water blanks, the limit of detection was 0.79 nmoles/g tissue for butadiene monoepoxide. The GC/MS results for tissues from air-exposed mice were not statistically different from those for water blanks. The butadiene monoepoxide levels in tissues from exposed mice are shown in Table 1. The data shown in Table 1 represent the results of one exposure; this exposure was repeated with similar results.

Table 1

Tissue Levels of Butadiene Monoepoxide Following Inhalation Exposure for 4 Hours to 100 ppm 1,3-Butadiene (Mean + SE, nmoles/g tissue)

Tissue	Butadiene-Exposed (n = 8)
Bone Marrow	3160 ± 860[a]
Blood	3.59 ± 0.70[a]
Lung	1.45 ± 0.29[a]
Liver	10.7 ± 4.2[a]
Heart	2.29 ± 0.67[a]

[a]Significantly different from the mean value for an air-exposed sample based on Student's *t* test using a Bonferroni correction for multiple comparisons with the criterion for significance set at $p < 0.05$.

The blood results fit well with previous data obtained in our laboratories using cryogenic distillation and radioanalysis. Our current blood butadiene monoepoxide value, when normalized to the exposure butadiene

concentration, is 36 pmoles/g tissue/ppm, quite close to the previously reported value of 26 pmoles/g tissue/ppm (Dahl, A. R. *et al. Environ. Health Perspect. 86*: 65, 1990).

Based on the results reported here, we suggest that the toxicity to the bone marrow in mice exposed to 1,3-butadiene is probably related to high levels of butadiene monoepoxide. Colagiovanni, D. B. *et al.* (*Proc. Natl. Acad. Sci. USA 90*: 2803, 1993) demonstrated that *in vitro* pretreatment of hematopoietic progenitor cells from C57BL/6 mice with butadiene monoepoxide resulted in the same hematopoietic defects seen in butadiene-exposed mice. Inhibition of stimulated colony formation was achieved using only pmolar amounts of butadiene monoepoxide. The levels of butadiene monoepoxide we found in the bone marrow following butadiene exposure, 3.16 μmoles/g tissue, were well above this threshold level for hematopoietic progenitor cell effects.

The high butadiene monoepoxide levels in bone marrow relative to those in blood may indicate any or all of the following: (1) bone marrow cells may produce butadiene monoepoxide *in situ*, (2) bone marrow may preferentially absorb butadiene monoepoxide from the blood, or (3) bone marrow cells may have only a limited capacity to further metabolize or otherwise clear butadiene monoepoxide. Metabolism of butadiene to butadiene monoepoxide could be carried out in bone marrow by either cytochrome P-450 or by myeloperoxidase. Our results support earlier findings (Tice, R. R. *et al. Environ. Mutagen. 9*: 235, 1987) that one possible reason for the exquisite sensitivity of the mouse to the carcinogenic effects of butadiene exposure may be the high rate of synthesis of butadiene monoepoxide and the slow rate of hydrolysis of this toxic metabolite in the mouse.

The results reported here, together with previously published results from a number of laboratories, suggest that before carcinogenicity data obtained in mice are used for risk assessment of butadiene toxicity in humans, further studies of the causes of mouse sensitivity to butadiene are in order.

(Research supported by the Chemical Manufacturers' Association under Funds-In-Agreement No. DE-FI04-91AL66351 with the U.S. Department of Energy under Contract No. DE-AC04-76EV01013.)

URINARY EXCRETION OF HYDROQUINONE AND CATECHOL BY WORKERS OCCUPATIONALLY EXPOSED TO BENZENE

*W. E. Bechtold and N. Rothman**

Although benzene is a known human carcinogen, the dose-response curve is poorly defined at low exposure levels. To better understand the toxicity of benzene at low doses, the National Cancer Institute will follow a cohort of 74,000 benzene-exposed Chinese workers for occurrences of leukemia. A sub-population was identified for a more thorough study of benzene biomarkers. The goal of the study will be to evaluate a variety of blood and urine biomarkers related to benzene exposure, metabolism, and biologic effects. These markers include benzene metabolites, blood protein adducts, P4502E1 metabolic activity, chromosomal abnormalities, lymphocyte micronuclei, glycophorin A red blood cell mutation frequency, ras mutations, and peripheral blood counts. Our role at ITRI will be to determine benzene metabolites and blood protein adducts; this report describes results of urinary metabolite analyses. All currently exposed subjects have been monitored during their full workshifts for air exposure to benzene using organic vapor monitoring badges. Readings from the badges were obtained on 5 consecutive days prior to biologic sampling. Industrial hygiene data and questionnaires are being processed.

For determination of internal dose, the benzene metabolites muconic acid (MUC), phenol (PHE), catechol (CAT), and hydroquinone (HQ) are of interest. Analysis of metabolites will provide a critical link between exposure concentration, uptake and metabolism, and short-term endpoints of toxicity. Further, measurement of metabolites will allow assignment of worker exposures when the industrial hygiene data are in doubt. For example, numerous workers performed in areas in which respirator use was mandated. However, these same workers were observed using the respirators only occasionally. The exposures of these individuals can be inferred by comparing their excretions of PHE and MUC with those of workers performing in well-defined exposure atmospheres.

Benzene metabolism to HQ is of particular interest, due to a postulated link between formation of this metabolite and bone marrow toxicity. Inoue, O. *et al.* (*Br. J. Ind. Med. 45*: 487, 1988) have been the only investigators who have explored the excretion of HQ by workers after benzene exposure. They concluded that workers exposed to less than 10 ppm benzene could not be distinguished from controls based on measurement of urinary HQ. These results suggest that humans are constantly exposed to this apparently toxic benzene metabolite at levels that would occur from a 10 ppm exposure. However, the method used by Inoue *et al.* (1988) was a highly nonspecific HPLC method. Backgrounds actually may be considerably lower. We will test for this by measuring HQ (excreted in the urine as a conjugate) by a selective and sensitive gas chromatography/ mass spectroscopy (GC/MS) method.

Benzene urinary metabolites were measured using an alteration of our previously described isotope dilution GC/MS assay (Bechtold, W. E. *et al. Am. Ind. Hyg. J. 52*: 473, 1991). ^{13}C-labeled analogues of the metabolites MUC, and PHE, CAT, and HQ as conjugates (sulfate and glucuronide) were available for use as internal standards. Concentrations were determined by calibrating against a primary standard solution. Urine samples or solutions of benzene metabolite standards were placed in a 15 mL centrifuge tube, with 100 μL of 88% formic acid and 50 μL of internal standard solution. The aqueous samples were extracted twice with 3 mL of ethyl acetate. The extraction step removed MUC. Since the PHE, CAT, and HQ exist as conjugates, they had to be hydrolyzed prior to analysis. To do so, 0.6 mL of concentrated HCl was added to the aqueous layer, and the mixture was incubated for 1 h at 100°C. After cooling, the urine was neutralized to pH 7 with 10 N NaOH, and 2 mL of ethyl acetate was added. The mixture was shaken and centrifuged until the layers separated. The ethyl acetate was removed and added to the previous extract. The combined extracts were evaporated to dryness in a cool nitrogen stream.

Benzene metabolites were analyzed by GC/MS. Prior to analysis, the analytes were chemically converted to volatile trimethylsilyl (TMS) derivatives, using bistrimethylsilyltrifluoracetamide. TMS derivatives were injected directly onto the GC/MS using the following conditions. The GC was equipped with an HP Ultra-1

*National Cancer Institute, Bethesda, Maryland

fused silica capillary column, 25 m x 0.25 mm with a 0.5-μm film thickness. The initial column temperature was 80°C for 1 min, followed by a temperature gradient at 10°C/min to 340°C. The ions monitored were 166, 254, 254, and 271 for PHE, CAT, HQ, and MUC, and 172, 260, 260, and 277 for the ^{13}C analogues, respectively. Standard curves were created by plotting the amount of added metabolite standard vs. the ratios of the integrated peaks for analyte and internal standards, and by fitting the data points by linear regression.

Initially 106 urine samples were analyzed in duplicate. Of these, 62 were unique urine samples; the remainder were blind duplicates, blanks, and spiked urine samples. The precision was greater than ± 5%. All measured values were well above the limits of sensitivity for the assay (about 10 ng/mg creatinine for all analytes).

No industrial hygiene data are currently available for comparisons of exposures with excreted metabolites. However, some conclusions can be made from the data. Of particular interest are shifts in the major metabolic pathways as a function of increased exposures. Concentrations of the toxic metabolites HQ and MUC were calculated relative to the inverse of PHE, and plotted against PHE (Figs. 1 and 2). Results indicate that as dose is decreased (as indicated by a decrease in concentration of PHE), the relative amounts of MUC and HQ increase. These results are consistent with previous animal studies. For example, a physiological model has been developed to describe the uptake and metabolism of benzene in rats and mice (Medinsky, M. A. *et al. Toxicol. Appl. Pharmacol.* 99: 193, 1989). Model simulations explored the effect of dose on the excretion of detoxication metabolites PHE and phenylmercapturic acid, and toxication metabolites MUC and HQ (experimentally, CAT could not be distinguished from PHE). Model simulations suggested that for both rats and mice at lower exposure concentrations HQ and MUC represented a larger fraction of the total benzene metabolized than at higher exposure concentrations where detoxication metabolites were predominant. The results presented here suggest that humans metabolize benzene similarly to the way rodents do.

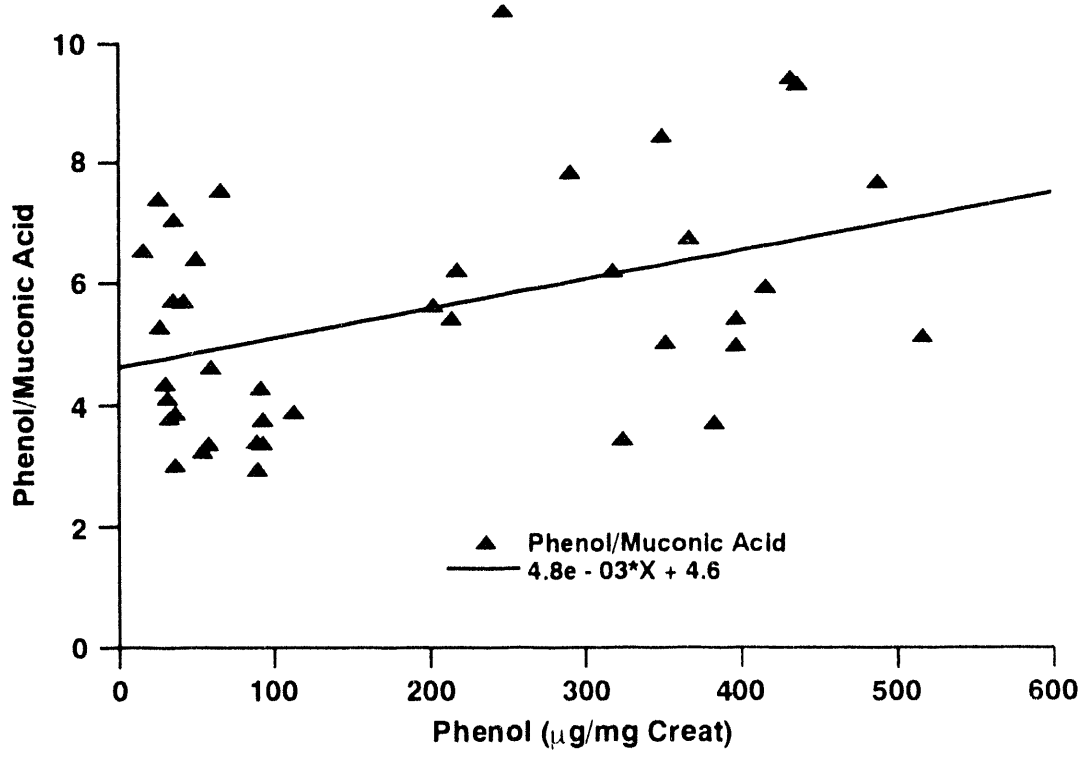

Figure 1. Concentrations of urinary phenol vs. phenol/muconic acid in urine samples of Chinese workers exposed to benzene.

In summary, benzene metabolites have been measured in urine samples from a group of Chinese workers occupationally exposed to benzene. Full interpretation of these data must wait until industrial hygiene data become available.

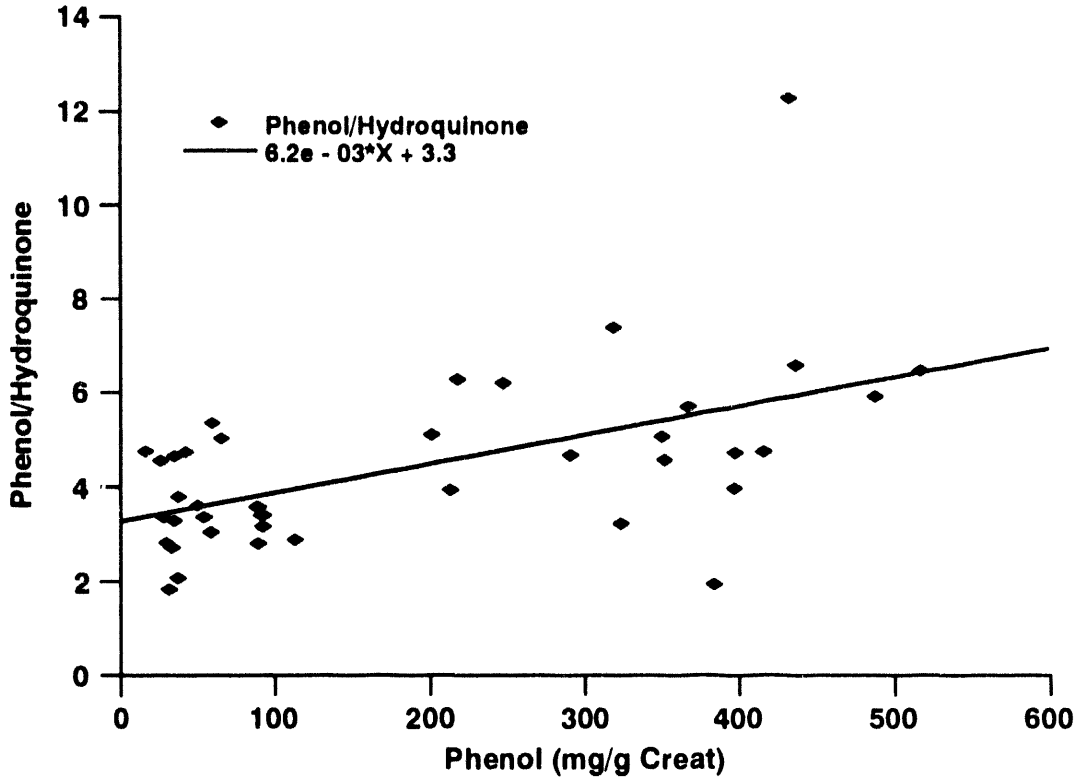

Figure 2. Concentrations of urinary phenol vs. phenol/hydroquinone in urine samples of Chinese workers exposed to benzene.

(Research sponsored by the Office of Health and Environmental Research, U.S. Department of Energy, under Contract No. DE-AC04-76EV01013.)

III. CARCINOGENIC RESPONSES TO TOXICANTS

EXPOSURE OF F344 RATS TO AEROSOLS OF $^{239}PuO_2$ AND CHRONICALLY INHALED CIGARETTE SMOKE

G. L. Finch, E. B. Barr, W. E. Bechtold, B. T. Chen, W. C. Griffith, M. D. Hoover, J. L. Mauderly, C. E. Mitchell, and K. J. Nikula

Workers in the nuclear industries may be exposed to radioactive materials such as $^{239}PuO_2$, and thus be at risk for the induction of lung cancer. Of additional concern is the possibility that interactions between $^{239}PuO_2$ and other carcinogens may increase the risks of cancer induction. An important and common lung carcinogen is cigarette smoke; however, the effect of cigarette smoking on lung cancer risk in individuals who also inhale $^{239}PuO_2$ is unknown. To better understand this relationship, we are studying the combined effects of inhaled $^{239}PuO_2$ and cigarette smoke on the induction of lung cancer in rats.

Three individual exposure blocks (Blocks A, B, and C) of from 690 to 790 male and female CDF®(F344)/CrlBR rats (purchased from Charles River Laboratories, Raleigh, NC) were placed on study during September 1991, February 1992, and May 1992 (Table 1). Rats were received at 4 ± 1 wk of age, held in Hazelton H2000 chambers (Lab Products Inc., Maywood, NJ) for 2 wk, and assigned to one of six experimental groups (Table 1). Beginning at 6 wk of age, groups of rats were exposed by the whole-body mode to either filtered air or to mainstream cigarette smoke (generated from 1R3 research cigarettes, Tobacco Health Research Inst., Lexington, KY; as described by Chen, B. T. *et al. J. Aerosol Med. 5(1)*: 19, 1992) for 6 h/day, 5 days/wk, for 6 wk. Target cigarette smoke exposure concentrations were either 100 or 250 mg total particulate matter (TPM)/m^3, except during the first week when the rats were exposed to 50% of the target concentrations.

Table 1

Experimental Design for the Chronic Study of the Combined Effects of Exposure to Cigarette Smoke and $^{239}PuO_2$ on Lung Cancer in Rats

		Approximate $^{239}PuO_2$ ILB[a]		
		0 Bq	400 Bq	Total:
Cigarette Smoke TPM	0 mg/m^3	Life: 232[b] Sac: 130	Life: 232 Sac: 100	Life: 464 Sac: 230
	100 mg/m^3	Life: 348 Sac: 130	Life: 348 Sac: 100	Life: 696 Sac: 230
	250 mg/m^3	Life: 174 Sac: 130	Life: 174 Sac: 100	Life: 348 Sac: 230
	Total:	Life: 754 Sac: 390	Life: 754 Sac: 300	Life: 1508 Sac: 690
			Experiment Total:	2198

[a]ILB = Initial lung burden.

[b]Number of rats included for either life-span exposure and observation (Life) or for assignment to serial sacrifice (Sac) groups.

At 12 wk of age, the rats were removed from the chambers and exposed nose-only to either filtered air or to aerosols of $^{239}PuO_2$ for 25 min (nominal mean values of 1.0 μm AMAD, σ_g = 1.6, 960 Bq/L air concentration) to achieve mean initial lung burdens (ILBs) of approximately 400 Bq. One week after the $^{239}PuO_2$ exposure, the rats were returned to the H2000 chambers, and cigarette smoke exposures were resumed.

To estimate the ILB and early clearance half-time for $^{239}PuO_2$, the rats were whole-body counted weekly for 6 wk for the gamma emitter ^{169}Yb which was fused as a radiolabel into the $^{239}PuO_2$ particles.

The rats will be exposed to cigarette smoke for 30 mo, or until survival falls to 10% of the total number of rats in any one experimental group and gender within the three exposure blocks. At monthly intervals, the rats are weighed and observed for clinical abnormalities. Moribund rats are euthanized, and a full necropsy is performed on all dead rats. As shown in Table 1, approximately two-thirds of the rats are being observed for life; the remaining one-third of the rats are designated for interim sacrifices. Rats from each exposure group from each block are included in the sacrifice schedule. The purposes of the interim sacrifices include (1) the collection of lung and lesion tissue for histopathological and morphometric analysis, (2) the quantitation of epithelial cell proliferation in selected rats using a 5-bromodeoxyuridine labeling technique, (3) the radiochemical analysis of ^{239}Pu for dosimetric evaluations, (4) the retention of frozen lung and blood samples for future molecular biological and biomarker studies, (5) the measurement of bone mass, and calcium and cadmium concentrations in lumbar vertebrae and femurs, and (6) the assessment of immunocompetence of lymphocytes obtained from spleens.

Additional in-life endpoints are being examined in selected groups of rats. These endpoints include (1) the periodic assessment of respiratory function, (2) the quantitation of clearance of inert radiolabeled ^{85}Sr-FAP tracer particles administered after 3 and 18 mo of smoke exposure, and (3) the measurement of nicotine and cotinine in urine at various times after initiation of exposure.

As of September 30, 1993, rats from Blocks A, B, and C had been exposed to cigarette smoke for 24, 20, and 17 mo, respectively. Mean cigarette smoke concentrations were within 5% of the targeted levels for all chambers. The chemical compositions of the smoke exposure atmospheres were consistent with our previous observations (Chen, B. T. *et al. Inhal. Toxicol. 1*: 331, 1989).

To date, survival has not been markedly affected by cigarette smoke exposure. Through 24 mo of exposure (25½ mo of age) of Block A, the cumulative surviving fractions of rats in the different exposure groups ranged from 45 to 73% for the six groups of males, and from 62 to 80% for the groups of females. Cigarette smoke-exposed rats gained less weight than chamber control rats. After 24 mo of exposing rats in Block A to 100 and 250 mg TPM/m^3, the male rats weighed 88 and 75% as much as controls, and the female rats weighed 80 and 78% as much as controls, respectively.

No other clinical manifestations have been associated with cigarette smoke and/or $^{239}PuO_2$ exposure levels to date. Initial $^{239}PuO_2$ ILBs and clearance rates, and clearance of the ^{85}Sr-FAP tracer particles, were significantly lower in smoke-exposed rats than in controls, as determined by an analysis of variance.

Gray mottling of the lungs and hypertrophy of bronchial lymph nodes have been observed at necropsy in rats exposed to cigarette smoke. Histopathological examination of a small number of rats exposed to cigarette smoke revealed alveolar macrophage pigmentation and hyperplasia, chronic-active inflammation, alveolar epithelial hyperplasia, interstitial fibrosis, and bronchial mucous cell hyperplasia in the lungs. The severity of these lesions appeared to increase with exposure time and concentration.

Through 24 mo of exposure, 35 rats had lung masses or nodules observed during necropsy that were histologically examined and confirmed as being neoplasms. Of these 35, 21 rats were from Block A, 8 were from Block B, and 6 were from Block C. The tumor phenotypes have included adenomas, adenocarcinomas, squamous cell carcinomas (all common types of radiation- or chemical-induced lung tumors in rats), a bronchial papilloma, and a carcinosarcoma (both rare lung tumors in rats).

Most of the tumors have been in rats exposed to both cigarette smoke and $^{239}PuO_2$. Figure 1 illustrates the prevalence (number of rats with tumors over the total number of rats examined at necropsy) of lung tumors observed in rats exposed to smoke for at least 12 mo, the approximate time at which the first tumor was observed. In the experimental group exposed to $^{239}PuO_2$ and 250 mg TPM/m^3, the distribution of the prevalence of the 16 rats with tumors of the 36 rats examined is 10 of 22 for Block A, 3 of 7 for Block B, and 3 of 7 for Block C. Thus, although most of the rats in the study are still alive, indications are that cigarette smoke and $^{239}PuO_2$ are interacting synergistically.

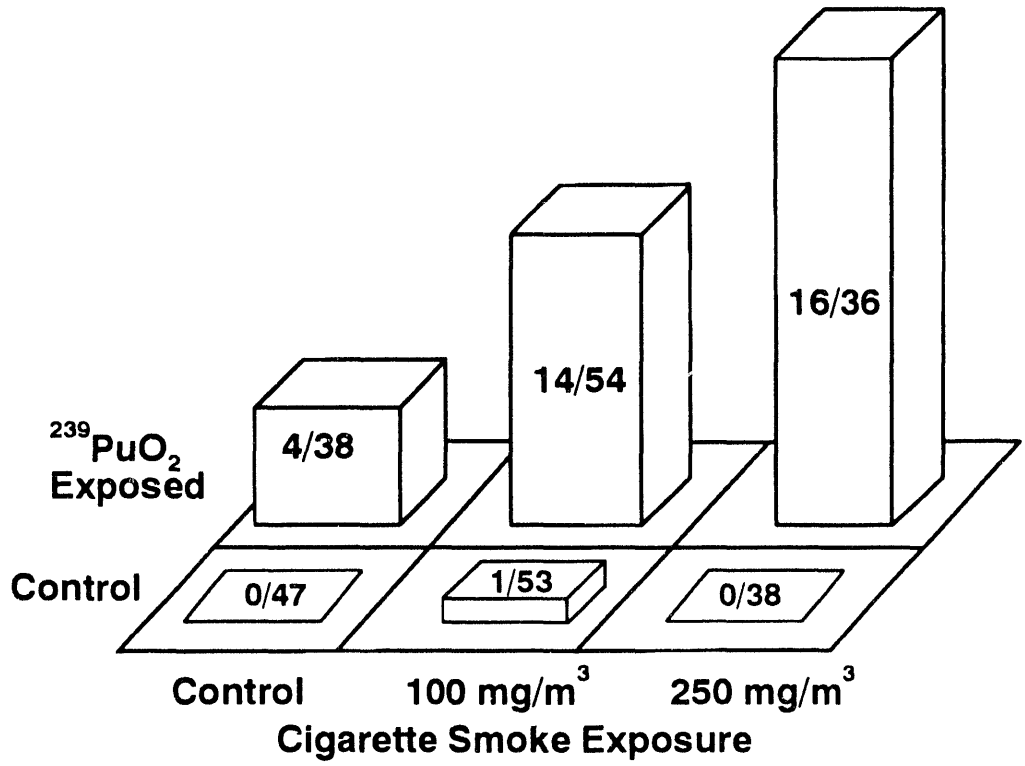

Figure 1. Prevalence by exposure group of lung tumors in rats on study for at least 12 mo. The number of rats with primary lung tumors over the total number of rats examined is indicated for each group.

This study is still in progress. At its conclusion, we anticipate that significant new information will be generated regarding the induction of cigarette smoke-induced lung cancer in rats, and the potential for interaction between cigarette smoke and $^{239}PuO_2$ exposure in the induction of lung cancer.

(Research sponsored by the Assistant Secretary for Defense Programs, U.S. Department of Energy, under Contract No. DE-AC04-76EV01013.)

EFFECTS OF COMBINED EXPOSURE OF F344 RATS TO INHALED $^{239}PuO_2$ AND A CHEMICAL CARCINOGEN (NNK)

D. L. Lundgren, S. A. Belinsky, K. J. Nikula, W. C. Griffith, and M. D. Hoover

Workers in the nuclear weapons facilities have a significant potential for exposure to radiation from external sources or from internally deposited radionuclides such as ^{239}Pu and to chemical carcinogens. Although the carcinogenic effects of inhaled ^{239}Pu and many chemicals have been studied individually, very little information is available on their combined effects (Fry, R. J. M. and R. L. Ullrich. In *Radiation Carcinogenesis*, Elsevier, New York, p. 437, 1986). One chemical carcinogen that workers could be exposed to is the tobacco-specific nitrosamine 4-(N-Methyl-N-nitrosamino)-1-(3-pyridyl)-1-butanone (NNK), a product of the curing and pyrolysis of nicotine in tobacco smoke (Hoffman, D. and S. S. Hecht. *Cancer Res. 45*: 935, 1985). NNK is rather organ-specific in that, regardless of the route of administration, tumors occur in the lungs of rats treated with the carcinogen (Rivenson, D. *et al. Cancer Res. 48*: 6912, 1988). Tumors also occur to a lesser extent in the liver, nasal passages, and pancreas.

The purpose of this study is to characterize the effects of combined exposure of rats to NNK and internally deposited plutonium, as well as to these agents alone. The rats are being observed to determine whether specific doses of NNK and internally deposited $^{239}PuO_2$ interact to increase cancer risk. Data are being collected on age-specific cancer incidence rates for cancers that occur spontaneously and as a result of exposure to alpha radiation of the lung with or without exposure to NNK. This information will aid in determining the appropriateness of different mathematical cancer risk models based upon observations of large populations of laboratory animals. A model for the development of lung tumors, illustrating the various rates to be taken into account in predicting the occurrence of lung tumors, has been presented (1986-87 Annual Report, p. 318). Our primary interest in this model is the rate at which the rats develop lung tumors and whether the combined exposure to radiation and a chemical carcinogen alters this rate.

The experimental design for this study has been previously summarized (1991-92 Annual Report, p. 118). Briefly, a total of 740 male 4 ± 1-wk-old CDF®(F344)/CrlBR rats purchased from Charles River Laboratories (Kingston, NY) are being used in the study. A block experimental design consisting of two blocks with 370 rats each was used to enter the rats into the study. The first block of rats was entered into this study in FY92. The second block of rats was entered into this study this year. Rats were randomized by weight for assignment to dose groups within each block. At death, all rats are necropsied, and major organs and all lesions for histological examination are fixed in 4% buffered paraformaldehyde for histologic examination.

For this study, the alpha dose to lungs was expected to induce a 15% incidence of lung tumors (1987-88 Annual Report, p. 245; Lundgren, D. L. *et al. Human Exp. Toxicol. 9*: 295, 1990; Lundgren, D. L. *et al. Health Phys. 60*: 353, 1991). The methods used for the inhalation exposures of rats to ^{169}Yb-labeled $^{239}PuO_2$ have been described (Lundgren *et al.*, 1991). Doses of NNK, dissolved in physiological saline, sufficient to result in a 15%, 50%, or 90% incidence of lung tumors when given by subcutaneous injection three times per week for 20 wk were used (Belinsky, S. A. *et al. Cancer Res. 50*: 3772, 1990). The high dose NNK group (50 mg kg^{-1}; 90% lung tumor incidence expected) was included in this study to provide tumors to be used in molecular biological studies to aid in understanding the interactions of the combined exposure to NNK and $^{239}PuO_2$. None of the rats in the 50 mg kg^{-1} group were exposed to $^{239}PuO_2$. The NNK injections began when the rats were 6 wk of age, and $^{239}PuO_2$ exposures occurred when the rats were 12 wk of age. Rats treated with 50 mg NNK kg^{-1} body mass had a slower rate of body weight gain than the other groups of rats in this study. The injections of the lower doses of NNK and exposure to $^{239}PuO_2$ have not affected body weight gain.

Because the exposure to the combination of $^{239}PuO_2$ and NNK may alter the lung tumor incidences and/or death rates, it is necessary to include interim sacrifices to determine the rate at which animals develop lung tumors (1986-87 Annual Report, p. 318; McKnight, B. and J. Crowely. *J. Am. Stat. Assoc. 79*: 639, 1984). Four rats at each interval per group exposed to ^{239}Pu were sacrificed from 8 through 360 days after exposure to obtain more detailed information on the clearance of ^{239}Pu for dosimetry purposes. Additional rats are scheduled

for sacrifice at 450 days after exposure. Additional data on ^{239}Pu clearance are being obtained from the necropsies of rats that die spontaneously.

The initial lung burdens (ILBs) and clearance half times for ^{239}Pu for rats in this study are summarized in Table 1. Only the mean ILB of the rats treated with 1.0 mg kg^{-1} NNK was significantly less than that in the controls. The early clearance half times of the inhaled ^{239}Pu, as determined from the whole-body counting of the ^{169}Yb radiolabel, were significantly slower (two-tailed Student's *t* test; $p < 0.05$) in the NNK-treated groups than in the controls. Completion of the radiochemical analyses of lung tissue for ^{239}Pu will provide data on the long-term retention in the various groups of rats. This should provide a clearer understanding of the effects of NNK treatment on ^{239}Pu clearance.

Table 1

Initial Lung Burden (ILB) and Clearance Half Times for ^{239}Pu in Rats in Both Blocks Exposed by Inhalation to Aerosols of $^{239}PuO_2$ With and Without Receiving NNK by Injection

NNK Dose[a] Day^{-1}	N	^{239}Pu ILB and Early Clearance Half Times	
		ILB (Bq ± SD)	Clearance Half Times (Days ± SD)[b]
Sham	136	480 ± 70	33 ± 4
0.3 mg kg^{-1}	145	470 ± 68	40 ± 12[c]
1.0 mg kg^{-1}	113	460 ± 76[d]	37 ± 12[c]

[a]None of the rats treated with 50 mg kg^{-1} body mass group was exposed to $^{239}PuO_2$.

[b]Based on the whole-body counting of the ^{169}Yb radiolabel for the ^{239}Pu corrected for the physical decay of the ^{169}Yb.

[c]Mean clearance half times significantly greater (two-tailed Student's *t* test; $p < 0.05$) from that in the sham-NNK-exposed rats.

[d]Mean ILB significantly less (two-tailed Student's *t* test; $p < 0.05$) than that in the sham-NNK-treated group.

As of September 30, 1993, 31 rats had died spontaneously or were euthanized when moribund, 84 had been sacrificed, three had been removed from study for reasons unrelated to this study, and 622 remained alive. Twenty-one of the rats that died or were euthanized were in the group treated with 50 mg NNK kg^{-1} body weight. The deaths of the remaining seven rats did not appear to be related to either the NNK treatment levels or to the $^{239}PuO_2$ exposure. This study will provide information on whether combined exposure to a chemical carcinogen (NNK) and alpha radiation from inhaled $^{239}PuO_2$ acts in an additive, synergistic, or antagonistic manner in inducing lung cancer in rats.

(Research sponsored by the Assistant Secretary for Defense Programs, U.S. Department of Energy, under Contract No. DE-AC04-76EV01013.)

COMBINED EXPOSURE OF F344 RATS TO BERYLLIUM METAL AND $^{239}PuO_2$ AEROSOLS

G. L. Finch, F. F. Hahn, W. W. Carlton, A. H. Rebar*, M. D. Hoover, W. C. Griffith, J. A. Mewhinney**, and R. G. Cuddihy*

Many workers in nuclear weapons industries have the potential for inhalation exposures to plutonium (Pu) and other agents, such as beryllium (Be) metal. Inhaled Pu deposited in the lung delivers high-LET alpha particle radiation and is known to induce pulmonary cancer in laboratory animals (BEIR-IV, 1988). Although the epidemiological evidence implicating Be in the induction of human lung cancer is weak and controversial, various studies in laboratory animals have demonstrated the pulmonary carcinogenicity of Be, and it is currently classified as a suspect human carcinogen (U.S. EPA/600/8-84/026F, 1987). We are investigating the potential interactions between Pu and Be in the production of lung tumors in rats exposed by inhalation to particles of plutonium dioxide ($^{239}PuO_2$), Be metal, or these agents in combination.

In our initial studies, a total of 2856 rats (F344/N; both male and female; 12 ± 1 wk old at exposure) reared at this Institute were exposed once pernasally in eight blocks of 354 or 360 animals. Blocks were entered into the study over a 15-mo period (October 1987 to January 1989; see the 1991-92 Annual Report, p. 112 for the experimental design matrix). Groups of 60 rats received $^{239}PuO_2$ (0.7 μm AMAD, 1.7 σ_g, 5-25 min exposure, 630 Bq/L), followed immediately by exposure to Be metal (1.4 μm MMAD, 1.9 σ_g, 8-50 min exposure, 200-1200 mg/m^3), or the appropriate air control. Rats received one of two target initial lung burdens (ILBs) of $^{239}PuO_2$ (56 or 170 Bq), and/or one of three target ILBs of Be metal (50, 150, or 450 μg).

Rats were designated for either serial sacrifice or for life-span observation. At death, a complete necropsy was performed, and lungs, other selected tissues, and all lesions were fixed in formalin for histological analysis. All rats involved in this study were dead as of March 1991.

We found that Be exposure significantly retarded the clearance of ^{239}Pu (1989-90 Annual Report, p. 125). We also observed significant mortality from acute pneumonitis of 33 and 64% of the male and female rats in the 450 μg group of Be metal within 3 wk of exposure, and further noted that for a given $^{239}PuO_2$ exposure group, increased levels of Be metal increased the mortality rate (1990-91 Annual Report, p. 99).

Histological evaluation of the lungs of the rats is in progress. As of September 30, 1993, lung tissues from all control rats and those exposed only to Be metal have been examined. The crude incidence of lung tumors (combined benign and malignant) is shown in Table 1. The most prevalent malignant neoplasm observed thus far is the bronchiolar/alveolar adenocarcinoma having alveolar, papillary, or tubular patterns. Other tumor types observed include adenosquamous carcinomas and squamous cell carcinomas. These results demonstrate a substantial incidence of Be metal-induced lung tumors in all exposure groups; in addition, a number of the Be-metal-exposed rats have multiple tumors (data not shown). Approximately 25% of the lungs of rats in the combined exposure groups have been histologically examined; crude incidences of malignant lung tumors in this group were given in our 1991-92 Annual Report, p. 112.

Our results to date reveal significantly higher incidences of lung tumors than expected based on extrapolations from a limited data base in the literature (Sanders, C. L. *et al. Health Phys. 35*: 193, 1978; Groth, D. H. *Environ. Res. 21:* 84, 1980; Nolibe, D. *et al. Commissariat A L'Energie Atomique 1984 Annual Report*, 1984). Because interactions between two carcinogens are best analyzed when lung tumor incidences from the individual agents are relatively low, a second phase of this study was initiated using lower ILBs of Be.

The experimental design for phase two of the combined effects study is shown in Table 2. This study is using CDF®(F344)/CrlBR rats purchased from Charles River Laboratories; significant design features include (1) the use of relatively large numbers of rats exposed to Be metal only to define dose-response relationships

*Purdue University, Lafayette, Indiana

**Currently at Waste Isolation Pilot Plant, U.S. D.O.E., Carlsbad, New Mexico

for Be metal-induced carcinogenicity, (2) the combined exposure of two Be metal dose groups with $^{239}PuO_2$, and (3) the addition of a group of rats exposed only to $^{239}PuO_2$ at a relatively higher initial dose rate, to mimic the increased cumulative radiation dose caused by Be metal-induced lung clearance reductions that are likely to occur in the combined exposure groups.

Table 1

Number of Rats Exposed to Be Metal or Controls Having Lung Tumors - Phase 1[a]

	Mean (± S.D.) Be Lung Burden[b] (μg)							
	Control		33 (± 14)		84 (± 30)		420 (± 230)	
	M	F	M	F	M	F	M	F
Number of rats examined:	107	103	114	117	109	108	56	35
Number with benign and/or malignant lung tumors:	2	0	71	97	97	104	50	35
Number with malignant lung tumors:	2	0	44	82	60	90	40	28

[a]For rats living 1 yr or more after exposure.

[b]Lung burdens estimated from measurement of Be burden for each rat at time of death and extrapolation from days after exposure back to exposure date using the formula ILB = $A_t \cdot \exp(0.0032t)$, where A_t is the quantity of Be present in lung at death, and t is the number of days from exposure to death. The exponential factor 0.0032 is a representative slope of a single component negative exponential function describing clearance of Be from rat lung (Finch, G. L. *et al.* In *Proceedings of the 4th International Conference on the Combined Effects of Environmental Factors* [L. Fechter, ed.], Department of Environmental Health Sciences, Johns Hopkins University, Baltimore, MD, p. 49, 1991).

Table 2

Experimental Design to Study the Combined Effects of $^{239}PuO_2$ and Be Metal in Rats - Phase 2

	$^{239}PuO_2$ ILB[a]			
Be Metal ILB	0 Bq	230 nCi	460 nCi	TOTAL
0 μg	270[b]	288	156	714
0.3 μg	288	–	–	288
1.0 μg	288	288	–	576
3.0 μg	288	–	–	288
10 μg	288	288	–	576
50 μg	156	–	–	156
TOTAL	1578	864	156	2598

[a]ILB = Initial lung burden.

[b]Number of rats per group. Equal numbers of males and females.

As of September 30, 1993, 50% of the rats comprising this phase of the study have been exposed. Properties of the exposure atmospheres are similar to those in the first study, except that the Be metal exposure occurs 1 day after the $^{239}PuO_2$ exposure, and the exposure mass concentrations of Be range from 0.8 to 140 mg/m^3. As before, the $^{239}PuO_2$ particles are labeled with ^{169}Yb (<3% by mass) to permit periodic external radioactivity counting through 42 days after exposure for determination of $^{239}PuO_2$ ILB. Early results indicate that exposure to Be metal decreased $^{239}PuO_2$ clearance compared to controls over this 42-day period. Clearance half-times for males and females combined were 39 ± 7 (S.D.), 76 ± 10, or 137 ± 17 days for groups of rats receiving 0, 1, or 10 μg target ILBs, respectively.

This study is continuing, with the exposure of the remaining animals planned in FY-1994. As the data are obtained and analyzed, this work will serve to define the pulmonary carcinogenicity of Be metal in the rat, and will provide information regarding the potential interaction between Be metal and $^{239}PuO_2$ in causing lung cancer.

(Research sponsored by the Assistant Secretary for Defense Programs, U.S. Department of Energy, under Contract No. DE-AC04-76EV01013.)

EFFECTS OF COMBINED EXPOSURE OF F344 RATS TO $^{239}PuO_2$ AND WHOLE-BODY X-RADIATION

D. L. Lundgren, F. F. Hahn, W. C. Griffith, W. W. Carlton, M. D. Hoover, and B. B. Boecker*

Many workers in the nuclear weapons industries have significant potential for exposure to both inhaled plutonium and external whole-body radiation. Inhaled plutonium delivers high-LET (linear energy transfer) alpha radiation, primarily to the pulmonary tissues, where it may add to, or multiply, the risk from low-LET external irradiation. The individual effects of these different types of radiation exposures have been studied in laboratory animals. These studies have included external exposure to high- and low-LET radiation or internal exposure to a variety of radionuclides irradiating specific organ systems with high- or low-LET radiation.

The purpose of this research was to characterize the lifetime effects of combined exposure of rats to external x-radiation and internally deposited plutonium, as well as to each agent alone. The animals were being observed to determine how specific exposure levels and combinations of radiation may interact to modify cancer risk. As part of the design of these studies, data based upon observations of large populations of laboratory animals were collected on cancer incidences as a function of age for cancers that occur spontaneously or from exposure to radiation. This information will aid in determining the appropriateness of different mathematical cancer risk models. A model for the development of lung tumors, illustrating the various rates to be taken into account in predicting the occurrence of lung tumors, has been published (1986-87 Annual Report, p. 318). Our primary interests in this model are the rates at which animals develop lung tumors and whether the combined radiations alter these rates.

Details of the experimental design for this study have also been presented (1986-87 Annual Report, p. 318). Briefly, a total of 3199 (1592 male and 1607 female) 11-to 13-wk old F344/N rats reared at this Institute were used. A block experimental design was used to enter rats into the study. Rats were randomized by litter for assignment to dose groups within each block so that biological variability would be distributed throughout each dose group. At death, all rats were necropsied, and major organs and all lesions were fixed in 10% neutral buffered formalin for histologic examination.

For this study, radiation doses to the lungs from inhaled $^{239}PuO_2$ and whole-body x-radiation that would result in 5% and 15% incidences of lung tumors were estimated from results of other studies of $^{239}PuO_2$ in rats and from previously published studies of the effects of whole-body x-radiation. The methods used for the inhalation exposures of rats to $^{239}PuO_2$ and their subsequent whole-body x-radiation have been described (1987-88 Annual Report, p. 251). Several interim sacrifices were conducted during the course of this study. Because the combined radiation may alter both the lung tumor incidence and the death rates, it was necessary to include interim sacrifices in order to determine the rates at which the animals developed lung tumors (McKnight, B. and J. Crowely. *J. Am. Stat. Assoc. 79*: 639, 1984). Data to determine the clearance patterns of the inhaled ^{239}Pu are being obtained from tissues collected during necropsies of serially sacrificed animals and animals that die spontaneously.

The mean initial lung burdens achieved in each experimental group and the corresponding potential average alpha doses to lung have been summarized (1990-91 Annual Report, p. 94). The initial lung burdens and radiation doses to the lungs, which were relatively consistent within each ^{239}Pu exposure level, were within the desired ranges.

The last rats in this study died during the past year. A final summary of the survival of the rats in each experimental group is presented in Table 1. No significant life shortening occurred among the rats exposed only to $^{239}PuO_2$ compared with the respective sham-inhalation-exposed rats. Within each X-ray exposure group, there was also no life shortening related to the $^{239}PuO_2$ exposures.

*Department of Veterinary Pathobiology, Purdue University, Lafayette, Indiana

In contrast, a dose-response relationship for life shortening occurred among the rats exposed to whole-body x-radiation with shorter survival times of female rats than male rats. Among the groups of rats that received 3.84 Gy of X rays, the median survival times were decreased by an average of 10% in the males and 18% in the females compared with the respective sham-X-ray- and $^{239}PuO_2$-exposed groups. Among those exposed to 11.5 Gy of X rays, the median survival times were decreased by an average of 28% in the males and 34% in the females compared with the respective sham X-ray and $^{239}PuO_2$-exposed groups.

Table 1

Survival of Rats in the Study of Combined Exposure to Inhaled $^{239}PuO_2$ and Whole-Body X-Radiation

Experimental Group Numbers	Exposure		Number Exposed[a]		Median Survival Time (MST) (days ± SE)	
	^{239}Pu ILB[b]	X-Ray[c,d]	Males	Females	Males	Females
I	Sham	Sham	160	160	617 ± 12	719 ± 13
II	56 Bq	Sham	192	191	618 ± 9	750 ± 13
III	170 Bq	Sham	182	182	607 ± 11	749 ± 14
IV	Sham	3.84 Gy	158	156	557 ± 10	594 ± 10
V	56 Bq	3.84 Gy	192	192	565 ± 10	620 ± 7
VI	170 Bq	3.84 Gy	188	191	549 ± 7	593 ± 13
VII	Sham	11.5 Gy	160	160	431 ± 11	485 ± 13
VIII	56 Bq	11.5 Gy	191	191	451 ± 9	473 ± 14
IX	170 Bq	11.5 Gy	172	183	449 ± 10	492 ± 12
		Totals	1595	1606		

[a]Includes spontaneous deaths and rats sacrificed for dosimetry and for determining the rate of lung tumor development.
[b]ILB = Initial lung burden.
[c]X-ray exposure divided into two split doses, one at 30 and the other at 60 days after exposure to $^{239}PuO_2$.
[d]Gy = 0.0096 x R.

The radiochemical analyses of lung samples from all rats exposed to $^{239}PuO_2$ have been completed. These data were used in up dating (Table 2) our preliminary data (1991-92 Annual Report, p. 115) on the retention of the initial lung burdens of ^{239}Pu in the rats in this study. The percentage of the initial lung burden in the long-term component of retention increased with increasing X-ray dose. However, the clearance half time of this component decreased with increasing X-ray dose. Further analyses is needed in order to better understand the differences in these retention patterns.

Histological evaluations have been completed on 2125 (66%) of the 3199 rats entered into this study and were reported last year (1991-92 Annual Report, p. 115). Histopathological evaluations of tissues from the remaining rats are in progress. Completion of this study will provide information on whether exposure to inhaled $^{239}PuO_2$ and whole-body x-irradiation are additive or synergistic for the induction of lung tumors in rats.

Table 2

Pulmonary Retention of ^{239}Pu in Rats Exposed to Whole-Body X-Radiation after Exposure by Inhalation to Aerosols of $^{239}PuO_2$

^{239}Pu ILB[a] (Bq)	X-Ray Exposure (Gy)[b,c]	N	Retention Parameters (± SD)[d]			
			100-A (%)	T_1 (days)	*A* (%)	T_2 (days)
56	Sham	344	88[e]	63 ± 6	12 ± 2	680 ± 160
170	Sham	330	89	53 ± 6	11 ± 1	800 ± 160
56	3.84	356	84	53 ± 7	16 ± 2	560 ± 100
170	3.84	330	84	45 ± 7	16 ± 2	520 ± 100
56	11.5	342	78	43 ± 6	22 ± 3	400 ± 65
170	11.5	332	83	46 ± 6	17 ± 2	490 ± 86

[a]ILB = Initial lung burden.
[b]See Table 1 for ^{239}Pu ILBs.
[c]Gy = 0.0096 x R.
[d]Retention described by: $Y(t) = (100\text{-}A)e^{-0.693t/T_1} + Ae^{-0.693t/T_2}$,
where 100-A and A are percentages of the initial lung burdens, and T_1 and T_2 are days after exposure to $^{239}PuO_2$.
[e]No ±SD was determined for 100-A because it was forced to equal 100%.

(Research sponsored by the Assistant Secretary for Defense Programs, U.S. Department of Energy, under Contract No. DE-AC04-76EV01013.)

EFFECTS OF THORACIC AND WHOLE-BODY EXPOSURE OF F344 RATS TO X RAYS

F. F. Hahn, D. L. Lundgren, W. C. Griffith, and B. B. Boecker

The risk of radiation-induced lung cancer has been determined from groups of people exposed to external X rays, radiation from atomic weapons explosions, or radon and its progeny. Data from numerous studies of laboratory animals have been reviewed for use in estimating lung cancer risk factors for people (Cuddihy, R. G. In *Proceedings of the 17th Annual Meeting of the National Council on Radiation Protection and Measurements*, Washington, DC, p. 133, 1982). However, some of the studies may have resulted in an underestimate of risk, because the relatively high radiation doses used resulted in life shortening and, theoretically, a reduction in tumor yield. Consequently, it has been concluded that only studies which include larger groups of animals (i.e., 500 per group) than previously used can address some of the questions on the dose-response relationships of inhaled radionuclides at relatively low doses (McClellan, R. O. *Health Phys.* 55: 279, 1988).

Based on previous results (1983-84 Annual Report, p. 251), we proposed to expose laboratory rats to relatively low, non-life-shortening doses of X rays or inhaled beta-emitting radionuclides as an experimental approach to estimating the risk of lung cancer in people. One study involved fractionated x-irradiation of the thorax in one group and the single or fractionated exposure of the whole body of two other groups of rats. This report summarizes the status of these studies. When completed, these results will be compared with those from a study conducted at Battelle Pacific Northwest Laboratory (Sanders, C. L. *et al. Health Phys.* 55: 455, 1988), of the effects of relatively low, alpha-radiation doses to lungs of rats exposed by inhalation to aerosols of $^{239}PuO_2$. The data will, in turn, be compared with other studies on the effects of radionuclides inhaled in relatively insoluble forms, especially those involving relatively low doses to the lungs, and with data on the effects of partial or whole-body x- or gamma-radiation.

The experimental design for this work has been reported (1986-87 Annual Report, p. 313). A total of 3871 (1933 male and 1938 female), 12-wk old, laboratory-reared, specific pathogen-free CDF®(F344)/CrlBR rats were used. Briefly, groups of rats were exposed either to fractionated doses of X rays to the thorax or to the whole body, on 10 successive workdays (M-F), or to a single, whole-body exposure. The total absorbed radiation doses were 3.5, 5.8, 11, and 38 Gy for the fractionated thoracic exposures, 3.5 and 5.8 Gy for the fractionated whole-body exposure, and 5.8 Gy for the single, whole-body exposure.

The rats were entered into this study in 12 blocks and randomly assigned to experimental groups by litter to randomize characteristics of a litter. At death, all rats were necropsied, and major organs and all other tissues with lesions were fixed in 10% neutral buffered formalin for histologic examination.

A Picker Vanguard X-ray therapy machine (Picker X-Ray Corp., Cleveland, OH) was used to irradiate the rats. This unit was operated at 280 kVp at 18 mA, with 1 mm Al and 0.5 mm Cu filters, resulting in an equivalent energy of 135 keV. The exposure rate was about 0.221 Gy (23 R) min^{-1} at 1 meter. The rats were placed on a turntable that rotated at two revolutions per minute during the exposures. The X-ray exposures were monitored with a Victoreen R-meter and LiF thermoluminescent dosimeters (Eberline, Albuquerque, NM). Plastic boxes covered with 6.4 mm Pb were constructed so that the bodies of the rats, restrained in standard plastic exposure tubes, were shielded while the thorax was exposed through an opening in the Pb shield. The exposure times ranged from approximately 1.5 to 26 min per exposure, depending on the exposure required.

All rats in this study are now dead; the survival times and patterns remain similar to those previously reported (1991-92 Annual Report, p. 121). As anticipated, the higher radiation doses reduced survival time. With fractionated thoracic irradiation, 38 Gy reduced survival about 10% in male and females, and 11 Gy reduced survival about 5% in females. With whole-body exposures, 5.8 Gy reduced survival 15 to 20% in both males and females, but 3.8 Gy did not affect survival.

Histopathology on the lungs has been completed on 70% of the animals. The primary lung tumors were classified as adenoma, adenocarcinoma, adenosquamous carcinoma, squamous cell carcinoma, and sarcomas. The

percentage of squamous cell carcinomas was higher in the lower dose groups, comprising 40% of the lung tumors observed after fractionated, whole-body exposure of 3.5 Gy. This increased percentage of squamous cell carcinomas at lower doses is in contrast to the frequency seen with inhaled beta-emitting radionuclides. With inhaled $^{144}CeO_2$ in rats, squamous cell carcinomas were more frequent and were a higher percentage of lung tumors at the higher radiation doses (Hahn, F. F. and D. L. Lundgren. *Toxicol. Pathol. 20*: 169, 1992). The reason for this difference in response to external x-irradiation and irradiation from an internally deposited beta-emitting radionuclide is unknown.

The lung tumor incidence shown in Table 1 is based on the histopathology completed to date. The results show that x-irradiation induced a significant increase in lung tumors, even at 3.5 Gy. They also show that the thoracic and whole-body exposure and single and fractionated exposures produced similar lung tumor incidences. This table should be interpreted with caution, however, because the histopathology is incomplete and not random. Further age-specific incidence analyses will be conducted when the histopathology is complete. These results will then be used to develop dose-response relationships for lung tumor induction in rats by x-irradiation.

Table 1

Lung Tumor Incidence Related to Dose

Dose (Gy)	Exposure Type	Total Exposed	Number Examined[a]	Crude Incidence (%) of Tumors[a]		
				Benign	Malignant	Total
0	Sham	1008	588	0.0	0.0	0.0
3.5	Fractionated thoracic	1005	585	0.5	1.9	2.4
3.5	Fractionated whole-body	300	294	0.0	1.7	1.7
5.8	Fractionated thoracic	500	289	1.4	3.1	4.5
5.8	Fractionated whole-body	503	497	0.8	3.0	3.8
5.8	Single whole-body	500	500	0.8	4.4	5.2
11	Fractionated thoracic	238	158	0.7	6.3	7.0
38	Fractionated thoracic	120	120	0.9	6.6	7.5

[a]Number with histopathology examination as of September 30, 1993.

Because similar dose-response data for X-ray-induced lung tumors are available from exposed human populations, this information will provide a valuable link between rats and people for x-radiation-induced lung cancers. When combined with results from studies of rats exposed to internally deposited alpha- or beta-emitting radionuclides, these data will aid in determining risk factors for humans exposed to such radionuclides.

(Research sponsored by the Office of Health and Environmental Research, U.S. Department of Energy, under Contract No. DE-AC04-76EV01013.)

EFFECTS OF INTRAPLEURAL INNOCULATION OF F344 RATS WITH SILICON CARBIDE WHISKERS AND CONTINUOUS GLASS FILAMENTS

N. F. Johnson and F. F. Hahn

Silicon carbide whiskers (SiCW) and continuous glass filaments (CGF) are used in the aerospace, automotive, and power generation industries as reinforcing materials in advanced ceramic composites. SiCW are single crystal structures that can have a fine fibrous morphology. The diameter of these fine fibers is typically 1 μm or less. CGF are coarse fibers with diameters of 10-30 μm. The fibrous morphology of SiCW is similar to that of asbestos. There is concern that exposure to SiCW may be associated with similar health risks known to occur following exposure to asbestos (pulmonary fibrosis, lung cancer, and mesothelioma). Recent *in vitro* studies in cultured lung epithelial cells and alveolar macrophages have shown that SiCW possess biological activity which is similar to that seen with asbestos (Johnson, N. F. *et al. Am. J. Ind. Med. 21*: 807, 1992). In contrast, the CGF did not display any adverse biological activity toward cultured cells. The *in vitro* cytotoxicity associated with SiCW indicates the necessity of undertaking *in vivo* studies with these materials.

A study was conducted to determine the *in vivo* mesothelioma-inducing potential of SiCW. In addition, *in vivo* studies were also conducted with CGF. The *in vivo* assay chosen was the intrapleural injection approach. This assay provides a useful screen to identify fibrous materials that do not produce a neoplastic response (Johnson, N. F. In *Fiber Toxicology*, Academic Press, San Diego, p. 43, 1993), and is simpler to conduct than inhalation exposures. However, fibers that produce a positive response in the intrapleural injection assay should be further assessed by the inhalation route of exposure (Johnson, 1993).

Two-hundred-and-twenty female F344/N rats, 6-8 wk old, from the Institute's colony were used for this study. The rats were randomly allocated to the experimental groups (Table 1). Each rat was injected intrapleurally with either saline, silicon carbide samples #1, #2, or #3, UICC crocidolite, or PRD-166 (a CGF) suspended in saline. These samples were identical to those used in previous cell culture studies (Johnson *et al.*, 1992). The rats were killed by intraperitoneal injection of sodium pentobarbital when moribund or when 20% of the longest surviving group of rats (injected with PRD-166) remained alive.

Table 1

The Occurrence of Pleural Mesotheliomas in the Various Treatment Groups

Sample	Number of Animals	Animals with Mesothelioma	Percent of Animals with Mesothelioma	Time of First Tumor	Mean Time to Tumor/Days (± Standard Error)
Saline	50	0	0	–	–
PRD-166	50	0	0	–	–
SiCW #1	30	27	90	320	465 ± 25
SiCW #2	30	26	87	273	499 ± 15
SiCW #3	30	7	23	349	651 ± 30
Crocidolite	30	17	57	416	608 ± 23

All rats were necropsied and examined for gross lesions. The spleen, kidneys, liver, heart, lungs, trachea, and larynx were removed and fixed in 10% neutral buffered formalin (10% NBF). The lungs were inflated with 10% NBF to 30 cm H_2O. The diaphragm and any identifiable lesion on the parietal chest wall and elsewhere in the thoracic cavity were also removed and immersed in 10% NBF. Fixed tissue was prepared for

conventional paraffin-embedding and examination by light microscopy using sections stained with hematoxylin and eosin. Only lung and thoracic lesions were routinely examined. The tumor incidence was determined from the number of rats that developed pleural mesotheliomas.

The animal survival data were analyzed by the Kaplan-Meier method. The Student's *t* test was used to determine whether the results from the exposed rats were significantly different ($p = 0.05$) from those of the controls.

The first death occurred from respiratory distress at 166 days after inoculation with SiCW #2, and the first tumor was found after 273 days with SiCW #2. Rats inoculated with SiCW #1 or #2 had the shortest life spans (Fig. 1). Rats treated with crocidolite, the positive control, had intermediate life spans compared to the rats treated with the SiCW #1 or #2 and to rats treated with saline vehicle control (Fig. 1). Rats treated with PRD-166 had life spans similar to the rats treated with saline. Rats treated with SiCW #3 had life spans between the saline- and crocidolite-treated rats. The life spans of the rats treated with SiCW #1 or #2 and crocidolite were significantly shorter than those of the saline-treated animals. The life spans of the rats treated with PRD-166 or SiCW #3 were not significantly different to those of the saline-treated rats.

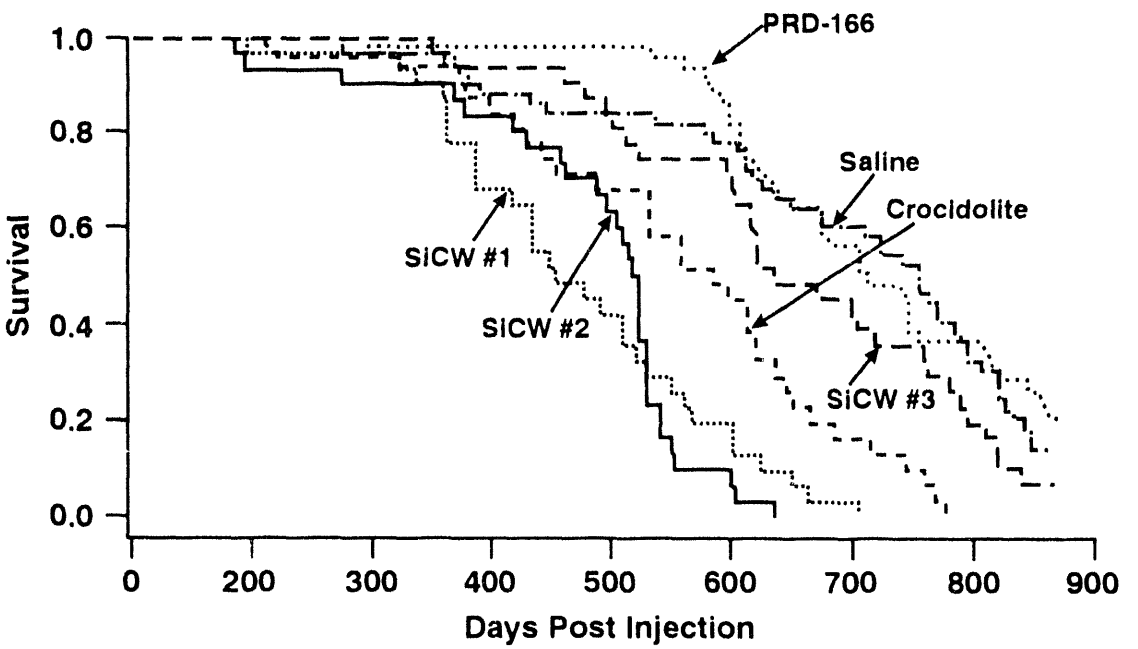

Figure 1. The fraction of rats surviving following intrapleural injection differs with the different inoculations. Saline and PRD-166 show a similar response, which is different from crocidolite, the positive control. SiCW #1 and #2 also show a similar response, which is also different from that of crocidolite.

Histopathological examination of the thoracic contents from all rats showed that the three samples of SiCW displayed varied abilities to induce pleural mesotheliomas (Table 1). SiCW #1 and #2 resulted in 90% and 87%, respectively, of the treated rats developing pleural mesothelioma. SiCW #3 resulted in 27% of the treated rats developing pleural mesotheliomas. The positive control (crocidolite) resulted in 57% of the treated rats developing pleural mesotheliomas. No tumors were identified in the saline or PRD-166-treated animals (Table 1). The tumors, with one exception, were sarcomatous in appearance and in all but one case involved the visceral pleura. Fibers were found in sections from all treatment groups with the exception of those animals treated with saline or PRD-166.

These results demonstrate that SiCW can induce mesotheliomas when introduced into the pleural cavity, and that two samples were as carcinogenic as asbestos. The marked responses with two of the three SiCW samples indicate that SiCW should be handled with care and treated as a suspect carcinogen until the results of long-term inhalation studies are available.

The difference in the biological activity of the three SiCW samples cannot be explained by differences in fiber morphology. The fiber length/diameter distributions were similar for all three. None of the samples contained a disproportionate number of long, thin fibers, which are thought to be important in fiber carcinogenesis (Stanton, M. F. *et al. J. Natl. Cancer Inst. 58*: 587, 1977). The *in vitro* activity of the three SiCW samples did not indicate the *in vivo* biological activity. These results showed that physico-chemical characterization and *in vitro* cytotoxicity studies cannot accurately predict *in vivo* activity. In addition, studying only one example of a class of fibrous materials may not reflect the biological activity of the individual members of the class.

There is a limited amount of published information detailing the toxicological properties of SiCW and CGF. The results of this intrapleural study support results from previous animal studies. Two studies have been reported involving SiCW implanted into the pleural cavity (Stanton *et al.*, 1977) and injected into the peritoneal cavity (Pott, F. *et al. Exp. Pathol 32*: 129, 1992). The study of Pott *et al.* (1992) gave an unequivocal positive result although many of the animals died of an infectious lung disease. In addition, the intraperitoneal route of administration may be overly sensitive to injected fibers and particles such as silica (Johnson, 1993). Stanton *et al.* (1977) reported a high incidence of pleural tumors in rats implanted with SiCW. In a subchronic inhalation study in rats, pleural thickening and increased cellularity of the lung parenchyma were observed at 26 wk after a 13-wk exposure to a high concentration of SiCW (6 h/day, 5 days/wk, 500-7500 f/cc) (Lapin, C. A. *et al. Fundam. Appl. Toxicol. 16*: 128, 1991). The significance of the pleural thickening is not known; however, this lesion has been reported following exposure to erionite in rats (Johnson, N. F. and J. C. Wagner. In *Biological Interaction of Inhaled Mineral Fibers and Cigarette Smoke*, Battelle Press, Columbus, p. 325, 1989) and refractory ceramic fibers in hamsters (Hesterberg, T. W. *et al.* In *Mechanisms of Fibre Carcinogenesis*, Plenum, New York, p. 531, 1992). In both studies, high incidences of mesotheliomas were reported.

The results of this study also show that CFG (PRD-166) did not induce mesotheliomas when injected into the pleural cavity of rats. Inhalation and intratracheal assays have not been reported for glass filaments. Large diameter glass fibers with similar diameters to glass filaments did not produce tumors following intrapleural implantation (Stanton *et al.*, 1977). Glass filaments did not produce a significant mesothelioma incidence following intraperitoneal inoculation of high doses (up to 250 mg) of the material (Pott *et al.*, 1992). This information combined with the negative *in vitro* data (Johnson *et al.*, 1992) and the fact that the diameter of this material precludes inhalation show that exposure to CGF should not represent a significant health hazard.

(Research sponsored by the Office of Health and Environmental Research, U.S. Department of Energy, under Contract No. DE-AC04-76EV01013.)

BONE TUMOR INCIDENCE IN BEAGLE DOGS THAT INHALED SOLUBLE RADIONUCLIDES

B. A. Muggenburg, F. F. Hahn, B. B. Boecker, K. J. Nikula, R. A. Guilmette, and W. C. Griffith

A number of the life-span studies of Beagle dogs conducted at ITRI involved the inhalation of soluble forms of radionuclides having different half-lives, metabolic characteristics, and radiation emissions. One purpose of these studies was to determine which organs would be at risk for the development of significant long-term biological effects. The skeletal system was considered to be one of the organs at higher risk for the development of cancers because several of these radionuclides were known to accumulate preferentially in bone.

The studies conducted with radionuclides that were relatively soluble in body fluids are listed in Table 1. Dogs in a particular study were exposed once, by inhalation, to one of these radionuclides except those exposed to $^{137}CsCl$, which was injected intravenously. In this list, ^{90}Sr has the greatest affinity for bone and deposits throughout the volume of the bone resulting in a large percentage of the dogs developing bone tumors (Table 2). After inhalation, ^{144}Ce and ^{91}Y translocate from the lung primarily to liver and skeleton. The physical half-life of ^{144}Ce is a little over 9 mo, while that of ^{91}Y is about 2 mo. Although nearly half of the activity translocated from lung deposited in bone, only one bone tumor was observed in the ^{144}Ce study, and none was observed in the ^{91}Y study. The $^{137}CsCl$ injected intravenously resulted in an accumulation in soft tissues and a general whole-body irradiation. Although tumors were observed in some organ systems, no bone tumors were observed. The alpha-emitting radionuclide ^{238}Pu (inhaled as $^{238}PuO_2$), which has a radioactive half-life of approximately 88 yr, was also a part of this series. Approximately equal fractions of the ^{238}Pu that entered the blood from the lung were deposited in the liver and skeleton. The ^{238}Pu was deposited primarily on bone surfaces and resulted in a large percentage of the dogs developing bone tumors.

Table 1

Studies of the Toxicity of Various Radionuclides Inhaled or Injected in Relatively Soluble Chemi ›s and Their Distribution Characteristics in the Skeleton

Radionuclide	pe of Radiation	Radioactive Half-life	Primary Tissue Distribution
^{90}Sr	beta	29 yr	Bone volume
^{144}Ce	beta, gamma	285 days	Bone surfaces and liver
^{91}Y	beta, gamma	59 days	Bone surfaces and liver
^{137}Cs	beta, gamma	30 yr	Muscle and soft tissues
^{238}Pu	alpha	88 yr	Bone surfaces and liver

Each study had a group of control dogs (Table 2). None of the control dogs associated with these studies developed bone tumors. However, three bone tumors have been observed in a group of over 250 control dogs from all longevity studies at the Institute.

Bone tumors in the exposed dogs were primarily osteosarcomas or soft tissue sarcomas primary to bone (fibrosarcoma, hemangiosarcoma, myxosarcoma). In the ^{90}Sr study, 36% of the bone tumors were hemangiosarcomas or fibrosarcomas. With $^{238}PuO_2$, less than 2% of the bone tumors were soft tissue sarcomas. The distribution of tumors within the skeleton from the ^{90}Sr was mainly in the skull and long bones of the limbs.

Table 2

Number of Bone and Bone-Associated Tumors Found in Dogs that Inhaled or Were Injected with Radionuclides

Radionuclide	Number of Dogs	Number of Dogs Surviving > 2 yr	Dogs with Bone Tumors	Dogs with Bone-Marrow Tumors	Dogs with Nasal-Mucosal Tumors	Dogs with Oral Mucosal Tumors
$^{90}SrCl_2$	66	54	30	2	3	1
$^{144}CeCl_3$	55	41	1	3	5	3
$^{91}YCl_3$	42	29	0	0	3	0
$^{137}CsCl$	54	41	0	0	4	3
$^{238}PuO_2$	144	142	90	0	0	1
Controls	85	85	0	0	0	0

Some other tumors observed in the dogs may be related to the accumulation of radioactivity in the skeleton. Tumors of the bone marrow (leukemias and myeloproliferative disorders) were noted in several dogs exposed to $^{90}SrCl_2$ or $^{144}CeCl_3$. Both of these radionuclides are beta emitters with prolonged retention in bone. No such tumors were seen in studies with $^{91}YCl_3$, $^{137}CsCl$, or $^{238}PuO_2$. Tumors of the nasal and sinus mucosa were also found in 5 to 10% of the dogs in each study with beta-emitting radionuclides. None was found in the dogs that inhaled $^{238}PuO_2$. Tumors of the oral mucosa were also found in dogs exposed to $^{90}SrCl_2$, $^{144}CeCl_3$, $^{137}CsCl$, or $^{238}PuO_2$. One hypothesis for the occurrence of these oral and nasal tumors is that radiation from the radionuclide in the bone surrounding the mouth, nasal cavity, and sinuses induced the tumors of the epithelial lining cells. In the case of ^{137}Cs, the soft tissue distribution of the radionuclide suggests this may not be the mechanism for that particular radionuclide. However, the tissue distribution of ^{137}Cs around the nose and mouth has not been studied closely. The inability of the alpha radiation from the ^{238}Pu in the bones surrounding the nasal cavity and sinuses to reach the epithelial lining cell might explain why only one tumor was observed in these tissues in the dogs that inhaled ^{238}Pu. No tumors of the nasal cavity have been observed in the control dogs associated with these studies or in a larger group of controls from other longevity studies.

Comparison of the number of bone tumors observed in dogs that inhaled or were injected with various beta-emitting or an alpha-emitting radionuclides suggests that the tumors occurred primarily in studies with the longer-lived radionuclides. Significant differences exist in the distribution of tumors within the skeleton and the occurrence of possible bone-associated tumors between the beta- and alpha-emitting radionuclides.

As these studies are completed through final reviews and analyses of the dosimetry, clinical, and histopathological data and publication of core manuscripts, the bone cancer risks across these studies and those in other DOE laboratories will be analyzed. Of particular interest will be the comparisons of bone cancer risk factors for chronic beta and alpha irradiation and the examination of studies in which few or no bone cancers were observed even though the skeleton was irradiated.

(Research sponsored by the Office of Health and Environmental Research, U.S. Department of Energy, under Contract No. DE-AC04-76EV01013.)

GROWTH RATE PATTERNS OF LUNG TUMORS IN BEAGLE DOGS EXPOSED TO $^{239}PuO_2$ OR $^{238}PuO_2$

*W. C. Griffith, J. H. Diel, B. A. Muggenburg, and S. J. Matthews**

Inhalation exposure studies have been conducted in Beagle dogs to investigate the risk of lung tumor induction by α-radiation from relatively insoluble inhaled particles of $^{238}PuO_2$ or $^{239}PuO_2$. This report investigates the growth rate patterns for lung tumors induced in these studies. These tumor growth rate patterns are of interest because they aid in evaluation of the dose-response relationships for inhaled Pu.

Knowledge of the tumor growth rate assists in analyzing dose-response relationships by providing a more appropriate estimate of the dose and the tumor incidence rate. At the time of death, the size of a lung tumor varies greatly, suggesting that lung tumors are present for differing lengths of time before death. The tumors may be detected before death during routine surveillance of the dogs, but their sizes at time of detection are again highly variable. A tumor's growth rate and its size at death can be used to estimate a time when it was a certain size, so that all dogs can be standardized to the same tumor size. A small uniform size is used so that the estimated time is closer to when the tumor is likely to have arisen. The calculation of the tumor incidence rate is simplified by use of a time point early in the development of the tumor when the tumor is not likely to have affected survival. Because of the long retention half-lives of ^{239}Pu and ^{238}Pu in the lung, the radiation dose is delivered over long time periods, with part of the dose delivered after a tumor is present. Estimation of a standardized time endpoint for a tumor will eliminate variability in the dose due to the time between when a tumor reaches a uniform size and death.

The objectives of this project were to (1) develop a method to measure pulmonary tumor dimensions from radiographs; (2) select an appropriate method of calculating volume from two-dimensional images on a radiograph; and (3) determine and analyze tumor growth rate and doubling time.

To estimate lung-tumor growth, radiographs of 174 dogs that developed pulmonary neoplasms were examined. Dogs from three studies were included: single and repeated inhalation exposures to $^{239}PuO_2$ and a single inhalation exposure to $^{238}PuO_2$. The criteria for selection in each data set were (1) a single tumor with discrete boundaries exhibited in both dorsoventral and lateral views and (2) three or more serial radiographs showing the tumor that were taken over at least a 1-mo period.

Some of the 174 radiographs examined exhibited clearly delineated tumors in one view only. Other radiographs were clouded by the diffuse nature of the tumor's edges in the lung, especially those involving bronchioloalveolar carcinomas. Twenty-nine cases met our criteria. Information pertaining to tumor classification, exposure history, and metastasis was collected for each dog selected. Radiographic films in which the tumors were clearly visible ranged over a period of 57 to 578 days. With the aid of a light box, both radiographic views, dorsoventral and lateral, of the tumor perimeters were traced on paper. The cross-sectional tumor perimeters resembled circles or ellipses. The number of tracings of each dog differed with the number of radiographs taken between the time that the tumor was first observed to when the dog died, and ranged from 3 to 14. The tracings were digitized using a Graf/Pen data collection software program that was developed at ITRI. The program approximated the area of each tumor by applying the trapezoidal rule.

In recent studies in dogs (Rooser, B. *et al. ACTA Oncology 26(3)*: 189, 1987; Perry, R. R. *et al. Am. J. Vet. Res. 53(10)*: 1740, 1992), tumor volumes have been computed by assuming the tumor configuration to be spherical or ellipsoidal. In this project, it was assumed that tumor growth was uniform in all directions. Geometrically similar figures (i.e., the ratio of the dimensions are the same) would then be projected in each set of dorsoventral and lateral radiographs. Similarity of figures implies that the ratio of the volumes is proportional to the ratio of the areas raised to the three-halves power. This relationship was the basis for computing tumor volume. Tumor volume was plotted against days prior to death after the first noted occurrence of the tumor in the radiographs (Fig. 1).

*Department of Energy/Associated Western Universities Teacher Research Associates Program (TRAC) Participant

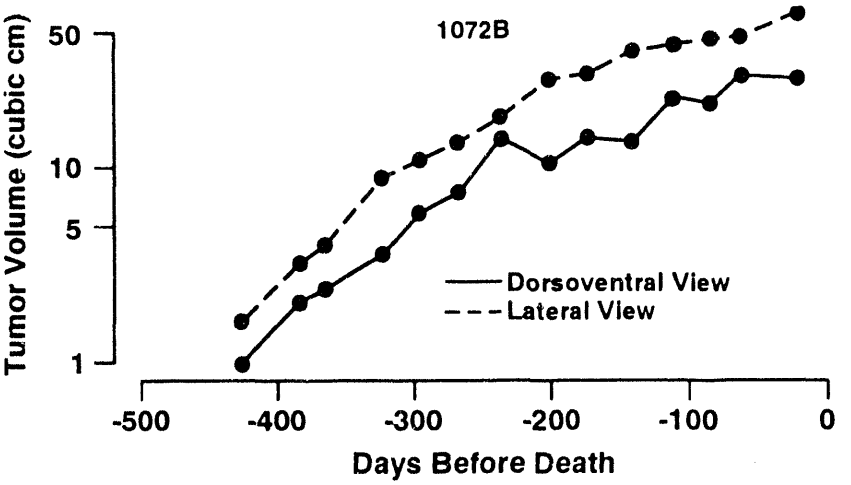

Figure 1. Example of tumor growth showing tumor volumes estimated from radiographs of dorsoventral and lateral views of the tumor at various times before death for dog 1072B.

Linear curves were estimated by least-squares regression for transformed data points for both dorsoventral and lateral views. The data were transformed by the natural logarithm of tumor volume as the dependent variable which was regressed on days prior to death as the independent variable. In most cases the slopes of the lines formed for both views appeared to be approximately the same. Single component exponential growth rates and doubling times were computed. Many of the curves appeared to be exponential. However, the growth rates of individual tumors differed among dogs. The data suggest that growth rates of Pu-induced lung tumors have doubling times ranging from 1 to 9 mo.

Further statistical analysis indicated that tumors which had maximum final volumes between 20 cm^3 and 125 cm^3 fell into two distinct groups of doubling times. One group had doubling times between 1 and 3 mo. Those for the other group ranged from 6 to 9 mo. There were no tumors with maximum volumes between 20 cm^3 and 125 cm^3 that had doubling times between 3 and 6 mo (Fig. 2).

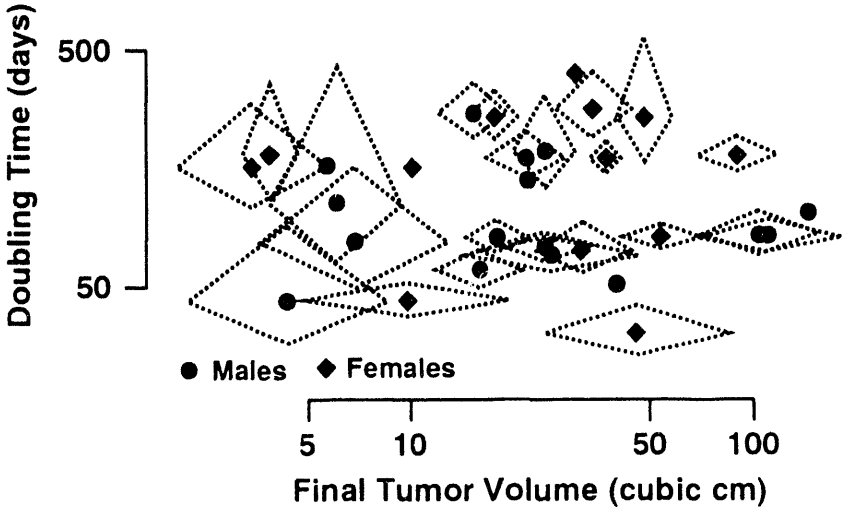

Figure 2. Tumor doubling times as a function of final tumor volume at death. The quadrilaterals illustrate the magnitude of the 95% confidence intervals determined from the linear regression for the doubling time and final tumor volume. The smaller quadrilaterals indicate that the doubling times and final volume are known more precisely. For points without quadrilaterals, the 95% confidence intervals were so broad in at least one direction that they did not fit onto the graph.

Tumor type, exposure history, and metastasis were factors that were considered for each dog. For the 29 cases reviewed, six of the tumors were classified as papillary adenocarcinoma, two as adenocarcinoma, one as adenosquamous carcinoma, one as squamous carcinoma, one as bronchioloalveolar carcinoma, and 18 as carcinoma. Metastasis occurred in 17 cases. No relationship among doubling times and gender, histologic type, age at death, lung burden, or metastasis was established.

The results of this study suggest that tumor growth rates can be used for estimation of the time at which lung tumors are a uniform size. The standard errors for the growth rates can be reduced by observation of the tumors over a longer period of time. The similar growth rates for both dorsoventral and lateral view data suggest that the sample size could be increased by focusing on the lateral-view radiographs. Frequently, observation of the dorsoventral view was obscured by the position of the tumor in relation to the heart. Relaxing the selection criteria to use these views would provide observations over longer periods of time.

The results of this study suggest estimation of the time when the lung tumors had a volume of about 1 cm^3 would be appropriate. This size of lung tumor is about as small as can be detected on a radiograph. This size of tumor is close to or inside the range of the data. Thus, it would only involve a small extrapolation. Also, the growth rate down to this size appears to be approximately exponential, so that the time estimated by this procedure is likely to have small bias.

The growth before a lung tumor reaches a volume of 1 cm^3 probably involves a period of much more rapid growth than those observed for the majority of tumors in this study. The slow growth rates in Figure 2 observed for many of the tumors would extrapolate back to times of origin, as a single cell, before the dog was exposed. This suggests these tumors have a period of more rapid growth, which is consistent with the observation in these studies that very few dogs have incidental lung tumors found at death when the dog dies of causes other than a lung tumor.

(Research sponsored by the Office of Health and Environmental Research, U.S. Department of Energy, under Contract No. DE-AC04-76EV01013.)

IV. MECHANISMS OF CARCINOGENIC RESPONSES TO TOXICANTS

ANALYSIS OF SPUTUM SAMPLES AND LUNG TUMORS FROM URANIUM MINERS FOR ALTERED GENE EXPRESSION

C. A. Carter, N. F. Johnson, S. A. Belinsky, and J. F. Lechner

Samples of sputum, bronchial brushings, and lung tumors have been obtained from cohorts of individuals exposed to elevated levels of high-linear energy transfer (LET) radiation, through the inhalation of radon progeny. In many instances, sputa and tissues from the same patient were collected for several years prior to and following detection of a lung tumor. These samples are being analyzed to identify the gene changes involved in lung cancer progression caused by high-LET radiation. An initial obstacle in detecting gene changes in sputum was the need to isolate the exfoliated epithelial cells from the inflammatory cells and mucus. The method we have developed is to first filter the sputum through nylon wool. The filtered material is then centrifuged. The resultant cell pellet is largely free of debris and mucus. Filtered sputum samples are then resuspended in phosphate buffered saline and stained with a pan anti-cytokeratin antibody. In this manner, epithelial cells are stained in suspension in filtered sputum samples, thereby excluding white blood cells. Cytokeratin-positive cells are collected using a FACStar Plus flow cytometer (Becton Dickinson, San Jose, CA). This method yields a highly purified population of epithelial cells that can then be stained for a variety of markers thought to be involved in lung cancer.

In a collaborative effort with researchers at St. Mary's Hospital, Grand Junction, CO, sputum samples and lung tissues collected from uranium miners from the Colorado Plateau are being analyzed for gene alterations known to be present in smoking-induced lung cancer. These specimens have been assessed for aberrant expression of the tumor suppressor gene p53 by immunohistochemical techniques. The p53 antibody used in this staining assay recognizes dysfunction of p53 because the abnormal proteins have an extended half-life. In the samples collected from Colorado Plateau miners, 7 of the 11 donors from which both sputum samples and bronchial brushings were obtained exhibited dysfunctional p53 by immunohistochemistry. The matching tumors obtained from these patients also have p53 gene dysfunctions. These studies will be continued; sputum samples will be double-stained for cytokeratin (to identify epithelial cells) and p53, and correlations will be made with the matching lung tissue sample. These studies will determine the onset of p53 dysfunction in these patients by examining sputum samples collected prior to the diagnosis of a lung tumor.

To further define the alterations exhibited by lung tumors associated with radon exposure, samples collected from the uranium mining belt in Grants, NM, have been analyzed for c-erbB-2 and p53 dysfunctions by immunohistochemistry. The results are shown in Table 1.

Table 1

High-LET Radiation: p53 and c-erbB-2 Gene Dysfunction Frequencies in Uranium Miners

	Squamous Cell Carcinoma	Adenocarcinoma	Small Cell Lung Cancer	Undiff.
p53	11/18	3/7	3/12	2/4
c-erbB-2	2/7	3/7	0/11	2/3

These results indicate that lung tumors associated with radon exposure display alterations of p53 and erbB-2 similar to gene alterations associated with smoking-induced lung tumors.

We are also examining the possibility of using F-and G-actin as markers for the detection of early lung cancer. In bladder cancer, F-actin is reduced (Rao, J. Y. *et al. Cancer Res. 51*: 2762, 1991) and concomitantly G-actin is increased (Rao, J. Y. *et al. Proc. Natl. Acad. Sci. USA*, in press) in premalignant and malignant

biopsy-confirmed cancer. To test whether this change in the actin ratio is also a hallmark of premalignant lung cancer, F-actin localization has been evaluated in normal human bronchial epithelial cells (NHBE), lung adenocarcinoma cells (Calu 6 cells), and metastatic bronchial carcinoma cells (Cha Go cells). Actin occurs as organized crisscrossing bundles of stress fibers distributed throughout the cells in NHBE cells. In the Calu 6 cells, F-actin stress fibers are reduced, occurring occasionally near the cell periphery. The cell center of Calu 6 cells is devoid of stress fibers, and F-actin aggregates are common. Cha Go cells display a sparse distribution of F-actin aggregates, and stress fibers are absent. This preliminary evidence indicates that *in vitro* F-actin is altered in malignant lung cells. These studies will continue using flow cytometry to quantitate the F-actin content in the cell lines described above. If these experiments are successful, F-actin and G-actin content will be assessed in sputum-derived lung epithelial cells obtained from cancer patients and uranium miners.

Described above is a model system for investigating the genetic alterations associated with early and late lung cancer in individuals exposed to high-LET radiation. Additionally, preliminary evidence indicates that markers such as F- and G-actin may serve as diagnostic markers to detect early lung cancer. The identification of genetic alterations associated with various stages of lung cancer in individuals exposed to high-LET radiation should lead to a greater understanding of the mechanism involved in lung cancer.

(Research sponsored by the Office of Health and Environmental Research, U.S. Department of Energy, under Contract No. DE-AC04-76EV01013).

A SCAFFOLD-ATTACHMENT-LIKE REGION ON HUMAN CHROMOSOME 9 IS AMPLIFIED IN SOME LUNG TUMOR SPECIMENS

W. A. Palmisano, C. H. Kennedy, and J. F. Lechner*

Numerous genetic alterations (e.g., deletions, amplifications, translocations, and point mutations) are frequently involved in carcinogenesis. Methods to identify these lesions have included restriction fragment length polymorphism analysis, differential cloning, and differential hybridization techniques. However, with recent advances in polymerase chain reaction (PCR) technology, an alternate one-step approach has been developed that allows the detection and isolation of DNA fragments which have undergone a genetic change. This technique, designated arbitrarily primed polymerase chain reaction (AP-PCR), uses a single primer of arbitrary sequence and produces a DNA fingerprint that can display qualitative and quantitative differences (polymorphisms) between closely related genomes (Williams, J. G. K. *et al. Nucleic Acids Res. 18*: 6531, 1990; Welsh, J. and M. McClellan. *Nucleic Acids Res. 18*: 7213, 1990; Peinado, M. A. *et al. Proc. Natl. Acad. Sci. USA 89*: 10065, 1992).

The objective of this study was to use AP-PCR to identify genetic alterations that are associated with lung cancer using tumor and adjacent normal human lung tissues obtained from the New Mexico Tumor Registry. High molecular weight DNA was isolated from eight tumor/normal pairs using a standard phenol-chloroform extraction method. Samples of DNA (500 ng) were amplified in 100 μL reaction volumes containing 10 mM Tris-Cl (pH 8.3), 50 mM KCl, 200 μM of each dNTP, 1 μM arbitrary primer, and 2.5 units of AmpliTaq® DNA polymerase (Perkin Elmer Cetus, Norwalk, CT). Samples were overlaid with mineral oil, denatured for 1 min at 94°C, then subjected to 35 rounds of amplification in a PTC-100™ thermal cycler (MJ Research, Inc., Watertown, MA) using the following thermal cycling program: 94°C for 5 sec; 42°C for 1 min; and 72°C for 1 min. After a final extension period of 5 min at 72°C, 20 μL of the resulting stage 1 products were subjected to an additional 15 rounds of amplification in a total volume of 200 μL using the same temperature profile; however, 20 μCi of α-[^{32}P]-dCTP were added and the final concentration of each dNTP was 2.0 μM. Samples of the resulting ^{32}P-labeled amplimers (5 μL) were electrophoresed through a 5% polyacrylamide gel under denaturing conditions and visualized by autoradiography.

Initially, a moderately well-differentiated, non-keratinizing squamous cell carcinoma and normal lung tissue from the same donor were used for AP-PCR amplification using the λgt10 reverse sequencing primer ($^{5'}$CTTATGAGTATTTCTTCCAGGGTA$^{3'}$) as an arbitrary primer. Comparison of the DNA fingerprints generated by this method revealed nearly identical banding patterns; however, among the dissimilar bands, one particular band was more intense in the tumor DNA fingerprint as compared to the corresponding band generated from normal lung DNA, suggesting the presence of several extra copies of this sequence in the tumor cell genome. This polymorphic band was excised from the gel, immersed in 50 μL of dH_2O, and heated at 72°C for 30 min. The resulting DNA (12.5 μL) was reamplified in a 50 μL reaction volume using the same PCR conditions used to produce stage 1 products, except that the annealing temperature was 55°C and only 15 rounds of amplification were performed. The reamplified DNA (1 μL) was cloned into the PCR™II vector using the TA cloning system (Invitrogen, San Diego, CA) and sequenced using a Sequenase® kit (United States Biochemicals Co., Cleveland, OH).

Comparison of the 393 bp DNA sequence (designated clone 1-5) with GenBank and EMBL data bases revealed that the sequence displays homology (60%) with a scaffold-attachment region (SAR) near the interferon β gene on chromosome 9. SARs are A+T rich DNA sequences responsible for organizing the chromosomal DNA into higher-ordered structures (i.e., loops) by binding to the nuclear scaffold and are believed to play a role in the control of gene expression and DNA replication (Roberge, M. and S. M. Gasser. *Mol. Microbiol. 6*: 419, 1992).

To determine the copy number of the polymorphic DNA present in the original tumor sample, the cloned band was excised with EcoR1 endonuclease, labeled with α-[^{32}P]-dCTP using a random-primed labeling kit

*Postdoctoral Fellow

(Boehringer Mannheim, Indianapolis, IN), and used as a probe for Southern analysis (Fig. 1). The results of this analysis, determined by densitometry, confirm the quantitative results obtained by AP-PCR and suggest that the DNA sequence is present in this squamous cell carcinoma at levels five-fold greater than that found in normal lung cells. To determine whether this polymorphism is common in lung cancers, seven other tumor/normal pairs from different donors were subjected to a similar analysis. Results of this experiment demonstrated that three of the seven tumors analyzed exhibited two- to nine-fold increases in copy number of the SAR-like DNA sequence, suggesting that this amplification may be a common event in lung cancers.

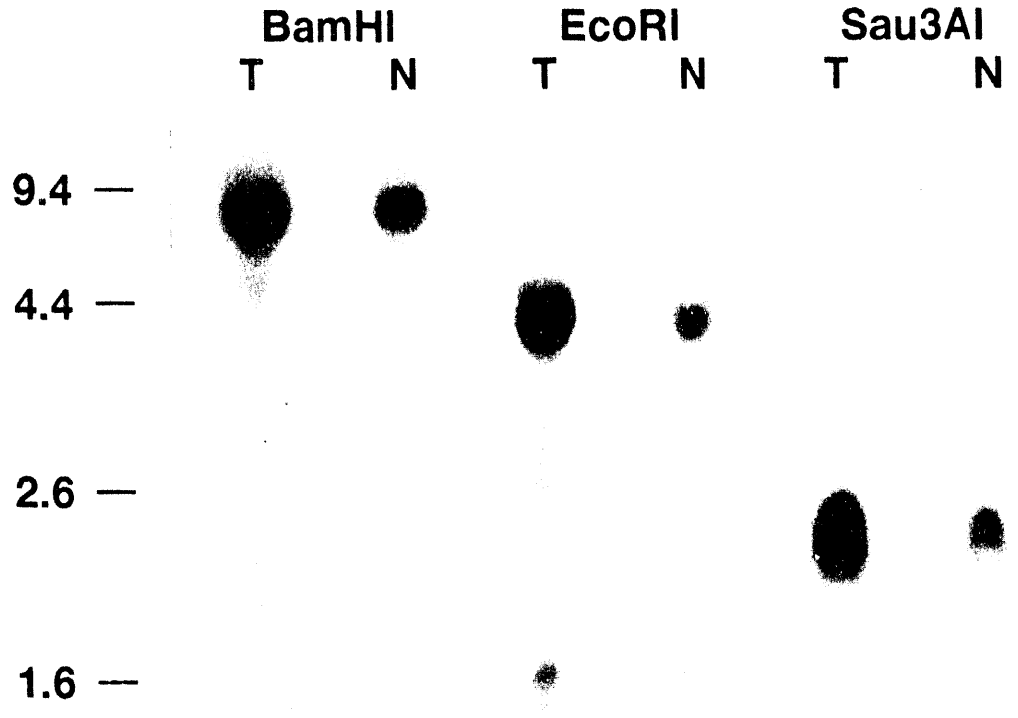

Figure 1. Southern analysis of tumor and normal DNA probed with clone 1-5. Samples of genomic DNA isolated from human lung tissues were digested with restriction endonucleases BamH1, EcoR1, and Sau3A1, electrophoresed through a 0.8% agarose gel, and transferred to a Nytran® membrane (Schleicher & Schuell, Keene, NH). The resulting blot was hybridized with ^{32}P-labeled DNA from clone 1-5 using standard aqueous hybridization conditions (Sambrook, J. *et al.* In *Molecular Cloning, A Laboratory Manual*, 2nd Ed., p. 9.52, Cold Spring Harbor Press, Cold Spring Harbor, New York, 1989), washed in 1X SSC/0.05% SDS buffer for 1 h at 68°C, and exposed to film for 61 h. The numbers at the left represent the sizes and positions of DNA standards in kilobase pairs.

A human/rodent somatic cell hybrid panel (Oncor®, Gaithersburg, MD), was used to determine that clone 1-5 is localized to chromosome 9, and recently, a genomic clone has been isolated from a chromosome 9 library (ATTC, Rockville, MD). In addition to DNA sequencing analysis, Northern blot analyses are being performed to determine if this genomic clone encompasses a transcribed gene. This clone will also be used for fluorescent *in situ* hybridization analyses to further map the chromosomal position of the scaffold-attachment-like region and to quickly screen other tumors to determine the prevalence of this amplification in human lung cancer. This information will reveal the nature of the increase in copy number of this region of DNA (i.e., amplification or aneuploidy) and may identify a novel gene involved in the etiology of lung cancer.

(Research sponsored by the Office of Health and Environmental Research, U.S. Department of Energy, under Contract No. DE-AC04-76EV01013.)

ISOLATION OF A PUTATIVE p53-CONTROLLED GENE BY POLYMERASE CHAIN REACTION AMPLIFICATION

C. H. Kennedy, W. A. Palmisano, and J. F. Lechner*

The tumor suppressor gene p53 has been described as the "guardian of the genome" based on its ability to cause arrest in the G_1 phase of the cell cycle after exposure of the cell to radiation and/or other DNA-damaging agents; this arrest allows the cell to repair DNA damage before entering the S phase (Lane, D. P. *Nature 358*: 15, 1992). The protein product of p53 has been shown to function as a sequence-specific transcription factor by binding to a dimeric consensus sequence of downstream effector genes (El-Deiry, W. S. *et al. Nature Genetics 1*: 45, 1992). It is probable that the expression of several genes is directly regulated by this mechanism. To date, four genes containing the consensus p53 protein-binding sequence have been identified: GADD45 (Kastan, M. B. *et al. Cell 17*: 587, 1992) and the mouse genes mdm-2 (Momand, J. *et al. Cell 26*: 1237, 1992), MCK (Zambetti, G. P. *et al. Genes Dev. 6*: 1143, 1992), and Thy1 (Bayle, J. H. *et al.*, unpublished results).

The focus of this project was to identify novel genes that are regulated by p53. Initially, the polymerase chain reaction (PCR) was used to amplify a putative p53-controlled downstream gene using genomic DNA prepared from normal human lung tissue. The 5′ primer for this amplification was the downstream half of the dimeric consensus p53 protein-binding sequence ($^{5'}$GACATGCCTG$^{3'}$ or $^{5'}$GACTTGCCTG$^{3'}$) that was described previously (Kern, S. E. *et al. Science 252*: 1708, 1991). The 3′ primer was the 5′ end of the highly repetitive Alu sequence ($^{5'}$ACCACGCCC$^{3'}$). Twenty-μL reactions were prepared for PCR using 0.5 U AmpliTaq® DNA polymerase (Perkin Elmer Cetus, Norwalk, CT), 2 μL of 10X PCR buffer (Perkin Elmer Cetus, Norwalk, CT), 0.2 mM of each dNTP, 1 μM of each primer, and 100 ng of DNA. The reaction mixtures were overlaid with oil, and the putative p53-regulated sequence was amplified by 35 cycles of the following thermal cycling program: 94°C for 5 sec (denaturing of DNA), 36°C for 1.5 min (primer annealing), and 72°C for 1 min (extension of DNA). The amplification products (stage 1 products) were used to prepare ^{32}P-labeled stage 2 PCR products. The stage 2 reaction was the same as above except that the final concentration of each dNTP was 2.0 μM, 1 μCi of α-[^{32}P]-dATP was added, and 2 μL of stage 1 product was used as the template. The DNA was amplified for 15 cycles using the same thermal cycle program. The ^{32}P-labeled products were electrophoresed through a 5% polyacrylamide gel and visualized by autoradiography.

PCR amplifications were carried out under either arbitrary conditions (i.e., only the 5′ or 3′ primer was present in the reaction mixture) or under specific conditions (i.e., both the 5′ and 3′ primers were used). By autoradiography, six bands were detected in the products of specific PCR that were not detected in the products of arbitrary PCR. These bands were excised from the gel, eluted into buffer, and reamplified. The products were then cloned using the TA Cloning™ system (Invitrogen, San Diego, CA). Subsequently, the cloned inserts were excised from the plasmid vector with EcoR1 endonuclease (Promega, Madison, WI) and gel-purified. Radioactive probes (^{32}P-labeled) were prepared from these clones by random-primed DNA labeling (Boehringer Mannheim, Indianapolis, IN) and used to screen a human placenta genomic cosmid DNA library (Clonetech, Palo Alto, CA). Only one of the six clones (designated 2-5) was found in this library.

Six cosmid colonies that hybridized with clone 2-5 were picked and expanded in liquid media (cosmid clones 2-7 to 2-12). The cosmid DNA was then purified and digested with endonucleases BamH1, EcoR1, and Pst1 (Promega, Madison, WI); all six showed the same restriction patterns. The Pst1 endonuclease-digested DNA from cosmid clone 2-8 was transferred to a Nytran membrane (Schleicher & Schuell, Keene, NH) and probed with clone 2-5 to determine which fragment contained the original PCR product. An 1100 bp fragment was detected, isolated, and subcloned into a Bluescript KS$^+$ cloning vector. Four of the resulting subclones (2-13 to 2-16) were found to hybridize with the original PCR product that contained the DNA sequence between the 3′ half of the dimeric consensus p53 protein-binding sequence and Alu (clone 2-5). One of these (clone 2-13) was sequenced using the Sequenase® kit (USB, Cleveland, OH) to determine if it contained the complete dimeric consensus p53 protein-binding sequence.

---

*Postdoctoral Fellow

These results are compared to the published consensus p53 protein-binding sequence identified previously by El-Deiry *et al.* (1992) in Table 1. These workers characterized 18 human genomic clones that bind p53 *in vitro* and determined the base possibilities for the different positions of the binding sequence. Only the G at the seventh position was found to be conserved in all 18 clones. In clone 2-13, a C was detected at this position suggesting that if this gene is controlled by p53, it is the first such gene to be reported that contains a base other than G at the seventh position of the binding sequence.

Table 1

Consensus p53 Protein-Binding Sequences

Position[a]	1	2	3	4	5	6	7	8	9	10
Literature[b]	A/G/t/c	G/A/t/c	A/G/c	C/t	A/T/c/g	T/A/g	G	T/C	C/T	T/C/a/g
2-13[c]	A	G	G	C	G	T	C	C	C	T
2-13[d]	o	G	A	C	A	A	G	C	C	T

[a]Positions 1 and 10 are the 5′ and 3′ ends, respectively, of one-half of the dimeric consensus p53 protein-binding sequence.

[b]Half-consensus p53 protein-binding sequence of El-Diery *et al.* (1992). Capital letters indicate the bases present in the majority of the clones, while small letters refer to bases present in only a small fraction (< 10%) of the clones.

[c]This sequence is the 5′ end of the putative dimeric p53-protein binding sequence detected in clone 2-13.

[d]This sequence is the 3′ end of the putative dimeric p53 protein-binding sequence detected in clone 2-13. The o refers to the fact that the two half-sequences run together (i.e., a total of 19 bases instead of 20); similar base omissions were noted in the consensus p53 protein-binding sequences reported by El-Diery *et al.* (1992).

In the future, the ability of p53 to regulate a gene within cosmid clone 2-8 will be assessed using a battery of lung cell lines that are either p53-wild type or -null. In these experiments, x-irradiated wild-type cells should show an induction of an mRNA that hybridizes with clone 2-8, whereas no hybridization should be detected in p53-null cells. Further, the remaining five original PCR amplification products will be used to screen other cosmid libraries in order to isolate their cognate genes. Ultimately, the role of these p53-regulated genes in the cell's response to high-linear transfer radiation will also be determined.

(Research sponsored by the Office of Health and Environmental Research, U.S. Department of Energy, under Contract No. DE-AC04-76EV01013.)

p53, ErbB2, and K-ras GENE DYSFUNCTIONS ARE RARE IN SPONTANEOUS AND PLUTONIUM-239-INDUCED CANINE LUNG NEOPLASIA

L. A. Tierney, F. F. Hahn, and J. F. Lechner*

Exposure to elevated levels of high-linear-energy-transfer (LET) radiation through the inhalation of radon progeny may result in as many as 20,000 new cases of lung cancer each year in the U.S. (Samet, J. M. *West. J. Med. 156*: 25, 1992). Underground miners are particularly at risk for acquiring lung cancer as a result of exposure through inhalation to radon progeny (Samet, J. M. *et al. Health Phys. 61*: 745, 1991). The molecular mechanisms by which alpha-radiation induces lung cancer are unclear. Several protooncogene (erbB2 and K-ras) and tumor suppressor gene (p53) alterations have been identified in lung cancer putatively caused by smoking, and to a lesser extent, by high-LET irradiation (Vahakangas, K. H. *et al. Lancet 339*: 576, 1992; Stegelmeier, B. L. *et al. Mol. Carcinog. 4*: 43, 1991; this report, p. 87).

The intent of this study was to determine if these gene dysfunctions are evident in high-LET radiation-induced or spontaneously occurring lung tumors of dogs. Therefore, 117 primary canine lung tumors from unexposed Beagle dogs and from animals exposed to $^{239}PuO_2$ through nose-only inhalation (1978-79 Annual Report, p. 141; 1981-82 Annual Report, p. 347) were examined for alterations in the expression of the protooncogene erbB2 and mutations in the K-ras protooncogene and the p53 tumor suppressor gene.

The canine form of the p53 protein was visualized by immunohistochemistry using SV40 virus T-antigen gene transformed canine airway epithelial cells developed by infection with a murine retroviral shuttle vector (pZipNeoSV(X)) (Pfeifer, A. M. *et. al. Proc. Natl. Acad. Sci. 90*: 5123, 1993). The T-antigen protein binds the p53 protein and increases its cellular half-life. Thus, the cells constitutively overexpress canine p53 protein in their nuclei. These cells were used to test a panel of commercially available anti-human p53 antibodies that recognize both mutant and wild-type forms of p53 protein. Bound antibody was detected by the avidin-biotin complex immunoperoxidase technique. The results showed that the polyclonal antibody CM-1 (Signet Laboratories) would effectively recognize canine p53 protein.

Rat and human mammary tumors frequently overexpress erbB2 oncoprotein. Previous investigators have reported that both the human and rat forms are recognized by several commercially available antibodies. Thus, sections of malignant canine mammary tumors and a formalin-fixed, paraffin-embedded preparation of a known erbB2 overexpressing human lung cell tumor line (A549, American Tissue Type Collection) were used to determine if these antibodies would also recognize canine erbB2. The results of these experiments showed that a monoclonal antibody preparation (Clone CB11, Signet Laboratories) would decorate canine erbB2.

Upon validating that these antibodies would recognize the canine forms of these proteins, immunohistochemistry for the detection of canine p53 and erbB2 in 5 μm paraffin sections was performed as previously described (Bennett, W. P. *et. al. Oncogene 6*: 1779, 1991; Kern, J. A. *et. al. Cancer Res. 50*: 5184, 1990) for p53 and erbB2 in human tissues, respectively. Overexpression of p53 protein in paraffin sections of lung tumor was considered indicative of a missense mutation in the conserved regions of the gene (Sundaresan, V. *et al. Oncogene 7*: 1989, 1992). The visual detection of erbB2 immunoreactivity in lung tumor epithelium was regarded as evidence of inappropriate expression of this oncoprotein, since it is expressed only at low levels in normal lung airway epithelium.

To analyze for activating mutations in the 12th, 13th, and 61st codons of K-ras, the coding sequences flanking exons 1 and 2 were amplified by polymerase chain reaction (PCR) from DNA extracted from paraffin sections containing predominately tumor tissue. The oligonucleotide primers and PCR conditions were as described by Kraegel, S. A. *et al.* (*Cancer Res. 52*: 4724, 1992). The canine PCR amplification products were sequenced directly using the dideoxymethod of Sanger, F. *et al.* (*Proc. Natl. Acad. Sci. USA 74*: 5463, 1977). DNA samples of canine tumors, with and without known K-ras-activating mutations (kindly provided by Dr. Kraegel, U.C. Davis) were sequenced blind, and in parallel with the ITRI samples, as a control for the

---

*UNM/ITRI Inhalation Toxicology Graduate Student

sequencing procedures. When the code was broken, the sequence results matched those reported by Kraegel and associates (Kraegel *et al.*, 1992).

Twenty-eight lung tumors representing a spectra of histotypes from dogs with spontaneous tumors (n = 9) and $^{239}PuO_2$ (n = 19)-exposed dogs were selected for analysis of activating mutations in codons 12, 13, or 61 of the K-ras oncogene. No K-ras mutations were detected in codons 12, 13, or 61 of either unexposed or $^{239}PuO_2$-induced lung tumors. In contrast, 14% (16/117) of the lung neoplasms showed elevated nuclear accumulation of p53 (Table 1). Adenosquamous and squamous cell histotypes were the most frequently perturbed regardless of exposure history and comprised 85% of all p53 dysfunctional tumors.

Table 1

ErbB2 and p53 Dysfunction in Canine Lung Tumors as Determined by Immunohistochemistry

		Gene Dysfunction			
Histologic Phenotype	Exposure Status	p53	%	erbB2	%
Papillary adenocarcinoma	$^{239}PuO_2$ exposed	0/26	(0)	5/25	(20)
	Unexposed	0/24	(0)	1/24	(4)
Bronchioloalveolar carcinoma	$^{239}PuO_2$ exposed	0/21	(0)	0/22	(0)
	Unexposed	1/7	(14)	2/7	(29)
Squamous cell carcinoma	$^{239}PuO_2$ exposed	6/19	(32)	5/19	(26)
	Unexposed	2/2	(100)	0/2	(0)
Adenosquamous carcinoma	$^{239}PuO_2$ exposed	4/12	(33)	6/13	(46)
	Unexposed	3/4	(25)	1/4	(25)
Adenocarcinoma[a]	$^{239}PuO_2$ exposed	0/1	(0)	1/1	(100)
	Unexposed	0/0	–	0/0	–

[a]Undifferentiated adenocarcinoma = histotype not represented in the unexposed dogs examined.

Twenty-three percent (25/111) of all tumors had evidence of erbB2 overexpression, and four of these co-overexpressed p53 protein, as well. Intrapulmonary metastasis from primary tumors overexpressing erbB2 also showed evidence of erbB2 gene dysfunction. No differences in erbB2 expression were noted between spontaneously occurring and plutonium-induced lung tumors nor was there a relationship between the total $^{239}PuO_2$ lung dose at death and altered erbB2 or p53 expression.

In summary, these data indicate that p53 and K-ras gene dysfunction, as a result of missense mutation, are infrequent events in spontaneous and $^{239}PuO_2$-induced lung neoplasia of laboratory-raised Beagle dogs. These results contrast human lung cancer observations, i.e., 30-40% of examined adenocarcinomas have K-ras-activating mutations (Bos, J. L. *Cancer Res. 49*: 4682, 1990), and 50-70% of all primary lung tumors show evidence of p53 gene dysfunction (Iggo, R. *Lancet 335*: 675, 1990). The results are comparable, however, with recent findings in other animal models of carcinogenesis in which mutations in p53 are, with few exceptions, infrequent. On the other hand, the lack of evidence for K-ras mutations in spontaneously occurring and $^{239}PuO_2$-induced lung cancer of dogs in this study contrasts markedly with the relatively high frequency of activating K-ras mutations in $^{239}PuO_2$-induced lung tumors of rats (Stegelmeier *et al.*, 1991). ErbB2 overexpression, however, compares favorably with that described in the literature for human lung malignancies, where approximately one-third of non-small-cell lung cancers overexpress this oncoprotein (Weiner, D. B. *et al. Cancer Res. 50*: 421, 1990). Overall, when compared and contrasted with existing human and rat data, the results of our investigations suggest that high-LET radiation causes cancer by mechanisms that may be predominantly species-specific.

(Research sponsored by the Office of Health and Environmental Research, U.S. Department of Energy, under Contract No. DE-AC04-76EV01013.)

p53 ALTERATIONS IN ^{239}Pu-INDUCED LUNG TUMORS IN F344 RATS

G. Kelly and F. F. Hahn

We have previously shown that 46% of rat lung tumors induced following exposure to aerosols of $^{239}PuO_2$ frequently contain activating mutations in the Ki-ras oncogene (Stegelmeier, B. L. *et al. Mol. Carcinog. 4*: 43, 1991). In addition, those tumors exhibiting a squamous morphology overexpress the epidermal growth factor receptor and its ligand, transforming growth factor α. These same genetic aberrations are frequently found in human non-small-cell lung cancer (Minna, J. D. *et al. Cold Spring Harbor Symposia on Quantitative Biology 61*: 843, 1986). An even more frequent alteration is a mutation of the p53 tumor suppressor gene (Caamano, J. *et al. Am. J. Pathol. 139*: 839, 1991). The p53 protein plays a critical role in a cell's response to DNA damage by inducing a pause or block at the G_1 to S boundary of the cell cycle (Kastan, M. B. *et al. Cancer Res. 51*: 6304, 1991; Lin, D. *et al. Proc. Natl. Acad. Sci. USA 89*: 9210, 1992). This G_1 block permits the cell to repair DNA damage before DNA synthesis. Cells lacking a functional p53 protein fail to pause for repair and consequently accumulate mutations into the genome at an accelerated rate. This study was designed to investigate if alterations in the p53 gene are common radiation-induced rat lung tumors.

Mutations within exons 5-8 of the p53 gene increase the cellular half-life of the protein, thereby facilitating detections by immunohistochemistry. In the present study, we investigated whether further correlations exist between genetic alterations in human non-small-cell lung cancer and alpha-particle-induced rat lung tumors by examining 38 $^{239}PuO_2$-induced rat lung tumors for increased levels of the p53 protein using immunohistochemistry.

Animal exposures, necropsies, and tissue preparation were as previously described (Herbert, R. A. *et al. Radiat. Res. 134*: 29, 1993). Briefly, 360 13 ± 2 wk old F344/N female rats from the Institute's colony were exposed by inhalation to a $^{239}PuO_2$ aerosol (3.7 kBq initial lung burden), and 140 control animals were similarly exposed to a sham aerosol. The animals were sacrificed at 7, 30, and 90 days after exposure, then at 90-day intervals thereafter for 24 mo. The left lung lobe and any gross lesions were fixed in paraformaldehyde and processed for histologic evaluation. The right lung lobe was snap-frozen in liquid N_2 and stored at -70°C.

Random 4 mm sections from the left lobe were embedded in paraffin, sectioned at 4 μm, and examined with a light microscope. Paraffin was removed from embedded tumor sections with xylene. The sections were rehydrated through a graded series of alcohol washes and rinsed in automation buffer (Biomead, Inc., Foster City, CA). Reactive epitopes were exposed using a brief treatment with trypsin (Elias, J. M. In *Immunohistopathology: A Practical Approach*, ASCP Press Inc., Chicago, p. 12, 1990). Endogenous peroxidase activity was blocked by treating the tissue with H_2O_2 at room temperature. Nonspecific antibody binding was blocked by incubating each slide with 2% normal goat serum for 30 min at room temperature. p53 specific immunoreactivity was then determined by incubation with anti-p53 antibody in phosphate buffered saline overnight at 4°C. Bound primary antibody was then detected by the standard ABC method (Vector Laboratories, Inc., Burlingame, CA).

The rat lung tumors examined included 25 squamous cell carcinomas, eight adenocarcinomas, three adenosquamous carcinomas and one fibrosarcoma. Formalin-fixed, paraffin-embedded sections of a nude mouse xenograft tumor were used as positive controls for p53 protein expression. This nude mouse tumor was obtained by injecting subcutaneously 1 x 10^6 RAT2 cells previously transfected with the SV-40 large T antigen (Bollag, B. *et al. J. Virol. 63*: 863, 1989). A rat lung epithelial cell line (LEC) (Li, A. P. *et al. Toxicology 27*: 257, 1983) served as negative controls for p53 expression. Normal serum at similar dilutions for each immunohistochemical assay served as an additional negative control. Two anti-p53 antibodies were used in these studies (CM1 polyclonal and DO7 monoclonal antibodies, Vector Laboratories, Inc., Burlingame, CA).

The slides were read in a blind fashion and scored according to intensity of staining pattern. Signal intensity greater than background was scored as a positive-staining neoplasm. Two rat lung tumors from animals exposed to aerosols of ^{239}Pu contained intensely staining nuclei indicative of elevated p53 protein levels. None of the remaining tumors expressed detectable levels of the p53 protein (Table 1).

Table 1

Summary of p53 Immunohistochemistry

Pulmonary Neoplasm	Number Examined	Number Positive	Percent Positive
Squamous Cell Carcinoma	25	2	8%
Adenosquamous Carcinoma	3	0	0
Adenocarcinoma	9	0	0
Fibrosarcoma	1	0	0
Total	38	2	5.3%

In contrast to human non-small cell lung cancer, mutations in the p53 tumor suppressor gene are not a frequent genetic alteration in plutonium-induced rat lung tumors (similar results have been noted for dog tumors caused by $^{239}PuO_2$ inhalation; p. 81, this report). There is a strong correlation between elevated immunohistochemical staining and point mutations in the p53 gene. This suggests that rodent lung carcinogenesis depends on alterations in tumor suppressor genes other than p53 or that it depends on alterations in ras rather than p53-mediated regulatory pathways. Recently direct interactions between ras and the serine/threonine proto-oncogene raf have been characterized (Vojtek, A. B. *et al. Cell 74*: 205, 1993). raf alterations occur frequently in lung tumors (Rapp, U. R. *et al. Lung Cancer 4*: 162, 1988). Those plutonium-induced rat lung tumors (54% in this cohort) containing both wild-type p53 and ras may contain alterations in raf. Current efforts are designed to investigate this possibility.

(Research sponsored by the Office of Health and Environmental Research, U.S. Department of Energy, under Contract DE-AC04-76EV01013.)

WILD-TYPE p53 EXPRESSION IN CULTURED LUNG EPITHELIAL CELLS EXPOSED TO ALPHA PARTICLES

*N. F. Johnson, R. J. Jaramillo, and A. W. Hickman**

Sparsely and densely ionizing radiations delay the passage of the cell through the cell cycle. This delay can occur in the G_1 and G_2 phases of the cell cycle. Recent studies have shown that the cell-cycle delay in G_1 induced by X rays is associated with elevated levels of the p53 protein (Kasten, M. B. *et al. Cancer Res. 51*: 6304, 1991). Wild-type p53 protein acts as a "checkpoint" protein to control transit of cells through the restriction point in the late G_1 phase of the cell cycle. The induced cell-cycle block following X-ray-induced DNA damage occurs, presumably, to allow time for repair of damaged DNA template. This investigation was undertaken to determine whether exposure to alpha particles results in increased expression of the p53 protein in a manner similar to that seen with exposure to X rays and to delineate whether such a response is dose-dependent.

Three experiments were conducted using a nontumorigenic lung epithelial cell (LEC) line derived from normal rat alveolar type II cells (Li, A. P. *et al. Toxicology 27*: 257, 1983). The cells were cultured in Ham's F-12 media supplemented with 10% fetal calf serum at 37°C in 5% carbon dioxide and air.

The purpose of the initial experiment was to determine the appropriate time to irradiate the cells after inoculating the culture dishes. Cells were trypsinized and reinoculated into dishes for set culture periods (2, 4, 6, 8, 12, 24, 36, 48, 60 or 72 h), trypsinized, and fixed in 70% methanol at -20°C for immunocytochemistry and flow cytometry. The fixed cells were stained with a monoclonal antibody that recognizes wild-type p53 protein (Oncogene Science, Inc., Uniondale, NY) or an immunoglobulin isotype antibody that recognizes a nonmammalian protein (Dako Corp., Carpinteria, CA). The antibody was detected using a biotinylated secondary antibody and a streptavidin/fluorescein fluorochrome. The positive control used was a rat fibroblast cell line derived by immortalization with the SV-40 large T antigen (Bolag, B. *et al. J. Virol. 63*: 863, 1989). The cells were also stained with RNase and propidium iodide for cell-cycle analysis.

The second experiment was to determine the peak response for p53 protein expression after irradiation. LECs were cultured for 48 h (70%-80% confluent), then exposed to 0.5 Gy alpha particles from a ^{238}Pu electroplated copper disc (Thomassen, D. G. *et al. Radiat. Prot. Dosim. 38*: 65, 1991), trypsinized, fixed at set periods after irradiation (2, 4, 6, 8, or 12 h), and stained as described above.

The third experiment was to determine the dose-response relationship. LECs were plated for 48 h, irradiated with graded doses of alpha particles (0, 0.01, 0.05, 0.1, 0.5, 1.0, or 2.0 Gy), trypsinized, and fixed 6 h after irradiation. The cells were stained as described above.

The cells stained for p53 and DNA content were analyzed by flow cytometry. Signals from forward light scatter, side-angle light scatter, and the fluorescence detectors were collected and stored for analysis. Only events associated with cells containing DNA were analyzed for p53 content. The number of p53-positive cells was determined by subtracting the number of events in each channel for control histograms from those for test histograms and correcting the figure for the number of events in each file.

The number of cells containing elevated levels of p53 protein increased following inoculation of the cells onto the culture dishes. The expression was maximal after 4-6 h and returned to background levels by 48 h. Cells that had been cultured for 48 h and exposed to 0.5 Gy alpha particles showed a maximal expression of p53 protein 4-6 h after irradiation. There was a nonlinear, dose-dependent increase in the number of cells expressing elevated levels of p53 protein following exposure to graded doses of alpha particles (Fig. 1). Cells containing increased levels of p53 protein were found in both the G_1 and G_2 phases of the cell cycle. A response was detected at the lowest dose used (0.01 Gy). At this dose, 9.5% of the cells in the G_1 phase of the cell cycle had increased levels of p53 protein.

---

*UNM/ITRI Inhalation Toxicology Graduate Student

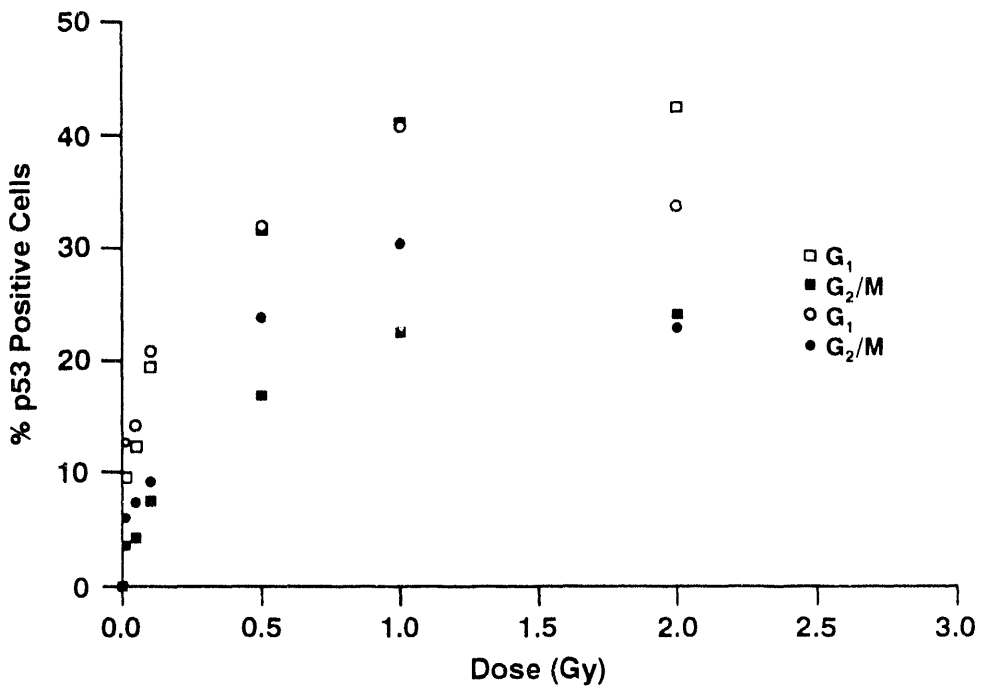

Figure 1. Percentage of cells staining positive for the p53 protein as a function of alpha-particle dose and cell-cycle phase (G_1 and G_2). Analyses are from two separate experiments (G_1: □, ○; G_2: ■, ●).

The presence of cells with increased levels of p53 protein in both G_1 and G_2 phases of the cell cycle is in contrast to the effect of X rays where the majority of positive cells are in the G_1 phase of the cell cycle (Kasten *et al.*, 1991). This difference may be related to the ability of alpha particles to cause greater chromosomal damage than X rays. The chromosomal damage would be expected to be repaired in the G_2 phase of the cell cycle prior to mitosis.

The nucleus is generally regarded as the target for alpha-particle damage. The estimated number of nuclei traversed by an alpha particle at 0.01 Gy is less than 3.5%. The difference between the number of cells expressing increased levels of p53 and the estimated number of nuclei hit suggests that the target for alpha particles is larger than the nucleus and that a hit cell may communicate with neighboring cells. A similar conclusion was drawn from an experiment in which the frequency of cells with sister chromatid exchange were greater than the number of nuclei traversed by an alpha particle (Nagasawa, H. and J. B. Little. *Cancer Res.* 52: 6394, 1992).

This latter study was also conducted at doses where only a small fraction of the nuclei were hit by an alpha particle, and dose-rate phenomena would be inoperative. Under these experimental conditions, a cell receives the lowest dose possible, i.e., one hit during the cell's life span. These results show that p53 expression may be a very sensitive indicator of DNA damage. In addition, there appear to be differences in the expression of p53 protein following alpha particle and X-ray exposure. Understanding these differences will provide information on how p53 acts as a cell-cycle checkpoint protein.

(Research sponsored by the Office of Health and Environmental Research, U.S. Department of Energy, under Contract No. DE-AC04-76EV01013.)

K-ras AND p53 ALTERATIONS IN LUNG TUMORS INDUCED IN THE F344 RAT BY X IRRADIATION

S. A. Belinsky, C. E. Mitchell, and F. F Hahn

The mutagenic properties of ionizing radiation have been demonstrated in many different *in vitro* systems (Breimer, L. H. *Br. J. Cancer 57*: 6, 1988). However, the molecular alterations underlying ionizing radiation-induced mutagenesis and the carcinogenic risk of low-dose exposure have not been clearly discerned. Point mutations primarily within codons 12, 13, or 61 of the K-ras gene are oncogenic and have been detected in lung tumors from humans and in chemically induced lung tumors in rats and mice (Rodenhuis, S. *et al. Cancer Res. 48*: 5738, 1988; Stowers, J. *et al. Cancer Res. 47*: 3212, 1987; Belinsky S. A. *et al. Mutat. Res. 233*: 105, 1990). Point mutations within exons 5-8 of the p53 gene inactivate this tumor suppressor gene; p53 alterations are present in approximately 50% of human lung cancers (Hollstein, M. *et al. Science 253*: 49, 1991). The purpose of this study was to determine whether the induction of lung tumors in the F344/N rat by X irradiation involves alterations in the K-ras and/or p53 genes.

Lung tumors were induced in F344 rats from the Institute's colony following thoracic or whole-body exposure to X rays (p. 64, this report). Exposures were fractionated and the total dose ranged from 3.5 to 12 Gy. Thirty-six tumors (18 adenocarcinomas, and 18 squamous cell carcinomas) were evaluated for alterations within the K-ras and p53 genes. Mutations present within codon 12 of the K-ras gene were detected by the BstN1 restriction fragment length polymorphism assay and identified by direct sequencing of K-ras exon 1 following amplification by the polymerase chain reaction (PCR). Exon 2 of the K-ras gene was examined by direct sequencing following PCR amplification. The prevalence for p53 gene dysfunctions was initially determined by immunohistochemistry using a polyclonal antibody (CM1) to the p53 protein. This procedure detects dysfunctional p53 genes with an 80% efficiency. The remaining mutations are detected using single strand conformation polymorphism (SSCP) technology. SSCP detects single base substitutions within DNA fragments up to 350 base pairs in length as shifts in electrophoretic mobility. Direct sequencing is then used to identify the mutation.

Activation of the K-ras gene was detected in only one tumor, an adenocarcinoma. The mutation was a G to A transition (GGT to GAT) within codon 12. Dysfunctional p53 protein was observed in three of 18 squamous cell carcinomas, but none of the adenocarcinomas demonstrated increased p53 protein (Table 1). The p53 staining characteristics differed among the three squamous cell tumors. In one tumor, the majority of squamous epithelium appeared to stain for p53 protein, while very focal staining was observed in another tumor. In the third tumor, staining appeared to be light and diffuse. For SSCP analysis of these three tumors, areas showing positive p53 immunoreactivity were microdissected from paraffin tissue sections, and the DNA isolated from this paraformaldehyde fixed tissue was amplified by PCR. SSCP analysis of exons 4-9 did not detect mutations in these three tumors. SSCP alterations in electrophoretic moblility were, however, detected in two other tumors (Table 1). One adenocarcinoma may have mutations in both exons 6 and 7, while an exon 5 mutation may be present in a squamous cell carcinoma. These exons will be sequenced to identify the actual mutation.

The results from this study indicate that alterations within the K-ras and p53 genes are rarely involved in the development of lung tumors induced in the rat by X rays. These results contrast with studies of human subjects and rodent lung tumors caused by other agents. Activation of the K-ras gene is detected in approximately 30% of human adenocarcinomas and 47% and 100% of lung tumors induced in the rat by high linear energy transfer radiation (plutonium) and tetranitromethane, respectively (Stegelmeier, B. L. *et al. Mol. Carcinog. 4*: 43, 1991; Stowers *et al.*, 1987). Thus, it is apparent that activation of the K-ras gene is strongly influenced by the initiating carcinogenic exposure. The lack of p53 alterations in rat lung tumors induced by X rays is consistent with studies using other compounds ongoing at the Inhalation Toxicology Research Institute (this report, p. 89). The lack of concordance between human and rat lung tumors for mutations within the p53 gene could be explained if mutations exist in other member genes of the p53 pathway (e.g., mdm1l; Oliner, J. D. *et al. Nature 358*: 80, 1992). The positive immunostaining of three squamous cell carcinomas suggests the potential for alterations within the p53 pathway. Future studies will focus on the identification of novel

oncogenes and tumor suppressor genes in X-ray-induced cancer and will also examine the genes that interact with p53.

Table 1

Immunoperoxidase Staining and SSCP Analysis of p53 in X-Ray-Induced Rat Lung Tumors

Tumor Type	Positive Immunostaining (Frequency)	SSCP[a] (Frequency)
Adenocarcinoma[b]	0/18	1/18
Squamous cell carcinoma	3/18	1/18

[a]Exons 4-9 of the p53 gene were evaluated by SSCP.
[b]This one adenocarcinoma appeared to have a mutation within both exons 6 and 7.

(Research sponsored by the Office of Health and Environmental Research, U.S. Department of Energy, under Contract No. DE-AC04-76EV01013.)

K-ras AND p53 ALTERATIONS IN LUNG TUMORS INDUCED IN THE F344 RAT BY DIESEL EXHAUST OR CARBON BLACK

D. S. Swafford, K. J. Nikula, and S. A. Belinsky*

The results of a study completed at ITRI (1991-92 Annual Report, p. 105) suggest that a high lung burden of carbonaceous particles, rather than mutagenic particle-associated organic compounds, is principally responsible for the carcinogenicity of inhaled diesel exhaust (DE) in rats. This conclusion is based on the failure of DE to produce an excess of lung tumors in F344/N rats over those produced by comparable lung burdens of carbon black (CB), a carbonaceous particulate that is virtually free of adsorbed organic compounds. In the current investigation, tumors from F344/N rats from the Institute's colony that were chronically exposed to either DE or CB were analyzed to determine if either activation of the K-ras oncogene or inactivation of the p53 tumor suppressor gene plays a role in the carcinogenicity of these particulates in the rat lung, and to determine whether patterns of genetic damage in these tumors support the hypothesis that particle-associated mutagenic compounds are not principally responsible for the induction of rat lung tumors by DE.

The K-ras protooncogene is frequently activated in human lung tumors and in experimentally induced tumors in rats and mice (Barbacid, M. *Ann. Rev. Biochem. 56*: 779, 1987). K-ras activation results from point mutation, usually in codons 12, 13, or 61. In animal models, compound-specific mutational profiles are often observed that are consistent with the base-mispairing effects of adducts between DNA and the experimental carcinogen. Variations in mutational spectra within the K-ras oncogene may thus reflect mechanistic properties of the initiating agent. In this system, a specific pattern of point mutations would suggest the participation of de-adsorbed mutagenic organic compounds in the carcinogenic effect of DE. The p53 tumor suppressor gene is also frequently altered in human lung tumors, and has been shown to be inactivated in experimentally induced tumors of the rat (Ohgaki, H. G. *et al. Cancer Res. 52*: 2995, 1992). The inactivation of this gene can result from point mutations, particularly within the conserved region of the gene (exons 4 through 9), although deletions and rearrangements elsewhere in the gene can also result in loss of function; thus, the p53 gene is subject to inactivation by various types of genetic damage. Examination of the incidence and spectra of alterations in these two genes in lung tumors induced by DE or CB should provide insight into the molecular mechanisms associated with the development of DE-caused tumors.

Tumor DNA was isolated from paraffin-embedded tissue sections using a quick-lysis method (Levi, S. *et al. Cancer Res. 51*: 3497, 1991), and specific gene fragments were amplified using the polymerase chain reaction (PCR) procedure. Because of the low concentration (< 100 pg) and substantial degradation of target DNA obtained from formalin-fixed, paraffin-embedded tissues and the need for high-purity gene fragment products for sequence analysis, a second PCR amplification was performed for each sample. Exons 4 through 9 of the p53 gene were then analyzed using the single-strand conformational polymorphism assay (SSCP) (Orita, M. *et al. Proc. Natl. Acad. Sci. 86*: 2766, 1989). Some samples, including those with apparent mutations, were sequenced by the dideoxy method (Tindal, K. R. and L. F. Stankowski. *Mutat. Res. 220*: 241 1989). Sequence data for p53 were compared to both the published sequence of the rat p53 gene and to samples of normal rat lung DNA isolated from paraffin-embedded sections by the same method used for the tumors.

Gene sequence information was corroborated by immunohistochemical (IHC) staining for the p53 protein. Point mutations within exons 5 through 8 result in an increased protein half-life which allows detection by IHC staining. Mutations in codon 12 of the K-ras gene were detected by BstN1 restriction endonuclease analysis (Kahn, S. M. *et al. Oncogene 6*: 1079, 1991), and direct sequencing was used to identify mutations present in codons 12, 13, or 61 of this gene. The sequence analysis and IHC results obtained to date are summarized in Tables 1 and 2.

These data suggest that the p53 and K-ras genes are infrequently altered in adenocarcinomas (AC) induced by either DE or CB. In squamous cell carcinomas (SCC), alterations in the K-ras gene appear to occur at a similar frequency to that seen in AC. Results indicate that the p53 gene is commonly inactivated in SCC (6/9),

*UNM/ITRI Inhalation Toxicology Graduate Student

and studies are in progress to identify the mutations within these samples. In addition, the number of tumor samples analyzed will be increased to 40 for AC (20 induced by DE and 20 induced by CB), and 10 for SCC. Furthermore, five AC obtained from unexposed F344/N rats will be included in the analysis to determine whether the pattern of alterations seen in the DE- or CB-induced tumors parallels that seen in spontaneous tumors with respect to these two genes. Although these results are preliminary, we have not observed a pattern of genetic alterations within K-ras or p53 that would suggest a differential mechanism between DE and CB carcinogenesis in the rat lung; however, the high incidence of p53 alterations detected in SCC indicates a potential role for inactivation of this gene in the development of tumors with squamous differentiation.

Table 1

Mutations Found in the K-ras and p53 Genes in
Rat Lung Tumors Arising from Exposure to DE or CB[a]

	p53 Exons						K-ras Codons		
Histotype	4	5	6	7	8	9	12	61	p53 IHC
Adenocarcinomas	0/17	0/17	1/10	0/15	0/18	0/18	1/20	1/16	0/25
Squamous cell carcinoma	0/3	0/3	0/8	1/8	1/8	0/8	1[b]/8	0/8	5[b]/9

[a]Values indicate number of tumors containing mutations over number of tumors evaluated. For IHC data, number of tumors with positive p53-dependent immunostaining is shown over the number of tumors evaluated.

[b]Indicates that number includes one mixed phenotype tumor (adenosquamous carcinoma). Only the portion of this tumor with squamous differentiation stained positive for p53 protein by IHC staining. Apparent alterations in p53 sequence are reported here when identified either by direct sequencing or by SSCP analysis. The K-ras mutations in codon 12 were confirmed by both direct sequencing and by BstN1 restriction endonuclease analysis.

Table 2

Comparison of K-ras and p53 Mutation Frequency
in Tumors Arising from Exposure to DE or CB[a]

	p53	K-ras		
Exposure	Exons 4-9	Codon 12 (GGT)	Codon 13 (GGC)	Codon 61 (CAA)
DE	6/21	1/21 (GAT)	0/21	1/16 (CAT)
CB	2/8	1/8 (GTT)	0/8	0/8

[a]Values shown indicate mutations detected by any of the methods used over the total number of samples evaluated. For the K-ras mutations, the sequence of the mutant is shown.

(Research sponsored by the Health Effects Institute under Funds-In-Agreement No. DE-FI04-93AL80314 with the U.S. Department of Energy under Contract No. DE-AC04-76EV01013.)

EPITHELIAL CELL KINETICS IN THE LUNGS OF F344 RATS THAT INHALE DIESEL EXHAUST OR CARBON BLACK

K. J. Nikula and I. Y. Chang

Diesel exhaust (DE), a complex mixture of gases, vapors, and soot particles, is a pulmonary carcinogen when inhaled chronically, at high concentrations, by rats. It is known that filtered DE is not a pulmonary carcinogen in rats, thus demonstrating that the carcinogenic response requires the presence of soot. A study conducted at ITRI in which rats were exposed to DE or the same concentrations of carbon black (CB), a carbonaceous particulate that is virtually free of adsorbed organic compounds, showed that the carcinogenic potencies of the two materials were nearly identical. This result suggested that the high lung burden of carbonaceous particles, rather than the mutagenic, soot-associated organic compounds, is principally responsible for the carcinogenicity of DE in rats (1991-92 Annual Report, p. 105).

Exposure-induced, sustained cell proliferation has been correlated with the induction of cancer (Butterworth, B. E. and T. L. Goldsworthy. *Proc. Soc. Exp. Biol. Med. 198*: 683, 1991). It has been proposed that (1) doses higher than expected for human exposures lead to increased cell proliferation, which accounts for much of the excess tumor incidence observed in bioassays, and (2) this carcinogenicity is not predictive for human cancer risk (Ames, B. N. and L. S. Gold. *Science 249*: 970, 1990).

To better understand the pathogenesis of the hyperplastic and neoplastic lung lesions induced by exposure to DE and CB, replicative and proliferative indices were quantitated in terminal bronchiolar epithelia, alveolar epithelia of focal hyperplastic lesions (referred to as focal lesions), which occur in the centriacinar region of the lung, and alveolar epithelia not included in the focal lesions (referred to as nonfocal lung). These data will show (1) if DE and CB induce the same or different proliferative responses with respect to magnitude over time and location, and (2) the location of the greatest, sustained proliferative response.

Groups of five male F344/N rats from the Institute's colony, 9 ± wk old, were exposed 16 h/day, 5 days/wk for 3, 6, or 12 mo to DE or CB at particle concentrations of 6.5 mg/m^3, or to filtered air (controls). To label S-phase nuclei, 0.78 mCi of tritiated thymidine (80.0 Ci/mmole) was delivered to each rat, via continuous infusion, over the last 6.5 days prior to sacrifice. Standard morphometric techniques were used to fix and sample the lungs and to determine the relative volume densities of a number of components of the alveolar parenchyma and indices of cell replication and proliferation (Elias, H. M. and D. M. Hyde. *Practical Stereology*, Karger, New York, 1983; Herbert, R. A. *et al. Radiat. Res. 134*: 29, 1993). The unit length labeling index (labeled epithelial nuclei/mm basal lamina) and the numeric density of epithelial nuclei (epithelial nuclei/mm basal lamina) were determined in the terminal bronchioles. The type II cell labeling index expressed as a percent (Type II LI; calculated from the ratio of labeled type II cells to the number of type II cells counted), the percent type II cells (calculated from the ratio of type II cells to the number of type II, type I, endothelial, and fixed interstitial cells), and the number of labeled type II cells per 4,000 lung cells (labeled II cells/4000 cells) were determined in the focal lesions and nonfocal lung. Unit length labeling index, Type II LI, and labeled II cells/4000 cells are indices of replication. These three indices are used with the numeric density of epithelial nuclei or the percent type II cells to evaluate cell proliferation. In a preliminary statistical analysis, differences in unit length labeling indices and numeric densities between groups were tested using a *t* test with a Bonferroni correction for multiple comparisons. Significance was set at an overall p value of less than 0.05. Statistical analyses of the data for the focal lesions and nonfocal lung have not been done.

The data for the terminal bronchioles, nonfocal lung, and the focal lesions are presented in Table 1. In the terminal bronchiolar epithelium, the unit length labeling indices of DE- and CB-exposed rats were significantly greater than those of controls at 3, 6, and 12 mo. The greatest unit length labeling indices were measured at 3 mo in both CB- and DE-exposed rats. The unit length labeling indices of DE-exposed rats were greater than those of CB-exposed rats at 3 and 6 mo, but not at 12 mo. The numeric densities in the terminal bronchioles were similar in all groups at all times.

Table 1

Indices of Cell Replication and Proliferation in the Lungs of Rats that Inhaled Diesel Exhaust or Carbon Black

Exposure Atmosphere[a]	Duration (mo)	ULLI[b]	ND[c]	Type II LI[d]		% II Cells[e]		L II/4000 Cells[f]	
				NF[g]	FL[h]	NF	FL	NF	FL
Air	3	4.0 ± 0.7[i]	146.4 ± 3.5	8.8 ± 0.8		10.5 ± 0.2		37.4 ± 7.4	
DE	3	16.1 ± 1.6	167.6 ± 17.0	11.8 ± 1.1	24.2 ± 0.6	15.3 ± 0.5	39.4 ± 0.7	69.0 ± 13.5	380.6 ± 18.1
CB	3	10.9 ± 0.6	161.2 ± 8.9	13.7 ± 0.6	27.1 ± 1.4	12.8 ± 0.4	38.5 ± 0.7	69.4 ± 7.8	411.4 ± 35.2
Air	6	1.9 ± 0.3	144.7 ± 7.9	6.3 ± 1.0		10.6 ± 0.5		27.4 ± 4.8	
DE	6	9.0 ± 0.8	138.5 ± 7.4	7.9 ± 0.3	13.4 ± 0.4	21.4 ± 0.6	45.0 ± 0.8	67.4 ± 4.6	239.8 ± 17.8
CB	6	5.9 ± 0.4	158.4 ± 6.2	8.8 ± 1.1	15.3 ± 0.3	16.0 ± 0.3	46.9 ± 0.1	56.1 ± 15.6	287.2 ± 11.1
Air	12	1.2 ± 0.2	148.6 ± 6.6	3.2 ± 0.7		11.4 ± 0.15		14.5 ± 3.2	
DE	12	8.4 ± 0.6	186.7 ± 9.6	5.1 ± 0.4	14.4 ± 1.0	24.0 ± 0.2	38.8 ± 0.7	48.8 ± 8.7	223.2 ± 16.9
CB	12	6.8 ± 0.6	164.0 ± 9.0	3.3 ± 0.3	11.1 ± 0.4	19.6 ± 0.4	40.6 ± 0.4	26.5 ± 5.2	180.5 ± 16.7

[a]Exposures were for 16 h/day, 5 days/wk to filtered air, diesel exhaust (DE), or carbon black (CB) at particle concentrations of 6.5 mg/m^3.
[b]Unit length labeling index defined as the labeled epithelial nuclei/mm terminal bronchiolar basal lamina.
[c]Numeric density defined as the number of epithelial nuclei/mm terminal bronchiolar basal lamina.
[d]Type II cell labeling index (ratio of labeled type II cells to the number of type II cells counted expressed as a percent).
[e]Percent type II cells (ratio of type II cells to the number of type II, type I, endothelial, and fixed interstitial cells expressed as a percent).
[f]Number of labeled type II cells per 4,000 lung cells.
[g]Nonfocal defined as areas of the pulmonary parenchyma that are not part of discrete focal lesions.
[h]Focal lesions defined as hyperplastic and inflammatory lesions principally located in the centriacinar pulmonary parenchyma. There were no FLs in air-exposed rats.
[i]Mean ± standard error, n = 5.

In the nonfocal lung, the Type II LIs were similar in rats exposed to filtered air, CB, or DE at 3, 6, and 12 mo; the Type II LIs decreased in all groups over time. The percent type II cells was greater in rats exposed to DE or CB than in controls at 3, 6, and 12 mo, and the percent type II cells was greater in DE- than CB-exposed rats at each time. The percent type II cells increased in rats exposed to DE or CB over time. The relatively large standard errors make the labeled II cells/4000 cells data difficult to interpret for the nonfocal lung, but the data are similar for the DE- and CB-exposed rats. The labeled II cells/4000 cells appeared to be greater in the DE-exposed rats compared to controls at 6 and 12 mo. The labeled II cells/4000 cells in the nonfocal lung decreased in all groups over time.

Focal lesions were not present in the control lungs. In the rats exposed to DE or CB, the Type II LIs in the focal lesions were two- to three-fold greater than the Type II LIs in the nonfocal lung of controls at each time. There was no consistent difference in Type II LIs between DE- and CB-exposed rats at any time. The percentages of type II cells in the focal lesions of the DE- and CB-exposed rats were similar at all times and were three- to four-fold greater than the percent type II cells in the nonfocal lung of controls. The labeled II cells/4000 cells in the focal lesions were (1) 10- to 15-fold greater than the labeled II cells/4000 cells in the nonfocal lung of controls, (2) were similar in the DE- and CB-exposed rats at each time, and (3) decreased over time.

The greater unit length labeling indices in DE- than CB-exposed rats at 3 and 6 mo suggest that DE induces a greater replicative response than CB in the terminal bronchioles at earlier times, but not after 12 mo of exposure. The lack of increase in the numeric densities of epithelial nuclei, especially the lack of increase at 3 and 6 mo, shows that although both DE and CB induce replication, neither DE nor CB cause proliferation. The unit length labeling index and numeric density of epithelial nuclei data suggest that DE and CB induce cell injury that leads to regenerative replication in the terminal bronchioles, and that the amount of injury and subsequent regeneration is greater for DE than CB at 3 and 6 mo of exposure.

In the nonfocal lung, the Type II LI data indicate that type II cell replication was not enhanced by DE or CB exposure, and that replication decreased in all groups over time. The labeled II cells/4000 cells index, which can be a more sensitive indicator of type II cell replication when there is concomitant hyperplasia, suggests that DE exposure caused a modest increase in replication compared to controls at 6 and 12 mo; these data also show that type II cell replication decreased in all groups by 12 mo. The percent type II cell data show that both DE and CB exposure caused type II cell hyperplasia in the nonfocal lung. The amount of hyperplasia increased over time and was greater for DE than CB. These percent type II cell data, in conjunction with the Type II LIs and the labeled II cells/4000 cells, indicate that a lack of differentiation of type II cells to type I cells, rather than enhanced replication of type II cells, may have been a significant factor in the type II cell hyperplasia in the nonfocal lung. Preliminary examination of the percent type I cells (data not shown) supports this speculation.

All three indices of replication and proliferation show that DE and CB induce similar, sustained proliferative responses in the focal lesions. The volume percent of the lung composed of interstitium of focal lesions increased in the DE- and CB-exposed rats (data not shown), further supporting the conclusion that the greatest sustained proliferation was in the focal lesions.

In the carcinogenicity study (1991-92 Annual Report, p. 105), the neoplasms induced by DE or CB exposure in rats appeared to arise from the alveolar epithelium of hyperplastic foci. The equivalent replicative and proliferative responses induced by DE and CB in these regions where the neoplasms apparently arise corroborate the tumor incidence and tumor site data from the carcinogenesis bioassay.

(Research sponsored by the Office of Health and Environmental Research, U.S. Department of Energy, under Contract No. DE-AC04-76EV01013.)

RAPID DETECTION AND QUANTITATION OF MUTANT K-ras CODON 12 RESTRICTION FRAGMENTS BY CAPILLARY ELECTROPHORESIS

C. E. Mitchell, S. A. Belinsky, and J. F. Lechner

Ras mutations are found in a large number of epithelial cell cancers and in subtypes of leukemia. The role of ras in the early stages of cancers as well as the interaction of ras genes with additional genetic alterations are areas of active investigation. A recent breakthrough has been made in detecting ras mutations with the use of the BstN1 endonuclease restriction fragment polymorphism (RFLP) assay (Kahn, S. M. *et al. Oncogene 6*: 1079, 1991). Although this assay can detect one mutant gene in a total population of 10,000 cells, it is labor-intensive, time-consuming, and nonquantitative.

Capillary gel electrophoresis (CE) is another recent innovation in the analysis of DNA fragments (Mayer, A. *et al. Arch. Pathol. Lab. Med. 115*: 1228, 1991). The advantages of this technique are decreased analysis time, single base resolution with oligos of > 100 bases, reduced sample requirements, automation, and especially quantitation. In this report, we examine the use of CE to separate and quantitate K-ras mutant and wild-type (WT) alleles following selection by BstN1 endonuclease digestion.

DNA was isolated from the following tumor cell lines: SW480, A549, Calu-1, SKlu-1, and H345. These cell lines were either homozygous or heterozygous for K-ras codon 12 mutations. Standard conditions for the polymerase chain reaction (PCR) amplification and BstN1 endonuclease digestions were used to amplify DNA and obtain the digestion fragments for analyses (Jiang, W. *et al. Oncogene 4*: 923, 1989). Following amplification and digestion, mutant and WT bands of 157 and 128 base pairs were formed, respectively. In the original RFLP procedure, these fragments were separated and analyzed by acrylamide gel (8%) electrophoresis. The gel fragments were then recognized by staining with ethidium bromide and photographed, and the relative concentrations of DNA in each band were estimated visually. Our new system uses CE analysis instead of acrylamide gel electrophoresis. Aliquots of the PCR amplification products are first added to Centricon 30 spin columns to remove salts and low-molecular-weight materials. The purified material is then separated on a fused silica capillary column filled with a hydrophilic low viscosity polymer by an Applied Biosystem Model 270-HT CE instrument and analyzed using a Model 600 data analyzing package.

Figure 1 shows the slab gel analysis of BstN1 fragments of SW480, Calu-1, SKlu-1, A549, and WT DNA. One-stage of 30 rounds of PCR amplification (single-stage PCR) was used to amplify the DNA. Mutant and WT bands in Calu-1 and SKlu-1 were clearly separated. In addition, homozygosity for the K-ras codon 12 mutation in SW-480 and A-549 cell lines was evident. Differences in the intensities of the stained bands were also observed; however, it was not possible to accurately determine the percent of the mutant band relative to the WT band.

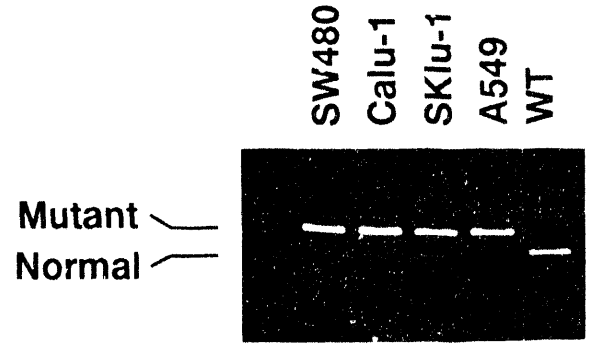

Figure 1. Polyacrylamide gel analysis of K-ras codon 12 mutant and wild-type (WT) BstN1 fragments of SW480, Calu-1, SKlu-1, A549, and WT. DNA was separated on a 8% acrylamide gel, stained with ethidium bromide, and photographed. Mutant and WT fragments are 157 and 128 base pairs in size, respectively.

In Figure 2, a representative CE electropherogram of BstN1 endonuclease digestion fragments of Calu-1 is depicted. The mutant and WT fragments in Calu-1 were both resolved. The OX174 fragments ranging from 72 to 1353 base pairs were also resolved by CE (data not shown). A volume integration was done on both mutant and WT bands, and the volume of the 157-bp band (mutant) was divided by the total volume. This value multiplied by 100 reflects the percentage of the mutant alleles in the population. These calculations showed that the percentages of mutant alleles in Calu-1 and SKlu-1 were 86 and 79%, respectively. It was also determined by multiple analysis of individual PCRs that the reproducibility of the analysis had an average coefficient of variation of ± 2.3%.

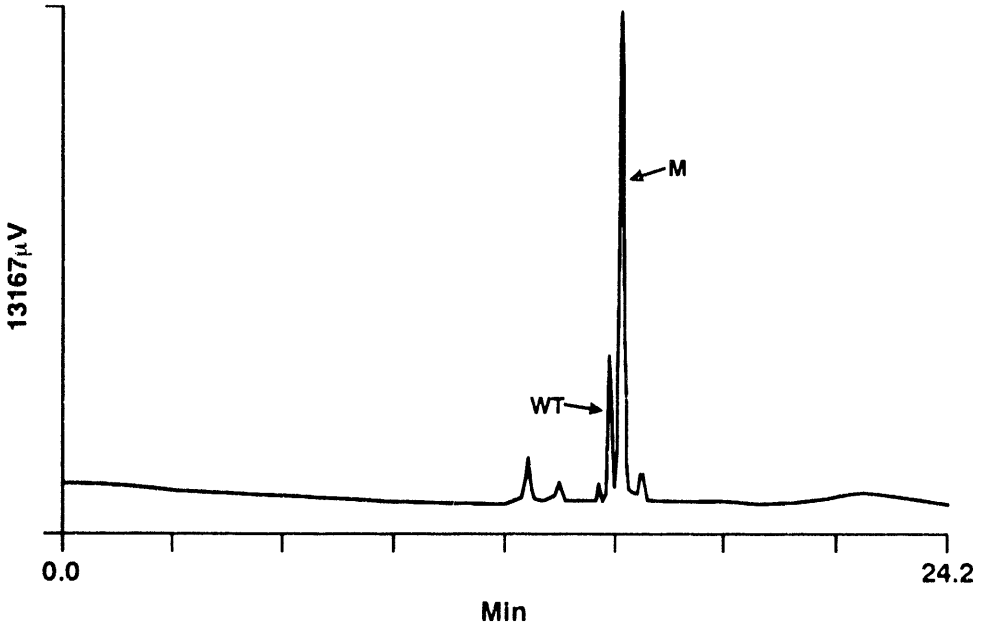

Figure 2. Electropherogram of BstN1 fragments from Calu-1. The DNA sample was separated on a fused silica capillary column filled with a hydrophilic low viscosity polymer. DNA was electrokinetically injected for 5 sec at -5 kV and separated at 12 kV. Detection of DNA was at 260 nm.

Results from this study show the applicability of CE to separate and, particularly, quantitate BstN1 K-ras codon 12 mutant and WT fragments. The reproducibility of the assay was evident over several experiments, and the percentages of mutant genes in the different cell line populations were similar to values reported by others using direct sequencing (Capon, D. *et al. Nature 304*: 507 1983). Although the single-stage PCR protocols using the BstN1 RFLP procedure can detect mutant alleles to the 1% level, studies to examine the role of ras gene mutations as early events in the initiation of cancer require a detection sensitivity of ~ 0.01%. To achieve this sensitivity, a second PCR following the BstN1 endonuclease digestion can be performed to selectively reamplify the mutant species which were left uncut by the BstN1 endonuclease.

Future studies will concentrate on using the two-stage PCR procedure in conjunction with the CE analysis to detect mutant alleles that occur at low frequencies. The cell lines in the present study will be used to validate the accuracy of the two-stage procedure in order to quantitate the percent of mutant alleles in the presence of WT alleles. Experiments with dilutions of mutant and WT DNA will be reconstructed to achieve a calibration curve with a sensitivity of 10^{-4}. Thus, the combined high sensitivity and quantitative capabilities of the CE should make it possible to quantitate the frequency of K-ras mutations in target and nontarget lung cell populations in animal models following exposure to carcinogens. This technology will also be applied as a screen for K-ras mutations in exfoliated cells collected in sputum or in a bronchial wash from persons at risk for lung cancer.

(Research sponsored by the Office of Health and Environmental Research, U.S. Department of Energy, under Contract No. DE-AC04-76EV01013.)

AN IMPROVED METHOD FOR THE ISOLATION OF TYPE II AND CLARA CELLS FROM A/J MICE

S. A. Belinsky, J. F. Lechner, and N. F. Johnson

The lung contains over 40 different types of cells (Sorokin, J. P. In *Morphology of Experimental Respiratory Carcinogenesis*, Oak Ridge, TN, AEC Symposium Series, p. 3, 1970). However, by identifying and isolating target cells for neoplasia, the effect of environmental and occupational exposures on nontarget cells can be eliminated. Previous studies have identified the alveolar type II cell and the Clara cell as progenitor cells for the development of human adenocarcinoma of the peripheral lung (Gazdar, A. F. and R. I. Linnoila, *Semin. Oncol. 15*: 215, 1988). In contrast, lung tumors appear to originate from the alveolar type II cell in the A/J mouse (Belinsky, S. A. *et al. Cancer Res. 52*: 3164, 1992). Thus, the comparison of the frequency and the nature of gene alterations between type II cells and Clara cells isolated from the A/J mouse may uncover factors seminal in the initiation and clonal expansion of neoplastic cells. The purpose of this study was to improve current procedures for isolating purified preparations of type II and Clara cells from mice for cellular and molecular analyses.

Current protocols for the sequential isolation of type II and Clara cells rely on protease digestion followed by centrifugal elutriation (Belinsky *et al.*, 1992). The process of centrifugal elutriation separates cells based on size and density. This isolation procedure routinely results in a type II cell preparation with a purity of 48%. The contaminating cells include Clara cells (16%), macrophages (20%), and small cells (16%). The typical purity of the Clara cell preparation is 43% with contamination by type II cells (20%), macrophages (20%), and small cells (17%). The low purity obtained by this approach is due primarily to the size distribution of mouse lung cells which overlap each other. Thus, while it was possible to enrich for type II or Clara cells out of the initial lung cell digest, high purity fractions have not been obtained.

The strategy used in the current study was to collect type II and Clara cell fractions using the previous elutriation protocol (Belinsky *et al.*, 1992) and further purify these fractions with an additional elutriation step using a different elutriation chamber. The flow diagram depicted in Figure 1 illustrates the complete elutriation procedure. Lung perfusion and digestion are essentially as described previously (Belinsky *et al.*, 1992). Lungs from 12 to 16 A/J mice were pooled for isolation of cells. The cell digest was injected into a standard elutriation chamber which can separate populations whose diameters differ by 2.5 to 5 μm. Four fractions were collected during this elutriation (Table 1). Fraction 1, which was collected at a rotor speed of 2500 rpm and a flow rate of 9.0 mL/min, was comprised mainly of cellular debris. Fraction 2, which was collected at 2300 rpm and a flow rate of 14 mL/min, consisted mainly of endothelial cells and lymphocytes (small cells). Type II cells were recovered in the third fraction at a rotor speed of 1200 rpm and a flow rate of 13 mL/min. The elutriator was then turned off, and the Clara cells (fraction 4) were collected as a pellet remaining within the standard chamber. Type II and Clara cells were concentrated by centrifugation at 2000 rpm for 10 min.

In the second part of the method, the Standard chamber was replaced with the Sanderson chamber which can elute populations whose diameter vary by only 1.5 to 2.5 μm. This chamber accommodates fewer cells than the Standard chamber (a factor of 3). The type II cells from the first elutriation were then injected into the chamber, and the first and second fractions were collected at a rotor speed of 2500 rpm and 8 mL/min. The first and second fractions contained debris and small cells, respectively. The type II cells were collected in fraction 3 at a speed of 1800 rpm and a flow rate of 10 mL/min. Clara cells originally contaminating the type II cell preparation were collected as a cell pellet remaining in the chamber; they were combined with the Clara cell fraction from the first elutriation (Fig. 1). This Clara cell fraction was further purified by elutriation using the same protocol for purification of the type II cells with the Sanderson chamber. Cell purity and yield during all three elutriations are indicated in Table 1. Type II and Clara cells were identified after staining with the modified Papanicolaou stain (Kikkawa, Y. and K. Yoneda, *Lab. Invest. 30*: 76, 1974) and the nitroblue tetrazolium stain (Devereux, T. R. and J. R. Fouts, *Methods Enzymol. 77*: 147, 1981), respectively. The purity of the type II cell preparation was increased from 48% to 73%, while the Clara cell contamination was reduced from 16% to 2.5% (Table 1). The purity of the Clara cell preparation was increased from 43% to 73%, and contamination by type II cells decreased from 20% to 12%. Viability of both cell populations was greater than 95% based on trypan blue exclusion.

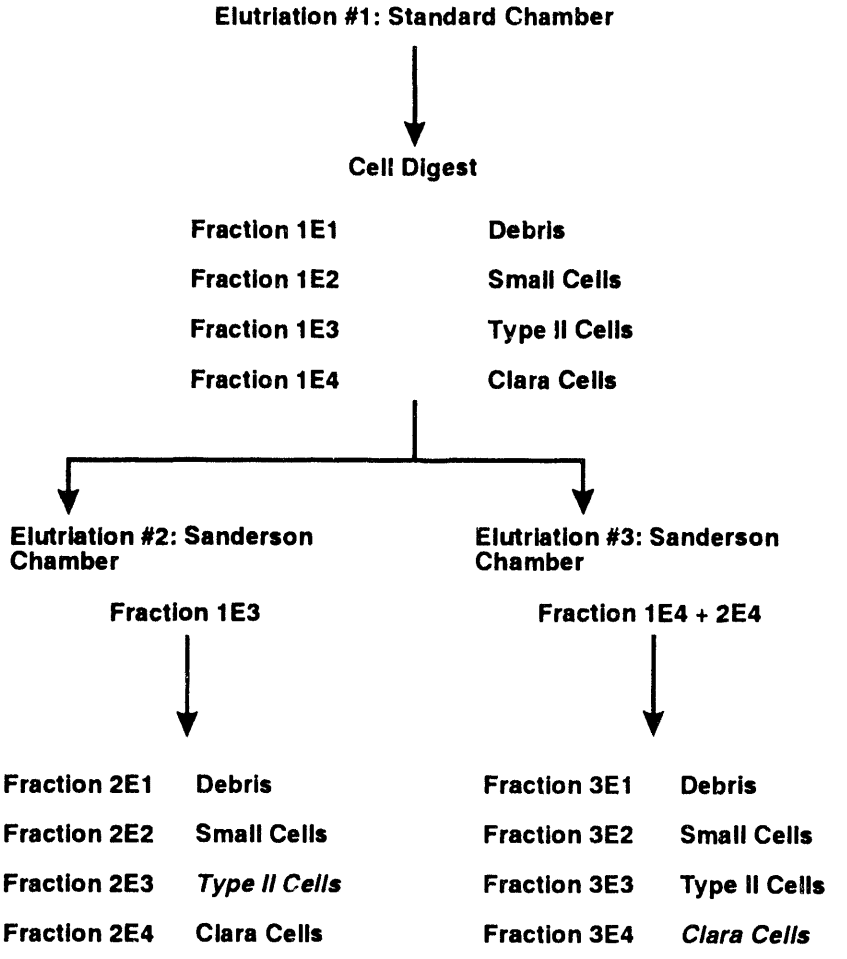

Figure 1. Flow diagram for isolation of type II and Clara cells from the mouse. High purity populations indicated by italicized type for type II and Clara cells are obtained in fractions 2E3 and 3E4, respectively.

Table 1

Purity and Yield of Type II and Clara Cells Isolated by Centrifugal Elutriation

Cell Fraction	Total Cells/Lung ($\times 10^6$)	Type II (%)	Clara (%)
Cell Digest	31 ± 2.0[a]	22 ± 2.0	16 ± 2.0
1E3	5 ± 0.2	48 ± 2.0	16 ± 2.0
1E4	3 ± 0.3	20 ± 7.0	43 ± 2.0
2E3	4 ± 0.6	73 ± 2.0	2 ± 1.0
3E4	1 ± 0.3	12 ± 2.6	73 ± 2.6

[a]Mean ± SEM from four cell isolations.

The ability of isolated type II and Clara cells to grow in culture was also examined. Cells were seeded on 60 mm polystyrene plates at a density of 50,000 cells. Prior to seeding, the plates were coated with FNC coating medium (BRFF, Inc., Rockville, MD). Growth of the cells in four different media (MCDB 151, M199, LHC9, and ITRI 1) known to promote growth of lung airway epithelial cell was assessed. All media were supplemented with insulin, transferrin, selenium, and cholera toxin and contained 2% or less fetal bovine serum. LHC9 and ITRI 1 contained pituitary growth extract and retinoic acid at concentrations also known to promote airway epithelial cell growth. Cells were fixed and stained with Giemsa 1 and 7 days after inoculating to determine colony-forming efficiency. Colonies of 5-6 Clara cells were observed frequently in ITRI 1 medium, and to a lesser extent with the other media. In contrast, type II cells did not replicate in any media; the cells appeared stellate with fine, long pseudopodia. These results suggest that Clara cells will undergo at least limited replication *in vitro*. Future studies will use DNA and RNA obtained from isolated type II and Clara cells to elucidate pathways involved in cell transformation following exposure to environmental carcinogens.

(Research sponsored by the Office of Health and Environmental Research, U.S. Department of Energy, under Contract No. DE-AC04-76EV01013.)

V. NONCARCINOGENIC RESPONSES TO INHALED TOXICANTS

INDUCTION OF NASAL CARBOXYLESTERASE IN F344 RATS FOLLOWING INHALATION EXPOSURE TO PYRIDINE

K. J. Nikula, R. Novak, I. Y. Chang, A. R. Dahl, and J. L. Lewis*

Heterocyclic amines such as pyridine constitute an important class of xenobiotics that is frequently used as solvents, intermediates in the production of agricultural chemicals (insecticides, herbicides), and in the manufacture of pharmaceuticals. Pyridine is a amphipathic solvent that is readily absorbed through inhalation, ingestion, or cutaneous exposure. A major metabolic pathway for pyridine is via cytochrome P-450 oxidation, and pyridine has been shown to induce cytochromes P-450 CYP1A1 and 1A2 in nasal tissues following inhalation exposures.

Carboxylesterases (CEs), which have high levels of activity in the olfactory mucosa, metabolize inhaled esters to toxic metabolites. The distribution of these esterases within the olfactory epithelium is known to be cell specific with the major localization occurring in the acinar cells of Bowman's glands and the apical cytoplasm of the sustentacular cells (1991-92 Annual Report, p. 190). Although CEs are not involved in the metabolism of pyridine, previous research suggested an increase in CE expression in hepatic microsomes following pyridine exposure. Because inhalation is a primary route of exposure to pyridine and because CE is sensitive to modulation by chemical exposure and mucosal lesions, we have examined the effect of pyridine inhalation on CE expression in the olfactory mucosa.

Twenty male F344/N rats (13-15 wk; 210-285 g) from the Institute's colony were used in this study. The nose-only exposures were conducted in two sets. In the first, five rats were exposed to filtered air (controls) and five to 444.0 ± 16.0 ppm pyridine 6 h/day for 4 days. In the second set, five rats were exposed to filtered air (controls) and five to 5.1 ± 0.4 ppm pyridine 6 h/day for 4 days.

Approximately 18 h following their final exposure to air or pyridine, the rats were sacrificed, and the nasal cavities were formalin fixed, decalcified, and sectioned transversely into four blocks (Young, J. T. *et al. Fundam. Appl. Toxicol. 1*: 309, 1981). The fourth block, which contains the caudal ethmoturbinates and caudal portion of the nasal septum, was paraffin embedded and cut into serial 5 μm sections. One section from each rat was stained with hematoxylin and eosin. Additional serial sections were immunostained for CE using Vectastain ABC immunoperoxidase reagents (Vector Laboratories, Burlingame, CA), diaminobenzidine chromogen, and primary antibody concentrations of 1:1000, 1:2000, 1:4000, 1:8000, 1:16,000, 1:32,000, 1:64,000, 1:128,000, 1:256,000, 1:512,000 CE-immunized goat sera. Serial sections (normal goat sera [NGS] controls) were reacted with the same 10 concentrations of NGS substituted for immunized goat sera in the primary incubation. One slide from each rat was stained according to the same procedure, but neither immunized nor NGS was applied (negative control slide for calibration of background optical density).

Immunostained nasal sections were analyzed by light microscopy and a semi-automatic image analysis system. The optical density of the CE-dependent immunoperoxidase reaction product was quantitated using the microdosimetry capabilities of an image analysis software package (Image Measure, Phoenix Technologies, Inc., Seattle, WA). The system was recalibrated (maximal [no light] and background optical density) for each rat.

The optical densities were determined bilaterally at 15 contiguous sites in the lamina propria on each side of the nasal septum. The data were used to devise a single descriptive value (mean total optical density) representing the average density of the immunoperoxidase reaction product at each primary antibody dilution for each animal. The process was repeated for the corresponding NGS slide. The mean total optical density for the NGS slide was subtracted from the mean total optical density for the immunized-goat sera slide to obtain a net mean total optical density at each serum dilution for each rat. The net mean values at each serum dilution were analyzed using a repeated measures analysis of variance.

---

*Institute of Chemical Toxicology, Wayne State University, Detroit, Michigan

Immunostaining of nasal tissue from air-exposed control rats with anti-CE (1:8000 dilution) showed a moderate positive staining of most cells of Bowman's glands that were located deep in the lamina propria. The majority of gland and duct cells that were located more superficially in the lamina propria were faintly stained. The apices of a few sustentacular cells lining the ethmoturbinates and septum were also faintly stained. At higher antibody concentrations, the immunostaining of the gland and duct cells increased in intensity, and all gland and duct cells showed at least some immunoreactivity. The gradient of immunostaining remained, so that the deeper glandular cells were more strongly immunoreactive than the superficial gland and duct cells. At the higher antibody concentrations, more of the sustentacular cells were positively immunostained. As the antibody concentrations decreased, the staining at all mucosal sites became less intense. At the highest dilutions, few to none of the gland or duct cells and none of the sustentacular cells were immunostained.

Immunostained nasal sections from rats exposed to 444 ppm pyridine vapor exhibited a cellular distribution of immunoreactive CE that was similar to that observed in air-exposed controls. However, there were exposure-related differences in the level of CE expression and in the extent of the immunostaining in Bowman's glands and the surface epithelium. There was strongly positive immunoreactivity of the deep glandular cells and strong to moderate positive immunoreactivity of the superficial glands and ducts with a 1:8000 concentration of anti-CE. Most fields did not exhibit an immunostaining gradient between the deep and superficial gland cells; they were equally immunoreactive throughout the depth of the lamina propria. Most sustentacular cells were immunostained; the intensity of the reaction varied from faint to strong. At higher antibody concentrations, all Bowman's gland and duct cells were strongly immunoreactive, and there was no gradient between the deep and superficial cells. The immunoreactivity of the sustentacular cells also became more intense and uniform. At weaker antibody concentrations, the intensity of the staining reaction decreased. Some fields exhibited a gradient between the superficial and deep gland or duct cells, but most did not.

At each antibody concentration, immunostained sections from rats exposed to 5 ppm pyridine vapor showed increased immunostaining of the superficial Bowman's gland and duct cells, as compared to controls, but the staining was not as intense as in the rats exposed to 444 ppm pyridine vapor. The immunostaining of the apices of the sustentacular cells was more intense and involved more of the epithelium than was the case for either the controls or the rats exposed to 444 ppm pyridine vapor.

The effect of pyridine exposure on the relative levels of immunoreactive CE is illustrated in Figure 1. The curve of optical density for the 444 ppm pyridine-exposed rats was significantly different from controls ($F_{1,8}$ = 12.5, p = 0.0083). The statistical analysis has not been completed for the dilution curve for the 5 ppm pyridine-exposed rats.

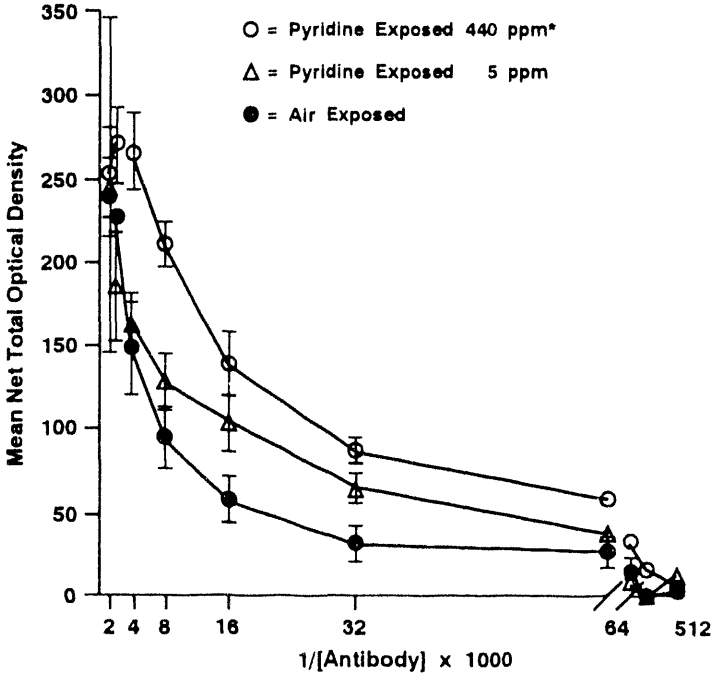

Figure 1. Dilution curves of immunohistochemical staining density in olfactory mucosae from rats exposed to either filtered air, 444 ppm, or 5 ppm pyridine. Mean net total optical density ± standard error of the mean are plotted at each serum dilution. The curve of optical density for 444 ppm pyridine-exposed animals is significantly different from controls. Optical density for staining of 5 ppm pyridine-exposed animals is plotted, but statistical analysis was not done.

These results indicate that CE can be induced in the nasal mucosa and describe the potential for toxic substances to induce enzymes not directly involved in their own metabolism, even following low-dose, short-term exposure. Increased expression of CE occurred in the rats exposed to the threshold limit value (5 ppm) for pyridine vapor in the workplace. Lastly, these results emphasize the importance of exposure history in predicting the metabolism of toxic substances.

(Research sponsored by the National Institutes of Health under Grant 5R01-ES03656-07 from the NIEHS by subcontract with Wayne State University under Funds-In-Agreement No. DE-FI04-89AL58635 with the U.S. Department of Energy under Contract No. DE-AC04-76EV01013.)

TOBACCO SMOKE-INDUCED ALTERATIONS OF RHODANESE AND CARBOXYLESTERASE IN THE OLFACTORY MUCOSAE OF F344 RATS

K. J. Nikula, L. A. Sachetti, G. L. Finch, B. T. Chen, and J. L. Lewis*

Nasal olfactory mucosa is often the first tissue to be exposed to inhalants. This mucosa contains enzymes that can detoxicate or activate inhaled toxicants. Inhalants may, in turn, alter the olfactory mucosa in numerous ways such as causing morphologic lesions, altering the cellular localization of enzymes, or altering enzyme activity. Rhodanese (RH) and carboxylesterase (CE) are two enzymes that are present in high levels in olfactory tissues, and their activities may protect the olfactory tissue, may protect other tissues, or, in the case of CE, may lead to local tissue damage. RH metabolizes cyanide to the less toxic thiocyanate ion (Westly, J. In *Advances in Enzymology* [E. F. Nordand and A. Meister, eds.], Wiley, New York, p. 327, 1973). Nasal CE can be protective, as in the metabolism of malathion. Alternatively, CE metabolizes inhaled acrylate esters and acetates to carboxylic acids and alcohols, which are known to be toxic to olfactory epithelium (Miller, R. R. *et al. Toxicol. Appl. Pharmacol. 75*: 521, 1984). Acetates, acrylate esters, and cyanide are constituents of tobacco smoke, which is a common nasal toxicant. RH activity is decreased in the nasal respiratory tissues of human smokers (Lewis, J. L. *et al. Toxicol. Appl. Pharmacol. 108*: 114, 1991). The effect of tobacco smoke exposure on the amount or activity of CE in human nasal mucosae is unknown. The amount of CE, as detected by immunohistochemical techniques, decreases in metaplastic and hyperplastic lesions of human respiratory mucosae (1991-92 Annual Report, p. 190). Based on these data, we hypothesized that tobacco smoke would induce lesions in rat nasal olfactory mucosae which would correlate with a decrease in the amount and activity of RH and CE.

We used 30 CD®(F344)/CrlBR rats purchased from Charles River Laboratories (equal numbers of males and females) exposed in whole body chambers to filtered air (controls) or mainstream 1R3 research cigarette smoke at concentrations of 100 (low smoke, LS) or 250 (high smoke, HS) mg total particulate matter/m^3. The exposure methods have been described in detail (Chen, B. T. *et al. J. Aerosol Med. 5*: 19, 1992). Six-week old rats were exposed for 6 h/day, 5 days/wk, for 32 wk.

Formalin-fixed, paraffin-embedded, transverse sections of rat nasal olfactory tissue (level 3 as described in Young, J. T. *Fundam. Appl. Toxicol. 1*: 309, 1981) from three males and three females per exposure group were used for histopathologic and immunohistochemical analyses. Serial sections were stained with hematoxylin, eosin, and alcian blue or reacted with polyclonal antibodies to RH (rabbit origin, 1:1200) or CE (goat origin, 1:8000). We used the same concentrations of normal rabbit or goat sera in place of the primary antibodies for the corresponding negative control slides. Vectastain ABC (Vector Laboratories, Burlingame, CA) immunoperoxidase reagents and diaminobenzidine chromagen were used to detect the immunoreactivity.

The biochemical assays for RH and CE activities were performed on tissue homogenates of rat ethmoturbinates, which are lined by olfactory mucosa. For each assay, two tissue pools, each composed of ethmoturbinates from two rats (n = 2) were used per exposure level. Mitochondrial and S-9 (cytoplasmic and microsomal) preparations were used for the RH and CE assays, respectively. RH biochemical activity was determined by measuring the rate of formation of thiocyanate (cyanide metabolism), whereas the CE biochemical activity was determined by measuring the rate of formation of p-nitrophenol (4-nitrophenyl butyrate metabolism). From these data we determined maximum velocity (Vmax), the enzyme affinity for its substrate (1/Km), and the capacity of each enzyme to metabolize its substrate at low substrate concentrations (Vmax/Km).

No histopathologic lesions were observed in the filtered air control olfactory mucosae. Both the LS-exposed and HS-exposed olfactory mucosae had proteinaceous globules in many of the sustentacular cells, particularly in lateral regions of the ethmoturbinates. There was a concomitant loss of neurons in the portions of the epithelium with extensive proteinaceous globules. In addition, the HS-exposed olfactory mucosa lining the dorsal nasal septum and dorsal meatus exhibited focal epithelial necrosis, attenuation, and loss of Bowman's gland acini in some sections.

*Department of Energy/Associated Western Universities Teacher Research Associates Program (TRAC) Participant

The filtered air control olfactory mucosae exhibited a fine, brown, granular RH-specific immunoreactivity that was most intense in the apical portions of sustentacular cells. Bowman's gland acinar and duct cells, and basal cells also showed RH-specific immunostaining, but fewer cells were affected, and the staining was less intense than in the sustentacular cells. Overall, LS-exposed olfactory mucosae exhibited a decrease in RH-specific immunoreactivity compared to controls. The decreased immunoreactivity was particularly evident in sustentacular cells. There was no RH immunoreactivity in the proteinaceous globules, and generally the sustentacular cells, with or without globules, exhibited less immunoreactivity. HS-exposed olfactory mucosae exhibited an increase in RH-specific immunoreactivity compared to controls. This increase was observed particularly in the apical portions of sustentacular cells. As in the LS mucosae, no RH immunoreactivity was detected in the proteinaceous globules of sustentacular cells, but sustentacular cells adjacent to those with globules and sustentacular cells in areas without globules were intensely immunoreactive.

The filtered air control olfactory mucosae exhibited intense, brown, granular CE-specific immunoreactivity primarily in the acinar cells of Bowman's glands. Immunostaining was also observed to a lesser extent in the apical portions of sustentacular cells, basal cells, and Bowman's duct cells. The LS-exposed olfactory mucosae exhibited intense immunoreactivity in Bowman's glands, as seen in controls, and there was intense immunostaining of the proteinaceous globules, resulting in more immunoreactivity in the LS mucosae compared to controls. The HS-exposed olfactory mucosae exhibited intense CE-specific immunostaining in the proteinaceous globules of the sustentacular cells. However, there was a significant loss of acinar cells of Bowman's glands in areas of epithelial necrosis and attenuation, and a loss of CE immunostaining that corresponded directly to the loss of Bowman's gland cells.

Compared to the filtered air control group, the Vmax of RH for cyanide metabolism decreased in LS-exposed olfactory mucosae and increased in the HS-exposed olfactory mucosae (Fig. 1). The LS-exposed olfactory mucosae exhibited a slight increase in affinity of RH for cyanide (decreased Km) as compared to the filtered air controls. The HS-exposed olfactory mucosae exhibited a slight decrease in affinity (increased Km) as compared to the controls. Overall, the ability of RH to metabolize cyanide at low concentrations (Vmax/Km) was similar among the three exposure groups.

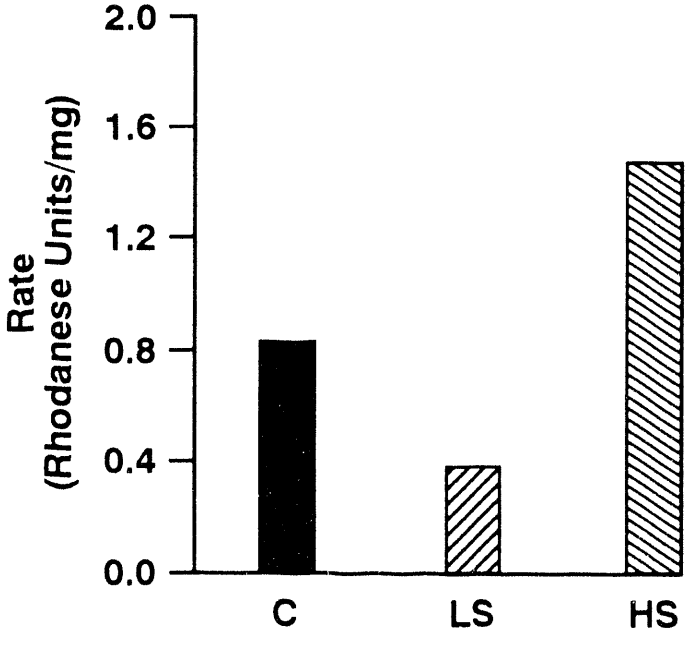

Figure 1. Maximum velocity of rhodanese for cyanide metabolism. Mean values are shown. Two tissue pools, each composed of mitochondrial preparations of ethmoturbinates from two rats (n = 2) were used for each exposure level. Actual rate values were 1.00, 0.66 [controls (C)]; 0.39, 0.37 [low smoke (LS)]; and 1.13, 1.83 [high smoke (HS)].

The Vmax of CE for 4-nitrophenyl butyrate metabolism in LS-exposed olfactory mucosae increased compared to the filtered air control group, whereas the Vmax of CE in the HS-exposed olfactory mucosae was similar to the control group (Fig. 2). The LS-exposed olfactory mucosae exhibited a slight decrease in affinity of CE for its substrate (increased Km) as compared to the controls. The affinity of CE for its substrate did not change in the HS-exposed mucosae compared to the controls. Overall, the Vmax/Km values for CE did not differ among the three exposure groups.

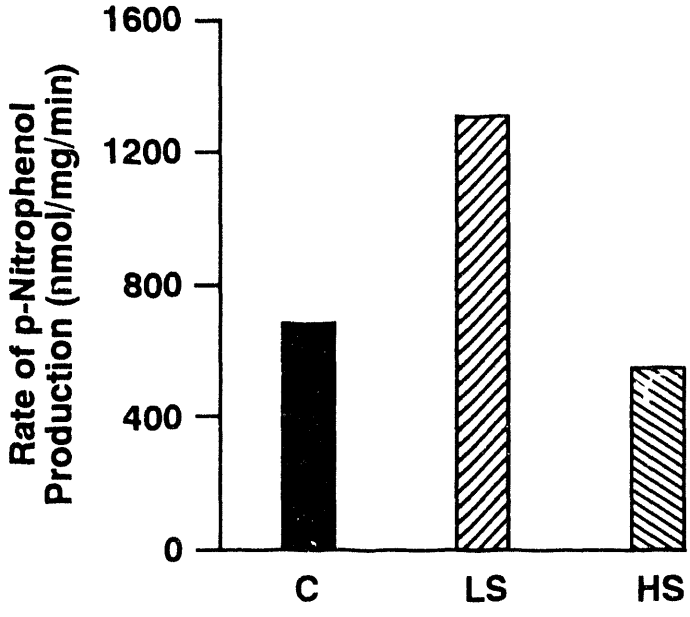

Figure 2. Maximum velocity of carboxylesterase for 4-nitrophenyl butyrate metabolism. Mean values are shown. Two tissue pools, each composed of S-9 preparations of ethmoturbinates from two rats (n = 2) were used for each exposure level. Actual rate values were 649.35, 710.73 [control (C)]; 1524.40, 1106.40 [low smoke (LS)]; and 646.00, 448.43 [high smoke (HS)].

In summary, RH appears to have been induced in those sustentacular cells without proteinaceous globules in the HS-exposed olfactory mucosae. On the other hand, RH immunoreactivity was either lost or significantly decreased, particularly in sustentacular cells, in the LS-exposed olfactory mucosae. Changes in RH Vmax corresponded to these differences in immunoreactivity. Although these alterations were observed in RH immunoreactivity and maximal velocity, there were inverse changes in Km such that the capacity of RH to metabolize its substrate at low substrate concentrations did not change overall. CE appears to have been induced in the proteinaceous globules of sustentacular cells in both LS- and HS-exposed olfactory mucosae. In the LS mucosae, the induction of CE in the globules correlated with an increase in Vmax. In the HS mucosae, the induction of CE in the globules was balanced by the loss of CE in the glands, which are the greatest reservoir of CE in normal mucosae, resulting in no change in Vmax. In conclusion, inhalation of tobacco smoke induces complex lesions that result in enzyme induction or loss of enzyme from specific cells found in the olfactory mucosae of rats. Despite these alterations, the capacities of RH or CE at low substrate concentrations were not changed in smoke-exposed rats compared to controls.

(Research sponsored by the Office of Health and Environmental Research, U.S. Department of Energy under Contract No. DE-AC04-76EV01013 and by the PHS/NIH under Grant R01-DC01714-01 from the National Institute on Deafness and Other Communication Disorders.)

EFFECTS OF INHALED ENDOTOXIN ON INTRAEPITHELIAL MUCOSUBSTANCES IN F344 RAT NASAL AND TRACHEOBRONCHIAL AIRWAYS

*J. R. Harkema and T. Gordon**

Gram-negative bacteria and their cell wall component endotoxin are ubiquitous in the environment. Exposure to airborne endotoxin can occur both occupationally (e.g., organic dusts in textile mills, swine confinement, and poultry buildings) and at home (e.g., inadvertent bacterial contamination of aerosols produced by ultrasonic humidifiers and evaporative coolers). Increased sputum production and chronic bronchitis are associated with occupational exposure to endotoxin-contaminated organic dusts (Dosman, J. A. *et al. Am. Rev. Respir. Dis. 126*: 75, 1980; Donham, K. *et al. Br. J. Ind. Med. 46*: 31, 1989; Rooke, G. B. *Chest 79*: 67S, 1981). Recent experiments in laboratory animals have suggested that airway-instilled endotoxin can increase the amount of stored mucosubstances in airway epithelium in the upper and lower respiratory tracts of rats (Harkema, J. R. and J. A. Hotchkiss. *Exp. Lung. Res. 17*: 743, 1991; Harkema, J. R. and J. A. Hotchkiss. *Am. J. Pathol. 141*: 307, 1992). Although these studies demonstrate that large amounts of endotoxin instilled in the airways of rats will increase mucous production, the effects of inhaled endotoxin at occupational concentrations have not been investigated. The present study was performed to (1) determine whether repeated exposure to occupationally relevant concentrations (0.3-50 $\mu g/m^3$) of inhaled endotoxin can alter the presence of stored mucosubstances in the rat and (2) establish a convenient *in vivo* animal model for studying the mechanisms involved in the production and release of mucosubstances.

Male CDR® (F344)/CrlBR rats (purchased from Charles River Laboratories) were exposed in whole-body inhalation chambers to either aerosolized, pyrogen-free saline (n = 9) or 0.3, 3.1, or 52.4 $\mu g/m^3$ endotoxin (n = 6 per group) for 3 h/day for 3 days with the exposure time starting at 24-h intervals. Endotoxin and saline aerosols were generated with a Babington-type nebulizer driven by medical-grade breathing air at 9 psi. Solutions of endotoxin, 0.35, 3.5, or 35 $\mu g/mL$ (*E. coli* 0127:B8), were made up with pyrogen-free, isotonic saline immediately prior to exposure. Exposure concentrations were determined by sampling the chamber atmosphere in the breathing zone of the animals twice during each exposure (Gordon, T. *et al. Appl. Occup. Environ. Hyg. 7*: 472, 1992). Chamber air was sampled at 1.07 L/min through 47 mm filters. Endotoxin was extracted from the filters, and the concentrations of endotoxin in the collected extracts were quantitated with a Limulus amebocyte lysate assay using a spectrophotometric microplate method.

At 24 h after the final inhalation exposure, rats were anesthetized with ketamine and exsanguinated via the heart. The nose, trachea, and lungs from each animal were fixed in 10% neutral buffered formalin. The tracheobronchial airways were fixed at a constant pressure of 25 cm of fixative. After fixation the nasal cavities were decalcified and coronally sectioned by methods previously described in detail (Harkema J. R. *et al. Toxicol. Pathol. 17*: 525, 1989; Young, J. T. *Fundam. Appl. Toxicol. 1*: 309, 1981). The most proximal nasal tissue section taken at the level immediately posterior to the upper incisor teeth was embedded in glycol methacrylate. One μm thick sections were cut from the embedded tissue and stained with Alcian Blue (pH 2.5)/Periodic Acid Schiff (AB/PAS) to identify acidic and neutral mucosubstances in surface epithelium lining the septum. Tissues from the mid-trachea and the intrapulmonary axial airway (generation 3) in the left lung lobe were similarly processed and stained for identification of intraepithelial mucosubstances.

The amount of AB/PAS-stained mucosubstances in (1) the surface epithelium lining both sides of the mid-nasal septum in the proximal nasal airway; (2) the surface epithelium overlying the cartilaginous and noncartilaginous regions of the mid-trachea; and (3) the surface epithelium lining the intrapulmonary axial airway of the left lung lobe in each rat were determined by image analysis and standard morphometric techniques (Harkema *et al.*, 1989). The data were expressed as the mean (± SE) volume density (Vs = nL/mm^2 basal lamina) of AB/PAS-positive mucosubstances within the epithelium.

Exposure to endotoxin produced a conspicuous mucous cell metaplasia and a dose-dependent increase in Vs in the surface epithelium lining the intrapulmonary airways (Fig. 1). Of the three regions of the respiratory tract

*Institute of Environmental Medicine, New York University Medical Center, Tuxedo, New York

examined, the surface epithelium of the intrapulmonary airways was the most sensitive to the mucosubstance-inducing effect of inhaled endotoxin. The quantity of Vs in the intrapulmonary airways was significantly increased (2.5-fold greater than saline-exposed controls) in rats exposed to as little as 0.3 $\mu g/m^3$ endotoxin. Intrapulmonary airways in rats exposed to 52.4 $\mu g/m^3$ and 3.1 $\mu g/m^3$ endotoxin had Vs seven- and four-fold greater, respectively, than controls. Significant increases in Vs were observed in the surface epithelium overlying the noncartilaginous portions of the mid-trachea only after exposure to 3.1 $\mu g/m^3$ or 52.4 $\mu g/m^3$ endotoxin (Fig. 2), while no significant changes were observed in the cartilaginous portions of the mid-trachea or in the nasal airways even at concentrations as high as 52.4 $\mu g/m^3$.

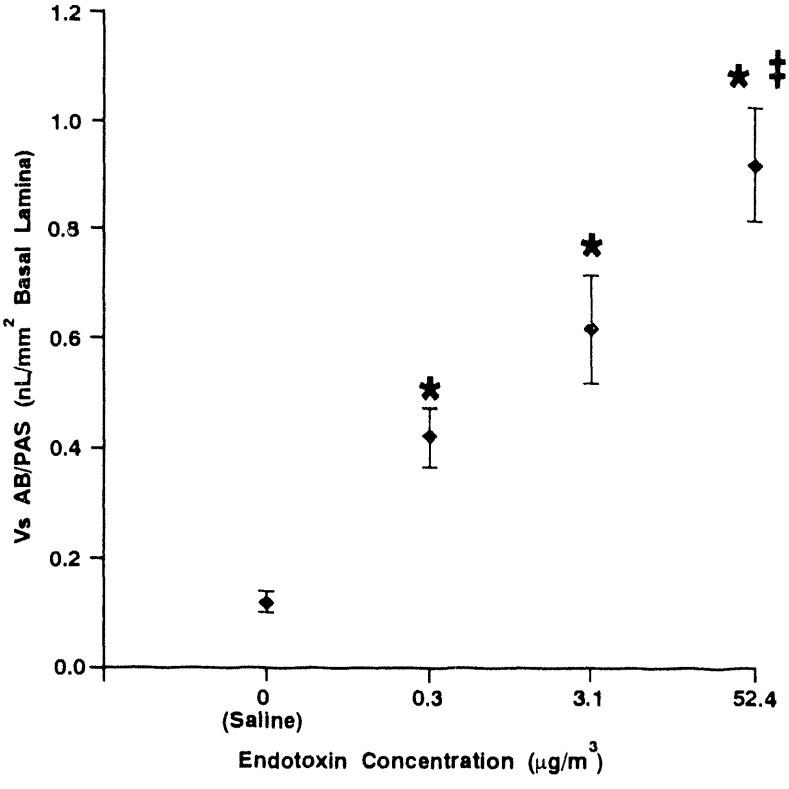

Figure 1. The effects of inhaled endotoxin aerosols on the amount of stored epithelial mucosubstances (mean ± SE) in the intrapulmonary airways (generation 3). Vs = Volume density of stored AB/PAS-stained mucosubstances in airway surface epithelium (Vs); * = Significantly greater from saline-exposed group, $p \leq 0.05$. ‡ = Significantly greater from 0.3 $\mu g/m^3$ endotoxin-exposed group, $p \leq 0.05$.

The results of the present study demonstrate a site-dependent difference in the degree of increase in the intraepithelial Vs induced by inhalation of endotoxin. Two possible explanations for the site-specific increase in intraepithelial Vs in response to aerosolized endotoxin are: (1) differential deposition of the inhaled particles throughout the conducting airways and (2) differences in the responsiveness of specific epithelial tissues to deposited aerosols of endotoxin. A difference in the sensitivity of the epithelial lining of a particular airway segment to endotoxin is probably a major factor contributing to the observed tissue-dependent response. Estimates of the minute ventilation (0.1 L/min; Stahl, W. R. *J. Appl. Physiol. 22*: 453, 1967) and total deposition of inhaled 2.5 μm particles in the respiratory tract (50%; Raabe, O. G. *et al.* In *Inhaled Particles IV, Part 1* [W. H. Walton, ed.], Pergamon, Oxford, p. 3, 1977) predict that approximately 9 to 900 ng endotoxin/rat were retained in the lungs during a 3-h exposure to 0.3 to 52.4 $\mu g/m^3$ endotoxin. Moreover, estimates of regional deposition of 2.5 μm particles in a rat suggest that most of the deposition would occur in the upper respiratory tract, and less than 10% of the inhaled particles would have impacted in the tracheobronchial region. Thus, the present results demonstrate that the epithelium of the tracheobronchial tree is extremely sensitive and the nasal septum is relatively insensitive in terms of the mucosubstance response to minute amounts of endotoxin. This difference in sensitivity could be due in part to different populations of epithelial cells in the various regions.

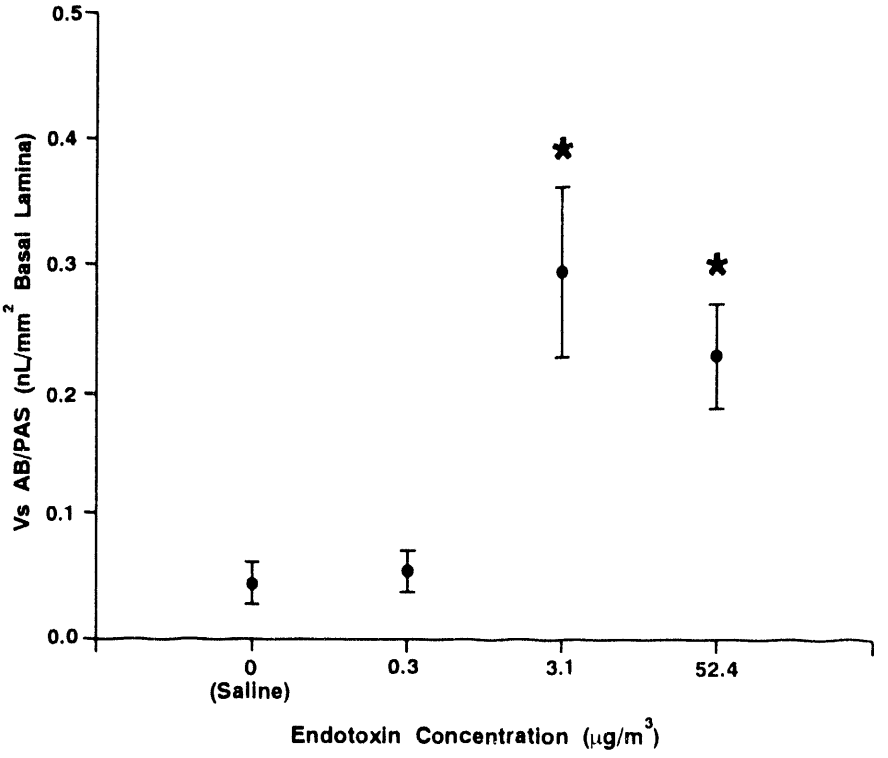

Figure 2. The effects of inhaled endotoxin aerosols on the amount of stored epithelial mucosubstances (mean ± SE) in the noncartilaginous portion of the mid-trachea. * = Significantly greater from saline-exposed group, $p \leq 0.05$.

In summary, the present study demonstrated that the control mechanisms regulating the stores of mucosubstances in the surface epithelium of rodent airways are very sensitive to the effects of inhaled endotoxin. The results of this study suggest that bacterial endotoxin, which contaminates organic dusts, may play an important role in the increase of sputum and the induction of chronic bronchitis reported for agriculturally and industrially exposed workers. In addition, endotoxin appears to be a rapid inducer of airway mucin production. Therefore, the present rat exposure regimen may provide an excellent *in vivo* model for studying the cellular signals involved in the induction of mucin glycoprotein production and secretion by intrapulmonary airway mucous goblet cells.

(Research sponsored by the Office of Health and Environmental Research, U.S. Department of Energy, under Contract No. DE-AC04-76EV01013, and by Public Health Service Grants ES-00260 and ES-04947.)

EFFECTS OF CHRONIC OZONE EXPOSURE ON AIRWAY MUCOSUBSTANCES IN THE F344 RAT

J. R. Harkema, K. E. Pinkerton, and C. G. Plopper**

Acute exposures to ozone induce secretory cell metaplasia and increased intraepithelial mucosubstances (IM) in nasal airways of rats (Harkema, J. R. *et al. Toxicol. Pathol. 17*: 525, 1989). The present study examined the effects of chronic ozone exposure on IM in nasal and tracheobronchial airways of F344/N (Simonsen Laboratories, Gilroy, CA) rats. Female and male rats were exposed to 0 (controls), 0.12, 0.5, or 1.0 ppm ozone, 6 h/day, 5 days/wk, for 20 mo. All rats were killed 1 wk after the end of the exposure. Tissues from (1) the proximal nasal passages (mid-lateral wall), (2) the mid-trachea (generation 0), (3) the left extrapulmonary bronchus (generation 1), (4) a small diameter, intrapulmonary airway in the left lobe (generations 5), (5) a large diameter, axial airway in the left lobe (generations 5), and (6) a small diameter, axial airway in the left lobe (generations 11) were processed for light microscopy and stained with Alcian Blue/Periodic Acid Schiff (AB/PAS) for detection of IM, as previously described in detail (Harkema *et al.*, 1989; Harkema J. R. and J. A. Hotchkiss. *Am. J. Pathol. 141*: 307, 1992). The amount of IM was quantitated by image analysis and standard morphometric techniques (Harkema *et al.*, 1989).

Intraepithelial mucosubstances in the mid-lateral wall of the proximal nasal passages of the 0.5 and 1.0 ppm ozone-exposed rats were 20-40 times greater than controls. IM in small diameter airways at generations 5 and 10 in the left lobe were 5-6 times greater in rats exposed to 1 ppm compared to controls. There was a 50% decrease in IM within the mid-trachea of rats exposed to 1 ppm compared to controls. No changes in the amount of IM were present in airways exposed to 0.12 ppm ozone. In addition, no changes in tracheobronchial IM were evident in rats exposed to 0.5 ppm. A summary of the effects of 1 ppm ozone on the IM throughout the respiratory tract is presented graphically in Figure 1.

The results of this study indicate that ozone-induced changes in IM are dependent on the concentration of ozone and the region of the airway examined. The nasal mucosa was significantly more responsive to the ozone exposures, in respect to induced changes in mucosubstance production, than all the other regions in the respiratory tract. Significant, but less dramatic increases in IM were also identified in distal pulmonary airways. This is the first study to demonstrate that chronic ozone exposures can induce alterations in the amount of IM in pulmonary airways as well as in nasal airways. The reason(s) for this regional difference in response is unknown, but is probably due in part to both tissue sensitivity and differences in dose to the airway tissue.

The ozone-induced lesions identified in this study may reflect deleterious effects on the normal functions of the mucocilary apparatus (e.g., mucociliary clearance) of upper and lower airways. If there is significant functional impairment to upper airway clearance mechanisms, this may allow more potentially harmful agents to reach distal airways. It has been suggested that chronic alterations in normal upper airway function may have a significant role in the development of small airway disease in the lungs (Proctor D. F. *et al. Ciba Found. Symp. 54*: 219, 1978). Ozone-induced changes in airway mucosubstances may lead to insufficient modification of inhaled air, which would then result in greater burdens of airborne pollutants to the lung parenchyma.

*School of Veterinary Medicine, University of California, Davis, California

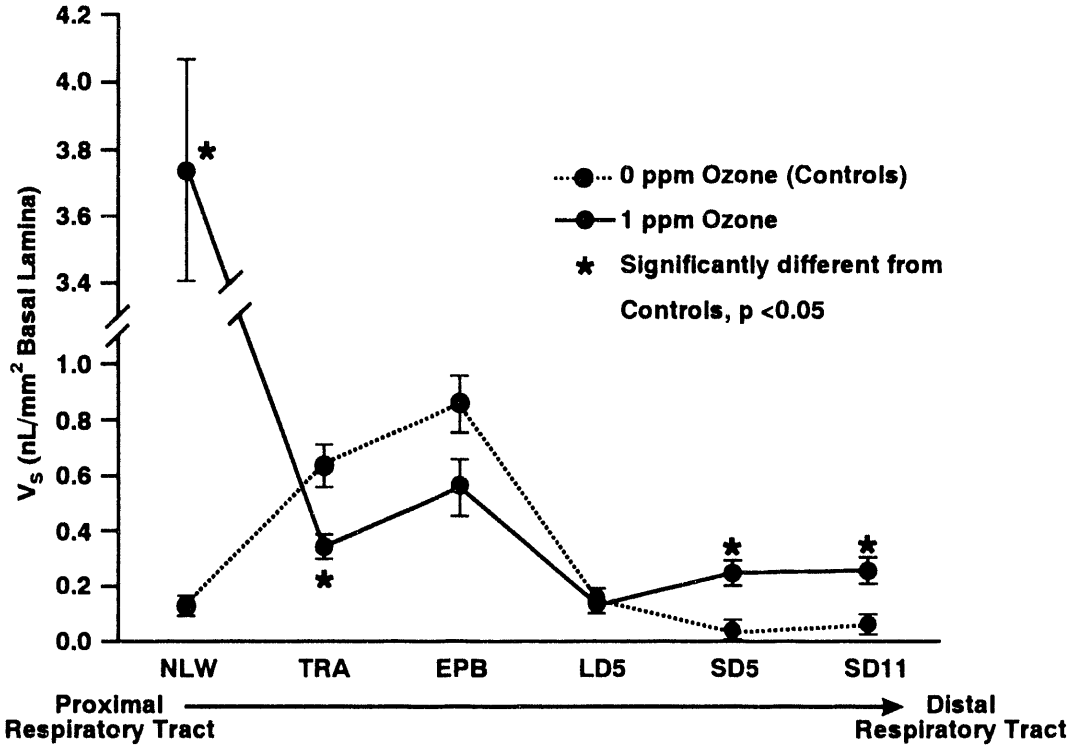

Figure 1. Ozone-induced changes in intraepithelial mucosubstances (IM) throughout the respiratory tract of F344/N rats. Vs = volume/surface area of IM expressed as nL of AB/PAS stained mucosubstance in the surface epithelium of the airway per mm^2 of underlying basal lamina. Group means are plotted. Bars are standard errors of the means. NLW = nasal lateral wall; TRA = mid-trachea; EPB = extrapulmonary bronchus; LD5 = large diameter intrapulmonary airway (generation 5); SD5 = small diameter intrapulmonary airway (generation 5); SD11 = small diameter intrapulmonary airway (generation 11). The natural logarithms of the morphometric data were used for statistical analyses. Data were tested for equality of group means by using an unpaired Student's *t* test with Bonferroni correction for multiple comparisons.

(Research supported by the Health Effects Institute under the Funds-In-Agreement DE-FI04-91AL75007 with the U.S. Department of Energy under Contract No. DE-AC04-76EV01013.)

COMPARISON OF TYPE II CELL AND NEUTROPHIL ALKALINE PHOSPHATASES

R. F. Henderson, G. Kelly, G. G. Scott, and J. J. Waide*

The analysis of bronchoalveolar lavage fluid (BALF) has been used to detect an inflammatory response in the lung. In addition to the usual markers of inflammatory response that are measured (neutrophil count, protein, lactate dehydrogenase activity), some investigators assay for alkaline phosphatase (AP) activity on the assumption that most of the AP comes from the type II cells as part of a secretory process or by lysis of the type II cells. Such an assumption is based on the fact that histochemical staining for AP indicates that the apical portion of the type II cell is the major site within the alveoli where AP is located (Miller, B. E. *et al. Exp. Lung Res. 12*: 135, 1987). Staining of AP in type II cells is used to help quantitate type II cell hyperplasia (Miller *et al.*, 1987). However, there are no published data to indicate the actual source of the AP that is in the epithelial lining fluid and sampled by BAL. If the BALF AP is actually coming from type II cells, the enzyme levels in BALF might be a valuable marker of type II cell activation leading to hypertrophy and hyperplasia, a common response to many inhaled toxicants (Miller, B. E. *et al. Lab Invest. 55*: 153, 1986). The first step in testing such an hypothesis is to determine if the type II cells are the primary source of AP in BALF.

To characterize the source(s) of AP in BALF, we have compared the APs in BALF with the APs in type II cells, neutrophils, serum, and various other organ sources of AP. The isoelectric focusing (IEF) pattern of AP in BALF from F344/N rats (Harlan Sprague Dawley, Indianapolis, IN) treated with α-quartz was compared with the IEF pattern of APs from rat serum, lung, heart, kidney, bone, liver, intestine, pulmonary type II cells, and neutrophils. Then the APs that had similar IEF patterns were characterized by heat stability profiles and differential inhibition by amino acids and chelating agents.

The IEF studies indicated that the BALF AP had two predominate bands that ran toward the anode. These same bands were observed as major bands in heart, lung, type II cell, and neutrophil samples, but were not observed or only faintly observed in kidney, liver, intestine, serum, or bone samples (1991-92 Annual Report, p. 67). Neutrophils are an important potential source of BALF AP because neutrophils are present in the alveoli during acute inflammatory responses.

Heat stability profiles and differential inhibition with amino acids and chelating agents were then used to characterize the AP in BALF, type II cells, and neutrophils to determine the most likely source of AP in BALF. The APs in all three samples were heat labile at 65°C for 10 min, but the BALF AP appeared to be more resistant than the other two AP samples to heating at 56°C (Table 1). None of the AP samples were inhibited by up to 40 mM L-phenylalanine or L-leucine (Table 1). L-homoarginine was more inhibitory toward BALF AP than the AP from neutrophils or type II cells. The BALF AP was also more sensitive to inhibition by the chelating agent (Table 1).

The results suggest that multiple isoenzymes of AP may be present in the samples. We will continue our research by fractionating the neutrophils and the type II cells into subcellular fractions to determine if the AP in one subcellular fraction matches that in the BALF AP. We will also isolate mRNA from the type II cells and from the neutrophils, and obtain cDNA clones of both type II cell and neutrophil AP. DNA sequence analysis of the cDNA clones will help establish the origin of the AP forms in BALF.

---

*UNM/ITRI Inhalation Toxicology Graduate Student

Table 1

Alkaline Phosphatase Activity (mIU/mg Protein) in BALF and Lung Cell Supernatants Chemically Inhibited or Heat Inactivated[a]

Inhibitor/Heat	Conc[b] (mM)	BALF	Type II	Neutrophils
Control		197	888	22
L-Phenylalanine	5.0	206	955	23
	10.0	192	910	24
	20.0	193	900	23
	40.0	189	919	23
L-Leucine	5.0	198	919	23
	10.0	198	886	22
	20.0	193	874	23
	40.0	179	846	22
L-Homoarginine	10.0	137	769	19
	20.0	62	655	17
	30.0	46	579	15
	40.0	43	515	13
EDTA Disodium	1.0	36	558	17
	2.5	16	282	11
	5.0	11	190	9
56°C, 10 min		84	48	4
65°C, 10 min		7	28	3

[a]Type II cells (0.9×10^6) and neutrophils (1.66×10^6) were incubated with phospholipase C, phosphatidylinositol specific (0.16 units) for 60 min at 37°C.
[b]Conc = concentration; BALF = bronchoavelolar lavage fluid.

(Research supported by the Office of Health and Environmental Research, U.S. Department of Energy, Contract No. DE-AC04-76EV01013.)

VI. MECHANISMS OF NONCARCINOGENIC RESPONSES TO INHALED TOXICANTS

CONSTRUCTION OF F344 RAT AND HUMAN cDNA LIBRARIES AND ISOLATION OF SPECIES-SPECIFIC CYTOCHROME P450 FAMILY 4 cDNAs

J. A. Hotchkiss, S. H. Lowell, and A. R. Dahl*

The cytochromes P450 are a superfamily of proteins that catalyze monooxygenation of xenobiotics and endogenous substrates. Isozymes of cytochrome P450 exhibit organ, tissue, and cell-type specificity which correlates with observed organ- and tissue-specific injury resulting from exposure to toxicants. In recent years, major progress has been made in the identification and localization of cytochromes P450 in the nasal cavities of laboratory animals and the determination of cytochrome P450-mediated metabolism in human nasal tissues. Because nasal metabolism can affect both the uptake and toxicity of inhalants, it is essential that differences in nasal metabolism between experimental animals and humans be evaluated so that expected effects in humans can be accurately predicted from animal data.

This report describes our approach to examine nasal metabolism in humans and F344 rats. Although it is possible to obtain sufficient nasal tissues from rats to purify specific enzymes of interest for *in vitro* metabolism studies, this approach cannot be routinely used for analyses of human nasal enzymes because of the quantities of tissues required. To minimize the ongoing need for rat and human nasal tissue samples, we have constructed rat and human nasal-tissue-specific cDNA libraries. These libraries will serve as the source of enzyme-specific cDNAs that will be used to express proteins of interest *in vitro* in quantities sufficient to perform metabolic analyses.

We have constructed two cDNA libraries from rat nasal tissues and one library from human nasal tissues. Ten male and 10 female F344/N (Taconic) rats (14 wk old) were used to obtain nasal tissue-specific RNA for construction of the cDNA libraries. Rats were deeply anesthetized with CO_2 and killed by exsanguination. Immediately after death, the heads were removed, depelted, and the nasal cavity was exposed by splitting the head longitudinally along the midline cranial suture. Tissues from two anatomic regions were dissected from the nasal cavity and immediately processed for isolation of total RNA according to the method of Chomzynski, G. and R. Sacchi (*Anal. Biochem. 162*: 156, 1987). The ethmoid turbinates and the posterior third of the nasal septum from each rat were removed and used as the source of olfactory epithelium. Nasal respiratory (e.g., mucociliary) and nasal transitional (e.g., nonciliated, nonsecretory) epithelia were obtained by removing the nasal septum, naso- and maxilloturbinates, and lateral wall mucosa from the region between the incisor teeth and the first molar teeth of the hard palate.

Human nasal tissue from the nasal septum and middle and inferior turbinates was obtained from 10 male (6 to 73 yr of age) and 10 female (24 to 51 yr of age) subjects undergoing therapeutic nasal tissue reductions at the Lovelace Medical Center, Albuquerque, New Mexico. The surface epithelium was primarily mucociliary respiratory epithelium with focal regions of squamous metaplasia and occasional inflammatory cell infiltrates. The cDNA libraries were constructed by Clontech Laboratories, Inc. (Palo Alto, CA) in the Lambda ZAP II (Stratagene; La Jolla, CA) bacteriophage cloning vector. Lambda ZAP II is an insertion vector that can accept up to 10 Kb of foreign DNA at six unique cloning sites located in the N-terminal region of the lacZ gene. Thus, recombinant phage may be recognized with blue/white color identification when plated on lac^- hosts in the presence of IPTG and X-gal. In addition, DNA sequences cloned into the multiple cloning site may be expressed as fusion proteins under the control of the lac promoter. The cDNA libraries were prepared using unidirectional priming (Oligo dT-Xho I primer) to increase the number of clones that can be detected using antibody screening. The characteristics of the three cDNA libraries are summarized in Table 1.

We initially screened the rat nasal respiratory/transitional and human nasal respiratory libraries for P450 family 4 isozymes. Our interest in P450 family 4 stems from its potential role in termination of inflammation, the importance of the 4B subfamily in the activation of aminoaromatic compounds to mutagens, and the reports of 4B in rabbit nasal tissues (Dahl, A. R. and W. M. Hadley. *CRC Crit. Rev. Toxicol. 21*: 345, 1991).

*Director, ENT Department, Lovelace Medical Center, Albuquerque, New Mexico

Consistent with this observation, 2-aminoanthracene, an aminoaromatic, is a potent mutagen when activated by either rat or rabbit nasal homogenates (Dahl, A. R. *Mutat. Res. 158*: 141, 1985).

Table 1

Summary of the Characteristics of the
F344 Rat and Human Nasal cDNA Libraries

Library Name	No. Independent Clones	Insert Size Range	Average Insert Size
Rat Respiratory/Transitional	1.6×10^6	0.8 to 5 K	1.6 K
Rat Olfactory	1.5×10^6	0.6 to 5 K	1.6 K
Human Respiratory	1.7×10^6	1.0 to 5 K	1.5 K

The libraries were screened with a P450 family 4-specific cDNA fragment using standard procedures (Sambrook, F. *et al. Molecular Cloning: A Laboratory Manual, 8th Ed.* Cold Spring Harbor Laboratory, Cold Spring Harbor, 1989). The P450 family 4-specific cDNA was made as follows. We synthesized a degenerate oligonucleotide (Model 391 PCR-Mate DNA synthesizer; Applied Biosystems, Inc., Foster City, CA) corresponding to the possible mRNA sequences coding for eight amino acids (Phe-Met-Phe-Glu-Gly-His-His-Asp-Thr) of a 16-amino acid sequence present in 100% of all published P450 family 4 sequences, but with less than a 50% identity with all other P450 families. A 585 bp cDNA fragment was synthesized by combined reverse transcription and polymerase chain reaction (PCR) amplification using total F344 rat liver RNA as the template for first-strand synthesis using an oligo-dT primer and the degenerate oligonucleotide as the 5'-amplimer. The cDNA fragment was ligated into a plasmid designed to accept PCR fragments (pCRII; Invitrogen, La Jolla, CA), amplified in *E. coli*, and both strands were sequenced (Sequenase; United States Biochemical, Cleveland, OH). The sequence was compared to all DNA sequences present in the Genbank and EMBL databanks using a DNA sequence analysis program (GCG DNA Sequence Analysis Version 7; Genetics Computer Group, Madison, WI). The top 25 sequences with the greatest degree of homology to the family 4 cDNA probe were all cytochrome P450 family 4 members that have been identified in rats, humans, mice, rabbits, and guinea pigs. Table 2 summarizes the degree of homology of our family 4-specific cDNA probe with published rat and human P450 family 4 members.

Table 2

Homology of P450 Family 4-Specific cDNA Probe with
Published Rat and Human P450 Family 4 Sequences

Species	Tissue	P450 Isozyme	% Homology
Rat	Liver	4A3	95
	Not Reported	4A2	85
	Kidney	4A1	75
	Lung	4B2	70
Human	Kidney	4A[a]	80
	Not Reported	4A11	78
	Lung	4B1	70

[a]Specific form not reported.

The degree of homology of the family 4-specific cDNA clone is great enough to preferentially hybridize with rat and human family 4 cDNAs present in the libraries, but should be general enough to hybridize with both 4A and 4B subfamilies if present.

We have performed the initial rounds of screening of the rat and human nasal respiratory libraries. We have isolated cDNA clones from both the human (3 positive/10^5 plaques screened) and rat (35 positive/10^5 plaques screened) libraries that range in size from 0.4 to 2 Kb. The largest clones from each library will be sequenced to determine their identity. Our goal is to isolate or construct full-length, species-specific, P450 family 4 cDNAs. We will subclone these cDNAs into a eukaryotic vector such as pSVL or pCMV4 for expression *in vitro*. Both vectors have been successfully used to express cloned heterologous P450 cDNAs in Cos 1 cells (Clank, B. J. and M. R. Waterman. *Methods Enzymol. 206*: 454, 1991).

In summary, we have produced F344/N rat and human nasal cDNA libraries. These libraries are being used as the source of species/tissue-specific cDNAs encoding xenobiotic-metabolizing enzymes such as cytochrome P450 family 4. The long-term goal of this project is to compare the xenobiotic-metabolizing activities of orthologous nasal P450 isozymes from rats and humans. We believe that the technique of cDNA-directed expression of specific P450 isozymes is essential in meeting this goal. These kinds of detailed metabolic analyses will help to provide a rational basis for predicting potential risks to humans based on pharmacokinetic data obtained from rodent exposures.

(Research sponsored by the Office of Health and Environmental Research, U.S. Department of Energy, under Contract No. DE-AC04-76EV01013.)

EFFECT OF NEUTROPHIL DEPLETION ON ENDOTOXIN-INDUCED MUCOUS CELL METAPLASIA IN PULMONARY AIRWAYS OF F344 RATS

J. A. Hotchkiss and J. R. Harkema

Endotoxins are major constituents of gram-negative bacterial cell walls and are presumed to induce injury to the lungs in gram-negative sepsis and bacterial bronchopneumonia. Although not directly chemotactic for neutrophils, endotoxins are more potent on a molar basis in inducing neutrophil influx than all other chemotactic factors tested. In addition, endotoxins are ubiquitous substances found in the domestic and occupational environment.

Intratracheal instillation of bacterial endotoxin results in an influx of neutrophils and an increase in epithelial cell DNA synthesis in intrapulmonary airways of F344 rats (1991-92 Annual Report, p. 160). Endotoxin instillation also results in a significant increase in both the number of mucous goblet cells in intrapulmonary airways and the amount of stored mucosubstances within these cells (Harkema, J. R. and J. A. Hotchkiss. *Am. J. Pathol. 141(2)*: 307, 1992). The mechanism of endotoxin-induced mucous cell metaplasia is unknown. However, other inhaled irritants that induce inflammatory cell infiltration, such as tobacco smoke, sulfur dioxide, and ozone, also increase the numbers of secretory cells in rat intrapulmonary airways. Intratracheal administration of neutrophil-derived elastase has also been shown to induce increases in intraepithelial mucosubstances and secretory cell numbers in rodent airways (Snider, G. L. *et al. Am. Rev. Respir. Dis. 129*: 155, 1984).

The purpose of this study was to examine the influence of inflammatory cells (i.e., neutrophils) on the induction of mucous cell metaplasia after endotoxin exposure. A total of 72 male F344/NHsd were randomly assigned to one of 12 experimental groups. Thirty-six rats were depleted of circulating neutrophils (neutrophil-deficient; ND) by intraperitoneal injection (i.p.) of a rabbit anti-rat neutrophil antisera (ANA; Accurate Chemical Co., Westbury, NY). The other 36 rats (neutrophil-sufficient; NS) were injected i.p. with normal rabbit serum (NRS). Eighteen hours after i.p. injection with ANA or NRS, the rats were briefly anesthetized with 4% halothane in O_2 and intratracheally instilled with 50 μg endotoxin (*E. coli* serotype 0111:B, Sigma Chemical Co., St. Louis, MO) in 500 μL sterile pyrogen-free saline (n = 12 NS and n = 12 ND), 500 μL of saline alone (n = 12 NS and n = 12 ND), or were not intratracheally instilled (n = 12 NS and n = 12 ND). Rats were sacrificed 24 or 48 h after intratracheal instillation. A blood sample was taken from the left ventricle at the time of sacrifice and analyzed for total and differential white blood cell counts. Immediately after death the lungs were removed and the left extrapulmonary bronchus temporarily clamped off, while the right lung lobes were lavaged with saline. The lavage fluid was recovered and analyzed for total and differential cell counts. The clamp was removed, and the entire lung was fixed with 10% neutral buffered formalin by intratracheal perfusion at a constant pressure of 30 cm of fixative. The left lobe was removed, a tissue block was removed by cutting perpendicular to the main (axial) intrapulmonary airway at a level corresponding to airway generation 2 and processed for light microscopy.

Sections from the proximal face of each tissue block were stained with Alcian Blue (pH 2.5)/Periodic Acid Schiff's sequence to identify acidic and neutral mucosubstances or with hematoxylin/eosin and Alcian blue (pH 2.5) for qualitative assessment of neutrophilic influx into the pulmonary airway epithelium. The main (axial) intrapulmonary airway at a level corresponding to airway generation 2 from each rat was analyzed with a computerized image analysis system (Harkema and Hotchkiss, 1992) to determine the volume density (Vs) of stored intraepithelial mucosubstances. Data were tested for equality of group means by using an unpaired Student's *t*-test with Bonferroni correction for multiple comparisons. The criterion for statistical significance was set at $p \leq 0.05$.

I.P. injection of ANA resulted in an 80 to 90% decrease in the number of all circulating white blood cells at both the 24 and 48 h sacrifice times. Rats injected with ANA had no detectable circulating neutrophils at either sacrifice time. The mean number of neutrophils (± SEM) recovered from the left lung lobe from each experimental group is presented in Figure 1. Intratracheal instillation of endotoxin resulted in a significant increase in neutrophils lavaged from the lungs of NS, but not ND, rats 24 and 48 h after instillation. Saline

instillation alone induced an influx of neutrophils into the lungs of NS rats sacrifice 24 h after instillation. However, 48 h after instillation the numbers of neutrophils recovered by lavage in saline-instilled NS rats were similar to non-instilled NS control animals.

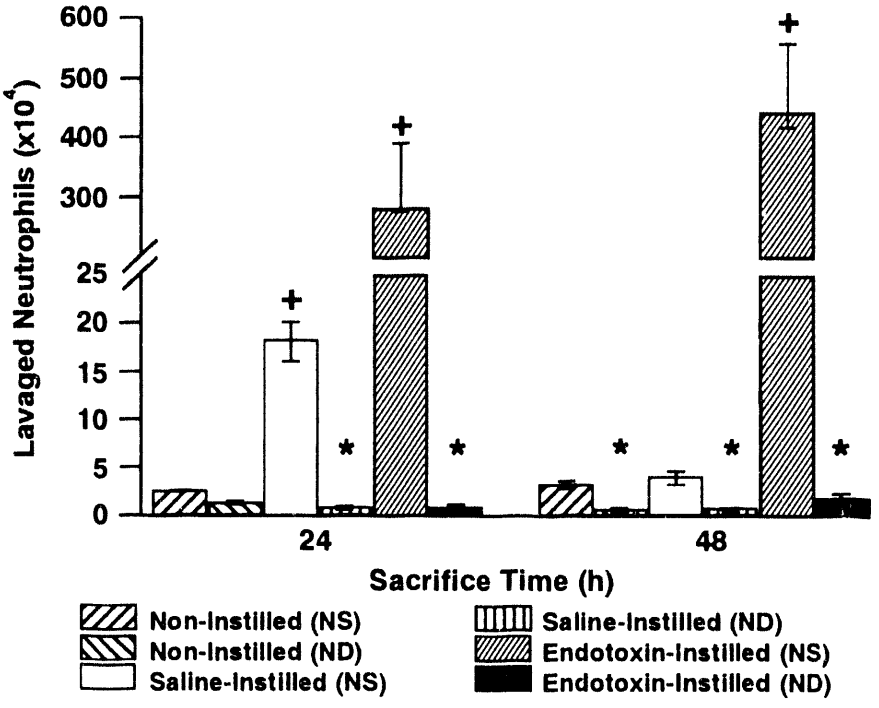

Figure 1. Number of neutrophils recovered by bronchoalveolar lavage from left lung lobes of NS and ND rats intratracheally instilled with endotoxin in saline, saline alone, or not instilled and sacrificed 24 or 48 h after instillation. Bars indicate the mean ± SEM. * = significantly different from similarly instilled, NS, group ($p \leq 0.05$). + = significantly different from non-instilled rats ($p \leq 0.05$).

Depletion of circulating neutrophils had no effect on the volume density of stored mucosubstances in non-instilled or saline-instilled rats. Therefore, at each sacrifice time, the data were combined and are presented as a single non-instilled or saline-instilled control group (Fig. 2). Endotoxin induced a significant increase in the volume density of mucosubstances 48 h after instillation in both NS and ND rats. However, endotoxin-instilled ND rats had an endotoxin-induced increase in IM that was only 40% of that observed in endotoxin-instilled NS rats.

In summary, we have examined the influence of inflammatory cell influx on endotoxin-induced mucous goblet-cell metaplasia in rat intrapulmonary airways. A single intratracheal instillation of 50 μg of endotoxin resulted in a large influx of neutrophils and an approximately nine-fold increase in stored mucosubstances. Depletion of circulating neutrophils by i.p. injection of ANA eliminated the endotoxin-induced neutrophil influx and markedly attenuated (approximately 50%), but did not prevent, the endotoxin-induced increase in stored mucosubstances. This suggests that infiltrating neutrophils contribute to the secretory cell metaplastic response of rat pulmonary airway epithelium exposed to bacterial endotoxin. This contribution might be made through direct interaction with the epithelium or indirectly through the release of soluble mediators (e.g., elastase).

In the future we will expose pulmonary airway explants to endotoxin *in vitro*. This will also prevent endotoxin-induced inflammatory cell influx and will determine if systemic factors are involved in endotoxin-induced mucous cell metaplasia. Results from these studies will help us to understand the pathogenesis of toxicant-induced mucous goblet cell metaplasia.

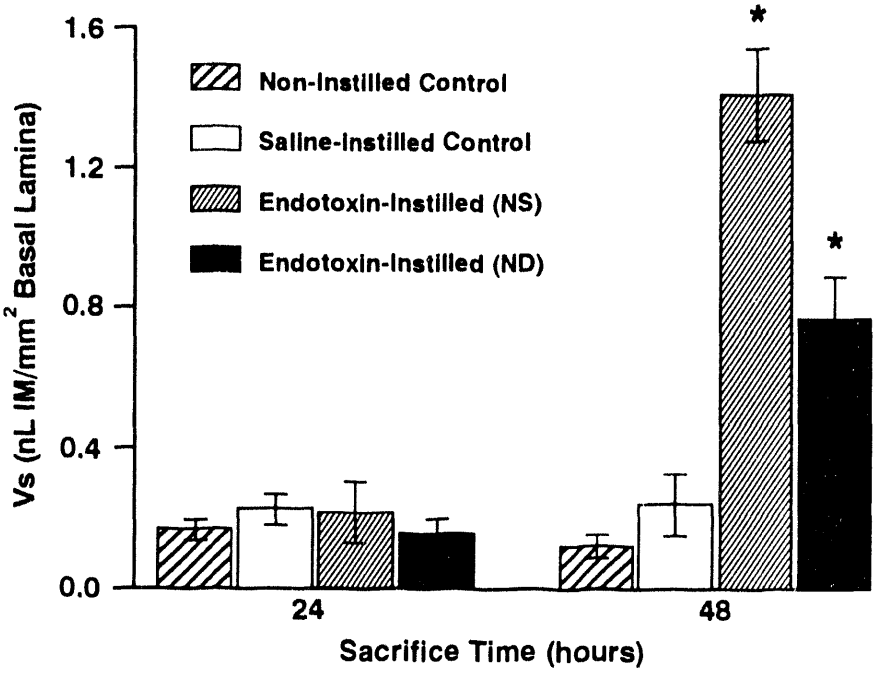

Figure 2. Amount of stored mucosubstances in the surface epithelium of pulmonary airways of NS and ND rats intratracheally instilled with endotoxin in saline, saline alone, or not instilled and sacrificed 24 or 48 h after instillation. Bars indicate the mean ± SEM. * = significantly different from non-instilled control ($p \leq 0.05$).

(Research sponsored by the Office of Health and Environmental Research, U.S. Department of Energy, under Contract No. DE-AC04-76EV01013.)

THE ROLE OF ANTIGEN IN THE DEVELOPMENT OF PULMONARY IMMUNE MEMORY

D. E. Bice, M. E. Cunniffe, G. E. Snow**, and B. A. Muggenburg*

Antibody-forming cells (AFC) are recruited from the blood into lung lobes exposed to antigen (Bice, D. E. *et al. Am. Rev. Respir. Dis. 126*: 635, 1982). These AFC produce antigen-specific antibody in the lung, providing an important pulmonary defense. In addition to AFC, immune memory cells are also present in the lung after a primary exposure to antigen (Mason, M. J. *et al. Reg. Immunol. 2*: 149, 1989; Jones, S. E. *et al. Mech. Ageing Dev. 68*: 191, 1993). The response of pulmonary immune memory cells to antigen challenge would help prevent repeated pulmonary infections. Although immune memory cells would be protective, the production of immune memory cells to inhaled allergens could also be pivotal in the production of lung diseases (e.g., asthma).

The mechanisms responsible for the development of immune memory in the lung are not understood. It is possible that immune memory cells are recruited into the lung from the blood as are AFC. However, it is also possible that immune memory cells are produced, or their number amplified, in the lung by interactions of immune cells with antigen retained in the lung. The goal of this study was to determine if the exposure of the lung to antigen is important in the recruitment and/or the development of pulmonary immune memory cells.

To study the role of antigen in the development of pulmonary immune memory, we used five female Beagle dogs. Based on the results of previous studies, primary immunization of two lung lobes with antigen and the exposure of one lung lobe to particles that induce inflammation were used to induced pulmonary immune memory cells in three lung lobes. If immune memory cells are recruited into the lung from blood like AFC, we hypothesized that these cells would enter not only lung lobes exposed to antigen, but also the lung lobe instilled with particles to induce inflammation. In contrast, if antigen is important in the recruitment of immune memory cells into the lung and/or if antigen retained in the lung after primary immunization is important in the development of immune memory cells, immune memory cells would be found only in the lung lobe exposed to antigen.

The antigen selected for this study was keyhole limpet hemocyanin (KLH), while ragweed pollen (*Ambrosia artemisiifolia*) (RWP) was instilled to induce inflammation. In a preliminary study, we determined that the level of inflammation produced by instillation of KLH or RWP was the same as indicated by the number of neutrophils and total protein in lung lavage fluid after exposure. For primary immunization, KLH was instilled (10 mg in 1 mL saline) into the left cardiac and left diaphragmatic lung lobes, while RWP was instilled (10 mg in 1 mL saline) into the right diaphragmatic lung lobe. The right intermediate lung lobe was instilled with 1 mL saline as a control. The levels of anti-KLH IgG in all four lung lobes and in blood were determined by an enzyme-linked immunosorbant assay (ELISA) evaluation of lung lavage and blood samples at 1, 4, 6, 8, 11, 13, 15, and 18 days after immunization (Jones *et al.*, 1993).

We have previously shown that the recruitment of AFC into the lung is not antigen-specific and that AFC enter lung lobes exposed to particles that induce inflammation (Bice *et al.*, 1982). Therefore, equally high levels of anti-KLH antibody were expected and observed in all three lung lobes instilled with either KLH or RWP (Fig. 1). The levels of anti-KLH IgG antibody in these three lung lobes were significantly higher than the level in lavage fluid from the saline control lung lobe (Fig. 1). The localized production of anti-KLH antibody in the lung lobes exposed to KLH as well as RWP supports the contention that AFC producing antibody in the lung after a primary immunization are not produced in the lung, but are recruited from the blood (Bice *et al.*, 1982). These observations also show that immune cells enter lung lobes exposed to antigen or agents that induce inflammation, regardless of the antigen-specificity of the immune cells (Bice *et al.*, 1982).

---

*Department of Energy/Associated Western Universities Summer Student Research Participant

**Department of Energy/Associated Western Universities Faculty Participant

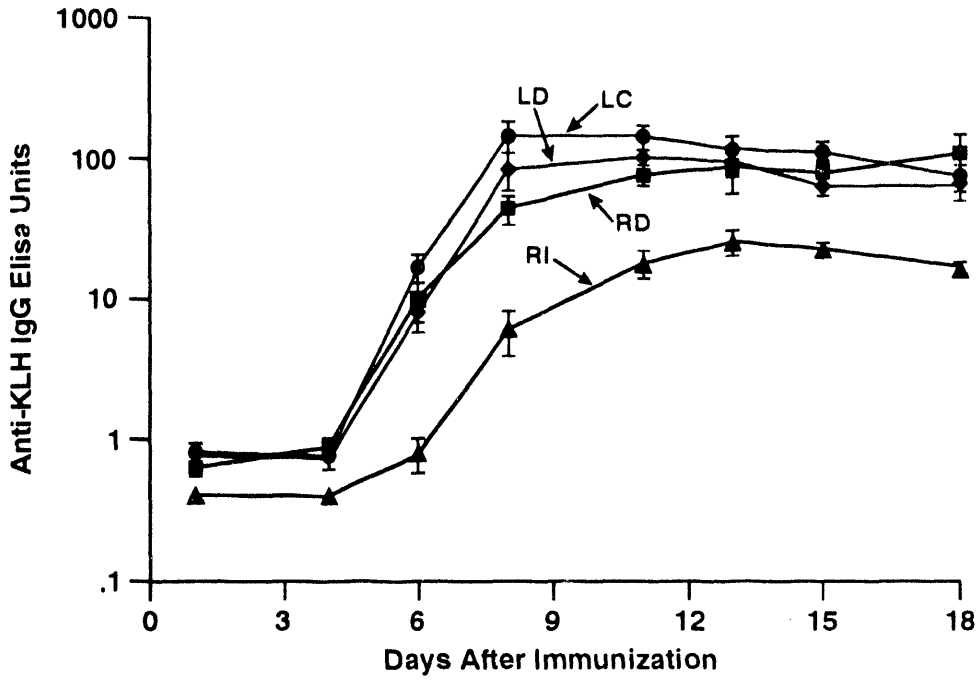

Figure 1. Levels (mean ± S.E.) of anti-keyhole limpet hemocyanin (KLH) IgG antibody present in lavage fluid from the left cardiac and left diaphragmatic lung lobes (LC, LD) instilled with KLH, the right diaphragmatic lung lobe (RD) exposed to ragweed pollen (RWP), and the right intermediate lung lobe (RI) instilled with 1 mL saline.

To evaluate the role of antigen in the recruitment and/or amplification of immune memory cells in the lung, the left cardiac (immunized with KLH) and the right diaphragmatic (exposed initially to RWP) lung lobes were challenged with KLH, while the left diaphragmatic (immunized with KLH) was challenged by instillation of RWP. All challenges were with 1.0 mg KLH in 1.0 mL saline. Blood and lavage samples were collected at 1, 4, 6, 8, 11, 13, and 15 days after challenge exposures, and the level of anti-KLH IgG was determined by ELISA.

The same level of anti-KLH IgG antibody was found in lavage fluid in the left cardiac lung lobe (initially exposed to KLH) and the right diaphragmatic lung lobe (initially exposed to RWP) after challenge with KLH (Fig. 2). The observation that an immune memory response was produced by a KLH challenge of a lung lobe exposed to RWP supports several conclusions. First, immune memory cells in the lung after primary immunization are recruited from the blood. If immune memory cells were produced in the lung during the development of a primary immune response, they would be antigen-specific, and no anti-KLH immune memory response would have been observed in a lung lobe initially exposed to RWP. Second, the recruitment of immune memory cells into the lung is not antigen-specific. Otherwise, no immune memory response would have been observed by KLH challenge of the lung lobe exposed to RWP. Third, there is no amplification of immune memory cells recruited into the lung by interaction with antigen retained in the lung. If immune memory functions were amplified by interactions of immune cells with antigen retained in the lung, a lower response would have been observed after challenge of the RWP lobe with KLH than observed after KLH challenge of the lung lobe immunized with KLH.

The level of anti-KLH IgG antibody in the left diaphragmatic lung lobe challenged with RWP was significantly lower than observed in either the left cardiac or right diaphragmatic challenged with KLH at 6 through 15 days after challenge (Fig. 2), although the level of anti-KLH antibody in this lung lobe was significantly higher than in the right intermediate control lung lobe. Based on previous observations, the elevated response in the left diaphragmatic lung lobe, in comparison to the level of anti-KLH IgG in the right intermediate control lung lobe, represents continued anti-KLH antibody production by AFC recruited into the lung after primary immunization. It is also possible that some AFC and antibody were recruited from the blood in

response to the inflammation produced by the challenge instillation of RWP. The elevated immune response observed in the left cardiac and right diaphragmatic lung lobes compared to that observed in the left diaphragmatic represents the response of anti-KLH memory cells in the lung (Mason *et al.*, 1989; Jones *et al.*, 1993).

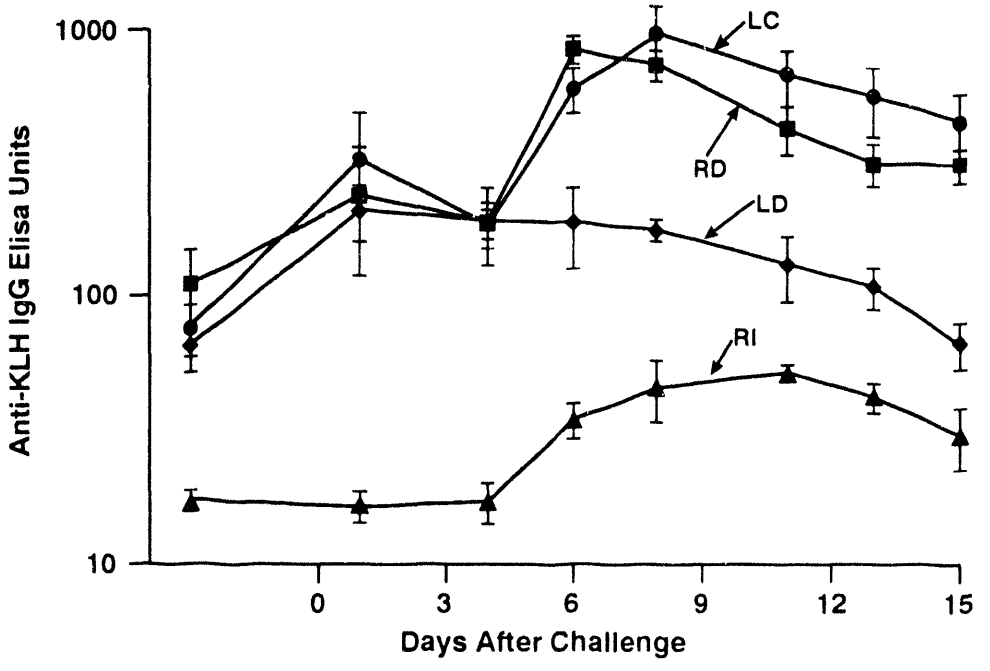

Figure 2. Levels (mean ± S.E.) of anti-keyhole limpet hemocyanin (KLH) IgG antibody present in lavage fluid from the left cardiac lung lobe (LC) immunized with KLH and challenged with KLH, the right diaphragmatic lung lobe (RD) exposed to ragweed pollen (RWP) and challenged with KLH, and the left diaphragmatic lung lobe (LD) immunized with KLH and challenged with RWP. The right intermediate lung lobe (RI) was instilled with 1 mL saline.

We conclude from these evaluations that immune memory cells in the blood enter the lung randomly, but at a higher frequency into any site of pulmonary inflammation. There is no further development or amplification of immune memory cells in the lung in response to contact with retained antigen. The local response of immune memory lymphocytes significantly elevates the level of pulmonary immunity above the response that could be produced only by the recruitment of AFC and antibody from the blood into a site of inflammation in the lung.

(Research sponsored by the Office of Health and Environmental Research, U.S. Department of Energy, under Contract No. DE-AC04-76EV01013).

PROGRESS TOWARD A MURINE MODEL OF GRANULOMATOUS LUNG DISEASE FROM INHALED BERYLLIUM

G. L. Finch, K. J. Nikula, D. S. Swafford, M. D. Hoover, and D. E. Bice*

The accidental inhalation exposure of people to beryllium (Be) can result in a spectrum of toxicologic responses. Of concern to this project is the induction of chronic beryllium disease (CBD) that typically occurs in a small percentage of exposed individuals. This disease is characterized by a Be-specific, immunologically mediated formation of granulomas within the lung (Haley, P. J. *Toxicol. Pathol. 19*: 514, 1991). Our efforts are oriented toward understanding the relationship between toxicity, immunologic responsiveness, and the physicochemical form of the Be to which an individual is exposed, as well as other exposure-related factors such as single versus repeated exposure. Central to this goal is the development of a laboratory animal model having Be-specific immune responses and pulmonary lesions typical of those seen in CBD.

Our previous efforts have involved studies of Beagle dogs, cynomolgus monkeys, and F344/N rats. We demonstrated that Be-exposed dogs and monkeys, but not rats, develop Be-specific cell immune responses and immune granulomatous lung lesions (Haley, 1991). More recently, we demonstrated that Strain A/J or C3H/HeJ mice that inhale Be metal develop a variety of lung lesions typical of CBD (1991-92 Annual Report, p. 171). Exposed mice formed pulmonary granulomas with a substantial component of T-helper lymphocytes. In addition, we observed a substantial degree of lymphocyte proliferation *in situ*, although we were not able to demonstrate the Be-specificity of this response using *in vitro* assays.

Development of a murine model that mimics human CBD would have a number of advantages over the use of dogs and monkeys. These include the availability of a number of syngeneic strains of mice, the existence of a wide range of cell markers and molecular probes, and more practical reasons such as the number of animals that can be studied. To this end, recent efforts have been oriented toward (1) evaluating the time course of pulmonary lesions in C3H mice exposed to a range of lung burdens of Be metal, (2) examining the development and potential resolution of Be-metal-induced lung lesions in Strain A/J versus C3H/HeJ mice, and (3) characterizing baseline lymphocyte proliferation characteristics in unexposed A/J and C3H mice.

To this end, we have collaborated with the project "Cancer Risks from Inhaled Beryllium Metal and $^{239}PuO_2$" in a dose-response toxicity study of inhaled Be metal in female C3H/HeJ mice (1991-92 Annual Report, p. 169). Beryllium was administered by a single, nose-only inhalation exposure to result in estimated initial lung burdens of 1, 4, 15, and 60 μg Be, and groups of six mice per exposure level were sacrificed periodically through 365 days post-exposure (dpe). In mice exposed to 15 or 60 μg, an analysis of bronchoalveolar lavage fluids revealed elevated numbers of neutrophils, increased amounts of total protein, and elevated activities of the enzymes lactate dehydrogenase and β-glucuronidase, all indicators of a chronic inflammatory response (Henderson, R. F. In *Concepts in Inhalation Toxicology*, Hemisphere Publishing Corp., New York, p. 415, 1989). Through 210 dpe, the numbers of lavagable lymphocytes were also significantly elevated in the 15 and 60 μg groups (Fig. 1).

Histologic analysis of lungs at 210 dpe revealed a minimal to mild increase in interstitial aggregates of lymphocytes and granulomas in the 1 μg group compared to controls. At the 4 μg burden, three of six mice were similar to controls, while the other three mice had mild increases in interstitial lymphocyte aggregates, discrete interstitial granulomas and mild granulomatous pneumonia characterized by alveolar macrophage hyperplasia, interstitial inflammation and fibrosis, and alveolar epithelial hyperplasia. The discrete interstitial lesions were moderate in severity in all mice at the 15 μg burden, and there was severe granulomatous pneumonia. All mice in the 60 μg group had severe granulomatous pneumonia and a marked increase in interstitial lymphocyte aggregates and discrete granulomas.

We are also collaborating on the project "Mechanisms of Chemically Induced Carcinogenesis" in a comparative study of the effects of inhaled Be in female Strain A/J and C3H/HeJ mice. Both strains received

*UNM/ITRI Inhalation Toxicology Graduate Student

Be initial lung burdens of 60 μg. Ten months after exposure, all 10 Be-exposed mice of both strains had similar lung lesions that consisted of severe granulomatous pneumonia. We concluded that either there were no strain-related differences, or that the lesions in the C3H/HeJ mice had a slightly reduced macrophage component and apparent toxic reaction to Be.

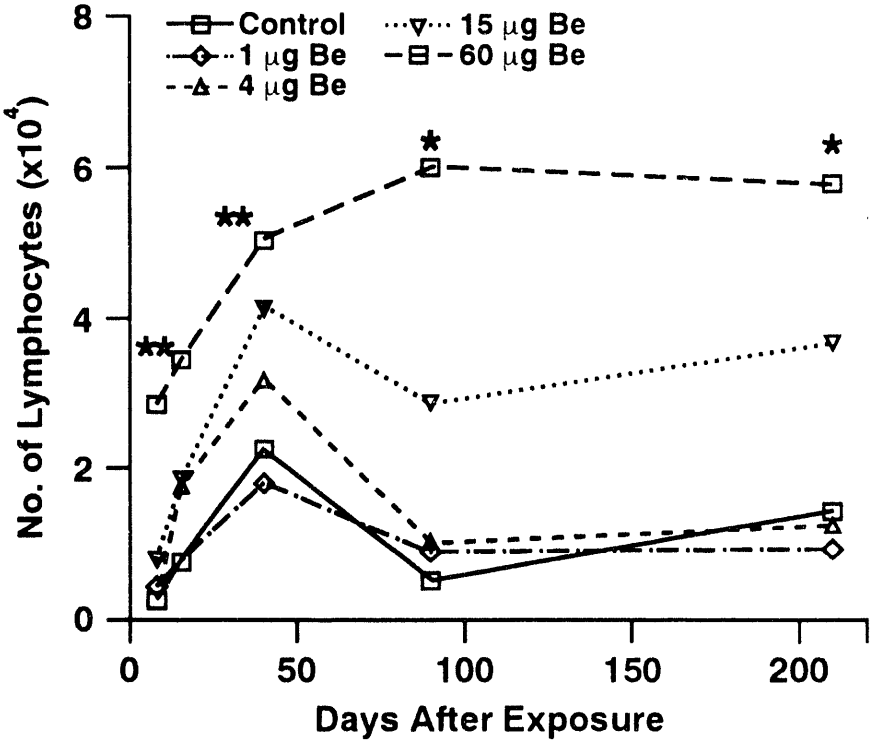

Figure 1. Absolute number of lymphocytes observed in bronchoalveolar lavage fluids from right lung lobes of mice exposed to a range of lung burdens of Be metal and sacrificed through 210 days after exposure. For each sacrifice time, asterisks denote the level of significance of difference between exposed groups and controls (*, $p < 0.05$; **, $p < 0.01$) using a Student's *t*-test with a Bonferroni correction for multiple comparisons.

To understand splenic lymphocyte proliferation characteristics in these two strains, A/J and C3H/HeJ mice were sacrificed between 20 and 22 mo after exposure. Spleen cells were harvested and placed in culture with $BeSO_4$ (1, 10, or 100 μM), phytohemagglutinin (PHA; 10 μg/mL), or culture medium alone. Cells were cultured for 3, 5, or 7 days, pulsed with tritiated thymidine (^{3}H-T), then harvested 18 h later for measurement of ^{3}H-T incorporation to indicate DNA synthesis. All cultures were run in triplicate. Proliferation was expressed as the stimulation index (SI; radioactivity in culture with $BeSO_4$ or PHA/radioactivity in cultures with medium alone).

Preliminary data have been obtained from splenic lymphocytes from two control A/J mice, three exposed A/J mice, three control C3H/HeJ mice, and one exposed C3H/HeJ mouse. No consistent, Be-specific responses have been observed in any of the mice, although borderline SI values of 4.6 and 5.9 were observed in cells stimulated by 1 μM $BeSO_4$ harvested at 7 days in an exposed C3H and an exposed A/J mouse, respectively. Substantial proliferation in response to the mitogen PHA was observed in all mice except for one control C3H/HeJ. With the exception of this mouse, there were no apparent differences in responses to $BeSO_4$ or PHA between control and exposed mice of either strain. Stimulation indices in response to PHA were greatest at 3 days, markedly reduced by 5 days, and lowest by 7 days in culture (data not shown).

Taken together, results from these experiments suggest that mice may react to Be exposure with many of the features of CBD. Work at the highest doses of Be metal, 60 μg, indicates that a pronounced, chronic, toxic reaction to Be predominates the pulmonary responses. Future efforts will use lower lung burdens, in the range of 4 to 15 μg, in an effort to decrease the magnitude of the toxic response, while still maintaining some

component of the lymphocytic response. Techniques such as lung cell elutriation of digested lung will provide populations of lung T-lymphocytes thought most likely to respond to Be. Because few differences in the nature and magnitude of pulmonary lesions or in the proliferative capabilities of cultured lymphocytes are evident between the A/J and C3H/HeJ mouse, and in light of the work of Huang, H. *et al.* (*Lab. Invest. 67*: 138, 1992), who demonstrated transient indications of Be-specificity in the reactions of Strain A/J mice, our future efforts will use this strain. We believe the use of these approaches will maximize the likelihood of developing a murine model that mimics the salient features of human CBD.

(Research sponsored by the Office of Health and Environmental Research, U.S. Department of Energy, under Contract No. DE-AC-04-76EV01013.)

VII. DEVELOPMENT OF THERAPEUTIC MODALITIES

TREATMENT OF THE PROSTATE GLAND USING A DIODE LASER

B. A. Muggenburg, F. F. Hahn, W. C. Griffith, V. Esch, and R. L. Conn***

Chronic prostatic hypertrophy is a common disease in older men. The hypertrophy of the prostatic tissue surrounding the urethra will often cause urinary retention and difficulty in micturition. Untreated, the disease can result in obstruction of the prostatic urethra. Current treatments include castration, surgical removal of prostatic tissue through the urethra, and yttrium-aluminum-garnett (YAG) laser treatment with the laser fiber placed in the prostatic urethra. The surgical and YAG laser treatment usually require hospitalization for several days. Because of the hospitalization, and the high cost of the YAG laser, a simpler and less expensive treatment modality is desirable.

An age-associated, chronic prostatic hyperplasia also occurs in dogs. The distribution of the hyperplastic tissue in the dog is more generalized and results in an enlargement of the gland. Although urethral narrowing or obstruction is rare, chronic infection within the hyperplastic areas is the most prevalent problem in the dog. However, the dog does provide a useful model for studies on the treatment of prostate problems in man because of the size, shape, and location of the prostate within the pelvis. These similarities provide the opportunity to use the same medical devices in the dog as in man. Because the landmarks for identifying locations within the prostate are present in the dog, procedures developed in the dog can be directly applied to man.

Indigo Medical, Inc. and ITRI have formed a collaborative research project to develop the diode laser for use in prostate surgery. Los Alamos National Laboratory and the Phillips Laboratory have contributed significantly to the development of the diode laser, the laser fibers, and diffusing tips. The studies were conducted at ITRI because of its unique laboratory animal facilities and staff.

The purpose of this study was to evaluate the safety of using a small diode laser to treat the prostate gland. The Beagle dog was selected for use for the reasons discussed above. The diode laser selected (Indigo Medical, Inc.) for evaluation has a power output of less than 10 watts (compared to approximately 100 watts from a YAG laser). In addition to small power output, the laser diffusing tip can actually be placed within the prostatic tissue. It is also expected that this system may be used on an outpatient basis.

The first studies, which were directed to establish "proof of principle," were performed as open surgical procedures through a laparotomy incision. The laser diffusing tips were placed in the prostate gland with temperature probes to establish a temperature profile around the tip during treatment and to correlate temperature with tissue damage using gross and histopathology methods.

A study was then conducted in dogs to establish the safety of treatment with 3 watts of power for 10 min in the right and left lobes of the prostate. The laser fiber was positioned in the prostate gland from the prostatic urethra using a rigid cystoscope. The dogs were serially sacrificed from 3 to 84 days after treatment. The dogs were clinically observed daily, and the body temperature and appetite were recorded during the first 3 days to establish morbidity during the immediate post-treatment period. Periodically, blood samples were taken for evaluation of blood loss post surgery, signs of infections or tissue damage, and recovery. The urethra and bladder were evaluated visually by cystoscopy, and the prostate gland was examined by ultrasound. The size of the prostate gland was also estimated by ultrasound. At sacrifice, the urinary tract and surrounding tissues were examined, photographed, and evaluated by histopathology.

For the first 3 days after treatment, all of the dogs had normal to above normal output of urine indicating tissue swelling did not obstruct the urethra. Body temperature was within normal range for all but one dog. Appetite was normal, and the dogs were active. Absolute monocyte and neutrophil numbers and alkaline phosphatase values in the peripheral blood were elevated on day 3 after treatment but were generally within the normal range by day 10. Prostatic volume tended to increase on day 3 after treatment but decreased in size

*Indigo Medical, Incorporated, Palo Alto, California

**Lovelace Medical Center, Albuquerque, New Mexico

thereafter until day 84 when the measurements were not statistically different from the baseline measurements (Fig. 1). Prostatic volume was analyzed using an estimate of variance pooled across all times. The 95% confidence intervals were calculated based upon the number of measurements available for each dog, and the mean of dogs at a particular time were weighted averages with the weight based upon the dogs' variance.

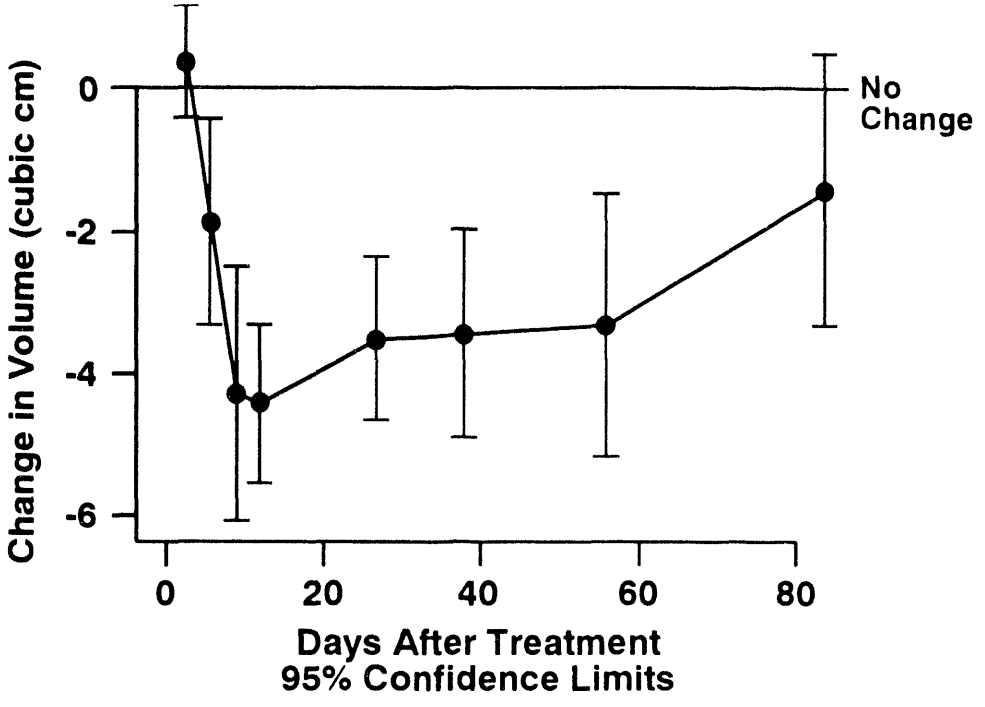

Figure 1. Prostatic volume as measured by ultrasound using a rectal probe. Average individual change from baseline. The straight line represents the volume before laser treatment.

Gross and histopathology showed large foci of coagulation necrosis around the area of treatment. At later times, this resulted in epithelial cyst formation in a few days, but more frequently atrophy and fibrosis were observed. Areas of moderate chronic inflammation were noted in some dogs at later times. These areas were sometimes distant to the treatment area. Based on these pathology findings, the increase in prostatic size immediately after treatment was interpreted as tissue reaction (inflammation and edema) to the laser-induced necrosis. As the prostate gland healed, the size decreased due to atrophy and fibrosis. The trend to increased size again at 84 days may have occurred because only three dogs were measured at that time, and one of these dogs had a very large prostate due to chronic prostatic hyperplasia, a condition that pre-dated the study.

These studies have shown that diode laser treatment of the prostate gland in dogs, using 3 watts for 10 min, results in necrosis of the prostate tissue, due to increased tissue temperatures around the laser diffusing tip. The dogs were clinically normal immediately after treatment except for signs of tissue injury as detected by hematology and clinical chemistry. As a result of treatment, the prostate gland decreased in size by atrophy and fibrosis, although in some dogs, cysts were formed in the gland. These studies support the potential use of diode laser treatment using the low power for treatment of benign prostatic hypertrophy in man.

(Research sponsored by Indigo Medical, Inc., under a Cooperative Research and Development Agreement No. IC91-20003 with the U.S. Department of Energy under Contract No. DE-AC04-76EV01013.)

VIII. THE APPLICATION OF MATHEMATICAL MODELING TO HEALTH ISSUES

MATHEMATICAL MODEL OF PARTICLE DEPOSITION FROM INHALED POLYDISPERSE AEROSOLS

H. C. Yeh, Y. Zhuang, and I. Y. Chang*

Mathematical modeling is an efficient and comparatively inexpensive approach in scientific research. Mathematical models for predicting respiratory tract deposition have been developed (Yeh, H. C. and G. M. Schum. *Bull. Math. Biol. 42*: 461, 1980). A previously developed deposition model has been incorporated into the proposed National Council on Radiation Protection Dosimetry model that describes particle deposition, clearance, and dosimetry in the human respiratory tract for inhaled radioactive materials (Chang, I. Y. *et al. Radiat. Prot. Dosim. 38 No. 1/3*: 193, 1991; Yeh, H. C. *et al.* In *Proceedings of the First Symposium on Pollution and Health Effects of Aerosols*, National Tsing Hua University, Taiwan, Republic of China, p. 44, 1991). As part of this model, a computer program was written to facilitate the model calculations for inhaled monodisperse particles. However, in the home or workplace, the aerosols are usually polydisperse, and the size distributions are likely to vary from environment to environment. The predicted inhaled particle deposition based on the mean (or median) particle diameter may not adequately describe the true exposure to polydisperse aerosols. In this report, we describe an update of our previous deposition model (Yeh and Schum, 1980) to compute the initial regional respiratory tract deposition pattern from inhaling polydisperse aerosols.

In that model, the respiratory tract was divided into three main regions, the naso-oro-pharyngo-laryngeal (NOPL), tracheobronchial (TB), and pulmonary (P) regions (Yeh, H. C. and J. R. Harkema. In *Gross Morphometry of Airways, 2nd Ed.* [D. E. Gardner *et al.*, eds.], Raven Press, New York, p. 55, 1993). The division of these regions is partially based on the functionality of the region and partially for convenience. In inhalation toxicology, the range of aerosol particle sizes of interest falls between 0.001 and 100 μm in diameter. The size distribution of these particles can, generally, be described by a log-normal function with a median diameter (e.g., mass median diameter [MMD]) and a geometric standard deviation (GSD), σ_g.

The modified model and its associated computer program involved the following steps: (1) taking into account the entrance effect of a tube on the diffusional deposition mechanism (Yeh, H. C. *Bull. Math. Biol. 36*: 105, 1972); (2) taking into account the inhalability of particles (American Conference of Governmental Industrial Hygienists Technical Committee. *Particle Size-Selective Sampling in the Workplace,* Cincinnati, OH, 1985); (3) using the latest data on nasal deposition (Cheng, Y. S. *et al. Radiat. Prot. Dosim. 38*: 41, 1991); and (4) facilitating computation of polydisperse aerosol deposition by integrating the deposition over the size distribution. The first three items involved the modification of deposition equations and minor computer coding update. The fourth item required the user to enter MMD and GSD data in addition to other usual parameters (such as breathing frequency, tidal volume, pause between breaths, etc.). For a given size distribution (i.e., an MMD and σ_g), the range of particle sizes of interest was set to MMD $\pm$ 4 σ_g, and that range covered 99.96% of all particles within the distribution. This range was subsequently divided into 40 equal size intervals on a log scale, and the mass (or number) fractions of particles for each interval were calculated. The mid-point of each interval was then taken as the particle size of interest for the deposition calculation. The regional deposition fractions thus calculated were multiplied by the mass fraction of that size interval of aerosols. Finally, the calculated results from all 40 intervals were summed together to obtain the regional deposition from inhaling a polydisperse aerosol.

Statistically, the polydispersities of aerosols are expressed by the GSDs, with the GSD = 1 for an ideal monodisperse aerosol. The GSDs of 1, 2, and 4 were chosen for sample calculations, and MMDs ranging from 0.001 and 100 μm were used to compute the regional depositions for investigating the effect of σ_g on deposition. The results of the total depositions are plotted on Figure 1. The results show that the total respiratory tract deposition increases with increasing polydispersity (i.e., increasing σ_g) for particles with MMDs between 0.5 and 2.0 μm, and MMD > 20 μm, and decreases for other particle sizes. Figure 2 shows the NOPL, TB, and P

*Department of Energy/Associated Western Universities Teacher Research Associates Program (TRAC) Participant

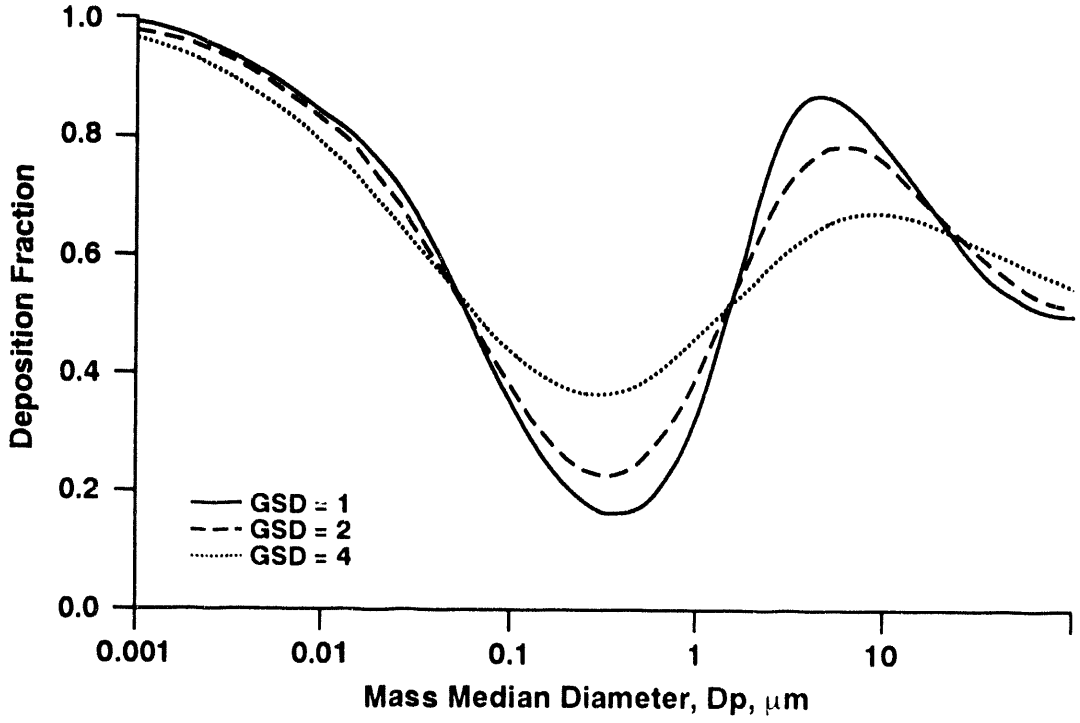

Figure 1. Calculated total deposition in the respiratory tract (tidal volume = 750 mL, breathing frequency = 15/min, GSD = geometric standard deviation).

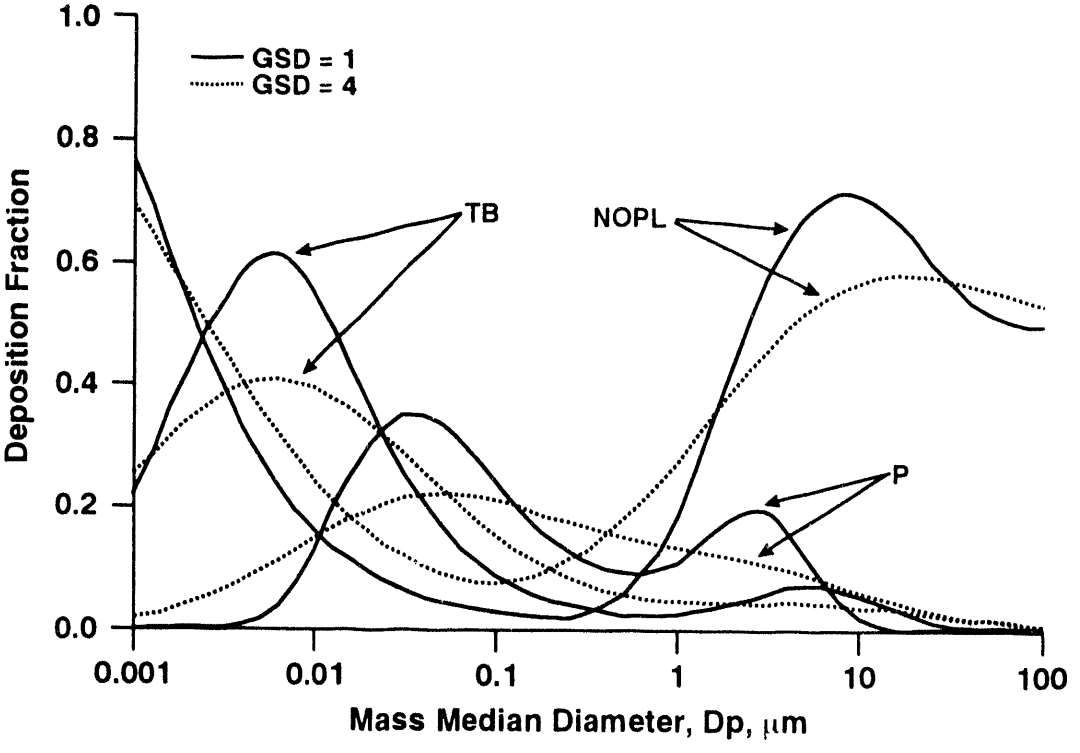

Figure 2. Calculated regional deposition in the respiratory tract for aerosols with geometric standard deviations (GSD) equal to 1 and 4 (tidal volume = 750 mL, breathing frequency = 15/min; NOPL = naso-oro-pharyngo-laryngeal, TB = tracheobronchial, P = pulmonary).

depositions, respectively, with σ_g equal to 1 and 4. For the NOPL region, the deposition increases with decreasing particle size for submicrometer particles, due to the diffusional deposition mechanism. On the other hand, the deposition increases with increasing particle size for micrometer-sized particles because sedimentation and inertial impaction mechanisms are important in this size range. However, for particles larger than about 5 μm, NOPL deposition starts to decrease; this is due to the decreasing inhalability of larger particles. For deposition of TB and P, two particle sizes are achieved (two peaks in deposition curves; around 0.005 μm and 6 μm for TB and 0.03 μm and 3 μm for P) for monodisperse particles (e.g., σ_g = 1). With increasing σ_g, the locations of the first peaks for both TB and P shift to larger sizes, and the second peak at MMD > 1 μm disappears as the effect of MMD on deposition decreases. When $\sigma_g \rightarrow \infty$, the effect of MMD diminishes. Finally, the results show that, for a finite value of σ_g, initial deposition in various regions may increase or decrease with increasing σ_g depending on the inhaled MMD. These changes in deposition are consistent with our current understanding of particle-size-specific mechanisms of deposition.

(Research sponsored by the Office of Health and Environmental Research, U.S. Department of Energy, under Contract No. DE-AC04-76EV01013.)

SENSITIVITY ANALYSIS OF THE ITRI ^{238}Pu BIOKINETIC MODEL

A. W. Hickman, W. C. Griffith, and R. A. Guilmette*

Plutonium-238 is used as the heat source for radioisotope thermoelectric generators (RTGs) in spacecraft (Bennett, G. L. *Nuclear Safety 32*: 1, 1991). Associated with this use is the potential for human exposure to ^{238}Pu, either occupationally as the result of an accident during manufacture of the RTGs or to the general population as the result of a launch-pad or re-entry accident involving the spacecraft. The ITRI ^{238}Pu biokinetic model (Hickman *et al.*, unpublished data), an adaptation of a canine model developed at this Institute (Mewhinney, J. A. and J. H. Diel. *Health Phys. 45*: 39, 1983), was developed for use following such exposures.

Inhaled particles containing ^{238}Pu undergo fragmentation in the lungs due to the high specific activity of ^{238}Pu. In the ITRI model, the rate of translocation of ^{238}Pu from the lungs to the systemic circulation, and from there to the other body organs, is determined by the rate of fragmentation of ^{238}Pu-containing particles and the rate of dissolution of particles and fragments. Mechanical clearance, which clears deposited material via the gastrointestinal tract, is not discussed here.

The fragmentation rate is described by the empirically derived equation (Mewhinney and Diel, 1983)

$$\lambda_F = ft^{a},$$

where f is the fragmentation constant, with units of days^{-a-1}; t is the time in days after exposure; and a is a dimensionless parameter. Individual particles lose mass according to the formula

$$\frac{dm}{dt} = -ks(t),$$

where k is the solubility rate constant in g cm^{-2} d^{-1} and $s(t)$ is the time-dependent surface area of the particle. For a population of particles with a log-normal distribution of particle sizes, the dissolution rate is a function of the following aerosol-specific parameters: k, the solubility rate constant; α_s and α_v, the particle surface and volume shape factors, respectively, which describe particle geometry; (ρ), the particle density; (D_m), the particle mass median diameter; (σ_g), the geometric standard deviation of D_m; and (R), the relative surface area of fragments compared to that of particles. More complete descriptions of the mathematics used to describe fragmentation and dissolution are given by Mercer, T. T. (*Health Phys. 13*: 1211, 1967), Mewhinney and Diel (1983), and Hickman, A. W. *et al.* (unpublished data).

Information on the physicochemical characteristics of an aerosol is usually not available following a human exposure incident. Therefore, the sensitivity of the model's prediction of urinary excretion to variations in the aerosol-associated parameters was tested. This was done by simulating exposure to a unit initial lung burden (ILB) (i.e., unit deposition of particles in the pulmonary region of the respiratory tract). All simulations were run using SimuSolv modeling and simulation software (SimuSolv Development Group, The Dow Chemical Company, Midland, MI) on a MicroVAX II computer (Digital Equipment Corporation, Maynard, MA). Test values of all parameters were selected to cover a range of expected values; default settings for all model parameters were those used previously in modeling the ^{238}Pu urinary excretion patterns for seven workers occupationally exposed to a ^{238}Pu ceramic aerosol (Hickman *et al.*, unpublished data).

Sensitivity testing of the model indicated that the shapes of the urinary excretion curves were least sensitive to changes in ρ and σ_g. In each case, the activity excreted at 1 day post exposure (dpe) varied by a factor of 2 or less over the range of values tested (ρ = 7 to 11 g cm^{-3}; σ_g = 1.1 to 3.5), and variation among the curves was greatest at 1 dpe. The basic shape of the urinary excretion curves did not change with changes in either parameter. All simulated urinary excretion curves converged at about 1500 dpe for both parameters.

---

*UNM/ITRI Inhalation Toxicology Graduate Student

Changes to f and a, the parameters in the fragmentation equation, had little effect on the level of peak excretion, which varied by 22% for f and 8% for a. The time at which the peak value of activity in the urine was obtained varied from 1720 to 2820 dpe for f (values tested = 5 x 10^{-5} to 5 x 10^{-3} d^{-a-1}) and from 1690 to 1990 dpe for a (values tested = 0.25 to 2). Increasing the value of either parameter decreased the time needed to approach the peak value, leading to an extended plateau for the higher values tested. All curves converged at about 2000 dpe for both f and a.

The model predictions proved to be more sensitive to changes in the value of the relative surface area of fragments compared to particles, R (Fig. 1). Increasing the value of R from 2 to 200 caused the level of peak excretion to increase by a factor of 31, from 3.8 x 10^{-4}% ILB d^{-1} to 1.2 x10^{-2}% ILB d^{-1}. The time needed to reach the peak value of activity in the urine decreased from 6080 dpe for R = 2 to 1240 dpe for R = 200. In addition, the curves remained divergent even at 20,000 dpe.

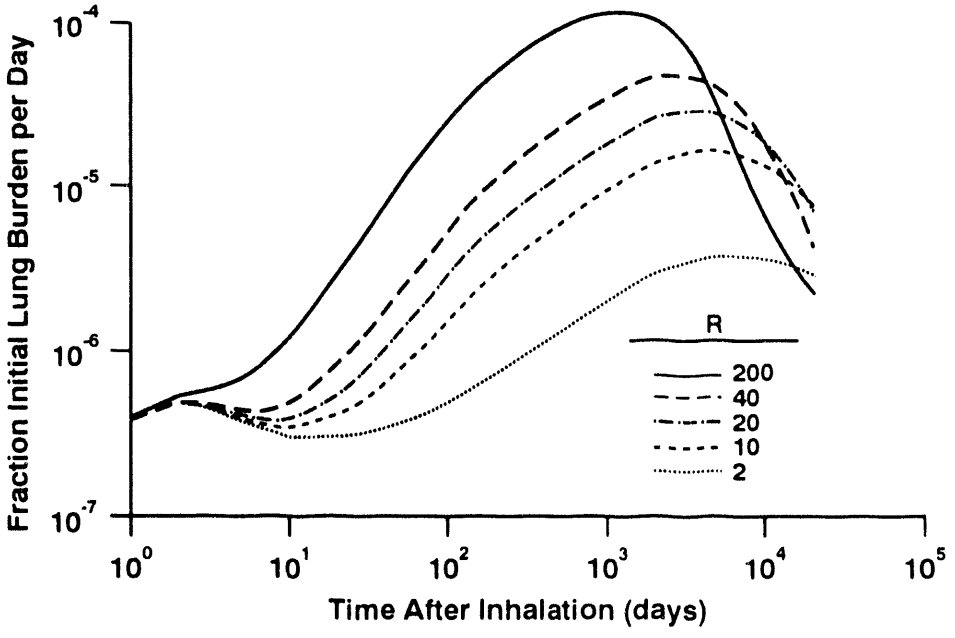

Figure 1. Effect of varying R, the relative surface area of fragments compared to particles, on the predicted daily rate of urinary excretion of ^{238}Pu.

The rate at which particles and fragments dissolve is proportional to the quantity $(\alpha_s/\alpha_v)\times(k/D_m)$. Often little is known about α_s or α_v for a given aerosol, and these parameters are difficult to measure. Therefore, sensitivity testing was not done on them. Any differences from spherical particles (α_s/α_v = 6) in an actual aerosol could be accounted for by modifications to k/D_m. However, if information on k and D_m was available, estimates of α_s/α_v would be needed to fit the predicted urinary excretion curve to available excretion data.

Because k and D_m are inversely related in the equation describing particle dissolution, an increase in the value of one is equivalent to a corresponding decrease in the value of the other. Therefore, only the effects of modifying k are described here. Changes to k (Fig. 2) influenced both excretion at 1 dpe (an effect unique to those factors associated with particle dissolution) and time and level of peak excretion. Excretion at 1 dpe varied by a factor of 350 over the range of values tested, from 1.9 x 10^{-5}% ILB d^{-1} for k = 2.5 x 10^{-11} g cm^{-2} d^{-1} to 6.8 x 10^{-3}% ILB d^{-1} for k = 2.5 x 10^{-7}. The level of peak excretion predicted varied by a factor of 60, from 6.2 x 10^{-4}% ILB d^{-1} for k = 2.5 x 10^{-11} to 3.6 x 10^{-2}% ILB d^{-1} for k = 2.5 x 10^{-7}. These values were attained at 5770 and 83 dpe, respectively. Curves for the highest values of k tested converged by about 10,000 dpe; however, those for the lowest values remained divergent at 20,000 dpe.

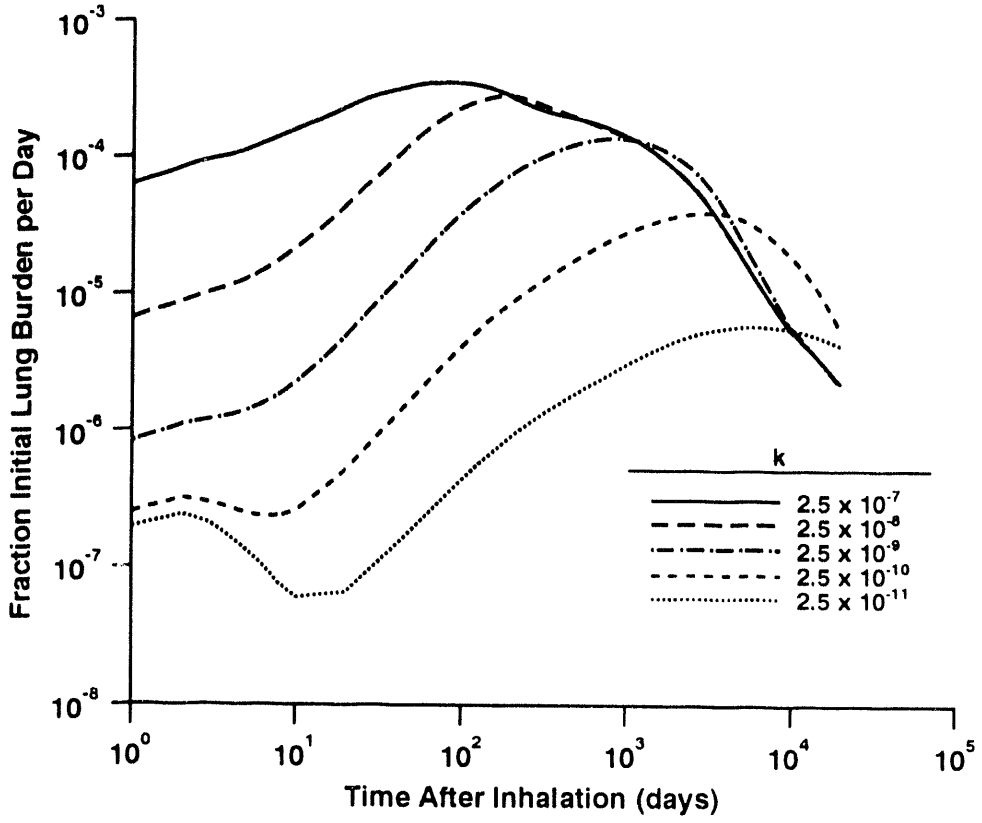

Figure 2. Effect of varying solubility rate constant k (g cm^{-2} d^{-1}) on predicted daily rate of urinary excretion of ^{238}Pu.

In the equation describing the dissolution rate for ^{238}Pu-containing particles and fragments, the parameter that actually varies is the ratio k/D_m. Therefore, it is possible to obtain the same value of k/D_m using many different values for the individual parameters. The values of k and D_m used to obtain a given value for k/D_m do not affect the estimated ILB received by an individual following exposure to ^{238}Pu. However, the choice of D_m determines the estimated intake that would deliver that ILB, because fractional deposition of material in the regions of the respiratory tract is affected by particle size.

In conclusion, sensitivity testing of the ITRI biokinetic model for ^{238}Pu indicates that predictions of urinary excretion are most sensitive to changes in the values of the solubility of the material inhaled (k) (or equivalently the particle size, D_m), particle geometry (α_s/α_v, which is coupled to k/D_m), and the ratio of fragment:particle surface area (R). The model is less sensitive to changes in the parameters governing the breakup of the inhaled material (f and a) and relatively insensitive to variation in density of the inhaled material (ρ) and the size distribution of the inhaled particles (σ_g). Because several of these variables are highly correlated, obtaining a unique set of best-fit parameters to describe a given inhalation exposure is difficult. This highlights the need for health protection personnel to maximize the collection of physical and chemical information on the exposure material, either by sampling known source materials or by capturing the materials as soon after an accident as possible.

(Research sponsored by the Office of Health and Environmental Research, U.S. Department of Energy, under Contract No. DE-AC04-76EV01013.)

INTAKE ASSESSMENT FOR WORKERS THAT INHALED ^{238}Pu AEROSOLS

*R. A. Guilmette, W. C. Griffith, and A. W. Hickman**

The United States space exploration program has relied on the use of radioisotope thermoelectric generators (RTGs) since 1961 for providing long-term dependable electric power to both its civilian and military spacecraft. All 37 RTGs have been powered by ^{238}Pu heat sources. Several known inhalation exposures involved with the production of the RTGs have occurred, and since the U.S. space program is projected into the 21st century, the potential for future worker exposures to ^{238}Pu will continue to exist.

Results from studies in which dogs inhaled $^{238}PuO_2$ aerosols provided the basis for the development of a mechanistically based biokinetic/dosimetric model that accounts for the fragmentation/dissolution characteristic of high specific activity ^{238}Pu particles. This model has now been applied to urinary bioassay data obtained from exposures that occurred at different ^{238}Pu production/fabrication facilities in the U.S.A. to predict the intakes, and to infer the aerosol particle physicochemical properties for which measurement data were lacking at the time of the exposure incidents.

The mathematical model used in this study was based on the original formulation of Mewhinney, J. A. and J. H. Diel (*Health Phys. 45*: 39, 1983) as modified for use in human exposure cases by Hickman, A. W. *et al.* (this report, p. 130). All simulations were done using SimuSolv (Dow Chemical Co., Midland, MI) modeling and simulation software that was implemented on a DEC MicroVAX II computer (Digital Equipment Corp., Maynard, MA).

The patterns of urinary excretion of ^{238}Pu for exposure cases from two facilities differed significantly from each other. These differences could be adequately treated by modifying only the values of variables directly related to the aerosol particles, i.e., no modifications to the systemic portion of the model were required. The exposure scenarios and associated urinary excretion patterns related to each facility are described separately since they each had unique features.

Facility 1 The ^{238}Pu exposures occurred during the disassembly of a ^{238}Pu heat source in a shielded hot cell. A leak in the plastic boot of a manipulator arm apparently resulted in a Pu aerosol being pumped into the work environment as a result of moving the manipulator. A continuous air monitor (CAM) alarm sounded, but was ignored because of a concurrent lightning storm, and because the CAM was not externally contaminated and could be reset manually. After 20-50 min, the CAM sounded again, but could not be reset, causing the workers then to use respiratory protection to finish their task. Seven workers were later determined to have had measurable intakes of ^{238}Pu based on urinary bioassay. No decorporation therapy was used on any of the workers. The inhaled ^{238}Pu aerosol was described as a "Pu ceramic," which probably means a PuO_2 material containing a Mo binder to allow the fabrication of heat source pellets. No other information on aerosol particle size, air concentration, or intrinsic solubility was available.

Four of seven workers had urinary excretion patterns similar to Case 6 (illustrated in Fig. 1). Of note is the pattern of urinary excretion during the first 200 days after exposure. In general, the lowest measured values occurred immediately after exposure, followed by a prolonged period of about 200 days during which the ^{238}Pu levels increased monotonically; thereafter, the ^{238}Pu levels maintained a plateau for about 4000 days. Then, levels appeared to decrease slowly. In workers having measurable urinary ^{238}Pu immediately after exposure, the magnitude of the increase in ^{238}Pu excretion was about a factor of 100. This urine excretion pattern was similar to the patterns observed in the ^{238}Pu dog study of Mewhinney and Diel (1983), but unlike those described for any other documented Pu exposure cases of which we are aware.

As can be seen, the fitted curve obtained from the ITRI model adequately describes the data for all but the very earliest urine values (Fig. 1). The parameter values resulting from the simulations suggested that the particle size of the deposited ^{238}Pu aerosol was 4.4 μm activity median aerodynamic diameter (AMAD), and that

*UNM/ITRI Inhalation Toxicology Graduate Student

the solubility rate constant was of the order of 8 x 10^{-10} g cm^{-2} d^{-1}. These particle-related parameters are responsible for the shape of the rising portion of the urinary excretion curve, and represent the period during which fragmentation of the ^{238}Pu particles and subsequent dissolution and translocation to blood were occurring. Thereafter, i.e., during the plateau period (t > 200 days), the shape of the urinary excretion curve is controlled by the systemic portion of the model. The fitted curves are consistent with assumed biological retention half times of 25 yr for liver and 50 yr for bone. The estimated initial lung burden (amount of ^{238}Pu deposited beyond the ciliated portion of the lung) for the illustrated case was 1700 Bq; the corresponding intake assuming a 4.4 μm AMAD aerosol was 30 kBq. The range of intakes for all seven workers was 1.4-30 kBq.

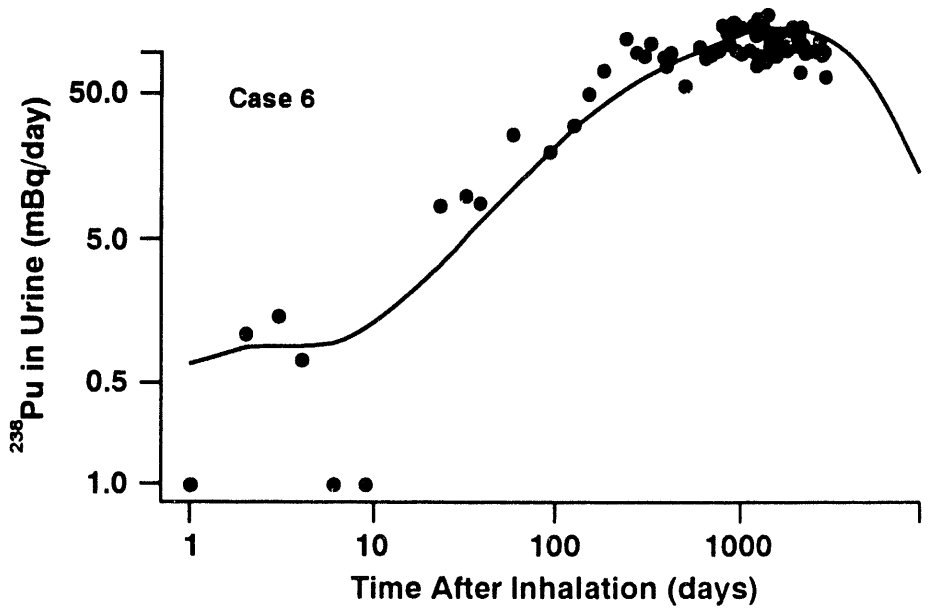

Figure 1. Urinary excretion of ^{238}Pu in one of seven male workers exposed at Facility 1 (closed circles). These cases had excretion patterns characteristic of the other workers whose data are not illustrated. The solid curve is from the model simulation.

Facility 2 A single acute exposure to ^{238}Pu occurred when a worker opened a purportedly empty ^{238}Pu shipping container in a laboratory. The can had not been opened for 7-20 yr. The worker carried the can to a radiation survey meter within the room; the survey meter alarm rang simultaneously with the room CAM. The worker replaced the lid on the can, and she and the other three workers in the room at the time evacuated immediately. The worker was given a single intravenous injection of DTPA and a laxative at 3 h post exposure; no other decorporation therapy was given. *In vivo* measurements over the thorax region were negative, and no information on particle size, chemical form or solubility of the ^{238}Pu aerosol was available.

Only urinary excretion data from the worker handling the can were provided for analysis (Fig. 2). In contrast to the urinary excretion pattern seen with the workers exposed at Facility 1, these data show a monotonically decreasing urinary excretion pattern suggestive of a much more soluble ^{238}Pu aerosol. Because the worker was treated with DTPA 3 h after exposure, the model was modified to account for the increased urinary excretion as follows. Excluding the ^{238}Pu excreted during the first day after exposure, the remainder of the DTPA-influenced urinary excretion was modeled by multiplying the value of the blood/urine transfer coefficient by 50, then decaying that modified value with a half time of 14 days [this is equivalent to expressing the blood/urine transfer function as $a(50e^{-bt} + 1)$, where a is the original blood/urine transfer constant, and b = ln(2)/14 days]. This approach to modeling the influence of DTPA on urinary excretion of Pu was based on the data of Hall, R. M. *et al.* (*Health Phys. 34*: 419, 1978) and the summarized cases in Volf, V. (IAEA Tech. Rpt. No. 184, 1978) in which workers exposed to Pu via wounds or inhalation were treated with discrete intravenous injections of DTPA.

The fitted curve derived from the model simulations is shown in Figure 2 overlaying the urinary excretion data. The model predictions suggest that the deposited particle size was 1.0 μm AMAD, the solubility rate

constant was 2 x 10^{-7} g cm^{-2} d^{-1}, the initial lung burden was 140 Bq, and the intake was 560 Bq. The dissolution rate constant is approximately equivalent to that expected from a class D solubility for Pu. Because of the lack of information on chemical form, it cannot be ascertained whether the observed high *in vivo* solubility was due to an intrinsically soluble form such as a nitrate, or due to long-term aging of a stored $^{238}PuO_2$ powder.

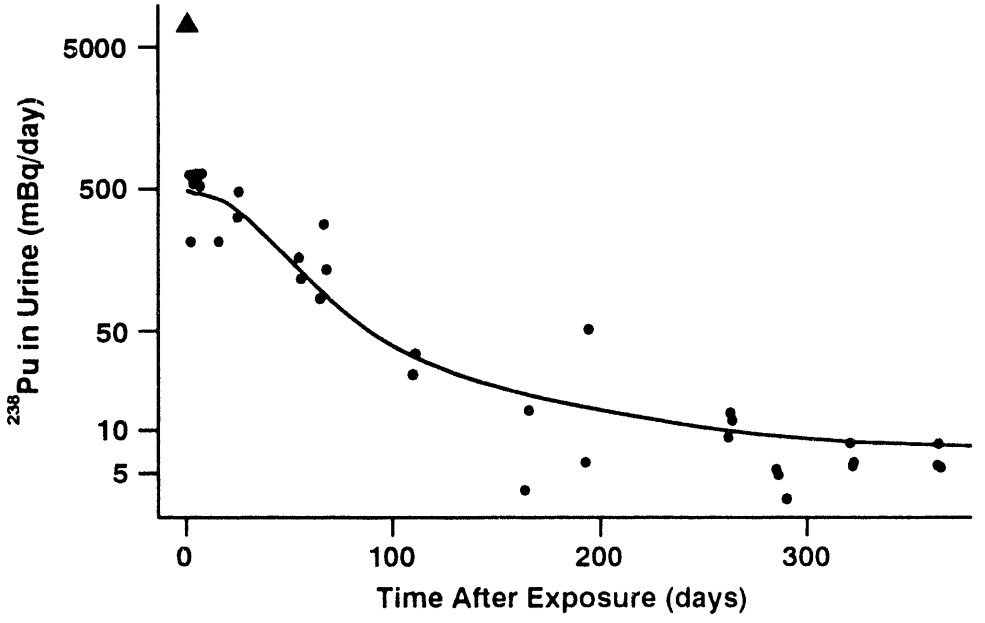

Figure 2. Urinary excretion of ^{238}Pu in a female worker exposed at Facility 2. The triangle represents the first day's excretion following a single DTPA injection; this data point was not included in the modeling. The solid curve is the result of the model simulation.

The urinary excretion patterns of the exposure cases from the two facilities described here were dissimilar. All seven cases from Facility 1 showed similar patterns suggesting that each worker inhaled an aerosol of similar *in vivo* solubility, and that the excretion patterns were similar to those seen in previous animal studies. The pattern for the exposure occurring in Facility 2 was better described by the traditional monotonically decreasing functions, albeit with a curve shape differing from the class D, W, or Y shapes. The differences in urinary excretion patterns in large part must be attributed to differences in *in vivo* solubility. Beyond that, however, it is not possible to determine whether these differences were due to differences in particle size or shape, chemical form, or intrinsic solubility. In general, such data are not available after accidents, but their value in retrospective dose assessment cannot be overemphasized.

The ability of the ITRI Pu model to describe the different urinary excretion patterns seen in the above exposure cases is confirmed by the two cases described above and reinforces the use of data from animal studies. However, the success of the model was not surprising, as the more complex mathematical structure needed to model the Diel/Mewhinney (1983) fragmentation mechanism provides a flexibility in manipulating the urinary excretion curve shapes beyond that possible with the current regulatory models. On the other hand, the modeling flexibility makes it more difficult to obtain unique sets of best-fit parameters, as several of the variables are highly correlated. For example, according to Mercer's dissolution theory, particle diameter and specific solubility are linearly but inversely related, and proportionate changes in either variable will produce the same changes in the urinary curve shape. Thus, lacking information on both will make the estimate of the intake more uncertain, as this quantity depends strongly on particle size. It is therefore incumbent on the health protection professional to be prepared to obtain as much physical and chemical characterization of the exposure material as possible, either prospectively by sampling known source materials, or by capturing the materials as soon after an accident as possible.

(Research sponsored by the Office of Health and Environmental Research, U.S. Department of Energy under Contract No. DE-AC04-76EV01013.)

NEW TOOLS FOR EVALUATING RESPIRATORY TRACT INTAKE OF ALPHA-EMITTING PARTICLES

B. R. Scott, M. D. Hoover, and G. J. Newton

The Department of Energy owns numerous facilities where workers routinely handle plutonium. Our research deals mainly with obtaining improved tools for evaluating possible respiratory tract intake by workers of high-specific-activity, alpha-emitting (HSA_α) and low-specific-activity, alpha-emitting (LSA_α) particles. Our reference for distinguishing between HSA_α and LSA_α particles is ^{239}Pu. Alpha-emitting particles with specific activity greater than that for ^{239}Pu represent HSA_α particles. Particles with specific activity not exceeding that for ^{239}Pu represent LSA_α particles.

The annual limit on intake (ALI) of a radionuclide (a secondary limit) has been used to meet the basic limits for occupational internal exposure to radionuclides. Associated with this limit is the derived air concentration (DAC). Both the ALI and the DAC are based on the implied assumption that when radioactive particles are airborne, they occur in large enough numbers that each tidal volume (TV) of air presented to a worker for inspiration likely contains radioactive particles of the type of interest. However, this assumption is not valid when the average concentration of radioactive particles of interest in the air is very much less than one particle per m^3, as can occur for air concentrations at, and above, the DAC when HSA_α particles are airborne. For a short-term stay in the work area with airborne HSA_α particles in such circumstances, use of DAC-h as a measure of exposure can be considerably biased toward overestimating the exposure.

Here we provide new, generic mathematical tools to facilitate calculating expected respiratory tract intake of HSA_α, and LSA_α particles. Our approach to evaluating the respiratory tract intake of particle-associated radioactivity includes the probability of particle inspiration (P_I), particle respiratory tract deposition probability (P_{Dep}), mechanical protection provided by a respirator, and other factors. Results acquired could be used to obtain adjusted DACs for HSA_α particles.

For very low concentrations of airborne radioactive particles, the number of these particles in TV of air presented to a worker for inspiration is likely to represent a Poisson random variable (i.e., have a Poisson distribution). Assuming a Poisson distribution of the radioactive particles of interest in TV of air presented for inspiration, we are providing new mathematical tools for evaluating their deposition in the respiratory tract. One tool, the particle *availability*, P_A, represents the probability that one or more of the radioactive particles of interest are contained in a TV of air presented for inspiration. A second mathematical tool is particle *unavailability*, $P_U = 1 - P_A$, which represents the probability that no particle is contained in a TV of air presented for inspiration. P_U is related to the average number ν of radioactive particles of interest per TV of air through $P_U = \exp[-\nu]$. The variable ν depends on the pattern of release of radioactive material from the source, particle size distribution, airflow patterns for the work environment, and on other covariates that include time after release of radioactive material from the source.

A third tool is the *attributable intake*, AI_i, of radioactivity in inhaled particles, specified for different particle-size groups. For particles of interest in the ith aerodynamic size group, AI_i is defined as the fraction of the total respiratory tract intake of radioactivity arising from airborne particles with aerodynamic diameters in the ith size group. The function AI_i depends on the exposure time and on the particle-size-group specific values for P_U, P_I, P_{Dep}, and the respirator particle-removal efficiency (when a respirator is used). A discussion of the equation for AI_i is beyond the scope of this report.

A fourth tool is the particle *relative specific activity*, S_r, a dimensionless factor that represents the specific activity of the radioactive particle divided by the specific activity of a reference particle. For PuO_2 particles, we selected $^{239}PuO_2$, with a specific activity of 2.26×10^9 Bq/g, as a reference. Particles of $^{239}PuO_2$ will therefore have a value for S_r of $(2.26 \times 10^9$ Bq/g$)/(2.26 \times 10^9$ Bq/g) or $S_r = 1$. For $^{238}PuO_2$, $S_r = 280$. Activity (A) of spherical PuO_2 particles can be evaluated as a function of S_r, aerodynamic diameter d_{ae} (in micrometers), and density ρ (g/cm^3) using

$$A \text{ (in Bq)} = k(\pi/6)\rho_o S_r d_{ae}^{\ 3}/(\rho/\rho_o)^{1/2} ,$$

where ρ_o represents unit density (i.e., 1 g/cm^3). The constant k equals (2.26 x 10^9 Bq/g) x (10^{-12} cm^3/μm^3) or 2.26 x 10^{-3} when particle density is in g/cm^3. Multiplying k by (π/6) and setting ρ_o = 1 (in g/cm^3), leads to the equation

$$A \text{ (in Bq)} = 1.183 \times 10^{-3} S_r d_{ae}^{\ 3}/\rho^{1/2} .$$

The Poisson variable v representing the average number of particles per TV was calculated as

$$v = DAC/(770A) ,$$

where the DAC is in Bq/m^3, and the constant 770 is the number of 1300 mL TV in 1 m^3 of air.

Calculated values for P_U for a 1300 mL TV of air, evaluated at the unadjusted DAC, are provided in Figure 1 for monodisperse spherical LSA_α ($^{244}PuO_2$, $^{242}PuO_2$, and $^{239}PuO_2$) and HSA_α ($^{238}PuO_2$, $^{240}PuO_2$, and $^{236}PuO_2$) particles as a function of the equivalent aerodynamic diameter. A density of 7 g/cm^3 was assumed. The indicated particles are arranged according to increasing S_r (see Table 1) with the $^{236}PuO_2$ particles having the highest value. At the unadjusted DAC, these particles are essentially unavailable for inspiration for particle sizes greater than 1 μm aerodynamic diameter. The ICRP intake limitation system is based on the implied assumption that P_U = 0. These results suggest that some adjustments to DACs for HSA_α particles could be made to account for particle availability (unavailability). Without such an adjustment, the calculated intake of HSA_α particles could be considerably overestimated.

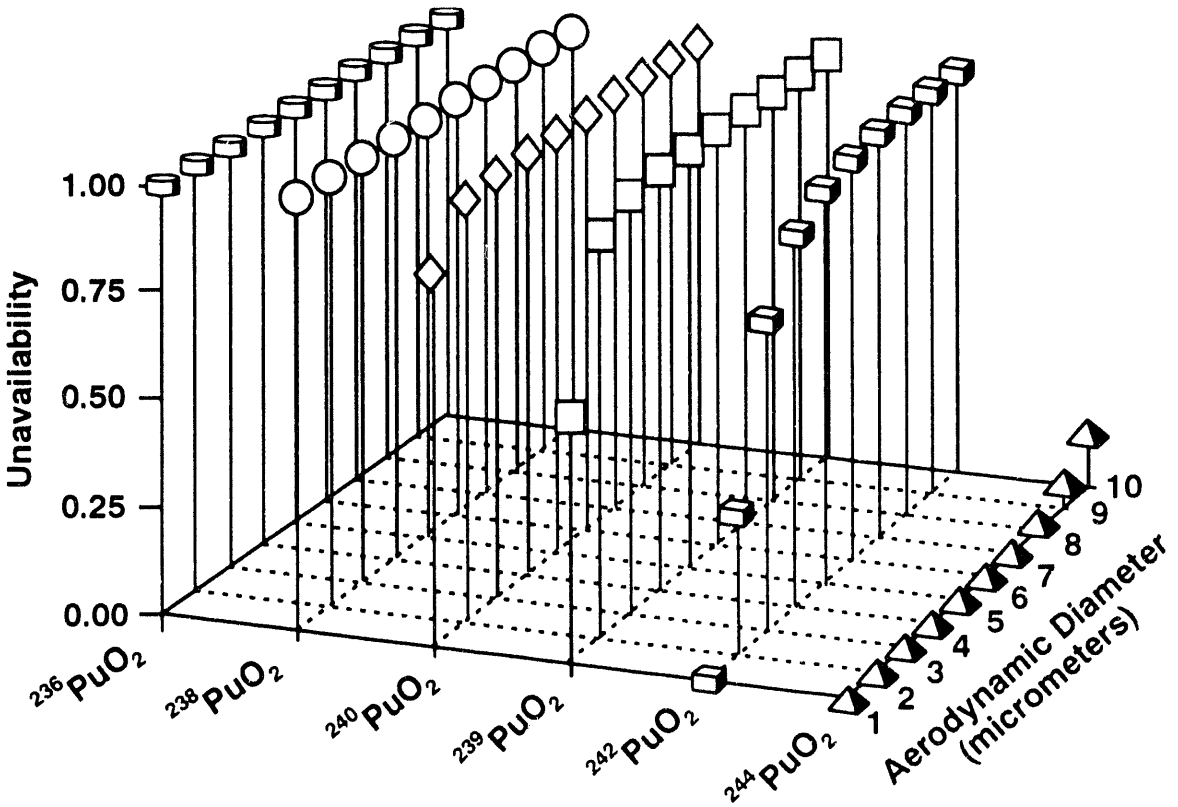

Figure 1. Vertical axis represents the probability (P_U) that no particle of PuO_2 of a specific type is contained in a tidal volume of air when the air activity concentration is 1 DAC (unadjusted). Results are presented for six different types of PuO_2 particles. The ICRP intake-limitation system is based on P_U = 0.

Table 1

Activity Intake Overestimation Factor for Monodisperse (1 μm) PuO_2 Particles Evaluated at Their Derived Air Concentration (DAC)

Type of Particle	Specific Activity Class	Relative Specific Activity[a]	DAC[b] (Bq/m^3)	P_A	Intake Over-estimation Factor[c]
$^{244}PuO_2$	LSA_α	2.9×10^{-4}	0.2	1.0	1.0
$^{242}PuO_2$	LSA_α	6.4×10^{-2}	0.2	1.0	1.0
$^{239}PuO_2$	LSA_α	1.0	0.2	0.44	2.3
$^{240}PuO_2$	HSA_α	3.7	0.2	0.15	6.7
$^{238}PuO_2$	HSA_α	2.8×10^{2}	0.3	0.003	300
$^{236}PuO_2$	HSA_α	8.5×10^{3}	0.6	0.0002	5000

[a]Specific activity divided by that for $^{239}PuO_2$.
[b]Unadjusted DAC.
[c]Applies to number of particles or total radioactivity because the particles are monodisperse.

The International Commission on Radiological Protection (ICRP) intake-limitation system for radionuclides, as applied to the respiratory tract, is based on assuming a polydisperse, particle-size distribution with an activity median aerodynamic diameter of 1 μm. When the actual particle-size distribution differs from that for which the ICRP intake limitation system is based, bias in calculated intake can arise. Although a method is being developed for evaluating this bias for polydisperse aerosols, the results are too preliminary to present here. However, some insights can be gained from calculations of particle intake overestimation when the particle size is monodisperse. A measure of particle intake overestimation (or radioactivity intake overestimation for a monodisperse particle size) is the *intake overestimation factor (IOF)* evaluated as $1/P_A$. Values for IOF were calculated for monodisperse PuO_2 particles with an aerodynamic diameter of 1 μm with the air activity concentration constrained to equal the unadjusted DAC for the same radionuclides considered in Figure 1. The results presented in Table 1 indicate that radioactivity intake could be considerably overestimated for $^{238}PuO_2$ when airborne particles have aerodynamic diameters on the order of 1 μm and larger, and particle availability is not accounted for. Similar conclusions apply to $^{236}PuO_2$; however, ^{236}Pu is seldom used in the workplace.

The problem of radioactive particle intake overestimation can arise for workers in the U.S. nuclear power industry where airborne hot β/γ particles may arise. Here, a hot β/γ particle refers to any particle with activity greater than or equal to 3.7 kBq (0.1 μCi) that emits β and/or γ radiations (National Council on Radiation Protection and Measurements, NCRP Report No. 106, 1989). Although hot β/γ particles are sometimes found on surfaces and on clothing of U.S. nuclear industry workers, airborne hot β/γ particles are extremely rare. Air concentrations of these hot β/γ particles are therefore likely to be very much less than 1 particle per m^3. Thus, particle availability should be considered when calculating respiratory tract intake of these particles by workers.

The results presented suggest that the current ICRP exposure-limitation system associated DAC may be overly conservative for HSA_α particles. We recommend that the DACs for HSA_α particles be adjusted to account for particle availability when appropriate. We also recommend that they be adjusted for the actual particle size distribution when possible. Some new research is needed to determine how best to carry out the recommended adjustments. When calculating the respiratory tract intake of hot β/γ particles by nuclear industry workers, it is also recommended that P_A be accounted for.

(Research sponsored by the Office of Health Physics and Industrial Hygiene Programs of the U.S. Department of Energy, under Contract No. DE-AC04-76EV01013.)

RISK OF LUNG CANCER MORTALITY AFTER INHALING BETA-GAMMA- OR ALPHA-EMITTING RADIONUCLIDES

B. R. Scott, M. E. Mueller, and B. B. Boecker*

The purpose of this project was to obtain risk estimates for lung cancer mortality for chronic internal exposure of humans to low-LET (linear energy transfer) beta and/or gamma (β/γ) or high-LET alpha (α) radiations arising from inhaled radioactive particles. The results presented here apply to single-exponential, decaying, dose-rate patterns. Two risk projection models were used: (1) the relative risk model (for central and upper bound estimates) and (2) the absolute risk model (for lower bound estimates) (Nuclear Regulatory Commission, NUREG/CR-4214, Rev. 1, Addendum 1, LMF-132, Washington, DC, 1991; Nuclear Regulatory Commission, NUREG/CR-4214, Rev. 1, Addendum 2, LMF-136, Washington, DC, 1993). Results of central risk evaluations, based on a relative risk model, are the focus of this report. Two benefits of using the relative risk model are (1) the ease of prospective risk evaluation (e.g., from the present to the end of the life span) and (2) the ease of transporting risk across populations (e.g., from the Japanese to Americans).

For central risk estimation, an age-dependent relative risk model was used to estimate lifetime risk for lung cancer mortality. With this model, the excess relative risk was 0.6 x RBE, per Gy, for persons under age 20 and 0.3 x RBE, per Gy, for persons 20 and older, where RBE represents relative biological effectiveness. Also, it was assumed that no risk was incurred before a latent period of 10 yr or a minimum age of 40. For β/γ and α irradiations, RBEs of 1 and 20 were used, respectively. Low-LET radiation exposures with different exponentially decaying patterns were simulated to obtain estimates of lifetime risk of lung cancer mortality as a function of age at initial exposure.

Excess relative risk coefficients for low-LET irradiations were based on Japanese survivors of the atomic bombs. A dose rate effectiveness factor of 2 was used to extrapolate from high dose rates to dose rates less than 0.1 Gy per h (International Commission on Radiological Protection. *Ann. ICRP 21*: 1, 1991). Different age groups (birth to 89 yr) were studied to compare the lifetime risk among ages at initial exposure groups. Results of animal studies (Hahn, F. F. *et al.* In *IRPA8, International Radiation Protection Association*, Vol. 1, p. 916, 1992) and our modeling results obtained for persons initially exposed as young adults (age 20 yr) were compared. Because the dose rate pattern could influence the estimated risk, different exponentially decaying dose rate patterns were generated to investigate their significance. Computer simulations were carried out using SAS software (*SAS User's Guide: Statistics, Version 5 Edition*, SAS Institute Inc., Cary, NC, 1985).

Figure 1 shows age-specific mortality rate data used in our relative risk evaluations. The points on the curve are actual data based on the 1978 Vital Statistics for the U.S. Population (*National Center for Health Statistics: 1978 Vital Statistics of the United States, Vol. II*, Public Health Service, DHHS Pub. No. [PHS] 81-1104, Hyattsville, MD, 1981). An empirical model was fitted to the points and is represented by the smooth curve. Our calculations compensated for competing risks using the U.S. Decennial Life Tables for 1979-1981 (*National Center for Health Statistics, Vol. I, No. 1, United States Life Tables*, Public Health Services, DHHS Pub. No. [PHS] 85-1150, Washington, DC, 1985).

Modeling results shown in Figure 2 indicate that the low-LET risk for lung cancer mortality should change with time after initial exposure, and the lifetime risk should depend strongly on age at initial exposure when insoluble β/γ-emitting particles are deposited in the lung via inhalation. The calculated lifetime risk decreased as the age at initial exposure increased. These results were obtained using an effective retention half time ($T_{1/2}$) of 500 days for insoluble β/γ-emitting particles in the lung and a potential infinite dose (i.e., cumulative dose evaluated over a very long time period) of 1 Gy. When the dose was varied, an approximately linear dose-response curve was obtained for doses less than 1 Gy.

---

*Department of Energy/Associated Western Universities Teacher Research Associates Program (TRAC) Participant

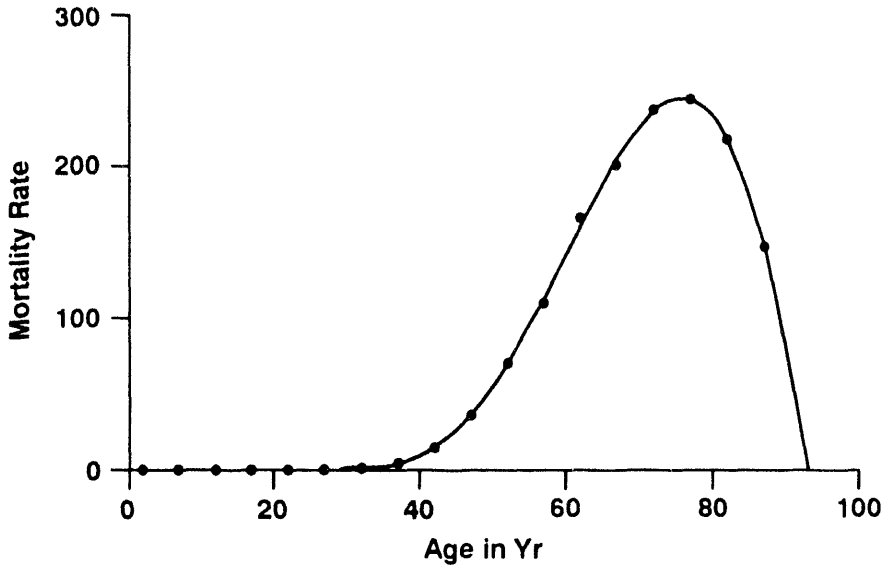

Figure 1. Age-specific mortality rate for U.S. population (deaths per 100,000 per yr).

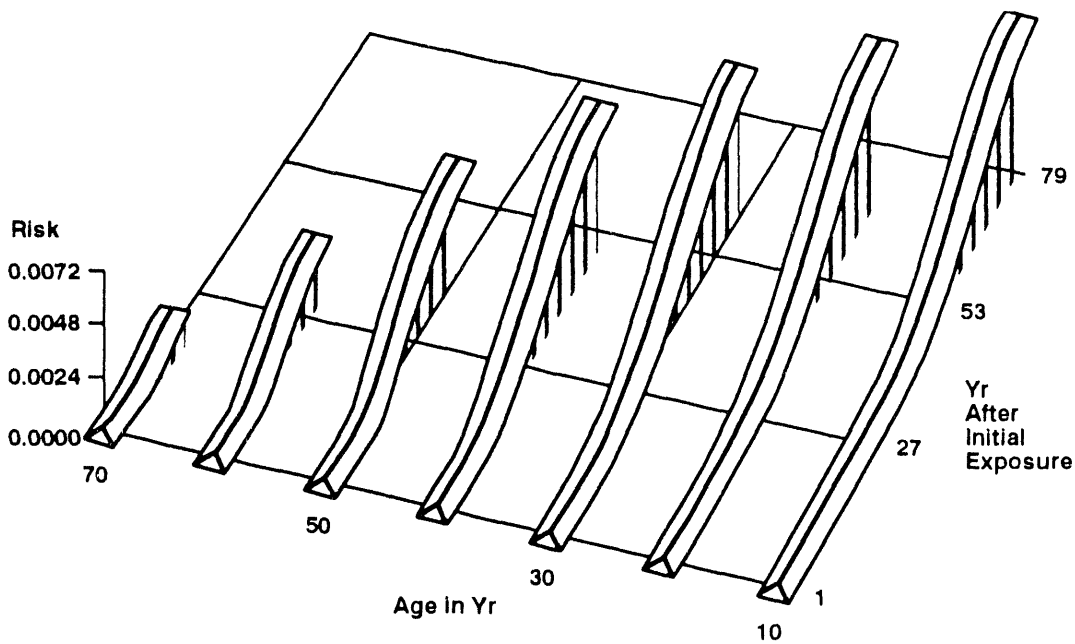

Figure 2. Model simulated risk of lung cancer mortality as a function of age at initial exposure and time after initial exposure, for an exponentially decaying pattern of β/γ irradiation with $T_{1/2}$ = 500 days. Deaths from competing risks were included in simulation.

The results of the comparisons between different dose rate patterns showed that for $T_{1/2}$ less than 1000 days, essentially the same risk coefficient was obtained. This means that for exposure at low dose rates, $T_{1/2}$ should not be an important factor for retention half times commonly used in risk assessment.

For exposure as a young adult to exponentially decaying dose rate patterns, the average risk per Gy for low-LET β/γ radiation was calculated to be 0.007/Gy, and for high-LET α radiation, it was calculated to be 0.14/Gy, for $T_{1/2}$ less than 1000 days. The low-LET estimate, 0.007/Gy, is almost identical to the estimate of 0.0065/Gy

(for usually fatal carcinomas) derived from studies with Beagle dogs (Hahn *et al.*, 1992). The high-LET estimate, 0.14/Gy, is smaller by a factor of 1.6 than the estimate of 0.23/Gy (carcinoma incidence) derived from the dog studies (Hahn *et al.*, 1992). This larger difference for high-LET radiation appears to be mainly related to uncertainty in the RBE for α radiation. We made the usual assumption that the RBE was 20. However, an RBE of 0.23/0.0065 = 35 is indicated by the dog data used. Using an RBE of 35 instead of 20 for α radiation, our risk coefficient would be 0.25/Gy in good agreement with the estimate of 0.23/Gy derived for inducing usually fatal lung carcinomas in dogs.

While central risk estimates for lung cancer mortality were presented for low-LET β/γ and high-LET α radiations separately, to obtain central risk estimates for combined exposure to β/γ and α radiations, simply add the low- and high-LET risk estimates (NRC, 1993). Subjective upper and lower bounds on risk for the combined exposure can be used to account for uncertainties (NRC, 1991, 1993).

In conclusion, our modeling results indicate the following for the lifetime risk of radiation-induced lung cancer mortality, for low dose rates, and for total doses less than 1 Gy: (1) the risk should be approximately a linear function of dose; (2) the risk should decrease as age at initial exposure increases; and (3) the risk should be independent of $T_{1/2}$ for $T_{1/2} < 1000$ days.

(Research sponsored by the Assistant Secretary for Defense Programs, U.S. Department of Energy, under Contract No. DE-AC04-76EV01013.)

IX. APPENDICES

APPENDIX A

STATUS OF LONGEVITY AND SACRIFICE EXPERIMENTS IN BEAGLE DOGS

Each annual report of the Inhalation Toxicology Research Institute from LF-38, 1967, through LMF-121, 1987-1988 included an appendix containing detailed tabular information on all dogs in the life-span studies of inhaled radionuclides and many sacrifices series associated with these studies. In LMF-121, similar kinds of summary tables were also included for dogs in long-term and life-span studies of injected actinides that were conducted at the University of Utah. All dogs remaining alive in the Utah studies were transferred to ITRI on September 15, 1987, where they are being maintained and studied for the remainder of their life spans. Responsibility for managing the completion of the Utah life-span studies has been assigned to ITRI. A small team of investigators at the University of Utah and investigators at ITRI are working together to complete the observations and summaries.

Along with other changes made in the regular ITRI Annual Report beginning with Report LMF-126, *Inhalation Toxicology Research Institute Annual Report, 1988-1989*, it was decided that the growing body of detailed information on these studies in dogs would no longer be included. Instead, separate periodic reports are being prepared that contain specific updated information on all ITRI and University of Utah long-term and life-span studies in Beagle dogs. The first three of these reports, entitled *Annual Report on Long-Term Dose-Response Studies of Inhaled or Injected Radionuclides* have been published for 1988-1989 as Report LMF-128, for 1989-1990 as Report LMF-130, and for 1990-91 as Report LMF-135. They describe the studies, updated experimental design charts, survival plots, pathology summaries and detailed tabular information on all dogs in a manner consistent with past practices. A similar report for the 1991-1993 period is now in preparation.

Recognizing that these data are of interest to a limited number of individuals, these reports are provided without charge to individuals requesting them. To obtain these reports, please send a request to:

Director
Inhalation Toxicology Research Institute
P. O. Box 5890
Albuquerque, NM 87185

LOVELACE BIOMEDICAL AND ENVIRONMENTAL RESEARCH INSTITUTE
Directors and Officers

R. O. McClellan, DVM, Chairman
D. J. Ottensmeyer, MD, Vice Chairman
J. L. Mauderly, DVM, President
R. K. Jones, MD, Vice President
B. B. Boecker, PhD, Asst. Secretary/Treasurer (non-director)
C. H. Hobbs, DVM, Asst. Secretary/Treasurer (non-director)
J. F. Lechner, PhD, Asst. Secretary/Treasurer (non-director)

J. P. Bundrant
N. Corzine
J. Doull, MD
B. D. Goldstein, MD
W. A. Gross, PhD
D. E. Kilgore, MD
J. Lovelace-Johnson
D. P. Pasternak, MD
M. W. Twiest, MD
A. C. Upton, MD

INHALATION TOXICOLOGY RESEARCH INSTITUTE
J. L. Mauderly, DVM, Director
R. K. Jones, MD, Associate Director
B. B. Boecker, PhD, Assistant Director
C. H. Hobbs, DVM, Assistant Director
J. F. Lechner, PhD, Assistant Director
D. E. Bice, PhD, Educational Coordinator

Scientific Groups

- Aerosol Science
  H. C. Yeh, PhD
- Chemistry and Biochemical Toxicology
  R. F. Henderson, PhD
- Molecular and Cellular Toxicology
  N. F. Johnson, PhD
- Pathology
  F. F. Hahn, DVM, PhD
- Pathophysiology
  J. M. Benson, PhD

Scientific Programs

- Aerosols
  Y. S. Cheng, PhD
- Applied Toxicology
  C. H. Hobbs, DVM
- Cancer Mechanisms
  J. F. Lechner, PhD
- Chemical Toxicology
  A. R. Dahl, PhD
- Pathogenesis
  J. R. Harkema, DVM, PhD
- Radiation Toxicology
  R. A. Guilmette, PhD

Research Support Sections and Units

- Analytical Chemistry
  W. E. Bechtold
- Animal Care
  D. G. Burt, DVM
- Biochemical Toxicology
  R. F. Henderson, PhD
- Biomathematics
  B. B. Boecker, PhD
- Chemistry
  A. R. Dahl, PhD
- Chronic Studies
  J. M. Benson, PhD
- Clinic
  B. A. Muggenburg, DVM, PhD
- Clinical Pathology
  F. F. Hahn, DVM, PhD
- Exposure
  E. B. Barr, MSEE
- Histopathology
  R. A. Smith
- Necropsy
  J. Hogan, BA

Administrative Support Units

- Computer
  J. H. Diel, PhD
- Engineering and Facilities
  J. A. Lopez, BSChE
- Financial Management
  K. M. Aragon, MBA
- Health Protection
  J. J. Thompson, PhD
- Human Resources
  B. K. Solari, BA
- Library
  S. E. Spurlock, MLS, MIS
- Procurement
  G. A. Allen
- Property Management
  P. F. Kaplan
- Quality Assurance
  D. L. Harris, MS
- Technical Communications
  P. L. Bradley, MA

INHALATION TOXICOLOGY RESEARCH INSTITUTE
Organizational Structure

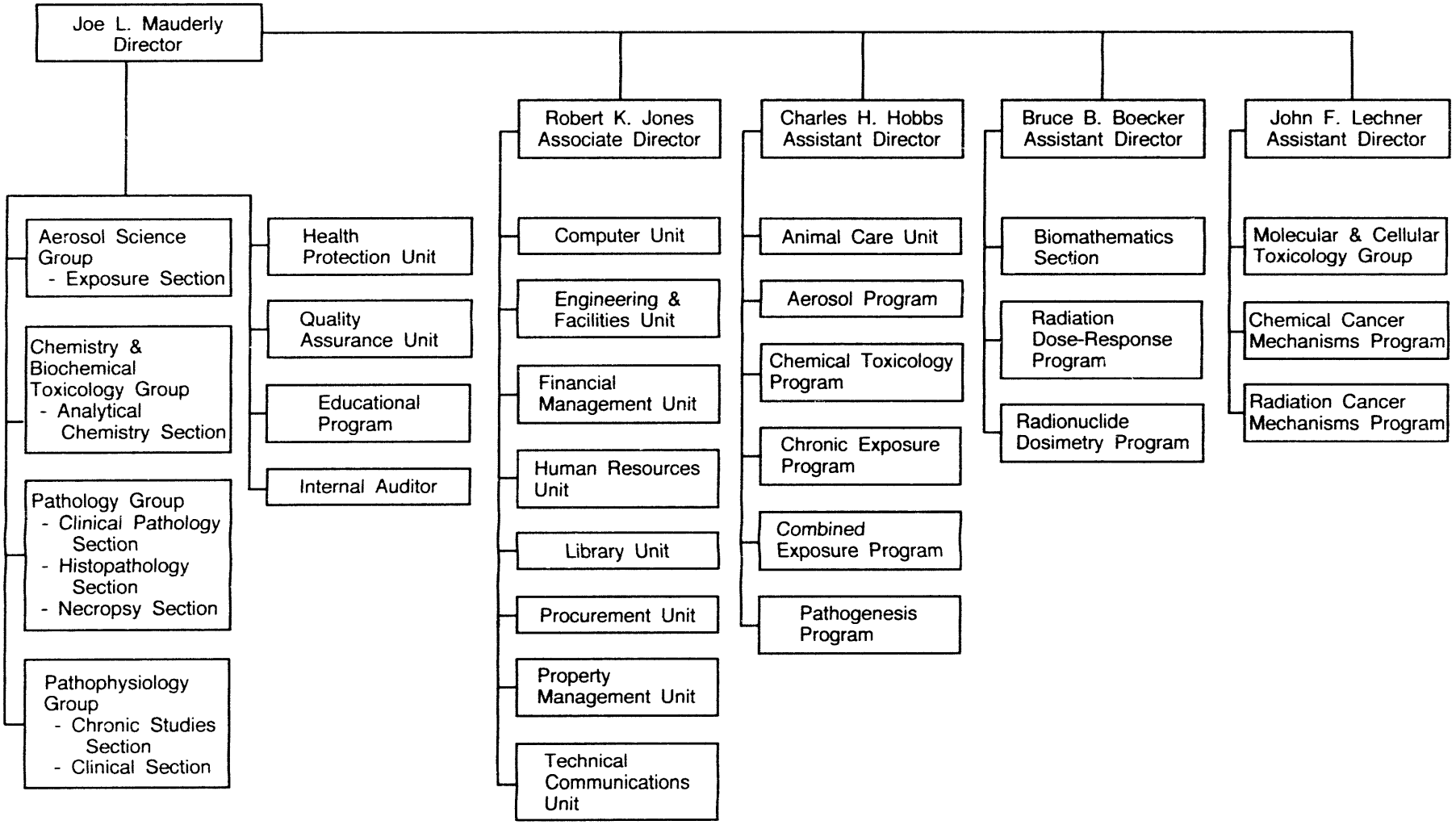

ADMINISTRATIVE SUPPORT

E. C. Bankey, MBA	Internal Auditor
L. L. Burton	Executive Secretary
M. G. Campos	Clerical Specialist
M. B. Morgan	Administrative Associate

AEROSOL SCIENCE GROUP

H. C. Yeh, PhD	Supervisor/Aerosol Scientist
B. T. Chen, PhD	Aerosol Scientist
Y. S. Cheng, PhD	Aerosol Scientist
G. A. Feather, BS	Research Technologist
A. F. Fencl, BS	Research Technologist
T. D. Holmes, BS	Sr. Research Technologist
M. D. Hoover, PhD	Aerosol Scientist
M. Marcinkovich	Research Technologist
M. M. Murphy, BS	Research Technologist
G. J. Newton, BS	Aerosol Scientist
K. D. Rohrbacher, BS*	Graduate Participant
S. M. Smith, BS	Graduate Participant
J. A. Stephens	Sr. Research Technologist
D. Yazzie	Research Technologist

Exposure Section

E. B. Barr, MSEE	Supervisor/Aerosol Scientist
R. D. Brodbeck	Technical Specialist
S. N. Lucas	Laboratory Technician
H. A. Sanchez	Laboratory Technician
R. K. White, BS	Technical Specialist
K. L. Williamson	Laboratory Technician
T. L. Zimmerman	Research Technologist

BIOMATHEMATICS SECTION

B. B. Boecker, PhD	Assistant Director
I. Y. Chang, MS	Biostatistician
W. C. Griffith, Jr., BS	Biomathematician
C. L. Sanders, PhD	Radiobiologist
B. R. Scott, PhD	Biophysicist

*Part-time employee.

CHEMISTRY AND BIOCHEMICAL TOXICOLOGY GROUP

R. F. Henderson, PhD	Supervisor/Toxicologist
M. L. Allen	Research Technologist
W. E. Bechtold, PhD	Chemist
L. K. Brookins, BS	Sr. Research Technologist
A. R. Dahl, PhD	Toxicologist
L. B. Galloway, BS	Research Technologist
P. M. Gerde, PhD*	Chemical Engineer
D. A. Kracko, BS	Research Technologist
M. R. Strunk, BA	Research Technologist
J. R. Thornton-Manning, PhD	Toxicologist
J. J. Waide, MS	Sr. Research Technologist

Analytical Chemistry Section

W. E. Bechtold, PhD	Supervisor/Chemist
K. R. Ahlert	Technical Specialist
L. I. Archuleta	Laboratory Technician
D. M. Sugino	Laboratory Technician

MOLECULAR AND CELLULAR TOXICOLOGY GROUP

N. F. Johnson, PhD	Supervisor/Exptl. Pathologist
S. A. Belinsky, PhD	Molecular Biologist
T. R. Carpenter, DVM	Graduate Participant
C. A. Carter, PhD	Cell Biologist
X. P. Galarza, BS	Research Technologist
A. W. Hickman, Jr., MS	Graduate Participant
R. J. Jaramillo, BS	Sr. Research Technologist
G. Kelly, PhD	Molecular Biologist
C. H. Kennedy, PhD	Molecular Toxicologist
D. M. Klinge, BS	Sr. Research Technologist
J. L. Lane, BS	Research Technologist
F. T. Lauer	Research Technologist
A. D. Magallanez, BS	Research Technologist
S. K. Middleton, BS	Research Technologist
C. E. Mitchell, PhD	Molecular Biologist
W. L. Pabich, BA	Research Technologist
M. M. Padilla	Research Technologist
W. A. Palmisano, PhD	Postdoctoral Participant
D. S. Swafford, BS	Graduate Participant
L. A. Tierney, DVM	Graduate Participant

PATHOLOGY GROUP

F. F. Hahn, DVM, PhD	Supervisor/Exptl. Pathologist
D. H. Aguilar	Clerical Specialist
D. E. Bice, PhD	Immunologist
C. J. Bresee, BS	Research Technologist
P. Y. Cossey, BS	Sr. Research Technologist
K. M. Garcia, BA	Sr. Research Technologist
J. R. Harkema, DVM, PhD	Experimental Pathologist
H. J. Harms, BS	Research Technologist
J. A. Hotchkiss, PhD	Cell Biologist
J. L. Lewis, PhD*	Toxicologist
K. J. Nikula, DVM, PhD	Experimental Pathologist
G. G. Scott, BS*	Graduate Participant
A. J. Williams, II, BS	Sr. Research Technologist

Clinical Pathology Section

F. F. Hahn, DVM, PhD	Supervisor/Exptl. Pathologist
D. A. Angerstein, AA	Research Technologist

Histopathology Section

R. A. Smith	Supervisor/Chief Res. Technologist
S. C. Barnett	Research Technologist
R. B. Garlick	Laboratory Technician
Y. N. Knighton	Laboratory Technician

Necropsy Section

J. Hogan, BA	Supervisor/Chief Res. Technologist
K. Avila, BS	Laboratory Technician-Trainee
B. Pacheco	Laboratory Technician-Trainee
J. L. Pitcher	Laboratory Technician
P. R. Romero-Stagg	Laboratory Technician

*Part-time employee.

PATHOPHYSIOLOGY GROUP

J. M. Benson, PhD	Supervisor/Toxicologist
L. F. Blair	Research Technologist
D. C. Esparza, BS	Sr. Research Technologist
G. L. Finch, PhD	Toxicologist
K. G. Gillett, BS	Sr. Research Technologist
R. A. Guilmette, PhD	Radiobiologist
A. M. Holmes	Research Technologist
D. L. Lundgren, PhD	Radiobiologist
E. J. Salas	Research Technologist
M. B. Snipes, PhD	Radiobiologist
B. M. Tibbetts, BA	Research Technologist
C. P. Vigil, BS	Research Technologist

Chronic Studies Section

J. M. Benson, PhD	Supervisor/Toxicologist
C. A. Dison	Research Technologist

Clinical Section

B. A. Muggenburg, DVM, PhD	Supervisor/Physiologist
M. A. Berry, DVM*	Clinical Veterinarian
T. R. Carpenter, DVM	Graduate Participant
M. A. Weinhold, AS	Research Technologist
M. E. Thompson	Laboratory Technician

ANIMAL CARE UNIT

D. G. Burt, DVM	Supervisor/Attending Veterinarian
B. K. Barnes*	Animal Caretaker
S. L. Batson, BS	Chief Animal Technologist
D. M. Bolton	Animal Technician
F. Campbell, Jr.	Animal Technician
D. M. Chavez	Animal Technician
D. T. Cordaro	Sr. Animal Technician
M. O. Crenner*	Animal Caretaker
F. E. Delgado	Animal Technician
J. M. Duran	Sr. Animal Technician
E. Garcia	Animal Technician
L. M. Martinez*	Animal Caretaker
A. D. Murrin	Clerical Specialist
J. L. Portillo-Palmer*	Animal Caretaker
J. Renard	Sr. Animal Technician
C. G. Romero	Animal Technician
P. J. Ryan	Animal Technician
S. Walker	Animal Technician
C. C. Ynostroza, AS	Sr. Animal Technician

COMPUTER UNIT

J. H. Diel, PhD	Supervisor/Computer Scientist
M. F. Conrad, AS	Research Technologist
J. L. Holmes, BS	Software Specialist
R. L. Lucero-Maldonado	Laboratory Technician
E. Taplin, BBA	Software Specialist

*Part-time employee.

ENGINEERING AND FACILITIES UNIT

J. A. Lopez, BChE	Supervisor/Facilities Engineer
E. Anzures	Electrical Maintenance Worker
D. Aragon	Lead Janitor
W. F. Beierman, BSEE	Assistant Facilities Engineer
R. T. Cossey, ASEE	Instrum. & Controls Maint. Worker/Tech. Specialist
F. D. Cox	Machinist, Sr. Research Technologist
J. A. Detmer	Technical Secretary
A. R. Espalin	General Maintenance Worker
D. Griego	Laboratory Assistant
J. C. Hawkins*	Laboratory Assistant
W. J. Jennings	Heating & Refrig. Maintenance Worker
T. A. Knowlton*	Laborer
A. F. Monnin	Sr. Research Technologist
S. J. Moya*	Laboratory Assistant
T. B. Orwat	Technical Specialist
B. D. Romero	Janitor
G. A. Saiz*	Laboratory Assistant
F. R. Torrez	HVAC Mechanic & Central Plant Operator

FINANCIAL MANAGEMENT UNIT

K. M. Aragon, MBA	Supervisor/Budget Officer
M. M. Gurule	Clerical Specialist
A. I. Medrano	Clerical Specialist
P. S. Ohl, BS	Accountant

HEALTH PROTECTION UNIT

J. J. Thompson, PhD	Supervisor/Health Protection Mgr.
A. C. Grace, MS	Environmental Restoration Coordinator
L. C. Haling	Executive Secretary
M. S. Hall, MS	Environmental Specialist
J. R. Lackey	Sr. Research Technologist
J. M. Mauser, MS	Environmental Restoration Engineer
K. L. Moline, AA	Research Technologist
G. R. Moore	Clerical Specialist
C. W. Pohl	Research Technologist
A. A. Powell*	Laboratory Assistant
P. S. Puckett*	Laboratory Assistant
P. E. Sanchez	Clerical Specialist
W. C. Schleyer, III, MS	Health Physicist
T. T. Simpson	Research Technologist

HUMAN RESOURCES UNIT

B. K. Solari, BA	Supervisor/Human Resources Manager
A. F. Baca	Surveillance Worker-Trainee
J. A. Davis, BS	Assistant Human Resources Manager
C. J. Dunsworth*	Clerical Specialist
T. J. Hoskins	Clerical Specialist
J. T. Nunez	Clerical Specialist
P. Padilla	Surveillance Worker
G. J. Quintana	Surveillance Worker-Trainee
R. L. Ripple	Clerical Specialist
I. J. Salinas	Surveillance Worker-Trainee

LIBRARY UNIT

S. E. Spurlock, MLS, MIS	Supervisor/Technical Librarian
C. S. Snidow	Clerical Specialist

PROCUREMENT UNIT

G. A. Allen	Supervisor
V. K. Aragon	Clerical Specialist
L. Vigil	Clerical Specialist

PROPERTY MANAGEMENT UNIT

P. F. Kaplan	Supervisor
A. J. Garcia	Clerical Specialist
K. Perales	Clerical Specialist

QUALITY ASSURANCE UNIT

D. L. Harris, MS	Supervisor/Quality Assurance Officer
T. A. Ahlert, BA	Administrative Specialist

TECHNICAL COMMUNICATIONS UNIT

P. L. Bradley, MA	Supervisor/Technical Editor
C. M. Herrera	Clerical Specialist
S. L. Perez	Clerical Specialist
W. L. Piper, BA	Clerical Specialist
S. F. Randock, BA	Clerical Specialist

*Part-time employee.

TASK FORCE ON LIFE-SPAN RADIATION TOXICITY STUDIES**

B. B. Boecker, PhD	Assistant Director
M. G. Campos	Clerical Specialist
I. Y. Chang, MS	Biostatistician
M. F. Conrad, AS	Research Technologist
J. H. Diel, PhD	Computer Scientist
K. M. Garcia, BA	Sr. Research Technologist
K. G. Gillett, BS	Sr. Research Technologist
W. C. Griffith, Jr., BS	Biomathematician
R. A. Guilmette, PhD	Radiobiologist
F. F. Hahn, DVM, PhD	Experimental Pathologist
B. A. Muggenburg, DVM, PhD	Physiologist
K. J. Nikula, DVM, PhD	Experimental Pathologist
M. B. Snipes, PhD	Radiobiologist

**Individuals have primary assignment in Scientific Groups or Units on preceding pages.

EDUCATIONAL PARTICIPANTS

Name	School/University	ITRI Group/Unit/Section
Department of Energy/Associated Western Universities Summer Student Research Participants		
Catherine J. Bresee	University of CA-Santa Cruz, CA	Molecular & Cellular Toxicology Group
Marie E. Cunniffe	Mount St. Mary's College, CA	Pathology Group
Ned Shane Cutler	The University of Utah, UT	Pathophysiology Group
Sara E. Dempster	Bryn Mawr College, PA	Chemistry & Biochemical Toxicology Group
Vivien Lim	Purdue University, IN	Pathology Group
Eloy E. Martinez	University of New Mexico, NM	Aerosol Science Group
Sandra J. Montano	University of New Mexico, NM	Aerosol Science Group
Marvin Oey	University of New Mexico, NM	Aerosol Science Group
Marcus Shoub	University of Arizona, AZ	Health Protection Unit
Devon J. Zastrow	New Mexico State University, NM	Chemistry & Biochemical Toxicology Group
Department of Energy/Associated Western Universities Teacher Research Associates Program (TRAC) Participants		
Thomas P. Carroll	St. Albans School, DC	Molecular & Cellular Toxicology Group
Donna L. Cassie	Palm Beach County, FL	Pathophysiology Group
Maureen A. Foutz	James A. Shank's High, FL	Chemistry & Biochemical Toxicology Group
Sandra J. Matthews	Eldorado High School, NM	Pathophysiology Group
Margie E. Mueller	Highland High School, NM	Biomathematics Section
Larry W. Rogers	Del Norte High School, NM	Engineering & Facilities Unit
Laurel A. Sachetti	Yorktown High School, NY	Pathology Group
Ying Zhuang	New Mexico Military Institute, NM	Aerosol Science Group
Department of Energy/Associated Western Universities Faculty Participant		
George E. Snow	Mount St. Mary's College, CA	Pathology Group
Department of Energy/Health Physics Fellows		
Michelle Lyn Hart	The Ohio State University, OH	Health Protection Unit
Mark N. Nel	University of Missouri, Columbia, MO	Aerosol Science Group

EDUCATIONAL PARTICIPANTS

Name	School/University	ITRI Group/Unit/Section
Student Employees - Summer 1993		
Laura A. Baca	University of New Mexico	Engineering & Facilities Unit
Brenda K. Barnes	University of New Mexico	Animal Care Unit
Nolan K. Bennett	NM Institute of Mining & Technology	Health Protection Unit
Gilbert Chavez	Occidental College, CA	Engineering & Facilities Unit
Mary O. Crenner	University of New Mexico	Animal Care Unit
Steven R. Figge	University of New Mexico	Animal Care Unit
Adam Gonzales	Colorado State University, CO	Animal Care Unit
Jarod T. Hage	Albuquerque Academy High School	Animal Care Unit
Jonathan C. Hawkins	University of New Mexico	Engineering & Facilities Unit
Felix P. Jiminez	Valley High School	Molecular & Cellular Toxicology Group
Paul P. Jones	Rio Grande High School	Animal Care Unit
Thomas A. Knowlton	University of New Mexico	Engineering & Facilities Unit
Dana M. Korczak	University of New Mexico	Animal Care Unit
Mark D. Manzanares	Valley High School	Library Unit
Leo M. Martinez	University of New Mexico	Animal Care Unit
Salomon J. Moya	University of New Mexico	Engineering & Facilities Unit
Luis Armando Najera	New Mexico State University	Engineering & Facilities Unit
Douglas J. Podzemny	University of New Mexico	Engineering & Facilities Unit
Jennifer L. Portillo-Palmer	University of New Mexico	Animal Care Unit
Adam A. Powell	University of New Mexico	Health Protection Unit
Paul S. Puckett	Albuquerque Technical Vocational Institute	Health Protection Unit
Donna M. Saavedra	University of New Mexico	Quality Assurance Unit
Gregory A. Saiz	University of New Mexico	Engineering & Facilities Unit
Jerold J. Sanchez	New Mexico State University	Health Protection Unit
Maria G. Sanchez	University of New Mexico	Animal Care Unit
John E. Schultz	University of New Mexico	Engineering & Facilities Unit
H. Denise Smith	University of New Mexico	Computer Unit
David J. Stichman	University of New Mexico	Animal Care Unit
Kyle Taylor	New Mexico State University	Health Protection Unit
Robert F. Valdez	University of New Mexico	Animal Care Unit
Brian S. Winkenweder	University of New Mexico	Pathophysiology Group

UNM/ITRI Inhalation Toxicology Graduate Students

Thomas R. Carpenter, DVM
Jennifer L. Francis
Albert W. Hickman, Jr.
Carlo M. Padilla
Kevin D. Rohrbacher
Gary G. Scott
Shawna M. Smith
Nicole D. Stephens
Deborah S. Swafford
Lauren A. Tierney, DVM

Postdoctoral Fellows

Courtney Nickell, PhD
William A. Palmisano, PhD

PROGRAM AND PROJECT TITLES	SPONSOR*	COORDINATOR
BRUCE B. BOECKER, ASSISTANT DIRECTOR		
Radiation Toxicology - R. A. Guilmette, Program Manager		
Effective Dose from Inhaled Nuclear Energy Materials	DOE/OHER	R. A. Guilmette
Dose-Response Relationships for Inhaled Radionuclides	DOE/OHER	B. A. Muggenburg
Radiation Dose and Injury to Critical Cells from Radon	DOE/OHER	N. F. Johnson
Deposition of Radon and Radon Progeny in the Respiratory Tract	DOE/OHER	H. C. Yeh
Toxicity of Injected Radionuclides - ITRI Effort	DOE/OHER	B. B. Boecker
Toxicity of Injected Radionuclides - Utah Effort	DOE/OHER	S. C. Miller
Health Effect Model for Reactor Accidents	NRC	B. B. Boecker
INSRP/BEES Panel	BNL	M. D. Hoover
Internal Dosimetry	WSRC	R. A. Guilmette
CHARLES H. HOBBS, ASSISTANT DIRECTOR		
Aerosols - Y. S. Cheng, Program Manager		
Biologically Relevant Properties of Energy Related Aerosols	DOE/OHER	H. C. Yeh
Dynamics of Radon Daughter Interactions with Indoor Aerosols	DOE/PHYS	Y. S. Cheng
Underground Aerosol Characterization at the WIPP Site	DOE/AL	G. J. Newton
Y-12 Radiological Protection Program	DOE/Y-12	M. D. Hoover
HQ Continuous Air Monitor Study	DOE/HQ	M. D. Hoover
Inhalation Hazards for Uranium Mill Tailings	DOE/UMTRAP	G. J. Newton
Characterization of Aerosols Produced by Surgical Procedures	NIOSH	H. C. Yeh
Evaluation of Respirators - II for Asbestos Fibers	NIOSH	Y. S. Cheng
Experimental Tests on Continuous Air Monitors	EG&G	M. D. Hoover
Idaho Gas Contamination	INEL	G. J. Newton
Plutonium Dispersal Study	SNL	G. J. Newton
Air Sampling Program at SNL Area V	SNL	G. J. Newton
Dissolution of Metal Tritides in Biological Systems	SNL	Y. S. Cheng
Russian Topaz-II Study	SNL	M. D. Hoover
NESHAP Studies	SNL	G. J. Newton
Independent Testing and Evaluation of SRS	DOE/WSRC	M. D. Hoover

PROGRAM AND PROJECT TITLES	SPONSOR*	COORDINATOR
Chemical Toxicology - A. R. Dahl, Program Manager		
Influence of Respiratory Tract Metabolism on Effective Dose	DOE/OHER	A. R. Dahl
Biological Markers of Human Exposure to Organic Compounds	DOE/OHER	W. E. Bechtold
Mechanisms of Granulomatous Disease from Inhaled Beryllium	DOE/OHER	G. L. Finch
Disposition of Inhaled Xenobiotics	NIEHS	R. F. Henderson
Nitrogen Heterocycles: Metabolic Effect and Toxicity	WSU	A. R. Dahl
Metabolism of 1,3-Butadiene, Butadiene Monoepoxide and Butadiene Diepoxide by Human and Mouse Liver and Lung Tissue Homogenates	CMA	R. F. Henderson
Exposure of B6C3F_1 Mice to 1,3-Butadiene	CMA	R. F. Henderson
Fate of Inhaled Vapors in Rats, Dogs, and Monkeys	NIH/NIEHS	A. R. Dahl
Carcinogenicity of Inhalants: A Dosimetric Approach	NIH/NIEHS	A. R. Dahl
Disposition of Inhaled Toxicants in the Olfactory System	NIH/NIDCD	J. L. Lewis
Toxicity of Nickel Compounds to the Respiratory Tract	NiPERA	J. M. Benson
Modeling in the Analysis of Toxic Effects on Complex Mixtures	HEI	W. E. Bechtold
Applied Toxicology - C. H. Hobbs, Program Manager		
Effects of L-Deprenyl on Physiologic Functions	DAHI	B. A. Muggenburg
Treatment of Chronic Prostatic Hypertrophy	IMI	B. A. Muggenburg
Combined Exposure, Plutonium-Cigarette Smoke	DOE/DP	G. L. Finch
Combined Exposure, Plutonium-Beryllium	DOE/DP	G. L. Finch
Combined Exposure, Plutonium-X Ray	DOE/DP	D. L. Lundgren
Combined Exposure, Plutonium-Chemical Carcinogen	DOE/DP	D. L. Lundgren
Combined Exposure, Radiation-Fiber	DOE/DP	D. L. Lundgren
Prechronic and Chronic Studies of Nickel Compounds	NIEHS	J. M. Benson
Chronic Inhalation of Hygroscopic Material in Rats	P&G	J. M. Benson
90-Day Study of Powdered Detergent Constituents Inhaled by F344 Rats	P&G	M. B. Snipes
Effects of Physical/Chemical HMs on Inflammatory and Proliferative Response Induced in the Lung	IPA	R. F. Henderson

PROGRAM AND PROJECT TITLES	SPONSOR*	COORDINATOR
Pathogenesis - J. R. Harkema, Program Manager		
Cellular & Biochemical Mediators of Respiratory Tract Disease	DOE/OHER	R. F. Henderson
Airway Epithelial Injury, Adaptation and Repair	DOE/OHER	J. R. Harkema
Role of Immune Responses in Respiratory Disease	DOE/OHER	D. E. Bice
Evaluation of Pulmonary Immune Responses to Viral Agents	UA	D. E. Bice
Rodent Immunity after Immunization of Nasal Airways	3M Company	D. E. Bice
Respiratory Function Alterations Following Chronic Ozone Inhalation in Rats	HEI	J. R. Harkema
Effect of Chronic Ozone Inhalation on Nasal Mucocilliary Apparatus in Rats	HEI	J. R. Harkema
Effects of Ozone on Airway Mucous Cells	NIH/HL	J. R. Harkema
JOHN F. LECHNER, ASSISTANT DIRECTOR		
Cancer Mechanisms - J. F. Lechner, Program Manager		
Links Between Radiation-Induced Lung Cancer in Laboratory Animals and People	DOE/OHER	F. F. Hahn
Pre-Malignant Events in Radiation-Induced Lung Cancer	DOE/OHER	J. F. Lechner
Lung Cancer in Uranium Miners - Gene Dysfunction	DOE/OHER	J. F. Lechner
Cellular Models of Radiation-Induced Lung Cancer	DOE/OHER	J. F. Lechner
Molecular Mechanisms of Radiation-Induced Cancer	DOE/OHER	G. Kelly
Gene Dysfunction in Chemical Induced Carcinogenicity	DOE/OHER	S. A. Belinsky
Identification of Target Genes Involved in Carbon Black and Diesel Induced Lung Cancer	HEI	S. A. Belinsky

* BNL - Brookhaven National Laboratory
CMA - Chemical Manufacturers Association
DAHI - Deprenyl Animal Health, Inc.
DOE/AL - Department of Energy Operations Office, Albuquerque
DOE/DP - Department of Energy, Defense Programs
DOE/HQ - Department of Energy, Headquarters
DOE/OHER - Department of Energy, Office of Health and Environmental Research
DOE/PHYS - Department of Energy, Physical and Technological Research
DOE/UMTRAP - Department of Energy, Uranium Mill Tailings Remediation Action Program
DOE/Y-12 - Y-12 Plant
EG&G - Rocky Flats Plant
HL - National Heart, Lung and Blood Institutes
HEI - Health Effects Institute
IMI - Indigo Medical, Inc.
INEL - Idaho National Engineering Laboratory
IPA - Institue of Polyacrylic Absorbents
NESHAP - National Emission Standards for Hazardous Air Pollutants
NIDCD - National Institute on Deafness and Communicable Diseases
NIEHS - National Institute of Environmental Health Sciences
NIH - National Institutes of Health
NIOSH - National Institute of Occupational Safety & Health
NiPERA - Nickel Producers Environmental Research Association
NRC - Nuclear Regulatory Commission
P&G - Proctor & Gamble
SNL - Sandia National Laboratories
UA - University of Arizona
WSRC - Westinghouse Savannah River Co.
WSU - Wayne State University

APPENDIX D

PUBLICATION OF TECHNICAL REPORTS

OCTOBER 1, 1992 - SEPTEMBER 30, 1993

LMF-136 - Abrahamson, S., M. A. Bender, B. B. Boecker, E. S. Gilbert and B. R. Scott: *Health Effects Model for Nuclear Power Plant Accident Consequence Analysis. Modification of Model Resulting from Addition of Effects of Exposure to Alpha-Emitting Radionuclides*, Addendum 2 to Report NUREG/CR-4214, Rev. 1, Part II.

LMF-137 - Bennett, W. C., J. J. Thompson and A. S. Shankar: *Site Environmental Report - 1991.*

LMF-138 - Finch, G. L., K. J. Nikula and P. L. Bradley (eds.): *Inhalation Toxicology Research Institute Annual Report - October 1, 1991 through September 30, 1992*, LMF-138, National Technical Information Service, Springfield, VA 22161.

APPENDIX E

ITRI PUBLICATIONS IN THE OPEN LITERATURE PUBLISHED, IN PRESS, OR SUBMITTED BETWEEN OCTOBER 1, 1992 - SEPTEMBER 30, 1993

Baron, P. A., M. Mazunder and Y. S. Cheng: Direct Reading Techniques Using Optical Particle Detection. In *Air Measurement: Principles, Techniques, and Applications*, Chapter 17 (K. Willeke and P. A. Baron, eds.), pp. 381-409, Van Nostrand Reinhold, New York, NY, 1993.

Barr, E. B. and Y. S. Cheng: Evaluation of the API Aerosizer Mach 2 Particle Sizer. In *Particles in Gases and Liquids 3: Detection, Characterization, and Control* (K. L. Mittal, ed.), pp. 131-139, Plenum Press, New York, 1993.

Bartczak, A., S. A. Kline, R. Yu, C. P. Weisel, W. E. Bechtold, B. D. Goldstein and G. Witz: Evaluation of Assays for the Identification and Quantitation of Muconic Acid, a Benzene Metabolite in Human Urine. *J. Toxicol. Environ. Health* (in press).

Bechtold, W. E. and R. F. Henderson: Biomarkers of Human Exposure. *J. Toxicol. Environ. Health* (in press).

Bechtold, W. E. and J. A. Hotchkiss: *Immunoaffinity Chromatography in the Analysis of Toxic Effects of Complex Chemical Mixtures*, Report to the Health Effects Institute, Cambridge, MA (submitted).

Bechtold, W. E., M. R. Strunk, I. Y. Chang, J. B. Ward, Jr. and R. F. Henderson: Species Differences in Urinary Butadiene Metabolites: Comparisons of Metabolite Ratios Between Mice, Rats, and Humans. *Toxicol. Appl. Pharmacol.* (submitted).

Bechtold, W. E., J. J. Waide, T. Sandstrom, N. Stjernberg, D. McBride, J. Koenig, and R. F. Henderson: Biological Markers of Exposure to SO_2 S-Sulphonates in Nasal Lavage. *J. Exposure Anal. Environ. Epidem.* (in press).

Benson, J. M.: *Final Report to the Nickel Producers Environmental Research Association, Inc.* (submitted).

Benson, J. M.: *Toxicokinetics of ^{63}Ni After Inhalation of Nickel Subsulfide*, Final Report to the National Toxicology Program (submitted).

Benson, J. M., E. B. Barr, W. E. Bechtold, Y. S. Cheng, J. K. Dunnick, W. E. Eastin, C. H. Hobbs, C. H. Kennedy and K. R. Maples: The Fate of Inhaled Nickel Oxide and Nickel Subsulfide in F344/N Rats. *Inhal. Toxicol.* (in press).

Bice, D. E.: The Lung as a Target Organ. In *Principles and Practice of Immunotoxicology*, pp. 125-142, Blackwell Scientific Publications, Oxford, UK, 1992.

Bice, D. E.: Pulmonary Responses to Antigen. *Chest 103*: 95S-98S, 1993.

Bice, D. E., S. E. Jones and B. A. Muggenburg: Long-Term Antibody Production after Lung Immunization and Challenge: Role of Lung and Lymphoid Tissues. *Am. J. Respir. Cell Mol. Biol. 8*: 662-667, 1993.

Boecker, B. B., M. D. Hoover, G. J. Newton, R. A. Guilmette and B. R. Scott: Evaluation of Strategies for Monitoring and Sampling Airborne Radionuclides in the Workplace. To be published in Proceedings of the *Workshop on Intake of Radionuclides: Detection, Assessment and Limitation of Occupational Exposure* held in Bath, UK, September 13-17, 1993 (in press).

Brooks, A. L., K. Rithidech, R. M. Kitchin, N. F. Johnson, D. G. Thomassen and G. J. Newton: Evaluating Chromosome Damage to Estimate Dose to Tracheal Epithelial Cells. In *Indoor Radon and Lung Cancer: Myth or Reality?* (F. T. Cross, ed.), pp. 601-614, Battelle Press, Richland, WA, 1992.

Chen, B. T., W. E. Bechtold and J. L. Mauderly: Description and Evaluation of a Cigarette Smoke Generation System for Inhalation Studies. *J. Aerosol Med. 5*: 19-30, 1992.

Chen, B. T.: Instrument Calibration. In *Aerosol Measurement: Principles, Techniques, and Applications*, Chapter 22 (K. Willeke and P. A. Baron, eds.), pp. 493-520, Van Nostrand Reinhold, New York, 1993.

Chen, B. T., J. V. Benz, G. L. Finch, J. L. Mauderly, P. J. Sabourin, M. B. Snipes and H. C. Yeh: Differences Between Internal and External Smoke Deposition in Rats After Nose-Only or Whole-Body Exposure to Cigarette Smoke. *Inhal. Toxicol.* (submitted).

Chen, B. T., R. Irwin, Y. S. Cheng, M. D. Hoover and H. C. Yeh: Aerodynamic Behavior of Fiber- and Disc-Like Particles in a Millikan Cell Apparatus. *J. Aerosol Sci. 24*: 181-195, 1993.

Chen, B. T., H. C. Yeh and C. H. Hobbs: Size Classification of Carbon Fiber Aerosols. *Aerosol Sci. Tech. 19*: 109-120, 1993.

Cheng, Y. S.: Condensation Detection and Diffusion Size Separation Techniques. In *Aerosol Measurement: Principles, Techniques, and Applications*, Chapter 19 (K. Willeke and P. A. Baron, eds.), pp. 427-451, Van Nostrand Reinhold, New York, 1993.

Cheng, Y. S.: Denuder Systems and Diffusion Batteries. To be published in *Air Sampling Instruments*, ACGIH, Cincinnati, OH (submitted).

Cheng, Y. S., E. B. Barr, I. A. Marshall and J. P. Mitchell: Calibration and Performance of an API Aerosizer. *J. Aerosol Sci. 24*: 501-514, 1993.

Cheng, Y. S. and B. T. Chen: Aerosol Sampler Calibration. To be published in *Air Sampling Instruments*, ACGIH, Cincinnati, OH (submitted).

Cheng, Y. S., B. T. Chen and H. C. Yeh: Performance of an Aerodynamic Particle Sizer. *Appl. Occup. Environ. Health 8*: 307-312, 1993.

Cheng, Y. S., B. T. Chen, H. C. Yeh, I. A. Marshall, J. P. Mitchell and W. D. Griffiths: The Behavior of Compact Non-Spherical Particles in the APS33B: Ultra-Stokesian Drag Forces. *Aerosol Sci. Technol. 19*: 255-267, 1993.

Cheng, Y. S., H. N. Jow and A. R. Dahl: *In Vitro* Dissolution and Radiation Dosimetry of Metal Tritides. To be published in *Proceedings of the 1993 Department of Energy Radiation Protection Workshop* held in Las Vegas, NV, April 13-15, 1993 (submitted).

Cheng, Y. S., Y. F. Su, H. C. Yeh and D. L. Swift: Deposition of Thoron Progeny in Human Head Airways. *Aerosol Sci. Tech. 18*. 1993.

Cheng, Y. S., Y. F. Su and T. B. Chen: Plate-Out Rates of Radon Progeny and Particles in a Spherical Chamber. In *Indoor Radon and Lung Cancer: Myth or Reality?* (F. T. Cross, ed.), pp. 65-79, Battelle Press, Richland, WA, 1992.

Cheng, Y. S., Y. F. Su, G. J. Newton and H. C. Yeh: Use of a Graded Diffusion Battery in Measuring the Activity Size Distributions of Thoron Progeny. *J. Aerosol Sci. 23:* 361-372, 1992.

Cheng, Y. S., C. C. Yu, C. J. Tung and P. K. Hopke: Neutralization of Thoron Progeny in Gases. *Health Phys.* (submitted).

Dahl, A. R. and J. L. Lewis: Respiratory Tract Uptake and Metabolism of Xenobiotics. *Ann. Rev. Pharmacol. Toxicol. 32*: 383-407, 1993.

Dahl, A. R. and P. Gerde: Uptake and Metabolism of Toxicants in the Respiratory Tract. *Environ. Health Perspect.* (in press).

Economou, P. J., J. F. Lechner and J. M. Samet: Familial and Genetic Factors in the Pathogenesis of Lung Cancer. To be published in *Epidemiology of Lung Cancer* (J. M. Samet, ed.) (in press).

El-Genk, M. S. and M. D. Hoover (eds.): *Proceedings of the 10th Symposium on Space Nuclear Power Systems*, CONF-930103, American Institute of Physics, New York, 1993.

Finch, G. L.: *In Vitro* Measurement of Macrophage Phagocytosis Using a Sheep Red Blood Cell Assay. To be published in *Methods in Toxicology*, Academic Press (in press).

Finch, G. L., B. T. Chen, E. B. Barr, I. Y. Chang and K. J. Nikula: Effects of Cigarette Smoke Exposure on F344 Rat Lung Clearance of Insoluble Particles. To be published in *Proceedings of the 4th International Inhalation Symposium "Toxic and Carcinogenic Effects of Solid Particles in the Respiratory Tract"* held in Hannover, Germany, March 1-5, 1993, ILSI Press, Washington, DC (in press).

Finch, G. L., P. J. Haley, M. D. Hoover, M. B. Snipes and R. G. Cuddihy: Responses of Rat Lungs to Low Lung Burdens of Inhaled Beryllium Metal. *Inhal. Toxicol.* (submitted).

Finch, G. L., P. J. Haley, M. D. Hoover and R. G. Cuddihy: Responses of Rats Lungs Following Inhalation of Beryllium Metal Particles to Achieve Relatively Low Lung Burdens. *Ann. Occup. Hyg.* (in press).

Finch, G. L., K. J. Nikula, B. T. Chen, E. B. Barr, I. Y. Chang and C. H. Hobbs: Effect of Chronic Cigarette Smoke Exposure on Lung Clearance of Tracer Particles Inhaled by Rats. *Fundam. Appl. Toxicol.* (submitted).

Gerde, P., B. A. Muggenburg, M. D. Hoover and R. F. Henderson: Clearance of Particles and Lipophilic Solutes from Central Airways. *Ann. Occup. Hyg.* (in press).

Gerde, P., B. A. Muggenburg, M. D. Hoover and R. F. Henderson: Disposition of Polycyclic Aromatic Hydrocarbons in the Respiratory Tract of the Beagle Dog. I. The Alveolar Region. *Toxicol. Appl. Pharmacol. 121*: 313-318, 1993.

Gerde, P., B. A. Muggenburg, P. J. Sabourin, J. R. Harkema, J. A. Hotchkiss, M. D. Hoover and R. F. Henderson: Disposition of Polycyclic Aromatic Hydrocarbons in the Respiratory Tract of the Beagle Dog. II. The Conducting Airways. *Toxicol. Appl. Pharmacol. 121*: 319-327, 1993.

Gerde, P., B. A. Muggenburg and R. F. Henderson: Disposition of Polycyclic Aromatic Hydrocarbons in the Respiratory Tract of the Beagle Dog. III. Mechanisms of the Dosimetry. *Toxicol. Appl. Pharmacol. 121*: 328-334, 1993.

Gordon, T. and J. R. Harkema: Effect of Endotoxin on Intraepithelial Mucosubstances in F344 Rat Nasal and Tracheobronchial Airways. *Am. J. Respir. Cell Mol. Biol.* (in press).

Guilmette, R. A. and T. J. Gagliano: Construction of a Model of Human Nasal Airways Using *In Vivo* Morphometric Data. *Ann. Occup. Hyg.* (in press).

Guilmette, R. A., W. C. Griffith and A. W. Hickman: Intake Assessment for Workers that Inhaled ^{238}Pu Aerosols. To be published in *Proceedings of the Workshop on Intake of Radionuclides: Detection, Assessment and Limitation of Occupational Exposure* held in Bath, UK, September 13-17, 1993 (in press).

Guilmette, R. A. and B. A. Muggenburg: Decorporation Therapy for Inhaled Plutonium Nitrate Using Repeatedly and Continuously Administered DTPA. *Int. J. Radiat. Biol. 63*: 395-403, 1993.

Hahn, F. F.: Chronic Inhalation Bioassays for Respiratory Tract Carcinogenesis. In *Toxicology of the Lung*, Chapter 16 (D. E. Gardner, J. D. Crapo and R. O. McClellan, eds.), pp. 435-459, Raven Press, New York, NY, 1993.

Hahn, F. F., W. C. Griffith, C. H. Hobbs, B. A. Muggenburg, G. J. Newton and B. B. Boecker: Biological Effects of ^{91}Y in Relatively Insoluble Particles Inhaled by Beagle Dogs. *Ann. Occup. Hyg.* (in press).

Hahn, F. F. and D. L. Lundgren: Pulmonary Neoplasms in Rats that Inhaled Cerium-144 Dioxide. *Toxicol. Pathol. 20:* 169-178,1992.

Haley, P. J.: Immunological Responses Within the Lung After Inhalation of Airborne Chemicals. In *Toxicology of the Lung*, Chapter 14 (D. E. Gardner, J. D. Crapo and R. O. McClellan, eds.), pp. 389-416, Raven Press, New York, 1993.

Haley, P. J., D. E. Bice, G. L. Finch, M. D. Hoover and B. A. Muggenburg: Animal Models of Human Disease: Chronic Beryllium Lung Disease. *Comp. Pathol. Bull. 25*: 3-4, 1993.

Haley, P. J., G. L. Finch, M. D. Hoover, J. A. Mewhinney, D. E. Bice and B. A. Muggenburg: Beryllium-Induced Lung Disease in the Dog Following Two Exposures to BeO. *Environ. Res. 59*: 400-415, 1992.

Harkema, J. R. and J. A. Hotchkiss: *In Vivo* Effects of Endotoxin on DNA Synthesis in Rat Nasal Epithelium. *J. Microscopic Res. Tech. 26*: 457-465, 1993.

Harkema, J. R. and J. A. Hotchkiss: Ozone- and Endotoxin-Induced Mucous Cell Metaplasias in Rat Airway Epithelium: Novel Animal Models to Study Toxicant-Induced Epithelial Transformation in Airways. *Toxicol. Lett. 68*: 251-263, 1993.

Harkema, J. R. and J. L. Mauderly: *Respiratory Function Alterations in Rats Following Chronic Ozone Inhalation*, Report to the Health Effects Institute, Cambridge, MA (submitted).

Harkema, J. R., K. T. Morgan, E. G. Bermudez, P. T. Catalano and W. C. Griffith: *Effects of Chronic Ozone Exposure on the Nasal Mucociliary Apparatus in the Rat*, Report to the Health Effects Institute, Cambridge, MA (submitted).

Harkema, J. R., C. G. Plopper, D. M. Hyde, J. A. St. George, D. W. Wilson and D. L. Dungworth: Response of Macaque Bronchiolar Epithelium to Ambient Concentrations of Ozone. *Am. J. Pathol. 143*: 857-866, 1993.

Henderson, R. F., W. E. Bechtold, P. J. Sabourin, K. R. Maples and A. R. Dahl: Species Differences in *In Vivo* Metabolism of 1,3-Butadiene. To be published in *Proceedings of the International Symposium on Health Hazards of Butadiene and Styrene* held in Espoo, Finland, April 18-21, 1993 (submitted).

Henderson, R. F. and S. A. Belinsky: Biological Markers of Respiratory Tract Exposure. In *Toxicology of the Lung*, Chapter 9 (D. E. Gardner, J. D. Crapo and R. O. McClellan, eds.), pp. 253-282, Raven Press, New York, 1993.

Henderson, R. F., K. E. Driscoll, R. C. Lindenschmidt, J. R. Harkema, E. B. Barr and I. Y. Chang: Response of the Lung to Instilled Versus Inhaled Particles. To be published in the *4th International Inhalation Symposium "Toxic and Carcinogenic Effects of Solid Particles in the Respiratory Tract"* held in Hannover, Germany, March 1-5, 1993, ILSI Press, Washington, DC (in press).

Henderson, R. F., J. A. Hotchkiss, I. Y. Chang, B. R. Scott and J. R. Harkema: Effect of Cumulative Exposure on Nasal Response to Ozone. *Toxicol. Appl. Pharmacol. 119*: 59-65, 1993.

Henderson, R. F. and J. L. Mauderly: Diesel Exhaust: An Approach for the Study of the Toxicity of Mixtures. To be published in *Toxicology of Chemical Mixtures: From Mechanisms to Real Life Examples* (R. S. H. Yang, ed.), Academic Press (submitted).

Henderson, R. F., P. J. Sabourin, W. E. Bechtold, B. Steinberg and I. Y. Chang: Disposition of Inhaled Isobutene in F344/N Rats. *Toxicol. Appl. Pharmacol.* (in press).

Henderson, R. F.: Short-Term Exposure Guidelines for Emergency Response - The Approach of the Committee on Toxicology. In *Chemical Risk Assessment in the DOD: Science, Policy, and Practice*, ISBN:0-936712-90-2, ACGIH, Inc., Cincinnati, OH, 1992.

Henderson, R. F., W. E. Bechtold and K. R. Maples: Biological Markers as Measures of Exposure. *J. Exposure Anal. Environ. Epidemiology 2*: 1-13, 1992.

Henderson, R. F. and J. L. Mauderly: The Toxicity of Particles from Combustion Processes. In *Toxicology of Combustion Products* (L. Manzo and D. F. Weetman, eds.), ISBN 88-7963-004-0, pp. 11-18, 1992.

Herbert, R. A., N. A. Gillett, A. H. Rebar, D. L. Lundgren, M. D. Hoover, I. Y. Chang, W. W. Carlton and F. F. Hahn: Sequential Analysis of the Pathogenesis of Plutonium-Induced Pulmonary Neoplasms in the Rat: Morphology, Morphometry, and Cytokinetics. *Radiat. Res. 134*: 29-42, 1993.

Herbert, R. A., B. S. Stegelmeier, N. A. Gillett, A. H. Rebar, W. W. Carlton, G. Singh and F. F. Hahn: Plutonium-Induced Proliferative Lesions and Pulmonary Epithelial Neoplasms in the Rat: Immunohistochemical and Ultrastructural Evidence for Their Origin from Type II Pneumocytes. *Vet. Pathol.* (in press).

Hobbs, C. H., K. M. Abdo, F. F. Hahn, N. A. Gillett, S. L. Eustis, R. K. Jones, J. M. Benson, E. B. Barr, M. P. Dieter, J. A. Pickrell and J. L. Mauderly: Summary of the Chronic Inhalation Toxicity of Talc in F344/N Rats and B6C3F$_1$ Mice. To be publshed in *Proceedings of the 4th International Inhalation Symposium "Toxic and Carcinogenic Effects of Solid Particles in the Respiratory Tract"* held in Hannover, Germany, March 1-5, 1993, ILSI Press, Washington, DC (in press).

Hoover, M. D., J. R. Harkema, B. A. Muggenburg, J. W. Spoo, P. Gerde, H. J. Staller and J. A. Hotchkiss: A Microspray Nozzle for Local Administration of Liquids or Suspensions to Lung Airways via Bronchoscopy. *J. Aerosol Med. 6*: 67-72, 1993.

Hoover, M. D. and G. J. Newton: Calibration and Operation of Continuous Air Monitors for Alpha-Emitting Radionuclides. To be published in *1993 DOE Radiation Protection Workshop* held in Las Vegas, NV, April 13-15, 1993 (submitted).

Hoover, M. D. and G. J. Newton: Radioactive Aerosols. In *Aerosol Measurement: Principles, Techniques, and Applications* (K. Willeke and P. A. Baron, eds.), pp. 768-798, Van Nostrand Reinhold, New York, 1993.

Hotchkiss, J. A., S. G. Kim, R. F. Novak and A. R. Dahl: Enhanced Expression of P450IIE1 Following Inhalation Exposure to Pyridine. *Toxicol. Appl. Pharmacol. 118*: 98-104, 1993.

Hotchkiss, J. A., M. A. Stam and J. R. Harkema: Platelet Activating Factor Stimulates Rapid Mucin Secretion in Rat Nasal Airways *In Vivo*. *Exp. Lung Res. 19*: 545-557, 1993.

Hotchkiss, J. A., S. J. Kennel and J. R. Harkema: A Rat Monoclonal Antibody Specific for Murine Type 1 Pneumocytes. *Exp. Mol. Pathol. 57*: 235-246, 1992.

Hubbs, A. F., K. J. Nikula, F. F. Hahn and D. L. Lundgren: Primary Intrathoracic, Extraskeletal Osteosarcoma in an F344/N Rat. *Vet. Pathol.* (in press).

Johnson, N. F.: The Limitations of Inhalation, Intratracheal, and Intercoelomic Routes of Administration for Identifying Hazardous Fibrous Materials. In *Fiber Toxicology* (D. Warheit, ed.), pp. 43-72, Academic Press, 1993.

Johnson, N. F. and G. J. Newton: Estimation of Radon Progeny Dose to the Peripheral Lung and the Effect of Radon Progeny Exposure on the Alveolar Macrophage. *Radiat. Res.* (submitted).

Johnson, N. F., G. J. Newton, and R. A. Guilmette: Effects of Acute Radon Progeny Exposure on Rat Alveolar Macrophage Number and Function. In *Indoor Radon and Lung Cancer: Myth or Reality?* (F. T. Cross, ed.), pp. 627-636, Battelle Press, Richland, WA, 1992.

Jones, S. E., D. R. Davila, P. J. Haley and D. E. Bice: The Effects of Age on Immune Responses in the Antigen-Instilled Dog Lung. Antibody Responses in the Lung and Lymphoid Tissues Following Primary and Secondary Antigen Instillation. *Mech. Ageing Dev. 68*: 191-207, 1993.

Kennedy, C. H., W. E. Bechtold, I. Y. Chang and R. F. Henderson: Effect of Dose on the Disposition of 2-Ethoxyethanol after Inhalation by F344/N Rats. *Fundam. Appl. Toxicol.* (in press).

Kennedy, C. H., K. B. Cohen, W. E. Bechtold, I. Y. Chang, A. E. Eidson, A. R. Dahl and R. F. Henderson: Effect of Dose on the Metabolism of 1,1,2,2,-Tetrabromoethane in F344/N Rats After Gavage Administration. *Toxicol. Appl. Pharmacol. 119*: 23-33, 1993.

LaBone, T. R., E. H. Carbaugh, W. C. Griffith, R. A. Guilmette and K. W. Skrable (eds.): *Evaluation of Savannah River Site Internal Dosimetry Registry Case 664 (U) - Report of An Adhoc Committee*, ESH-HPT-920178, Savannah River Site, Aiken, SC, 1992.

Lechner, J. F. and J. L. Mauderly: Sequence of Events in Carcinogenesis - Initiation and Promotion, Protooncogenes and Tumor Suppressor Genes. To be published in *Proceedings of the 4th International Inhalation Symposium "Toxic and Carcinogenic Effects of Solid Particles in the Respiratory Tract"* held in Hannover, Germany, March 1-5, 1993, ILSI Press, Washington, DC (in press).

Lewis, J. L. and A. R. Dahl: Olfactory Mucosa: Composition, Enzymatic Localization, and Metabolism. To be published in *Handbook of Clinical Olfaction and Gustation* (R. L. Doty, ed.), Marcel Dekker, New York (in press).

Lewis, J. L., F. F. Hahn and A. R. Dahl: Transport of Inhaled Toxicants to the Central Nervous System: Characteristics of a Nose-Brain Barrier. To be published in *The Vulnerable Brain and Environmental Risks, Volume 3, Special Hazards from Air* r (R. L. Isaacson and K. F. Jensen, eds.), Plenum, New York, (in press).

Lewis, J. L., K. J. Nikula, R. F. Novak and A. R. Dahl: Comparative Localizations of Carboxylesterase in F344 Rat, Beagle Dog, and Human Nasal Tissue. *Anatom. Rec.* (in press).

Lundgren, D. L., F. F. Hahn, J. H. Diel, and M. B. Snipes: Repeated Inhalation Exposure of Rats to Aerosols of $^{144}CeO_2$. I. Lung, Liver, and Skeletal Dosimetry. *Radiat. Res. 132:* 312-324, 1992.

Lundgren, D. L., F. F. Hahn, and J. H. Diel: Repeated Inhalation Exposure of Rats to Aerosols of $^{144}CeO_2$. II. Effects on Survival and Lung, Liver, and Skeletal Neoplasms. *Radiat. Res. 132:* 325-333, 1992.

Maples, K. R. and A. R. Dahl: Levels of Epoxides in Blood During Inhalation of Alkenes and Alkene Oxides. *Inhal. Toxicol. 5*: 43-54, 1993.

Maples, K. R. and N. F. Johnson: Epithelial and Mesothelial Cell Phagosomal pH: Potential Effect on Fiber Reactivity. *Cell Biol. Toxicol.* (submitted).

Maples, K. R., K. J. Nikula, B. T. Chen, G. L. Finch, W. C. Griffith and J. R. Harkema: Effects of Cigarette Smoke on the Glutathione Status of the Upper and Lower Respiratory Tract of Rats. *Inhal. Toxicol. 5*: 389-401, 1993.

Maples, K. R. and N. F. Johnson: Fiber-Induced Hydroxyl Radical Formation: Correlation with Mesothelioma Induction in Rats and Humans. *Carcinogenesis 13*: 2035-2039, 1992.

Mauderly, J. L.: Contribution of Inhalation Bioassays to the Assessment of Human Health Risks from Solid Airborne Particles. To be published in *Proceedings of the 4th International Inhalation Symposium "Toxic and Carcinogenic Effects of Solid Particles in the Respiratory Tract"* held in Hannover, Germany, March 1-5, 1993, ILSI Press, Washington, DC (in press).

Mauderly, J. L.: Current Assessment of the Carcinogenic Hazard of Diesel Exhaust. *Toxicologic and Environmental Chemistry* (in press).

Mauderly, J. L.: Non-Cancer Pulmonary Effects of Chronic Inhalation Exposure of Animals to Solid Particles. To be published in *Proceedings of the 4th International Inhalation Symposium "Toxic and Carcinogenic Effects of Solid Particles in the Respiratory Tract"* held in Hannover, Germany, March 1-5, 1993, ILSI Press, Washington, DC (in press).

Mauderly, J. L.: Toxicological Approaches to Complex Mixtures. *Environ. Health Perspect.* (in press).

Mauderly, J. L.: Toxicological and Epidemiological Evidence for Health Risks from Inhaled Engine Emissions. *Environ. Health Perspect.* (in press).

Mauderly, J. L., E. B. Barr, A. F. Eidson, J. R. Harkema, R. F. Henderson, J. A. Pickrell and R. K. Wolff: Pneumonconiosis in Rats Exposed Chronically to Oil Shale Dust and Diesel Exhaust, Alone and in Combination. *Ann. Occup. Hyg.* (in press).

Mauderly, J. L., M. B. Snipes, E. B. Barr, S. A. Belinsky, J. A. Bond, A. L. Brooks, I. Y. Chang, Y. S. Cheng, N. A. Gillett, W. C. Griffith, R. F. Henderson, C. E. Mitchell, K. J. Nikula and D. G. Thomassen: *Pulmonary Toxicity of Inhaled Diesel Exhaust and Carbon Black in Chronically Exposed Rats*, Report to the Health Effects Institute, Cambridge, MA (in press).

Mauderly, J. L. and N. A. Gillett: Changes in Respiratory Function. In *Pathobiology of the Aging Rat, Vol. 1, Blood and Lymphoid, Respiratory, Urinary, Cardiovascular, and Reproductive Systems* (U. Mohr, D. L. Dungworth and C. C. Capen, eds.), pp. 129-142, ILSI Press, Washington, DC, 1992.

Mitchell, C. E., W. E. Bechtold and S. A. Belinsky: Metabolism of Nitrofluoranthenes by Rat Lung Subcellular Fractions. *Carcinogenesis 14*: 1161-1166, 1993.

Muggenburg, B. A., R. A. Guilmette, W. C. Griffith, F. F. Hahn, N. A. Gillett and B. B. Boecker: The Toxicity of Inhaled Particles of $^{238}PuO_2$ in Dogs. *Ann. Occup. Hyg.* (in press).

Newton, G. J., W. E. Bechtold, M. D. Hoover, F. Ghanbari, P. S. Herring and H. N. Jow: A Case Study on Determining Air Monitoring Requirements in a Radioactive Materials Handling Area. To be published in *Proceedings of the 1993 DOE Radiation Protection Workshop* held in Las Vegas, NV, April 13-15, 1993 (submitted).

Newton, G. J., R. G. Cuddihy, H. C. Yeh and B. B. Boecker: Design and Performance of a Recirculating Radon Progeny Aerosol Generation and Animal Inhalation Exposure System. In *Indoor Radon and Lung Cancer: Reality or Myth?* (F. T. Cross, ed.), pp. 709-729, Battelle Press, Richland, WA, 1992.

Nickell-Brady, C., F. F. Hahn, G. L. Finch and S. A. Belinsky: Analysis of K-ras, p53, and c-raf-1 Mutations in Beryllium-induced Rat Lung Tumors. *Carcinogenesis* (submitted).

Nikula, K. J., M. B. Snipes, E. B. Barr, W. C. Griffith, R. F. Henderson and J. L. Mauderly: Influence of Particle-Associated Organic Compounds on the Carcinogenicity of Diesel Exhaust. To be published in *Proceedings of the 4th International Symposium "Toxic and Carcinogenic Effects of Solid Particles in the Respiratory Tract"* held in Hannover, Germany, March 1-5, 1993, ILSI Press, Washington, DC (in press).

Nikula, K. J., J. D. Sun, E. B. Barr, W. E. Bechtold, P. J. Haley, J. M. Benson, A. F. Eidson, D. G. Burt, A. R. Dahl, R. F. Henderson, I. Y. Chang, J. L. Mauderly, M. P. Dieter and C. H. Hobbs: Thirteen-Week, Repeated Inhalation Exposure of F344/N Rats and B6C3F$_1$ Mice to Ferrocene. *Fundam. Appl. Toxicol. 21*: 127-139, 1993.

Schuyler, M., K. Gott, B. Edwards and K. J. Nikula: Experimental Hypersensitivity Pneumonitis: Effect of CD4 Cell Depletion. *Am. Rev. Respir. Dis.* (in press).

Scott, B. R., C. W. Langberg and M. Hauer-Jensen: Models for Estimating the Risk of Ulcers in the Small Intestine After Localized Single or Fractionated Irradiation. *Br. J. Radiol.* (submitted).

Shyr, L. J., P. J. Sabourin, M. A. Medinsky, L. S. Birnbaum and R. F. Henderson: Physiologically Based Modeling of 2-Butoxyethanol Disposition in Rats Following Different Routes of Exposure. *Environ. Res.* (in press).

Shyr, L. J., J. H. Diel, I. Y. Chang and R. A. Guilmette: The Use of Autoradiographic Data for Estimating Tumor Cell Dose in Alpha Immunotherapy. In *Fifth International Radiopharmaceutical Dosimetry Symposium*, pp. 589-599, Oak Ridge Associated Universities, Oak Ridge, TN, 1992.

St. George, J. A., J. R. Harkema and C. G. Plopper: Cell Populations and Structure-Function Relationships of Cells in the Airways. In *Toxicology of the Lung*, Chapter 4 (D. E. Gardner, J. D. Crapo and R. O. McClellan, eds.), pp. 81-110, Raven Press, New York, 1993.

Swift, D. L., Y. S. Cheng, Y. F. Su and H. C. Yeh: Design, Characterization and Use of Replicate Human Upper Airways for Radon Dosimetry Studies. In *Indoor Radon and Lung Cancer: Reality or Myth?* (F. T. Cross, ed.), pp. 213-226, Battelle Press, Richland, WA, 1992.

Taya, A., J. A. Mewhinney, and R. A. Guilmette: Subcellular Distribution of ^{241}Am in Beagle Lungs Following Inhalation of $^{241}Am(NO_3)_3$ Aerosols. *Ann. Occup. Hyg.* (in press).

Thomassen, D. G.: Mitogens in Bovine Pituitary for Rat Tracheal Epithelial Cells. *In Vitro Cell. Dev. Biol. 29A*: 187-188, 1993.

Thomassen, D. G.: Neoplastic Progression of Rat Tracheal Epithelial Cells is Associated with a Reduction in the Number of Growth Factors Required for Clonal Proliferation in Culture. *In Vitro Cell. Dev. Biol. 29A*: 498-504, 1993.

Thomassen, D. G., G. J. Newton and R. A. Guilmette: Preneoplastic Transformation of Rat Tracheal Epithelial Cells by Inhaled Radon Progeny. In *Indoor Radon and Lung Cancer: Myth or Reality?* (F. T. Cross, ed.), pp. 637-648, Battelle Press, Richland, WA, 1992.

Ward, J. B., M. M. Ammenheuser, W. E. Bechtold, E. B. Whorton and M. S. Legator: hprt Mutant Lymphocyte Frequencies in Workers at a 1,3-Butadiene Production Plant. *Environ. Health Perspect.* (in press).

Yamada, Y., Y. S. Cheng, H. C. Yeh, and D. L. Swift: Deposition of Ultrafine Monodisperse Particles in a Human Tracheobronchial Cast. *Ann. Occup. Hyg.* (in press).

Yeh, H. C.: Electrical Techniques. In *Aerosol Measurement: Principles, Techniques, and Applications*, Chapter 18 (K. Willeke and P. A. Baron, eds.), pp. 410-426, Van Nostrand Reinhold, New York, 1993.

Yeh, H. C. and J. R. Harkema: Gross Morphometry of Airways. In *Toxicology of the Lung*, Chapter 3 (D. E. Gardner, J. D. Crapo and R. O. McClellan, eds.), pp. 55-80, Raven Press, New York, NY, 1993.

Yeh, H. C., Y. S. Cheng, Y. F. Su and K. T. Morgan: Deposition of Radon Progeny in Nonhuman Primate Nasal Airways. In *Indoor Radon and Lung Cancer: Reality or Myth?* (F. T. Cross, ed.), pp. 235-248, Battelle Press, Richland, WA, 1992.

Yuan, J. W., J. A. Krieger, K. R. Maples, J. L. Born and S. W. Burchiel: Immunotoxic Polycyclic Aromatic Hydrocarbons Reduce Intracellular Glutathione Levels in the A20.1 Murine B Cell Lymphoma. *Fundam. Appl. Toxicol.* (submitted).

APPENDIX F

PRESENTATIONS BEFORE REGIONAL OR NATIONAL SCIENTIFIC MEETINGS AND EDUCATIONAL AND SCIENTIFIC SEMINARS

OCTOBER 1, 1992 - SEPTEMBER 30, 1993

Barr, E. B.: Operation of Chronic Exposure Systems (Laboratory Demonstration). Current Concepts in Inhalation Toxicology - A Short Course, Albuquerque, NM, October 26-29, 1992.

Bechtold, W. E.: Biomarkers of Exposure to Benzene. 31st Hanford Symposium on Health and the Environment, Richland, WA, October 20-23, 1992.

Bechtold, W. E. and J. A. Hotchkiss: Analysis of the Toxic Effects of Complex Mixtures Using Immunoaffinity Chromatography. Ninth Health Effects Institute Annual Meeting, Monterey, CA, December 6-9, 1992.

Bechtold, W. E., K. T. Kelsey and J. B. Ward: Measurement of 1,2-Dihydroxy-4-(N-Acetylcysteinyl-S-) Butane in Urine as a Biomarker of Exposure to 1,3-Butadiene. International Symposium on Health Hazards of Butadiene and Styrene, Espoo, Finland, April 18-21, 1993.

Bechtold, W. E.: Absorption, Distribution, and Excretion. General Toxicology I Pharmacy 480/580 Course, University of New Mexico, Albuquerque, NM, September 1 and 8, 1993.

Bechtold, W. E.: Species Differences in the Disposition and Toxicology of 1,3-Butadiene. Toxicology Program Seminar, College of Pharmacy, University of New Mexico, Albuquerque, NM, October 13, 1993.

Belinsky, S. A., G. Kelly and J. F. Lechner: Molecular Tools in Toxicology Studies (Laboratory Demonstration). Current Concepts in Inhalation Toxicology - A Short Course, Albuquerque, NM, October 26-29, 1992.

Belinsky, S. A., D. S. Swafford, C. E. Mitchell and K. J. Nikula: Identification of Target Genes Involved in Carbon Black and Diesel-Induced Lung Cancer. Ninth Health Effects Institute Annual Meeting, Monterey, CA, December 6-9, 1992.

Belinsky, S. A.: Gene Dysfunction in the Development of Chemically Induced Cancer. DOE/OHER Review, ITRI, Albuquerque, NM, December 11, 1992.

Belinsky, S. A.: Kras and p53 Mutations in Rodent Lung Tumors. Fourth International Agency for the Study of Lung Cancer, Arlie, Virginia, April 13-16, 1993.

Belinsky, S. A.: Gene Dysfunctions Involved in the Development of Lung Tumors in Rats. Workshop on Adenocarcinoma of the Lung: Current Knowledge Regarding Etiologic Factors, Bethesda, MD, May 10-11, 1993.

Belinsky, S. A., C. E. Mitchell and F. F. Hahn: Gene Alterations in X-Ray-Induced Lung Tumors for the F344/N Rat. American Association for Cancer Research, Orlando, FL, May 19-22, 1993.

Belinsky, S. A.: Environmental Effects on Normal and Cancer Cells - Determinants of Lung Growth: Development vs. Cancer, Bethesda, MD, September 9-10, 1993.

Bice, D. E.: Pulmonary Immunotoxicology. Current Concepts in Inhalation Toxicology - A Short Course, Albuquerque, NM, October 26-29, 1992.

Bice, D. E., C. L. Astry and J. R. Harkema: Comparison of Antibody Immunity after Intratracheal or Intranasal Immunization. 1993 American Lung Association/American Thoracic Society International Conference, San Francisco, CA, May 16-19, 1993.

Boecker, B. B.: Respiratory Tract Dosimetry Models for Radionuclides. Current Concepts in Inhalation Toxicology - A Short Course, Albuquerque, NM, October 26-29, 1992.

Boecker, B. B.: ICRP Dosimetry Models for the Respiratory Tract: Indicators of Progress in Assessing Risk from Inhaled Radionuclides. WERC Seminar Series, University of New Mexico, Albuquerque, NM, March 12, 1993.

Boecker, B. B.: Inhalation Toxicology of Radioactive Materials. Radioactive Waste Management Videoconference Training Series, Waste-Management Education and Research Consortium, Albuquerque, NM, March 31, 1993.

Boecker, B. B.: Biological Effects of Ionizing Radiation. Radioactive Waste Management Videoconference Training Series, Waste-Management Education and Research Consortium, Albuquerque, NM, March 31, 1993.

Boecker, B. B., M. D. Hoover, G. J. Newton and R. A. Guilmette: Evaluation of Strategies for Monitoring and Sampling Airborne Radionuclides in the Workplace. CEC/DOE Workshop on Intake of Radionuclides, Bath, U.K., September 13-17, 1993.

Brodbeck, R.: Operation of Acute Exposure Systems (Laboratory Demonstration). Current Concepts in Inhalation Toxicology - A Short Course, Albuquerque, NM, October 26-29, 1992.

Chang, I. Y.: Computer Modeling Approaches (Laboratory Demonstration). Current Concepts in Inhalation Toxicology - A Short Course, Albuquerque, NM, October 26-29, 1992.

Chang, I. Y. and P. Gerde: Models for Chemical Uptake and Toxicokinetics. Topical Meeting on the Technical Basis for Measuring, Modeling, and Mitigating Aerosols, September 27-30, 1993.

Chen, B. T., H. C. Yeh and C. H. Hobbs: Electrical Classification of Fiber Aerosols. American Association for Aerosol Research, San Francisco, CA, October 12-16, 1992.

Chen, B. T. and K. R. Maples: Generation and Characterization of Gases and Vapors (Laboratory Demonstration). Current Concepts in Inhalation Toxicology - A Short Course, Albuquerque, NM, October 26-29, 1992.

Chen, B. T., W. E. Bechtold, G. L. Finch, J. A. Lopez and J. J. Thompson: Thermal Oxidation of Cigarette Smoke Exhaust. 1993 American Industrial Hygiene Conference and Exposition, New Orleans, LA, May 15-21, 1993.

Cheng, Y. S. and E. B. Barr: Calibration and Performance of an API Aerosizer. American Association for Aerosol Research, San Francisco, CA, October 12-16, 1992.

Cheng, Y. S.: Inhalation Exposure Systems. Current Concepts in Inhalation Toxicology - A Short Course, Albuquerque, NM, October 26-29, 1992.

Cheng, Y. S. and E. B. Barr: Intercomparison of Cyclone Cassette Personal Samplers for Respirable Mass Fractions. American Industrial Hygiene Conference and Exposition, New Orleans, LA, May 15-21, 1993.

Cheng, Y. S.: Aerosol Generation and Characterization. National Institute of Safety Research. Seoul, Korea, December 17, 1992.

Cheng, Y. S., J. M. Benson, E. B. Barr and C. H. Hobbs: Inhalation Toxicology of Nickel Compounds. National Institute of Safety Research. Seoul, Korea, December 17, 1992.

Cheng, Y. S., B. T. Chen and K. R. Maples: Generation and Characterization of Gases and Vapors, National Institute of Safety and Research, Seoul, Korea, December 17, 1993.

Cheng, Y. S. and H. N. Jow: Dissolution Rate and Radiological Dosimetry of Metal Tritides. DOE Tritium Focus Group Meeting, Livermore, CA, March 9-11, 1993.

Cheng, Y. S., H. C. Yeh, S. Q. Simpson and D. L. Swift: Head Airway Geometry and Aerosol Deposition in Human and Laboratory Animals. Seminar at the National Taiwan University, Taipei, Taiwan, April 10, 1993.

Cheng, Y. S., H. C. Yeh, S. Q. Simpson and D. L. Swift: Deposition of Ultrafine Aerosol in the Nasal Passages of Human Volunteers. NRC Radon Dosimetry Workshop, Albuquerque, MN, April 13, 1993.

Cheng, Y. S. and H. N. Jow: *In Vitro* Dissolution and Radiation Dosimetry of Metal Tritides. DOE Radiation Protection Workshop, Las Vegas, NV, April 13-15, 1993.

Cheng, Y. S.: Radon Studies at ITRI. Physics Department, New Mexico Institute of Mining and Technology, Socorro, NM, April 23, 1993.

Dahl, A. R.: Inorganic Toxicology. Chemistry Department, University of Colorado, Boulder, CO, October 16, 1992.

Dahl, A. R.: Deposition and Disposition of Inhaled Gases and Vapors. Current Concepts in Inhalation Toxicology - A Short Course, Albuquerque, NM, October 26-29, 1992.

Dahl, A. R.: Disposition of Inhaled Gases and Vapors (Laboratory Demonstration). Current Concepts in Inhalation Toxicology - A Short Course, Albuquerque, NM, October 26-29, 1992.

Dahl, A. R.: Influence of Respiratory Tract Metabolism on Effective Dose. DOE/OHER Review, ITRI, Albuquerque, NM, December 11, 1992.

Dahl, A. R. and L. K. Brookins: A Method for Measuring Vapor Uptake in the Nose and Lungs of Rats Having Patent Respiratory Tracts and During Cyclic Breathing. 1993 Annual Meeting of the Society of Toxicology, New Orleans, March 14-18, 1993.

Dahl, A. R.: Factors Influencing Xenobiotic Metabolism in Nasal, Respiratory and Olfactory Mucosae. Experimental Biology 93 Meeting, New Orleans, LA, March-April, 1993.

Dahl, A. R., D. Zastrow and J. A. Hotchkiss: Advances in Comparative Nasal Enzymology Between F344 Rats and Humans. Workshop on Nasal Toxicity and Dosimetry of Inhaled Xenobiotics: Implications for Human Health, Research Triangle Park, NC, September 20-22, 1993.

Finch, G. L., B. T. Chen, E. B. Barr, I. Y. Chang and K. J. Nikula: Effects of Cigarette Smoke Exposure on Rat Lung Clearance of Insoluble Particles. Toxic and Carcinogenic Effects of Solid Particles in the Respiratory Tract, Hannover, Germany, March 1-5, 1993.

Finch, G. L., L. Reddick, M. D. Hoover and K. J. Nikula: Effects of Inhaled Beryllium Metal on Mouse Clearance and Toxicity. 1993 Annual Meeting of the Society of Toxicology, New Orleans, March 14-18, 1993.

Finch, G. L.: Chronic Beryllium Disease Research at the Inhalation Toxicology Research Institute. Toxic Materials Advisory Committee Meeting, Sandia National Laboratory, Albuquerque, NM, April 6-7, 1993.

Finch, G. L.: Cancer Risks from Exposure to Ionizing Radiation and Chemical Carcinogens. BEIR-IV Phase I Committee Workshop, Radon: Molecular and Cellular Radiobiology, Washington, DC, August 26, 1993.

Finch, G. L.: Life-span Study of Rats Exposed to Cigarette Smoke and $^{239}PuO_2$. Toxicology Program Seminar, College of Pharmacy, University of New Mexico, Albuquerque, NM, September 15, 1993.

Funk, L. M., S. Q. Simpson, R. Singh and D. E. Bice: Bronchodilating Agents Inhibit Tumor Necrosis Factor Alpha Gene Expression. American Lung Association/American Thoracic Society International Conference, San Francisco, CA, May 16-19, 1993.

Gerde, P., B. A. Muggenburg, A. R. Dahl and R. F. Henderson: The Diffusion-Limited Clearance of Lipophilic Compounds from Lungs: A Novel Dosimetry Concept. Annual Meeting of the Society of Toxicology, New Orleans, March 14-18, 1993.

Griffith, W. C.: Statistical Design for Inhalation Studies (Laboratory Demonstration). Current Concepts in Inhalation Toxicology - A Short Course, Albuquerque, NM, October 26-29, 1992.

Griffith, W. C.: Effect of Demographic Factors on Fallout Pu Liver Burdens. Conference on Bioassay, Analytical and Environmental Radiochemistry, Santa Fe, NM, November 2-6, 1992.

Griffith, W. C.: Comparison of the New ICRP and NCRP Lung Retention Models. Health Physics Course, School of Engineering, University of New Mexico, Albuquerque, NM, December 16, 1992.

Griffith, W. C.: Health Effects of Inhaled Pu. Committee on Nuclear Weapons Safety for the Secretary of Defense. Defense Nuclear Agency, Albuquerque, NM, March 30, 1993.

Griffith, W. C.: The New NCRP Lung Model. National Academy of Science, BEIR VI Phase I Committee Workshop, Radon Dosimetry, Albuquerque, NM, April 19, 1993.

Guilmette, R. A.: Clearance of Particles Deposited on Canine Conducting Airways. GSF-Munchen, Neuherburg, Germany, March 11, 1993.

Guilmette, R. A.: Clearance of Particles Deposited in Canine Conducting Airways. GSF-Frankfurt, Frankfurt, Germany, March 15, 1993.

Guilmette, R. A., W. C. Griffith, K. J. Nikula and M. B. Snipes: Clearance of Particles Deposited in the Conducting Airways of Beagle Dogs. American Lung Association/American Thoracic Society International Conference, San Francisco, CA, May 16-19, 1993.

Guilmette, R. A.: Inhaled Radionuclides: Biokinetics, Dosimetry, and Therapy. Health Physics Society Annual Meeting, Atlanta, GA, July 11-15, 1993.

Guilmette, R. A., W. C. Griffith and A. W. Hickman: Intake and Dose Assessment of Workers that Inhaled ^{238}Pu Aerosols Using the ITRI ^{238}Pu Biokinetic/Dosimetric Model. CEC/DOE Workshop on Intake of Radionuclides, Bath, U.K., September 13-17, 1993.

Guilmette, R. A., Y. S. Cheng, H. C. Yeh and D. L. Swift: Deposition of 0.005-12 μm Monodisperse Particles in a Computer-Milled MRI-Based Nasal Airway Replica. Workshop on Nasal Toxicity and Dosimetry of Inhaled Xenobiotics: Implications for Human Health, Research Triangle Park, NC, September 20-22, 1993.

Hahn, F. F., W. C. Griffith, B. A. Muggenburg, M. B. Snipes and B. B. Boecker: Pulmonary Effects of Inhaled Beta-Emitting Radionuclides. Annual Meeting of the European Society for Radiation Biology, Frankfurt, Germany, October 4-8, 1992.

Hahn, F. F., W. C. Griffith and D. L. Lundgren: Dose-Response Relationships and Risk Estimates for Lung Carcinomas in Rats that Inhaled $^{239}PuO_2$ or $^{144}CeO_2$. Annual Meeting of the European Society for Radiation Biology, Frankfurt, Germany, October 4-08, 1992.

Hahn, F. F.: Respiratory Tract Cancer. Current Concepts in Inhalation Toxicology - A Short Course, Albuquerque, NM, October 26-29, 1992.

Hahn, F. F.: Links Between Radiation-Induced Lung Cancer in Lab Animals and People. DOE/OHER Review, ITRI, Albuquerque, NM, December 11, 1992.

Hahn, F. F., D. L. Lundgren, W. C. Griffith and B. B. Boecker: Long-Term Effects of Thoracic or Whole-Body Exposure of Rats to X-Rays. Joint Meeting of the Radiation Research Society/North American Hypothermia Society, Dallas, TX, March 25, 1993.

Harkema, J. R. and K. J. Nikula: Morphometric Techniques for Evaluating Pulmonary Toxicology (Laboratory Demonstration). Current Concepts in Inhalation Toxicology - A Short Course, Albuquerque, NM, October 26-29, 1992.

Harkema, J. R.: Noncancerous Airway and Parenchymal Diseases. Current Concepts in Inhalation Toxicology - A Short Course, Albuquerque, NM, October 26-29, 1992.

Harkema, J. R. and J. A. Hotchkiss: *In Vivo* Effects of Endotoxin on DNA Synthesis in Rat Nasal Epithelium (presented by K. J. Nikula). 1992 American College of Veterinary Pathologists Annual Meeting, San Diego, CA, November 17-20, 1992.

Harkema, J. R. and J. L. Mauderly: Effects of Chronic Ozone Exposure on Airway Mucosubstances in the Rat. Ninth Health Effects Institute Annual Meeting, Monterey, CA, December 6-9, 1992.

Harkema, J. R., K. Pinkerton and C. Plopper: Effects of Chronic Ozone Exposure on the Nasal Mucociliary Apparatus in the Rat. Ninth Health Effects Institute Annual Meeting, Monterey, CA, December 6-9, 1992.

Harkema, J. R., E. G. Bermudez and K. Morgan: Respiratory Function Alterations Following Chronic Ozone Inhalation in Rats. Ninth Health Effects Institute Annual Meeting, Monterey, CA, December 6-9, 1992.

Harkema, J. R.: Airway Epithelial Injury, Adaptation and Repair. DOE/OHER Review, ITRI, Albuquerque, NM, December 11, 1992.

Harkema, J. R., K. Pinkerton and C. Plopper: Effects of Chronic Ozone Exposure on Airway Mucosubstances in the Rat. 1993 Annual Meeting of the Society of Toxicology, New Orleans, March 14-18, 1993.

Harkema, J. R., J. A. Hotchkiss, D. G. Burt and C. H. Hobbs: Strain-Related Differences in Ozone-Induced Mucous Cell Metaplasia in the Nasal Epithelium of Rats. American Lung Association/American Thoracic Society International Conference, San Francisco, CA, May 16-19, 1993.

Harkema, J. R., J. A. Hotchkiss, D. G. Burt and C. H. Hobbs: Strain-Related Differences in Ozone-Induced Mucous Cell Metaplasia in the Nasal Epithelium of Rats. Workshop on Nasal Toxicity and Dosimetry of Inhaled Xenobiotics: Implications for Human Health, Research Triangle Park, NC, September 20-22, 1993.

Henderson, R. F.: Use of Lavage Fluid Analysis to Detect Response of Lung to Inhaled Particles. R. J. Reynolds Co., Winston-Salem, NC, January 27, 1993.

Henderson, R. F.: Response of Lung to Low Molecular Weight Polyacrylate Polymers. Rohm & Maas Co., Philadelphia, PA, February 8, 1993.

Henderson, R. F., K. Driscoll, R. Lindenschmidt, J. R. Harkema, E. B. Barr and I. Y. Chang: Response of the Rat Lung to Inhaled Versus Instilled Particles. Toxic and Carcinogenic Effects of Solid Particles in the Respiratory Tract, Hannover, Germany, March 1-5, 1993.

Henderson, R. F., K. R. Driscoll, R. Lindenschmidt, J. R. Harkema, E. B. Barr and I. Y. Chang: Response of Rat Lung to Inhaled Versus Instilled Particles. Annual Meeting of the Society of Toxicology, New Orleans, March 14-18, 1993.

Henderson, R. F., W. E. Bechtold, P. J. Sabourin, K. R. Maples and A. R. Dahl: Species Differences in *In Vivo* Metabolism of 1, 3-Butadiene. International Symposium on Health Hazards of Butadiene and Styrene, Espoo, Finland, April 18-21, 1993.

Henderson, R. F.: Species Differences in Metabolism of 1,3-Butadiene. Chancellor's Distinguished Lecture, University of California, Irvine, April 26, 1993.

Henderson, R. F.: Chemicals: Friends or Foe? Chancellor's Distinguished Lecture, University of California, Irvine, April 27, 1993.

Henderson, R. F., J. R. Harkema, D. G. Burt and C. H. Hobbs: Rat Strain and Substrain Differences in Response to Ozone. American Lung Association/American Thoracic Society International Conference, San Francisco, CA, May 16-19, 1993.

Hobbs, C. H., J. M. Benson and R. D. Brodbeck: Calibration and Quality Assurance for Inhalation Toxicology Studies (Laboratory Demonstration). Current Concepts in Inhalation Toxicology - A Short Course, Albuquerque, NM, October 26-29, 1992.

Hobbs, C. H., K. M. Abdo, F. F. Hahn, N. A. Gillett, S. L. Eustus, R. K. Jones, J. M. Benson, E. B. Barr, M. P. Dieter, J. A. Pickrell and J. L. Mauderly: Chronic Inhalation Toxicity of Talc in F344/N Rats and B6C3F_1 Mice (presented by J. L. Mauderly). Toxic and Carcinogenic Effects of Solid Particles in the Respiratory Tract, Hannover, Germany, March 1-5, 1993.

Hobbs, C. H., F. F. Hahn, N. A. Gillett, S. L. Eustus, R. K. Jones, J. M. Benson, E. B. Barr, M. P. Dieter, J. A. Pickrell and J. L. Mauderly: Chronic Inhalation Toxicity of Talc in F344/N Rats and B6C3F_1 Mice. Annual Meeting of the Society of Toxicology, New Orleans, March 14-18, 1993.

Hoover, M. D. and G. J. Newton: Technical Bases for Selection and Use of Filter Media in Continuous Air Monitors for Alpha-Emitting Radionuclides. American Association for Aerosol Research, San Francisco, CA, October 12-16, 1992.

Hoover, M. D.: Characterization of Exposure Atmospheres. Current Concepts in Inhalation Toxicology - A Short Course, Albuquerque, NM, October 26-29, 1992.

Hotchkiss, J. A., J. S. Kimball, L. K. Herrera, G. E. Hatch, K. T. Morgan and J. R. Harkema: Regional Differences in Ozone-Induced Nasal Epithelial Cell Proliferation in F344 Rats: Comparison with Computational Mass Flux Predictions of Ozone Dosimetry. Workshop on Nasal Toxicity and Dosimetry of Inhaled Xenobiotics: Implications for Human Health, Research Triangle Park, NC, September 20-22, 1993.

Hotchkiss, J. A., W. A. Evans, K. R. Maples, B. T. Chen, G. L. Finch and J. R. Harkema: Regional Differences in the Effects of Cigarette Smoke on Stored Mucosubstances in Respiratory Epithelium of the F344 Rat Nasal Septum. Workshop on Nasal Toxicity and Dosimetry of Inhaled Xenobiotics: Implications for Human Health, Research Triangle Park, NC, September 20-22, 1993.

Johnson, N. F. and Y. S. Cheng: Fiber Aerosols. Topical Meeting on the Technical Basis for Measuring, Modeling, and Mitigating Toxic Aerosols, Albuquerque, NM, September 27-30, 1993.

Kelly, G.: Molecular Mechanisms of Radiation-Induced Lung Cancer. DOE/OHER Review, ITRI, Albuquerque, NM, December 11, 1992.

Kelly, G., T. Carpenter and N. F. Johnson: Simian Virus 40 Large T Antigen Expression in *Saccharomyces Cerevisiae*. American Association for Cancer Research, Orlando, FL, May 19-22, 1993.

Kennedy, C. H., W. A. Palmisano and J. F. Lechner: A Novel Technique to Study Toxicant-Caused Gene Expression Alterations in Human Airway Cells. Congress on Cell and Tissue Culture. Meeting of the Tissue Culture Association, San Diego, CA, June 5-9, 1993.

Lechner, J. F.: Gene Dysfunction in Lung Cancer from Uranium Miners. UNM Cancer Center, Albuquerque, NM, November 24, 1992.

Lechner, J. F.: Premalignant Events in Radiation-Induced Lung Cancer. DOE/OHER Review, ITRI, Albuquerque, NM, December 11, 1992.

Lechner, J. F.: Cellular Models of Radiation-Induced Lung Cancer. DOE/OHER Review, ITRI, Albuquerque, NM, December 12, 1992.

Lechner, J. F.: Lung Cancer in Uranium Miners - Gene Dysfunction. DOE/OHER Review, ITRI, Albuquerque, NM, December 12, 1992.

Lechner, J. F. and J. L. Mauderly: Sequence of Events in Carcinogenesis - Multistage Carcinogenesis, Initiation, Promotion, Progression, Protooncogenes and Tumor Suppressor Genes. Toxic and Carcinogenic Effects of Solid Particles in the Respiratory Tract, Hannover, Germany, March 1-5, 1993.

Lechner, J. F.: Gene Aberrations in Alpha-Radiation-Caused Lung Cancer. The Steno Institute, University of Aarhus, Aarhus, Denmark, March 8, 1993.

Lechner, J. F.: Early Detection of Gene Changes Leading to Lung Cancer. Lovelace Medical Foundation Environmental Health Symposium, Albuquerque, NM, April 30, 1993.

Lechner, J. F., S. A. Belinsky, G. Saccomanno, J. Samet, W. P. Bennett and L. A. Tierney: Alpha Radiation-Caused Lung Cancer. American Lung Association/American Thoracic Society International Conference, San Francisco, CA, May 16-19, 1993.

Lechner, J. F.: Molecular Signatures of High-LET Radiation-Induced Lung Cancer: Animal Models, Cell Models, and Uranium Miners. BEIR-IV Phase I Committee Workshop, Radon: Molecular and Cellular Radiobiology, Washington, DC, August 26, 1993.

Lechner, J. F.: *In Vitro* Inhalation Toxicology. Xenometrix, Inc., Boulder, CO, September 24, 1993.

Lewis, J. L.: Structural and Metabolic Characteristics of Olfactory Toxicity and Their Potential Role in CNS Toxicity. European Science Foundation's Mechanisms of Toxicity Conference Series, San Feliu de Guixois, Costa Brava, Spain, November 10-15, 1992.

Lewis, J., K. J. Nikula, R. Novak, I. Y. Chang and A. R. Dahl: Induction of Nasal Carboxylesterase Following Inhalation Exposure to Pyridine. Annual Meeting of the Society of Toxicology, New Orleans, March 14-18, 1993.

Lewis, J. L., K. J. Nikula and L. A. Sachetti: Induced Xenobiotic Metabolizing Enzymes Localized to Eosinophilic Globules in Nasal Epithelium of Toxicant-Exposed F344 Rats. Workshop on Nasal Toxicity and Dosimetry of Inhaled Xenobiotics: Implications for Human Health, Research Triangle Park, NC, September 20-22, 1993.

Lopez, J. A.: Design of Exposure Facilities (Laboratory Demonstration). Current Concepts in Inhalation Toxicology - A Short Course, Albuquerque, NM, October 26-29, 1992.

Lopez, J. A.: Use of Facility Operator Aids in a Research Laboratory. U.S. Department of Energy Conduct of Operations Workshop, Tampa, FL, May 5, 1993.

Lopez, J. A.: Operator Aid Configuration Management Workshop. U.S. Department of Energy Albuquerque Operations Office, Albuquerque, NM, May 27, 1993.

Lundgren, D. L., F. F. Hahn, R. A. Guilmette and W. W. Carlton: Carcinogenic Effects of Inhaled $^{244}CmO_2O_3$ in Rats. Health Physics Society Annual Meeting, Atlanta, GA, July 11-15, 1993.

Lundgren, D. L.: ITRI Long-Term Rodent Studies. National Radiobiological Archives Workshop, Washington, DC, August 16-17, 1993.

Lundgren, D. L.: Report on the NIOSH Workshop on Bioaerosols. Topical Meeting on the Technical Basis for Measuring, Modeling, and Mitigating Aerosols, Albuquerque, NM, September 27-30, 1993.

Maples, K. R., W. E. Bechtold, A. R. Dahl and R. F. Henderson: Butadiene Monoepoxide Levels are Greater in Bone Marrow than in Blood Following Inhalation of 1,3-Butadiene in B6C3F_1 Mice. Annual Meeting of the Society of Toxicology, New Orleans, March 14-18, 1993.

Mauderly, J. L.: Physiology of Regional Responses to Inhaled Toxicants. Current Concepts in Inhalation Toxicology - A Short Course, Albuquerque, NM, October 26-29, 1992.

Mauderly, J. L.: Respiratory Function Evaluation (Laboratory Demonstration). Current Concepts in Inhalation Toxicology - A Short Course, Albuquerque, NM, October 26-29, 1992.

Mauderly, J. L., K. J. Nikula and M. B. Snipes: Influence of Particle-Associated Organic Compounds on Carcinogenicity of Diesel Exhaust. Ninth Health Effects Institute Annual Meeting, Monterey, CA, December 6-9, 1992.

Mauderly, J. L., M. B. Snipes, E. B. Barr, S. A. Belinsky, W. E. Bechtold, W. C. Griffith, R. F. Henderson, C. E. Mitchell and K. J. Nikula: Influence of Particle-Associated Organic Compounds on Carcinogenicity of Diesel Exhaust. Ninth Health Effects Institute Annual Meeting, Monterey, CA, December 6-9, 1992.

Mauderly, J. L., K. J. Nikula and M. B. Snipes: Influence of Particle-Associated Organic Compounds on Carcinogenicity of Diesel Exhaust. NIOSH Lung Disease Branch, Morgantown, WV, February 1, 1993.

Mauderly, J. L.: Implications of "Lung Overload" for Health Effects of Inhaled Dusts. International Council on Metals in the Environment, Health Advisory Panel, Pasadena, CA, February 8, 1993.

Mauderly, J. L.: Contribution of Inhalation Bioassays to the Assessment of Human Health Risks from Solid Airborne Particles. Fourth International Symposium on Toxic and Carcinogenic Effects of Solid Particles in the Respiratory Tract, Hannover, Germany, February 28-March 5, 1993.

Mauderly, J. L., R. F. Henderson, K. J. Nikula and M. B. Snipes: Non-Cancer Effects of Chronic Inhalation Exposure of Animals to Solid Particles. Fourth International Symposium on Toxic and Carcinogenic Effects of Solid Particles in the Respiratory Tract, Hannover, Germany, February 28-March 5, 1993.

Mauderly, J. L., E. B. Barr, W. C. Griffith, R. F. Henderson, K. J. Nikula and M. B. Snipes: Importance of Soot-Borne Organic Mutagenic Compounds in Pulmonary Carcinogenicity of Diesel Exhaust in Rats. Annual Meeting of the Society of Toxicology, New Orleans, March 14-18, 1993.

Mauderly, J. L., W. C. Griffith, R. F. Henderson, K. J. Nikula and M. B. Snipes: Importance of Soot-Associated Organic Mutagenic Compounds in Pulmonary Carcinogenicity of Diesel Exhaust in Rats. Ninth Congress of ISAM Aerosols in Medicine, Garmisch-Partenkirchen, Germany, March 30-April 4, 1993.

Mauderly, J. L.: Progress in Understanding Mechanisms of the Effects of Inhaled Particles. American Lung Association/American Thoracic Society International Conference, San Francisco, CA, May 16-19, 1993.

Mauderly, J. L.: Health Effects of Engine Exhaust. Symposium on Topics in Pulmonary Health, Regional American Association for the Advancement of Science Meeting, Albuquerque, NM, May 24, 1993.

Mauderly, J. L.: Current Assessment of the Carcinogenic Hazard of Diesel Exhaust. Third International Congress on Toxic Combustion Byproducts, Cambridge, MA, June 14-16, 1993.

Mauderly, J. L.: Particle-Induced Lung Tumor Response in Rats vs. Other Species. Relative Species Sensitivity Workshop, Institute for Polyacrylate Adsorbents, Rochester, NY, August 26-27, 1993.

Mauderly, J. L.: Selected Current Issues for Inhaled Particles. Topical Meeting on the Technical Basis for Measuring, Modeling, and Mitigating Toxic Aerosols, Albuquerque, NM, September 28-30, 1993.

Muggenburg, B. A. and R. F. Henderson: Bronchoalveolar Lavage for Evaluating Pulmonary Disease (Laboratory Demonstration). Current Concepts in Inhalation Toxicology - A Short Course, Albuquerque, NM, October 26-29, 1992.

Muggenburg, B. A., R. A. Guilmette, W. C. Griffith, F. F. Hahn, N. A. Gillett and B. B. Boecker: Toxicity of Inhaled Particles of $^{238}PuO_2$. Institutfur Radiologie, Kribsforschungszentrum, Heidelberg, Germany, March 12, 1993.

Muggenburg, B. A., K. J. Nikula, I. Y. Chang and B. B. Boecker: The Toxicity of Injected $^{137}CsCl$ in Laboratory Dogs. National Radiobiological Protective Board, Chilton, Didcot, U.K., March 15, 1993.

Muggenburg, B. A.: Therapy for Exposed Individuals. Topical Meeting on the Technical Basis for Measuring, Modeling, and Mitigating Toxic Aerosols, Albuquerque, NM, September 27-30, 1993.

Newton, G. J., M. D. Hoover and W. C. Griffith: Determination of Particle Location of Filters Using an Automatic Optical Imaging System. American Association for Aerosol Research, San Francisco, CA, October 12-16, 1992.

Newton, G. J. and Y. S. Cheng: Generation and Characterization of Particles and Mists (Laboratory Demonstration). Current Concepts in Inhalation Toxicology - A Short Course, Albuquerque, NM, October 26-29, 1992.

Nikula, K. J.: Gross and Cellular Anatomy of the Respiratory Tract. Current Concepts in Inhalation Toxicology - A Short Course, Albuquerque, NM, October 26-29, 1992.

Nikula, K. J., G. L. Finch, M. D. Hoover and D. S. Swafford: Granulomatous Lung Disease from Inhaled Beryllium in Mice. 1992 American College of Veterinary Pathologists Annual Meeting, San Diego, CA, November 17-20, 1992.

Nikula, K. J., M. B. Snipes, E. B. Barr, W. C. Griffith, R. F. Henderson and J. L. Mauderly: Influence of Soot-Associated Organic Compounds on Pulmonary Carcinogenicity of Diesel Exhaust in Rats. Toxic and Carcinogenic Effects of Solid Particles in the Respiratory Tract, Hannover, Germany, March 1-5, 1993.

Samet, J.: Lung Cancer in Uranium Miners - A Tissue Resource. DOE/OHER Review, ITRI, Albuquerque, NM, December 12, 1992.

Schery, S. and Y. S. Cheng: Radon Progeny Dynamics: Indoors and Outdoors. Topical Meeting on the Technical Basis for Measuring, Modeling, and Mitigating Toxic Aerosols, Albuquerque, NM, September 27-30, 1993.

Schleyer, W. C.: Process Knowledge at ITRI. Annual Defense Waste Generators Workshop, Las Vegas, NV, September 29, 1993.

Scott, B. R., C. W. Langberg and M. Hauer-Jensen: Weibull Models for the Prevalence of Ulcers in the Small Intestine after Localized Single or Fractionated Irradiation. Joint Meeting of the Radiation Research Society/North American Hypothermia Society, Dallas, TX, March 20-25, 1993.

Scott, B. R., M. D. Hoover and G. J. Newton: New Tools for Evaluating Respiratory Tract Intake from Exposure to High-Specific-Activity, Alpha-Emitting Particles. Topical Workshop on the Technical Basis for Measuring, Modeling, and Mitigating Toxic Aerosols, Albuquerque, NM, September 27-30, 1993.

Scott, B. R.: Adjustment to Exposure Limits. Topical Meeting on the Technical Basis for Measuring, Modeling, and Mitigating Toxic Aerosols, Albuquerque, NM, September 27-30, 1993.

Snipes, M. B.: Clearance of Deposited Particles. Current Concepts in Inhalation Toxicology - A Short Course, Albuquerque, NM, October 26-29, 1992.

Snipes, M. B.: Deposition and Clearance of Inhaled Particles (Laboratory Demonstration). Current Concepts in Inhalation Toxicology - A Short Course, Albuquerque, NM, October 26-29, 1992.

Snipes, M. B., E. B. Barr, I. Y. Chang, R. F. Henderson, K. J. Nikula and J. L. Mauderly: Particle Clearance and Sequestration in Lungs of Rats Exposed Chronically to Diesel Exhaust or Carbon Black (presented by J. L. Mauderly). Ninth Health Effects Institute Annual Meeting, Monterey, CA, December 6-9, 1992.

Snipes, M. B., W. C. Griffith, K. J. Nikula and R. A. Guilmette: Clearance of Particles Deposited in the Conducting Airways of Beagle Dogs. Ninth Congress of the International Society for Aerosols in Medicine, Garmisch-Partenkirchen, Germany, March 30-April 4, 1993.

Snipes, M. B.: Do Species Differences in Retention Patterns of Particles in the Lung Influence Biological Responses? University of Berne, Berne, Switzerland, April 6, 1993.

Snipes, M. B., E. B. Barr, I. Y. Chang, R. F. Henderson, K. J. Nikula and J. L. Mauderly: Particle Clearance and Distribution Patterns in Rat Lungs as Influenced by Chronic Inhalation of Diesel Exhaust or Carbon Black. American Lung Association/American Thoracic Society International Conference, San Francisco, CA, May 16-19, 1993.

Snipes, M. B.: Dissolution and Clearance of Inhaled Particles. Topical Meeting on the Technical Basis for Measuring, Modeling, and Mitigating Aerosols, Albuquerque, NM, September 27-30, 1993.

Swafford, D. S.: Identification of Genetic Alterations Induced in Lung Tumors Formed in F344/N Rats by the Inhalation of Diesel Exhaust or Carbon Black. Toxicology Program Seminar, College of Pharmacy, University of New Mexico, Albuquerque, NM, November 4, 1992.

Tierney, L. A., S. A. Belinsky, C. A. Carter, G. Saccomanno, M. Anderson and J. F. Lechner: X-Ray-Induced Lung Tumors in the F344 Rat. Fourth International Conference on Anticarcinogenesis and Radiation Protection, Baltimore, MD, April 19-23, 1993.

Weissman, D. D. E. Bice, R. Crowell and M. Schuyler: Primary Immunization Via the Human Respiratory Tract: Local Antibody Responses. The American Association of Immunologists/Clinical Immunology Society, Denver, CO, May 21-25, 1993.

Williams, P. L., K. Randerath and J. L. Mauderly: Statistical Analysis of Correlated Measurements of DNA Adduct Formation in Lungs of F344 Rats Exposed to Diesel Exhaust or Carbon Black. Ninth Health Effects Institute Annual Meeting, Monterey, CA, December 6-9, 1992.

Yeh, H. C., Y. S. Cheng, S. M. Smith and D. L. Swift: Deposition of 0.001-0.2 μm Ultrafine Particles in the Nasal Airway of Adults and Children. American Association for Aerosol Research, San Francisco, CA, October 12-16, 1992.

Yeh, H. C., R. S. Turner, R. K. Jones, B. A. Muggenburg, J. Smith, L. S. Martin and P. W. Strine: Characterization of Aerosols Produced During Surgical Procedures. 1993 American Industrial Hygiene Conference and Exposition, New Orleans, LA, May 15-21, 1993.

APPENDIX G

SEMINARS PRESENTED BY VISITING SCIENTISTS

OCTOBER 1, 1992 - SEPTEMBER 30, 1993

Dr. Richard D. Irons, Health Sciences Center, University of Colorado, Denver, CO: *Studies on the Mechanism(s) of Chemical Leukemogenesis: A Comparison of Benzene and Butadiene*, December 15, 1992.

Dr. Adnan A. Elfarra, Comparative Biosciences & Environmental Toxicology, University of Wisconsin, Veterinary Medicine, Madison, WI: *1,3-Butadiene Bioactivation*, December 17, 1992.

Dr. Robert A. Leboeuf, Procter and Gamble Company, Miami Valley Labs, Cincinnati, OH: *Transformation of Syrian Hamster Embryo Cells at pH 6.70 for Assessing the Carcinogenic Potential of Chemicals and Studying Multistage Carcinogenesis*, January 18, 1993.

Dr. Richard J. Lemen, St. Luke's Clinic, University of Arizona Health Sciences Center, Tucson, AZ: *An Update of Adenovirus Bronchiolitis in Normal and Ragweed Sensitized Beagle Puppies*, January 22, 1993.

Dr. Don Jacobs, Department of Vascular Surgery, Medical College of Wisconsin, Milwaukee, WI: *Peripheral Ischemia and Reperfusion Injury*, January 27, 1993.

Dr. Theodore T. Puck, Distinguished Professor, Department of Medicine, University of Colorado Health Sciences Center, Denver, CO: *Reverse Transcription, Genome Exposure and Cancer*, January 28, 1993.

Mr. Gene A. Runkle, Director, Health Protection Division, DOE Field Office, Albuquerque, NM: *Radiation Safety Visit to the Former USSR*, January 29, 1993.

Dr. Peter Foiles, American Health Foundation, Valhalla, NY: *Carcinogen Adducts as Markers in the Study of Chemical Carcinogenesis*, February 23, 1993.

Dr. Ian Gilmour, Health Effects Research Laboratory, U.S. Environmental Protection Agency, Research Triangle Park, NC: *The Interaction of Air Pollutants with Infectious or Allergenic Agents*, March 12, 1993.

Dr. Ainsley Weston, Department of Community Medicine, Division of Environmental & Occupational Medicine, The Mount Sinai Medical Center, New York, NY: *Inherited and Acquired Host Factors in Human Lung Cancer Risk*, April 13, 1993.

Dr. Eric Ansoborlo, Atomic Energy Commission, Pierrelatte, France: *Uranium Experience in France*, April 28, 1993.

Dr. Graham Patrick, MRC Radiobiology Unit, Chilton, Didcot, UK: *Particle Clearance from Alveoli Studied by Subpleural Microinjection*, May 13, 1993.

Dr. Ming J.W. Chang, Department of Public Health, Chang Gung Medical College, Tao-Yuan, Taiwan: *Studies on the Chemical and Biological Monitoring of Exposure to Environmental Toxicants*, May 14, 1993.

Dr. Carol Schnizlein-Bick, Indiana University School of Medicine, Indianapolis, IN: *Local Immunity in Lung Associated Lymph Nodes in a Mouse Model of Histoplasmosis*, May 27, 1993.

Dr. Chandrakant P. Giri, Center for Food Safety and Applied Nutrition, FDA, Division of Toxicological Research, Laurel, MD: *cDNA Subtraction Library Approach to Identify and Clone TGF-β1 Inducible Growth Suppressor Genes from Human Bronchial Epithelial Cells*, June 15, 1993.

Dr. Robert M. Strieter, Department of Internal Medicine, Division of Pulmonary and Critical Care, University of Michigan, Ann Arbor, MI: *The Role of IL-8 in the Recruitment of Neutrophils into the Lung*, June 17, 1993.

Dr. Charlene A. McQueen, Department of Pharmacology and Toxicology, University of Arizona College of Pharmacy, Tucson, AZ: *Aromatic Amine Toxicity: Genetics and Risk*, July 7, 1993.

Dr. Frank H.Y. Green, Department of Pathology, The University of Calgary, Calgary, Canada: *Responses of Human Lungs to Mineral Dust*, July 15, 1993.

APPENDIX H

ADJUNCT SCIENTISTS
AS OF NOVEMBER 30, 1993

Dr. Carol Basbaum
Department of Anatomy
University of California School of Medicine
San Francisco, CA 94143

Dr. William W. Carlton
Department of Veterinary Microbiology,
Pathology and Public Health
School of Veterinary Medicine
Purdue University
West Lafayette, IN 47907

Dr. Frank D. Gilliland
Cancer Center
New Mexico Tumor Registry and
Department of Medicine
University of New Mexico
Albuquerque, NM 87131

Dr. Terry Gordon
Institute of Environmental Medicine
Long Meadow Road
Tuxedo, NY 10987

Dr. William M. Hadley
Dean, College of Pharmacy
University of New Mexico
Albuquerque, NM 87131

Dr. Richard Hayes
NIH, NCI
6130 Executive Boulevard
Executive Plaza North 418
Rockville, MD 20892

Dr. Steve Kleeberger
Division of Physiology
Department of Environmental Health
Johns Hopkins University
615 N. Wolfe Street
Baltimore, MD 21205

Dr. Donna Kusewitt
The Lovelace Institutes
2425 Ridgecrest S.E.
Albuquerque, NM 87108

Dr. Douglas Mapel
Pulmonary Division
Department of Medicine
University of New Mexico
Albuquerque, NM 87131-5271

Dr. Raymond F. Novak
Wayne State University
Institute of Chemical Toxicology
Detroit, MI 48201

Dr. Judy Raucy
College of Pharmacy
University of New Mexico
Albuquerque, NM 87131

Dr. Alan H. Rebar
School of Veterinary Medicine
Purdue University
West Lafayette, IN 47907

Dr. Jonathan M. Samet
Pulmonary Division
Department of Medicine
The University of New Mexico
Albuquerque, NM 87131

Dr. Thomas Sandström
Department of Lung Medicine
University Hospital
S-901 85 Umea, Sweden

Dr. Steven Q. Simpson
Pulmonary Division
Department of Medicine
University of New Mexico
Albuquerque, NM 87131

Dr. David L. Swift
Johns Hopkins University
School of Hygiene and Public Health
Baltimore, MD 21205

Dr. Jonathan B. Ward
University of Texas Medical Branch
2.102 Ewing Hall, S-10
Galveston, TX 77555-1010

Dr. Ross Zumwalt
Office of Medical Investigation
Assistant Chief Medical Investigator
University of New Mexico
School of Medicine
Albuquerque, NM 87131

APPENDIX I

EDUCATION ACTIVITIES AT THE INHALATION TOXICOLOGY RESEARCH INSTITUTE

ITRI has always had educational programs that encourage students to select careers in science. Our programs provide research opportunities in inhalation toxicology and pulmonary biology for precollege, undergraduate, graduate students, postdoctoral fellows, and visiting scientists. These programs are important because fewer students are selecting careers in science, although there are continuing needs for scientists. A goal of our educational programs is to help provide scientists who will be available to fill positions needed by the Department of Energy.

Precollege Students

To stimulate an interest in science in precollege students, we provide tours and demonstrations at our Institute and support students who participate in science fairs. We also provide the opportunity for high school students to work in our research laboratories. This program has worked well during the last three summers, and we will have high school students working in our laboratories in FY-1994.

To support precollege education, ITRI provides research opportunities for middle school and high school science teachers. One program, the Summer Teacher Enrichment Program (STEP), is specifically for New Mexico teachers. A second program is the Teacher Research Associates Program (TRAC) for teachers throughout the United States. Teachers in these programs are involved in all steps of a scientific study, including the design of experiments, the conduct of experimental assays, evaluation of data, and the presentation of scientific results. The direct involvement of teachers in all phases of a research project provides them with information valuable to students interested in careers in science. The STEP and TRAC participants have been very enthusiastic about their work at ITRI and have found various ways to incorporate their experiences into the classroom. We will have eight high school teachers in these two programs at our Institute during the summer of FY-1994.

Since its beginning in 1984, 33 New Mexico middle school and high school science teachers have participated in research at ITRI through STEP. TRAC started in 1989, and 16 high school teachers have been supported at our Institute by this program. There were four STEP and four TRAC teachers in these programs at ITRI during the summer of FY-1993.

In FY-1993 a Field Task Proposal was submitted to obtain funding for a program in "Environmental Health Science - Educational Awareness." We anticipate funding of this program in FY-1994. An important objective of this program will be to provide interactions between ITRI and science teachers at high schools to stimulate interest by precollege students in environmental health science.

Our staff continued their involvement in precollege education as science fair judges and as tutors and mentors.

Undergraduate Students

There are three programs at ITRI for undergraduate students. The first is for undergraduate students who are science majors and who plan to continue their education with postgraduate training. Students in this program are provided the opportunity to initiate and complete a scientific investigation under the direction of an ITRI staff member. By being involved in the design of the study, the conduct of the experiments, analysis of the data, and the presentation of results, the students gain an understanding of research and experience the excitement of new discovery. Nine students carried out research at ITRI during the past summer.

A second program is for students in the Waste-management Education and Research Consortium (WERC). The mission of WERC is to expand the national capability in the management of hazardous, radioactive, and solid wastes. Four WERC students were provided opportunities to participate in waste-management activities at ITRI in FY-1993.

The third educational program for undergraduate students provides work opportunities for engineering students. Six students worked in various areas of engineering at ITRI during the summer of FY-1993. A total of 545 students have received educational opportunities at ITRI since 1966.

We continue to encourage students from the New Mexico universities to apply for our summer research programs. The continued participation of WERC students at ITRI has increased the number of New Mexico students participating in education programs at ITRI. We will continue to encourage more students from New Mexico to participate in our summer research programs to provide opportunities students in our state and to attract a higher number of minority applicants.

Graduate Students

Our Inhalation Toxicology Research Institute/University of New Mexico (UNM) Graduate Program in Inhalation Toxicology provides the opportunity for students to obtain the Ph.D. degree. Course work is completed at UNM, and the research portion of the doctoral degree is carried out at ITRI, with a staff member from our Institute serving as the research advisor. Two new students were accepted into this graduate program in FY-1993. We have continued to obtained support from industry for our graduate program. Both Lilly Laboratories and E. I. duPont de Nemours & Company continued to contribute funds that support the attendance of students at scientific meetings and as well as stipend support.

In addition to the ITRI-UNM program, graduate students attending other universities can also carry out the research necessary for their graduate degrees at the Institute. All course work for the advanced degree is completed at the university before the student starts research at ITRI. The advanced degree is awarded by the participating university upon completion of all degree requirements. Since 1968, 33 graduate students have conducted all or part of their research at ITRI.

Our graduate programs take advantage of the complementary academic resources available at universities and the research resources available at ITRI. For example, we established joint graduate programs in pathology with the schools of Veterinary Medicine at Colorado State and Purdue Universities. Graduate veterinary students complete the research portion of a Ph.D. degree at ITRI as part of their residency program in pathology. A program in health physics has recently been established with Texas A&M University, with funding from the Department of Energy.

Postgraduate Students

We provide research appointments to recent doctoral graduates to continue in their research training. Students in life science, chemistry, veterinary medicine, or engineering carry out research under the direction of ITRI staff members. This program is designed to develop research capabilities both in inhalation toxicology and one or more of the areas of basic pulmonary biology. It continues to be difficult to find qualified postdoctoral participants, and during FY-1993 we had only one postdoctoral fellow participating in research at our Institute. A continuing goal is to increase the number of postdoctoral participants at our Institute.

University Faculty and Industrial Scientists

Opportunities are available for scientists from universities or industry to visit the Institute or collaborate in research at ITRI. The length of these visits ranges from a few days, to obtain information or learn techniques, to up to a full year, to conduct research. During FY-1993, participants included scientists from UNM, the Albuquerque Veterans Medical Center, Purdue University, and the California Polytechnic State University.

Other Educational Activities

Several of our staff members hold academic appointments and present lectures to university students. ITRI also holds periodic workshops in inhalation toxicology. These workshops have received international recognition. The book, "Concepts in Inhalation Toxicology", published in 1989 from the workshop held in 1987, has become a key text in the field. The last workshop was held in October 1992, and approximately 90 attendees benefitted from the lectures and laboratory demonstrations.

David E. Bice, Ph.D.
Education Coordinator

APPENDIX J

AUTHOR INDEX

FIRST AUTHOR	PAGE NUMBERS
Bechtold, W. E.	50
Belinsky, S. A.	87, 96
Benson, J. M.	43, 45
Bice, D. E.	119
Carter, C. A.	75
Chen, B. T.	5, 13, 15
Cheng, Y. S.	1, 8, 29
Dahl, A. R.	35
Finch, G. L.	53, 58, 122
Gerde, P.	38
Griffith, W. C.	71
Guilmette, R. A.	133
Hahn, F. F.	64
Harkema, J. R.	105, 108
Henderson, R. F.	110
Hickman, A. W.	130
Hoover, M. D.	18, 21
Hotchkiss, J. A.	113, 116
Johnson, N. F.	66, 85
Kelly, G.	83
Kennedy, C. H.	79
Lewis, J. L.	32
Lundgren, D. L.	56, 61
Maples, K. R.	47
Mitchell, C. E.	94
Muggenburg, B. A.	69, 125
Newton, G. J.	23, 26
Nikula, K. J.	91, 99, 102
Palmisano, W. A.	77
Scott, B. R.	136, 139
Snipes, M. B.	40
Swafford, D. S.	89
Tierney, L. A.	81
Yeh, H. C.	10, 127

US GOVERNMENT PRINTING OFFICE 1994 - 840-226

DATE
FILMED
4/18/94
END